FLUCTUATIONS IN THE LATTICE BOLTZMANN METHOD

A Dissertation
Submitted to the Graduate Faculty
of the
North Dakota State University
of Agriculture and Applied Science

By

Goetz August Kähler

In Partial Fulfillment
for the Degree of
DOCTOR OF PHILOSOPHY

Major Department:
Physics

November 2012

Fargo, North Dakota

ProQuest LLC.
789 East Eisenhower Parkway
P.O. Box 1346
Ann Arbor, MI 48106 - 1346

North Dakota State University

Graduate School

Title

FLUCTUATIONS IN THE LATTICE BOLTZMANN METHOD

By

Goetz August Kähler

The Supervisory Committee certifies that this *disquisition* complies with North Dakota State University's regulations and meets the accepted standards for the degree of

DOCTOR OF PHILOSOPHY

SUPERVISORY COMMITTEE:

Alexander J. Wagner
Chair

Dan Kroll
Co-Chair

Sylvio May

Iskhandar Akhatov

Approved by Department Chair:

November 7, 2012 Dept. Chair

ABSTRACT

The implementation of fluctuations in the lattice Boltzmann method has made significant progress in the last 10 years. The significance of incorporating noise to all non-conserved degrees of freedom was a significant recent discovery that was based on a simplified Langevin treatment of the linarized Boltzmann equation. However, for non-vanishing mean velocities significant deviations in the correlation functions were observed. In this thesis we show how we can largely remove these deviations by incorporating fully velocity dependent moment transforms and thus recover a fluctuation dissipation theorem that is valid for a larger range of velocities. Furthermore we show that the remaining deviations can be attributed to the collision operator of the linearized Boltzmann equation not being identical to the one of the BGK collision which forms the basis of most modern lattice Boltzmann applications. Finally we show that the locally velocity dependent transforms significantly improve the stability of fluctuating lattice Boltzmann simulations at low particle densities.

ACKNOWLEDGEMENTS

Writing this thesis and conducting the research involved was a challenge intellectually but also personally. That probably is the definition of a worthwhile experience. I am grateful to have enjoyed significant support from many during this time, the department, family and friends.

First and foremost I must mention my academic advisor, Alexander Wagner, who, despite at times significant doubt and difficulties of mine supported me at all times and maintained belief that I could move this project forward. I hope that the results at least in part justify his trust.

My fellow grad students Stephan Löw, Eric Foard, and Ben Lu with whom I spent many cheerful and frightful moments must be mentioned. The enjoyment working our ways through grad school was largely due to the fairness and cameradery shared among us. Eric is now working at his first postdoc position in Rome and Stephan is finishing up his own thesis at the time of this writing. Ben unfortunately did not finish yet and is dealing with health problems. Hopefully these can be resolved and he can finish his degree soon.

I need to mention Stefan Possin, whom I've had the pleasure of knowing since first grade. He probably knows me better than any other person and has been a steady source of support when things didn't go smoothly and good humor when they did. He provided the all important perspective from the outside of the physics world.

DEDICATION

To my parents, Ruth Moderow and Sebastian Kähler, my friend Stephan Possin and Liisa Locker.

TABLE OF CONTENTS

LIST OF FIGURES

1. INTRODUCTION

Over the last 25 years the lattice Boltzmann method has been increasingly successful as a versatile practical tool in computational soft matter physics. Like its predecessor, the lattice gas automata, it was originally conceived for purposes of hydrodynamic simulations [1]. Here it has found significant success, largely due to its performance, adaptability, and ease of parallel implementation. It even found applications outside of its original field and has, for example, been applied to the nonlinear Schroedinger equation [2, 3, 4] and electrodynamics [5, 6, 7].

However, as it is based on the Boltzmann transport equation where the collision integral was constructed according to Boltzmann's Stosszahlansatz [8] its original inception did not include fluctuations at all. This is a key difference to lattice gas automata (LGA) which describe the system in consideration by means of discrete particles that move on a grid and interact by a set of predefined collisions that conserve mass, momentum and energy but limit the collisions to happen at fixed angles due to the lattice. Due to their particle based nature, LGA based methods intrinsically contain fluctuations. It has been shown that thermal LGA models can be constructed such that they reproduce the dynamic structure factors of real fluids [9].

As the correct implementation of thermal fluctuations is a key component of the successful reproduction of mesoscopic fluid behavior there has been significant interest in the last years to reintroduce fluctuations to the lattice Boltzmann method (LBM) in a way that is consistent with statistical mechanics. The motivation stems from the need to apply the LBM to several phenomena based on Brownian motion. The pioneering publication in the field was Ladd's work on colloidal particles suspended in a fluctuating lattice Boltzmann fluid [10]. This was a significant step in reintroducing fluctuations into the lattice Boltzmann method and allowed for investigation of a wide range of microscopic phenomena otherwise inaccessible to the method. Examples

here are domain growth in porous media [11], or dynamics in polymer solutions [12]. However, recently it was discovered that his method does not, in fact, reproduce the correct fluctuations except in the limit of long wavelengths. The reason is that Ladd's implementation introduces a random noise term only on the stress degrees of freedom, not the additional non-conserved modes. This was corrected first by Adhikari *et al* [13] who argued in the spirit of a Langevin treatment [14] of the linearized Boltzmann equation [15, 16, 17]. The theory put fourth by Fox and Uhlenbeck (and others) requires that all non-conserved degrees of freedom have noise term attached, not only the non-conserved hydrodynamic ones, i.e. the stress degrees of freedom.

The work on this thesis started out of a desire to develop a fluctuating lattice Boltzmann code for critical phenomena. After an early analysis of Adhikari's derivation [13] the question of the validity of the fluctuation dissipation theorem (FDT) arose even for the simple case of the ideal gas. The derivation presented there is reliant on an orthogonality condition which defines an eigenvector representation of the collision operator. This condition is, in principle, dependent on the streaming velocity, as shown, for example, in Fox's and Uhlenbeck's fundamental work on the fluctuating linearized Boltzmann equation [15]. However, Adhikari's implementation avoids this velocity dependence completely which has the effect that the derivation of the fluctuation dissipation theorem provided is strictly only valid for vanishing velocities. In [15] it is shown that this condition needs to depend on the equilibrium distribution function but in Adhikari's derivation the equilibrium distribution is only considered to zeroth order which has the convenient result that the eigenvector representation of the collision operator becomes independent of the local velocities. Motivated to investigate the effects of the velocity independent noise and the advantages of the Adhikari implementation over the Ladd implementation we implemented both of them and investigated the structure factors of density and momentum for vanishing mean

velocity and a fixed mean flow velocity. This early analysis was published in paper 2. Here we discussed that while for vanishing velocity we found very good agreement with the theory, we also observed significant Galilean invariance violations if a flow field was introduced. We attributed this to the simplification of the orthogonalization condition between the transformation matrices used in the multi-relaxation time method used to implement the fluctuating lattice Boltzmann method.

To avoid the use of only the zeroth order approximation of the equilibrium distribution, i.e. removing the restriction of vanishing velocities, in the orthogonality condition seemed the best and most straight-forward solution. However, it was, at first, not clear whether a velocity dependent set of transforms would allow for the preservation of hydrodynamic equations. We investigated this and found a general method of deriving hydrodynamics based on the asymptotic expansion of the equilibrium distribution. We could show that hydrodynamic equations can be reproduced provided that the first four velocity moments of the equilibrium distribution are fulfilled equivalently to those in the continuous case. We do not, however, require detailed knowledge of the base velocity set used for the particular lattice Boltzmann implementation provided the aforementioned moment equations are fulfilled. More importantly, however, we found that hydrodynamics are preserved independently of the addition of conserved quantities to the hydrodynamically relevant moments. This last result is particularly useful because it allows for the inclusion of the first and second moments of the equilibrium distribution in the orthogonality condition of the multi-relaxation time transforms. These extra degrees of freedom in turn allow for including the additional terms in the multi-relaxation time transforms implying that we can use the second order velocity dependent terms in the orthogonality condition of the eigenvector transforms of the collision operator. This discussion and the results were published in paper 3 and form the second chapter in this thesis.

Having shown that hydrodynamic equations could still be reproduced we implemented a fluctuating lattice Boltzmann method on the example of a D2Q9 system with velocity dependent transforms. This discussion is presented in paper 4. Here we discussed that it is now possible to include these fluctuations at non vanishing velocities and that the deviations in the correlation functions from those we expect from the fluctuation dissipation theorem are indeed, significantly smaller. We also derive the FDT and can show that it holds independent of the mean velocity of the fluid, limited by the velocity dependent range where the equilibrium distribution remains non-negative. Furthermore we show that the Adhikari derivation of the FDT is intrinsically only correct for the case of the wave vector $\mathbf{k} = 0$.

Finally, after showing the validity of the fluctuation dissipation theorem for all $\mathbf{u}$ in paper 4, we investigated the behavior of our fluctuating lattice Boltzmann implementation if we use entirely local parameters for the noise terms in the iteration in chapter 5. Here we leave the arguments put fourth by the Langevin type theory and only choose very basic physical assumptions as justification. We find that choosing entirely local parameters for the collision operator at a lattice site that enter the collision, i.e. density, momentum, and also the relaxation time, significantly improves stability of the fluctuating lattice-Boltzmann simulation. Furthermore we show that this local approach reproduces distribution functions that, at the low density limit, that are much closer to the expected Poisson distributions one expects from statistical mechanics. Finally we apply our method to the simple non-equilibrium case of a Poiseuille flow. We can show in this computer experiment that our method does reproduce a viscosity that depends on the local temperature instead of a constant lattice Boltzmann temperature.

In the remainder of this introduction we briefly discuss the Boltzmann equation as all the work presented in this thesis as the concepts and nomenclature used in

this document are all rooted this fundamental part of statistical mechanics. We then briefly review the Langevin description of Brownian motion and it's application to the linearized Boltzmann equation. Finally the lattice Boltzmann method is introduced with particular emphasis on the multi-relaxation time implementations.

1.1. The Boltzmann Transport Equation

1.1.1. The Distribution Function and the Collision Integral

In 1872 Ludwig Boltzmann published what would become one of his most famous papers [8]. His aim was to find the connection between the second law of thermodynamics and microscopic particle mechanics based on Newton's equations. In particular he was looking for the explanation of the irreversibility of thermodynamics which exists in stark contrast to the time-reversibility of Newton's equation of motion. To derive thermodynamics from Newtonian mechanics he introduced the probability density $f(\mathbf{x}, \mathbf{v}, t)$, a quantity that describes the probability to find one particle moving with velocity $\mathbf{v}$ at position $\mathbf{x}$ and time t. This is also called the one-particle distribution function. The mathematical representation of the position and velocity space is called μ-space which has a dimensionality of $2D$ where D is the actual physical dimension of the system under consideration. One may also interpret f such that $f(\mathbf{x}, \mathbf{v}, t)$ d $\mathbf{x}$ d $\mathbf{v}$ describes the number of particles that are found at time t in the small μ-space interval $\boldsymbol{x} + \Delta\mathbf{x}, \mathbf{v} + \Delta\mathbf{v}$. We will return to this interpretation later. This interval should be considered very small with respect to macroscopic length scales but large enough so that it contains a large number of particles. Then f can be considered a continuous function. How will this distribution function then change as a function of time? After a time Δt particles at position $\mathbf{x}$, having velocity $\mathbf{v}$ will move to a position $\mathbf{x}' = \mathbf{x} + \mathbf{v}\Delta t$. The velocity may change due to some long-range interactions that are in common to all particles at position $\mathbf{x}$. It is feasible to

subsume these long range effects into a local force term $\mathbf{F}(\mathbf{x})$ which gradually changes the velocity to $\mathbf{v}' = \mathbf{v} + \frac{\mathbf{F}(\mathbf{x})}{m}\Delta t$ where m is the particle mass. However, there are also more drastic changes in the velocity, possible due to collisions between particles. Typically these collisions occur on a time scale much faster than Δt here and will cause a discontinuous change in the velocity of the particle. The rate of change of this probability distribution is then given by the total time differential[1] (sometimes also called material derivative)

$$D_t f(\mathbf{x}, \mathbf{v}, t) = \left(\partial t + v_\alpha \partial_\alpha + \frac{F_\alpha}{m}\partial_{v_\alpha}\right) f(\mathbf{x}, \mathbf{v}, t) = C \tag{1}$$

where C describes the change in f due to collisions of the particles. In order to describe the rate of change in f due to these particle collisions Boltzmann introduced the collision operator C. Boltzmann assumed here the case of a dilute gas where collisions of more than two particles are considered negligible. Then C depends only on $f_2(\mathbf{x}_1, \mathbf{x}_2, \mathbf{v}_1, \mathbf{v}_2, t)$, the probability density to find two particles with their respective positions and velocities at time t. Note here that because the rate of change of the distribution function is written as an entirely local quantity it is implied that $\mathbf{F}$ only represents forces external to the interval $\mathbf{x}+\Delta\mathbf{x}$. The probability of finding two particles at the same position ($\mathbf{x}_1 = \mathbf{x}_2 = \mathbf{x}$) is then $f_2(\mathbf{x}, \mathbf{v}_1, \mathbf{v}_2, t)$ where "same position" is understood in the context of the scattering parameter b being much smaller than Δx. Here Boltzmann introduced his Stosszahlansatz or molecular chaos assumption which implies that prior to collision the particles are completely uncorrelated and as-

[1]Throughout this manuscript we will abbreviate partial differentials in this fashion, that is $\partial_t = \frac{\partial}{\partial t}$, $\partial_\alpha = \frac{\partial}{\partial x_\alpha}$, and $\partial_{v_\alpha} = \frac{\partial}{\partial v_\alpha}$ Furthermore it is implied that Greek subscripts α, β, γ, δ resemble the $1, ..., D$ components of Cartesian vectors and we imply the use of the Einstein convention, that is, that we sum over like indices implicitly.

sumes that f_2 factorizes into two one-particle distribution functions and that higher order correlations vanish such that

$$f_2(\mathbf{x}, \mathbf{v}_1, \mathbf{v}_2, t)\ \mathrm{d}\ \mathbf{x} = f_1(\mathbf{x}, \mathbf{v}_1, t) f_1(\mathbf{x}, \mathbf{v}_2, t)\ \mathrm{d}\ \mathbf{x}. \tag{2}$$

As we are only concerned with one-particle distribution functions in the remainder of this manuscript we change notation and use the subscript of f to indicate the velocity of the system state such that $f(\mathbf{x}, \mathbf{v}_1, t) = f_1(\mathbf{x}, t)$. The rate of change of the evolution equation for the dilute gas with instantaneous and short range interaction, i.e. binary collisions can then be described by

$$\left\{\partial_t + v_\alpha \partial_\alpha + \frac{F_\alpha}{m}\partial_{v_\alpha}\right\} f_1(\mathbf{x}, t) = \int \left(f_{1'} f_{2'} - f_1 f_2\right) P_{12\to 1'2'}\ \mathrm{d}\ \mathbf{v}_2\ \mathrm{d}\ \mathbf{v}_{1'}\ \mathrm{d}\ \mathbf{v}_{2'}, \tag{3}$$

where $P_{12\to 1'2'}$ is the probability of two particles with initial velocities $\mathbf{v}_1$ and $\mathbf{v}_2$ to collide such that their final velocities are $\mathbf{v}_{1'}$ and $\mathbf{v}_{2'}$. This is the well-known Boltzmann transport equation [8, 18, 1]. The collision integral describes the rate of change of the current local distribution $f_1(\mathbf{x}, t)$ of particles moving with $\mathbf{v}_1$ due to the local interaction with other particles. Then while in Eq. (3) $\int f_1 f_2 P_{12\to 1'2'}\ \mathrm{d}\ \mathbf{v}_2\ \mathrm{d}\ \mathbf{v}_{1'}\ \mathrm{d}\ \mathbf{v}_{2'}$ represents the loss in f_1 due to a collision, $\int f_{1'} f_{2'} P_{1'2'\to 12}\ \mathrm{d}\ \mathbf{v}_2\ \mathrm{d}\ \mathbf{v}_{1'}\ \mathrm{d}\ \mathbf{v}_{2'}$ gives the gain in f_1 due to collisions that yield a particle moving with $\mathbf{v}_1$. This necessitates that collisions are reversible, i.e. that for every collision $\{\mathbf{v}_1, \mathbf{v}_2\} \to \{\mathbf{v}_{1'}, \mathbf{v}_{2'}\}$ there exists an inverse collision $\{\mathbf{v}_{1'}, \mathbf{v}_{2'}\} \to \{\mathbf{v}_1, \mathbf{v}_2\}$ with equal collision probability $P_{12\to 1'2'} = P_{1'2'\to 12}$ [18]. As the collision is considered instantaneous and local, $\mathbf{x}$ and t remain unchanged.

1.1.2. The Equilibrium Distribution

Now consider a system of identical structureless particles. Eventually it will evolve to an equilibrium state. This state is defined to be such that collisions no

longer change the distribution function, i.e. $\frac{\partial f}{\partial t} = 0$. We thus define the equilibrium distribution as the solution of the Boltzmann equation Eq. (3) that is independent of time, i.e. $\frac{\mathrm{d}\, f^0(\mathbf{x},\mathbf{v},t)}{\mathrm{d}\, t} = 0$. This is equivalent to having a system for which the collision integral in Eq. (3) vanishes, i.e.

$$\int \left(f^0_{1'} f^0_{2'} - f^0_1 f^0_2\right) P_{12\to 1'2'}\ \mathrm{d}\ \mathbf{v}_2\ \mathrm{d}\ \mathbf{v}_{1'}\ \mathrm{d}\ \mathbf{v}_{2'} = 0. \tag{4}$$

To find $f^0(\mathbf{x},\mathbf{v},t)$ it is thus sufficient to have

$$f^0_{1'}(\mathbf{x},t) f^0_{2'}(\mathbf{x},t) = f^0_1(\mathbf{x},t) f^0_2(\mathbf{x},t). \tag{5}$$

Huang [18] then shows the necessity of Eq. (5) by proving that if $f(\mathbf{x},\mathbf{v},t)$ satisfies Eq. (3) then one can write for Boltzmann's H-functional,

$$H(t) = \int\ \mathrm{d}\ \mathbf{x}' f(\mathbf{x},\mathbf{v},t) \ln f(\mathbf{x},\mathbf{v},t), \tag{6}$$

that $\mathrm{d}\ H(t)/\ \mathrm{d}\ t \leq 0$. As part of that proof he finds that requiring $\frac{\mathrm{d}\, H}{\mathrm{d}\, t} = 0$ is equivalent to Eq. (5). We can thus use Eq. (5) to solve for the equilibrium distribution. We begin by taking the logarithm

$$\ln f^0_{1'}(\mathbf{x},t) + \ln f^0_{2'}(\mathbf{x},t) = \ln f^0_1(\mathbf{x},t) + \ln f^0_2(\mathbf{x},t). \tag{7}$$

Since $\{\mathbf{v}_1, \mathbf{v}_2\}$ and $\{\mathbf{v}_{1'}, \mathbf{v}_{2'}\}$ describe the initial and final velocities of all possible collisions Eq. (7) can be interpreted as a conservation law. Now if an arbitrary quantity $\eta(\mathbf{x},\mathbf{v})$ is a conserved quantity such that $\eta(\mathbf{x},\mathbf{v}_1) + \eta(\mathbf{x},\mathbf{v}_2) = \text{const}$ for the

collision of two molecules with velocities $\mathbf{v}_1$ and $\mathbf{v}_2$ then $\eta(\mathbf{x}, \mathbf{v}) = \ln f^0(\mathbf{x}, \mathbf{v})$ is a solution of Eq. (7). The general solution is then

$$\ln f^0(\mathbf{x}, \mathbf{v}) = \eta_1(\mathbf{x}, \mathbf{v}) + \eta_2(\mathbf{x}, \mathbf{v}) + ... \tag{8}$$

Where the η_1, η_2, ... represent all conserved quantities. In the case of an ideal gas we have $2 + D$. The conserved quantities are energy ϵ, the D components of the momentum vector v_α and the mass density ρ and relate to the velocity moments $\frac{1}{2}mv^2$, mv_α and m respectively. Then

$$\epsilon = \int m\frac{1}{2}\mathbf{v}^2 f(\mathbf{v}) \text{ d } \mathbf{v} \tag{9}$$

is the mean energy density, where we have assumed potential energy to be negligible,

$$j_\alpha = \int m v_\alpha f(\mathbf{v}) \text{ d } \mathbf{v} \tag{10}$$

the mean momentum and

$$\rho = \int m f(\mathbf{v}) \text{ d } \mathbf{v} \tag{11}$$

the mean density. In Eq. (8) we claim that $\ln f^0$ is a linear combination of all conserved quantities because Eq. (7) is invariant under a collision. This means that we have

$$\rho_1 + \rho_2 = \rho_{1'} + \rho_{2'} \tag{12}$$

$$j_{\alpha,1} + j_{\alpha,2} = j_{\alpha,1'} + j_{\alpha,2'} \tag{13}$$

$$\epsilon_1 + \epsilon_2 = \epsilon_{1'} + \epsilon_{2'}. \tag{14}$$

Then

$$\ln f^0(\mathbf{x}, \mathbf{v}) = \ln A - \frac{C}{2}(\mathbf{v} - \mathbf{B})^2 \tag{15}$$

and thus

$$f^0(\mathbf{x}, \mathbf{v}) = Ae^{-\frac{C}{2}(\mathbf{v}-\mathbf{B})^2} \tag{16}$$

where A, B_α and C are $D+2$ constants which we determine by taking the velocity moments corresponding to the conserved quantities ϵ, $\mathbf{u}$ and n. We solve for these constants by taking the moments corresponding to the conserved quantities. For the number density we find

$$n = \int \mathrm{d}\ \mathbf{v} f^0 = A \int \mathrm{d}\ \mathbf{v} e^{-\frac{C}{2}(\mathbf{v}-\mathbf{B})^2} = A\left(\frac{\pi}{C}\right)^{D/2}. \tag{17}$$

Thus $C > 0$ and $A = \left(\frac{C}{\pi}\right)^{D/2} n$. Similarly the mean velocity is found as

$$u_\alpha = \frac{1}{n}\int \mathrm{d}\ \mathbf{v} f^0 v_\alpha = \frac{A}{n}\int \mathrm{d}\ \mathbf{v} v_\alpha e^{-\frac{C}{2}(\mathbf{v}-\mathbf{B})^2} = B_\alpha. \tag{18}$$

For the energy conservation we integrate over $(\mathbf{v}-\mathbf{u})^2$ which yields the energy contained in the system due to all motion except for that of the center of mass, or equivalently by the equipartition theorem, the temperature,

$$\frac{D}{2}k_B T = \frac{1}{2n}\int \mathrm{d}\ \mathbf{v} f^0 (\mathbf{v}-\mathbf{u})^2 = \frac{A}{2n}\int \mathrm{d}\ \mathbf{v}'\mathbf{v}'^2 e^{-\frac{C}{2}\mathbf{v}'^2} = \frac{S_D A}{Dn}\int_0^\infty \mathrm{d}\ v' v'^{2+(D-1)} e^{-\frac{C}{2}v'^2} = \frac{D}{4C}. \tag{19}$$

Note here that this is correct only if $\mathbf{u}$ is the mean velocity of the particles in the entire system concerned. Later in the discussion of fluctuating lattice Boltzmann we will encounter a local definition of temperature which depends on the velocity at the lattice site, and, because temperature is defined microscopically as the unbiased estimator of the variance of the velocity, depends on the particle number considered

$$k_B T = \frac{1}{D}\frac{1}{n-1}\sum_{i=1}^{n}\left(\mathbf{v}_i - \langle \mathbf{v} \rangle\right)^2. \tag{20}$$

In Eq. (19) we have used the translation $v'_\alpha = v_\alpha - u_\alpha$ and spherical coordinates to simplify the integration and S_D a pre-factor from the spherical integration ($S_1 = 2$, $S_2 = 2\pi$, $S_3 = 4\pi$...). Thus

$$C = \frac{1}{2k_BT} \text{ and } A = n\left(\frac{1}{2\pi k_BT}\right)^{\frac{3}{2}}. \tag{21}$$

We have carried out this integration in 3 dimensions but it is valid for any D and thus we find the equilibrium distribution

$$f^0(n, \mathbf{v}, \mathbf{u}, T) = \frac{n}{(2\pi k_BT)^{\frac{D}{2}}}\, e^{-\frac{(\mathbf{v}-\mathbf{u})^2}{2\pi k_BT}}. \tag{22}$$

Here it is assumed that n, $\mathbf{u}$ and k_bT are global mean values. We will later in this thesis discuss these considerations quantities local to a discretization cell required by the fluctuating lattice Boltzmann implementation depending on local quantities.

1.1.3. The Bhatnagar-Gross-Krook Approximation

As it is often used in applications of the lattice Boltzmann method and in particular in all problems discussed later in this thesis it is expedient to introduce the Bhatnagar, Gross, and Krook [19] approximation to the collision operator. Bhatnagar, Gross, and Krook were investigating wave propagation in ionized gases, a much more complicated problem than the simple mono-atomic gas discussed here, and argued that Boltzmann's collision in Eq. (3)integral could often times be approximated by a simple relaxation of the current local distribution function to the equilibrium distribution scaled by at time constant τ such that

$$C\left(f(\mathbf{x}, \mathbf{v}, t)\right) = \frac{f^0[n(\mathbf{x}, t), \mathbf{u}(\mathbf{x}, t), T(\mathbf{x}, t)] - f\left(\mathbf{x}, \mathbf{v}, t\right)}{\tau}. \tag{23}$$

Here τ relates to the mean time between collisions. This simplified collision operator just uses the fact that collisions tend to relax the current distribution function $f(\mathbf{x}, \mathbf{v}, t)$ towards the equilibrium distribution $f^0(n, \mathbf{u}, T)$. Interestingly this simplified collision operator was only mentioned by Bhatnagar, Gross and Krook's as a generally known and used approximation. With the BGK collision term the Boltzmann Eq. (3) equation simplifies to

$$\left(\partial_t + v_\alpha \partial_\alpha + \frac{F_\alpha}{m}\partial_{v_\alpha}\right) f(\mathbf{x}, \mathbf{v}, t) = \frac{1}{\tau}\left\{f^0\left[n(\mathbf{x}, t), \mathbf{u}(\mathbf{x}, t), T(\mathbf{x}, t)\right] - f(\mathbf{x}, \mathbf{v}, t)\right\}. \quad (24)$$

We need to mention here that, in principle, the relaxation time τ does not need to be constant for all degrees of freedom. For example, in Fox and Uhlenbeck's treatment of the fluctuating linearized Boltzmann equation [15] the collision operator is decomposed into eigenvalues that are constructed as linear combinations of the distribution function. The collision operator then can be expressed in terms of eigenvalues. As discussed in the discrete case for the multi-relaxation time representation of the lattice Boltzmann method in section 1 we can associate these eigenvalues with relaxation times. Thus the relaxation times are associated with their corresponding hydrodynamic moments. This can be used to independently access hydrodynamic parameters such as bulk and shear viscosities.

1.1.4. Hydrodynamic Equations

The hydrodynamic equations describe the macroscopic behavior of a gas or a fluid. In terms of the Boltzmann equation it is important to recognize that the non-conserved moments relax quickly due to the collision whereas the moments corresponding to conserved quantities relax much slower as they are not altered in the collision but are only altered due to the streaming. Therefore the behavior of macroscopic quantities is governed by the long term behavior of these conserved quantities,

i.e. density, momentum and energy. The equations describing this long term behavior are the hydrodynamic equations. In the context of this thesis we will only consider second order hydrodynamics, i.e. the Navier-Stokes equations, and will omit terms of higher order than two in $\mathbf{u}$ of the distribution function. Requiring the density, momentum and energy to be conserved locally then implies that they are not changed in the collision, i.e.

$$\int \mathrm{d}\,\mathbf{v}\frac{1}{\tau}\left(f^0 - f\right) = 0 \tag{25}$$

$$\int \mathrm{d}\,\mathbf{v}v_\alpha\frac{1}{\tau}\left(f^0 - f\right) = 0 \tag{26}$$

$$\int \mathrm{d}\,\mathbf{v}v^2\frac{1}{\tau}\left(f^0 - f\right) = 0 \tag{27}$$

Consequently the moments of the current local distribution function have to equal those of the equilibrium distribution

$$\rho = \int \mathrm{d}\,\mathbf{v}f = \int \mathrm{d}\,\mathbf{v}f^0 \tag{28}$$

$$j_\alpha = \int \mathrm{d}\,\mathbf{v}v_\alpha f = \int \mathrm{d}\,\mathbf{v}v_\alpha f^0 \tag{29}$$

$$\epsilon = \int \mathrm{d}\,\mathbf{v}v^2 f = \int \mathrm{d}\,\mathbf{v}v^2 f^0. \tag{30}$$

Two different approaches are commonly used in the literature. The first one is based on the asymptotic expansion of the distribution function f around the equilibrium distribution f^0. Then taking the velocity moments of the Boltzmann equation Eq. (23) corresponding to the conserved quantities (i.e. 1 for conservation of mass, v_α for momentum, and v^2 for energy) yields the hydrodynamic equations. Because density, momentum and energy are conserved quantities, the corresponding moments of the distribution function and the equilibrium distribution vanish and consequently

the corresponding moment integrals over the BGK collision expression $\frac{1}{\tau}(f^0 - f)$ in Eq. (24) vanish as well.

This is actually independent of the form of the collision operator but particularly easy to see in this case. Taking velocity moments of the Boltzmann equation corresponding to the respective conserved quantities as suggested by Grad [20, 21] leads directly to the conservation equations. For mass conservation we thus take the zeroth order velocity moment of Eq. (24)

$$\partial_t \int \mathrm{d}\ \mathbf{v} f + \partial_\alpha \int \mathrm{d}\ \mathbf{v} v_\alpha f + \frac{\mathbf{F}}{m} \int \mathrm{d}\ \mathbf{v} \partial_v f = \frac{1}{\tau} \int \mathrm{d}\ \mathbf{v} \left(f^0 - f\right), \tag{31}$$

and obtain the continuity equation

$$\partial_t n + \partial_\alpha (n u_\alpha) = 0. \tag{32}$$

Similarly, for momentum conservation we integrate Eq. (24) over v_α

$$\partial_t \int \mathrm{d}\ \mathbf{v} v_\alpha f + \partial_\beta \int \mathrm{d}\ \mathbf{v} v_\alpha v_\beta f v_\alpha + \frac{F_\beta}{m} \int \mathrm{d}\ \mathbf{v} \partial_{v_\beta} v_\alpha f = \frac{1}{\tau} \int \mathrm{d}\ \mathbf{v} v_\alpha \left(f^0 - f\right), \tag{33}$$

which leads, to second order, to the Navier-Stokes equation

$$\partial_t \left(n u_\alpha\right) + \partial_\beta \left(\rho u_\alpha u_\beta\right) = -\partial_\alpha (n k_b T) + \partial_\beta [\eta(\partial_\beta u_\alpha + \partial_\alpha u_\beta - \frac{2}{3} \partial_\gamma u_\gamma \delta_{\alpha\beta})]. \tag{34}$$

Here we have used the BGK approximation to express the distribution function in terms of the equilibrium distribution

$$f_i = f_i^0 - \tau \left(\partial_t v_\alpha \partial_\alpha + \frac{F_\alpha}{m} \partial_{v_\alpha} \right). \tag{35}$$

Finally, in the same spirit, energy conservation is obtained by integrating the Boltzmann equation over $(\mathbf{v}-\mathbf{u})^2$

$$\partial_t \int \mathrm{d}\,\mathbf{v} v^2 f + \partial_\alpha \int \mathrm{d}\,\mathbf{v} v_\alpha v^2 f + \frac{\mathbf{F}}{m} \int \mathrm{d}\,\mathbf{v} \partial_v v^2 f = \frac{1}{\tau} \int \mathrm{d}\,\mathbf{v} v^2 \left(f^0 - f\right), \quad (36)$$

where the mean velocity $\mathbf{u}$ is subtracted to remain consistent with the definition of temperature. Then, after some algebra and again with Eq. (35), the heat equation is obtained

$$\partial_t k_b T + u_\alpha \partial_\alpha k_b T = -\frac{2}{3}\partial_\alpha u_\alpha k_b T + \frac{1}{n}\partial_\alpha \left(\frac{5 n k_b T}{3}\partial_\alpha k_b T\right) + \tau \partial_\alpha u_\beta \left(\partial_\alpha u_\beta + \partial_\beta u_\alpha - \frac{2}{3}\partial_\gamma u_\gamma \delta_{\alpha\beta}\right). \quad (37)$$

In addition to this method due to the asymptotic expansion of the distribution function around the equilibrium distribution one may employ a Chapman-Enskog expansion [22] and formally expand the distribution function into two time scales, sound-wave propagation and hydrodynamic interaction, and then calculate the moments treating the different time scales as if they do not interact.

Both approaches produce identical equations up second order although for the Chapman-Enskog multi-scale expansion sometimes different values for time and spacial scaling are assumed leading to formal differences in the results [23].

1.2. Fluctuations in the Linearized Boltzmann Equation

1.2.1. The Langevin Equation

Fluctuations in kinetic theory are most commonly described by a Langevin-type treatment of the linearized Boltzmann equation [16, 24, 15, 17, 25]. Langevin's assumption [14, 26] was that a particle in a fluid is free to move but experiences

friction and a random force $\mathbf{F}(t)$ due to the interaction with other particles. The equations of motion are then

$$m\frac{d\mathbf{u}(t)}{dt} = -\gamma m\mathbf{u}(t) + \mathbf{F}(t) \tag{38}$$

$$\frac{d\mathbf{x}(t)}{dt} = \mathbf{u}(t) \tag{39}$$

where $\mathbf{u}$ is the particle's velocity, m it's mass, γ the constant of friction due to the mean interaction with other particles and $\mathbf{F}$ the random force acting on the particle due to higher order terms in the particle-particle interactions. We can then introduce the net instantaneous force due to collisions $\mathfrak{F}(t)$ and find for its average over an ensemble of particles at fixed low velocity $\bar{\mathbf{u}}$ [17]

$$\langle\mathfrak{F}(t)\rangle_{\mathbf{u}} = -m\gamma\bar{\mathbf{u}} + O(\mathbf{u}^2). \tag{40}$$

Now $\mathbf{F}(t) = \mathfrak{F}(t) + m\gamma\mathbf{u}(t)$ can be interpreted as remainder of the net force due to a collision after the mean has been subtracted. To avoid drift $\langle\mathbf{F}\rangle = 0$ Langevin then suggested interpreting $\mathbf{F}$ as a Gaussian distributed random variable such that

$$\langle\mathbf{F}(t)\mathbf{F}'(t)\rangle = c\delta(t' - t) \tag{41}$$

where c is a constant independent of $\mathbf{u}$ and t. Here c is the variance of the distribution of the $\mathbf{F}$ and Eq. (41) becomes the predecessor to the fluctuation-dissipation theorem (FDT) as it defines the distribution function provided $\langle\mathbf{F}\rangle = 0$.

1.2.2. The Linearized Boltzmann Equation

As discussed in section 1.1 in equilibrium the one particle distribution takes the form of the Maxwell-Boltzmann distribution Eq. (42). In equilibrium the expectation value of the equilibrium distribution is what we call the global equilibrium distribution

$$\bar{f}^0 = f^0(\bar{n}, \bar{\mathbf{u}}, k_B T) = \frac{\bar{n}}{(2\pi k_B T)^{\frac{D}{2}}}\, e^{-\frac{(\mathbf{v}-\bar{\mathbf{u}})^2}{2\pi k_B T}}, \tag{42}$$

where $\bar{n}$, $\bar{\mathbf{u}}$ and T are the equilibrium values of the particle number density, the velocity and the temperature, respectively. Near equilibrium it is then reasonable to express the current local distribution function as a linear expansion around f^0

$$f(\mathbf{x}, \mathbf{v}, t) = \bar{f}^0(\bar{n}, \bar{\mathbf{u}}, k_B T)(1 + h\,(\mathbf{x}, \mathbf{v}, t))\,. \tag{43}$$

Assuming that there is no external force present the distribution function in equilibrium does not change as a function of temporal or spatial coordinates and $\bar{f}^0 = \bar{f}^0_1 = \bar{f}^0_2 = \bar{f}^0_{1'} = \bar{f}^0_{2'}$. Then with Eq. (43) the probability exchange term in the collision operator can be written as

$$\begin{aligned}(f_{1'} f_{2'} - f_1 f_2) &= \bar{f}^0 \left(\bar{f}^0 + h_{1'} + h_{2'} + \frac{h_{1'} h_{2'}}{\bar{f}^0} - \bar{f}^0 - h_1 - h_2 - \frac{h_1 h_2}{\bar{f}^0} \right) \\ &\approx \bar{f}^0\,(h_{1'} + h_{2'} - h_1 - h_2)\,. \end{aligned} \tag{44}$$

The terms quadratic in h are neglected and hence this treatment of the collision is called *linearized* Boltzmann equation. It can be written in terms of $h\,(\mathbf{x}, \mathbf{v}, t))$ such that

$$\{\partial_t + v_\alpha \partial_\alpha\}\, h(\mathbf{x}, \mathbf{v}_1, t) = \int \bar{f}^0_1\,(h_{1'} + h_{2'} - h_1 - h_2)\, P_{12\to 1'2'}\ \mathrm{d}\ \mathbf{v}_2\ \mathrm{d}\ \mathbf{v}_{1'}\ \mathrm{d}\ \mathbf{v}_{2'}. \tag{45}$$

This equation is used in the subsequent treatment of fluctuations and is the foundation of all theoretical discussion of fluctuations in the lattice Boltzmann method.

1.2.3. The Fluctuation Dissipation Theorem of the Linearized Boltzmann Equation

We now follow [15, 25] in a brief outline of deriving a fluctuation dissipation theorem (FDT) for the linearized Boltzmann equation. According to Fox and Uhlenbeck the collision integral in Eq. (45) can be rewritten such that

$$\{\partial_t + v_\alpha \partial_\alpha\}\, h(\mathbf{x}, \mathbf{v}_1, t) = \int f_1^0 K(\mathbf{v}_1, \mathbf{v}_2) h(\mathbf{x}, \mathbf{v}_2, t)\ \mathrm{d}\ \mathbf{v}_2 + C(\mathbf{x}, \mathbf{v}, t), \tag{46}$$

where $K(\mathbf{v}_1, \mathbf{v}_2)$ is the collision kernel that is symmetric, isotropic and has non-negative eigenvalues. One can define [2]

$$a(\mathbf{x}_1, \mathbf{v}_1, t) = \sqrt{f^0(v_1)} h(\mathbf{x}_1, \mathbf{v}_1, t) \tag{47}$$

$$A(\mathbf{x}_1, \mathbf{v}_1; \mathbf{x}_2, \mathbf{v}_2) = v_\alpha \partial_\alpha \delta(\mathbf{x}_1 - \mathbf{x}_2)\delta(\mathbf{v}_1 - \mathbf{v}_2), \tag{48}$$

$$S(\mathbf{x}_1, \mathbf{v}_1; \mathbf{x}_2, \mathbf{v}_2) = \sqrt{f^0(v_1)}\sqrt{f^0(v_2)} K(\mathbf{v}_1, \mathbf{v}_2)\delta(\mathbf{x}_1 - \mathbf{x}_2), \tag{49}$$

and write Eq. (45) as

$$\partial_t a(\mathbf{x}_1, \mathbf{v}_1, t) + \int A(\mathbf{x}_1, \mathbf{v}_1; \mathbf{x}_2, \mathbf{v}_2) a(\mathbf{x}_2, \mathbf{v}_2, t)\ \mathrm{d}\ \mathbf{x}_2\ \mathrm{d}\ \mathbf{v}_2 = \tag{50}$$

$$- \int S(\mathbf{x}_1, \mathbf{v}_1; \mathbf{x}_2, \mathbf{v}_2) a(\mathbf{x}_2, \mathbf{v}_2, t)\ \mathrm{d}\ \mathbf{x}_2\ \mathrm{d}\ \mathbf{v}_2. \tag{51}$$

According to Fox and Uhlenbeck this is the standard regression equation of a Gaussian Markov process that takes the form

$$\frac{d}{dt} a_i + A_{ij} a_j = -S_{ij} a_j, \tag{52}$$

[2] In the original publications an erroneous $\sqrt{f^0(v_1)}$ factor appears in the definition of A which we omit here.

where the advection operator is antisymmetric $A_{ij} = -A_{ji}$ and the collision operator symmetric $S_{ij} = S_{ji}$. Adding a random variable $\sqrt{f^0 v_1 \xi(\mathbf{x}, \mathbf{v}_1, t)}$ to the right hand side of Eq. (50) introduces the noise and, after canceling $\sqrt{f^0}$, Eq. (50) becomes

$$\{\partial_t + v_\alpha \partial_\alpha\} h(\mathbf{x}, \mathbf{v}_1, t) = \int f_1^0 \left(h_{1'} + h_{2'} - h_1 - h_2\right) P_{12 \to 1'2'} \, \mathrm{d}\, \mathbf{v}_2 \, \mathrm{d}\, \mathbf{v}_{1'} \, \mathrm{d}\, \mathbf{v}_{2'} + \xi(\mathbf{x}, \mathbf{v}_1). \tag{53}$$

If the random variable ξ is chosen as a Gaussian with zero mean Fox and Uhlenbeck find the fluctuation dissipation theorem for the linearized Boltzmann equation to be

$$\langle \xi(\mathbf{x}_1, \mathbf{v}_1, t) \xi(\mathbf{x}_2, \mathbf{v}_2, t \rangle = 2K(\mathbf{v}_1, \mathbf{v}_2) \delta(\mathbf{x}_1 - \mathbf{x}_2) \delta(t_1 - t_2). \tag{54}$$

The noise amplitude can now be computed in terms of the eigenvalues of the collision operator K. The kernel K is decomposed into eigenvectors ψ_i with corresponding eigenvalues λ_i such that the eigenfunctions fulfill

$$\int \frac{f^0(\mathbf{v})}{n} \psi_i(\mathbf{v}) \psi_j(\mathbf{v}) \, \mathrm{d}\, \mathbf{v} = \delta_{ij}, \tag{55}$$

where n is the particle number density and it is assumed that K has a discrete spectrum. The kernel then can be written as

$$K(\mathbf{v}_1, \mathbf{v}_2) = \sum_{i=1}^{\infty} \lambda_i \psi_i(\mathbf{v}_1) \psi_i(\mathbf{v}_2) \tag{56}$$

and, correspondingly, the noise term ξ can be decomposed to

$$\xi(\mathbf{x}, \mathbf{v}, t) = \sum_{i=1}^{\infty} \tilde{\xi}_i(\mathbf{x}, t) \psi_i(\mathbf{v}). \tag{57}$$

The FDT can now be expressed in terms of eigenfunction decomposition

$$\langle \tilde{\xi}_i(\mathbf{x_1}, t)\tilde{\xi}_j(\mathbf{x}_2, t)\rangle = 2\lambda_i\delta_{ij}\delta(\mathbf{x}_1 - \mathbf{x}_2)\delta(t_1 - t_2) \tag{58}$$

where it is understood that the noise term of the eigenfunctions corresponding to conserved quantities vanishes $\tilde{\xi}_{i,cons} = 0$. It should be noted that this eigenvector treatment of the Boltzmann equation is the continuous equivalent to the derivation for the discrete multi-relaxation time formalism of the lattice Boltzmann equation given in section II of paper 4 and discussed in section 1. The decomposition of the the Kernel K into eigenmodes is the direct equivalent of the moment space representation in multi-relaxation time lattice Boltzmann discussed in section 1.3.2.

1.3. The Lattice Boltzmann Method

The lattice Boltzmann method is a computational method based on a direct discussion of the previous sections. It is most commonly used for simulating gas and fluid flows, and, unlike many other algorithms for the same goal the LBM is not based on the direct discretization of the Navier-Stokes equation. Instead a discretized version of the Boltzmann transport equation Eq. (3), which we have already discussed in this introduction, is used. The state of the system is described by means of the one particle distribution function $f(\mathbf{x}, \mathbf{v}, t)$ and in lattice Boltzmann all three of these parameters are discretized: The time t moves in a discrete time step Δt which is usually chosen as $\Delta t = 1$. The position $\mathbf{x}$ is discretized on a lattice and the velocities $\mathbf{v}$ are represented by a set of base velocities v_i that to connect different lattice points and are indexed by i. The number of these base velocities fixes the total degrees of freedom and is determined by the order of velocity moments needed in order to reproduce the differential equations for which a model is set up. In principle lattice Boltzmann method is not limited to simulating just hydrodynamics and other partial

differential equations can be mapped. A particular realization of the lattice Boltzmann method is described as a DDQQ implementation where D gives the dimension of the implementation and Q the number of base velocity vectors. The particle densities are usually denoted as $f_i(\mathbf{x}, t)$ where i is the index of the previously defined base velocity set. The most general form of the lattice Boltzmann equation (LBE) is given by

$$f_i(\mathbf{x} + \mathbf{v}_i, t + 1) - f_i(\mathbf{x}, t) = \Omega_i(f_1, \cdots, f_N). \tag{59}$$

Here Ω is the collision operator. With respect to the work contained in this thesis it is sufficient to use the BGK expression. Then, in the case of a single relaxation time model $\Omega_i = (1/\tau)(f_i^0 - f_i)$. This was first suggested by Qian and d'Humieres [27, 28]. In the case of hydrodynamics the equilibrium distribution takes the form of an expansion of Eq. (42). Various different forms are in use [28, 29] but the one that has seen the most use is the second order expansion of the form

$$f_i^0(\mathbf{x}, t) = nw_i \left[1 + \frac{1}{\theta}\mathbf{u}.\mathbf{v}_i + \frac{1}{2\theta^2}\left(\mathbf{u}.\mathbf{v}_i\right)^2 - \frac{1}{2\theta}\mathbf{u}.\mathbf{u}\right], \tag{60}$$

In practice the algorithm is separated into a streaming and a collision step. The collision step consists of calculating the local conserved quantities and the equilibrium distribution values to which the current local distribution values are relaxed. The streaming then involves moving the densities f_i according to their corresponding base velocity vector $\mathbf{v}_i$ on the lattice. We have derived a general proof of the validity of hydrodynamic equations for the BGK lattice Boltzmann method in paper 3 in this thesis.

1.3.1. Isothermal Lattice Boltzmann

In most lattice Boltzmann methods energy conservation is omitted [1, chapter 14] and continuity and Navier-Stokes equations are considered sufficient. The kinetic temperature is

$$\rho k_b T = \frac{1}{D} \int \mathrm{d}\ \mathbf{v} f^0 \left(\mathbf{v} - \mathbf{u}\right)^2, \tag{61}$$

or, in the discrete lattice Boltzmann case,

$$\rho k_B T = \frac{1}{D} \sum_i^Q f_i^0 \left(\mathbf{v}_i - \mathbf{u}\right)^2. \tag{62}$$

To be precise one should also include here the factor of $n/(n-1)$ that ensures that the unbiased estimator is used as in Eq. (20), however, this is often omitted. The temperature enters the second and higher order moments of the distribution function and in the lattice Boltzmann method is often fixed due to the constraints of the base velocity set through the third order velocity moment

$$\sum_i v_{i\alpha} v_{i\beta} v_{i\gamma} f_i^0 = \rho\theta \left(u_\alpha \delta_{\beta\gamma} + u_\beta \delta_{\gamma\alpha} + u_\gamma \delta_{\alpha\beta}\right) + \rho u_\alpha u_\beta u_\gamma + Q_{\alpha\beta\gamma}. \tag{63}$$

Here the u^3 term is often not properly reproduced in lattice Boltzmann implementations and has to be corrected for by introducing Q which is assumed to be small but may lead to Galilean invariance issues [30]. The commonly used expression for the equilibrium distribution Eq. (60) is an example for this. In the D2Q9 base velocity set which we discuss extensively in papers 2 and 4, the components of the velocity vector $v_{i,x}$ and $v_{i,y}$ only take values of $\{-1, 0, 1\}$ such that $v_{i\alpha}^3 = v_{i\alpha}$. Then consistency of the third Eq. (63) and first moments $\sum_i f_i^0 v_{i\alpha} = \rho u_\alpha$ fixes the lattice Boltzmann temperature to $\theta = \frac{1}{3}$.

1.3.2. The Multi-Relaxation Time Representation

The multi-relaxation time (MRT) method refers to a deviation from the plain BGK approximation. The collision is performed on linear combination of the distribution functions f_i such that a relaxation time τ can be chosen for each relevant hydrodynamic degree of freedom. In the example of isothermal lattice Boltzmann method the only hydrodynamic degrees of freedom that remain are bulk and shear viscosities. However, when it is desirable to obtain independent access of these parameters, a MRT implementation has to be chosen. The general approach then consists of applying a matrix transform with elements m_i^a to the vector of f_i such the new moment becomes

$$M^a = \sum_i m_i^a f_i. \tag{64}$$

The corresponding back transform is then

$$f_i = \sum^a n_i^a M^a \tag{65}$$

and the fulfill the orthogonality condition

$$\sum_i m_i^a n_i^b = \delta^{ab}. \tag{66}$$

The matrix elements are not necessarily identical. Throughout this manuscript superscript indices refer to the moment space representation and subscript refers to velocity space. Unlike the components of spatial coordinates for which we imply Einstein summation, summation of either of these indices is always done explicitly. The main idea is then that we can write a collision matrix such that it becomes diagonal in the moment representation with a BGK-style relaxation time on each moment such

that $\Lambda^{ab} = \frac{1}{\tau^a}\delta^{ab}$. This requirement defines the moments M^a to be the eigenvectors of the collision matrix Λ. The lattice Boltzmann equation will then appear as

$$f_i(\mathbf{x} + v_i, t+1) - f_i(\mathbf{x}, t) = \sum_a n_i^a \left\{ \sum_b \Lambda^{ab} \left[M^b(\mathbf{x}, t) - M^{b,0}(\mathbf{x}, t) \right] \right\}. \tag{67}$$

The modern form of MRT representations was pioneered by d'Humieres [27] although in the development history of the lattice Boltzmann method a similar approach to a matrix collision operator with kinetic modes as eigenvectors was an actual predecessor to the BGK approximation [1, chapter IV]. There, however, microscopic collision dynamics were still taken into account, a feature that was abandoned with the introduction of the BGK method. Regarding the implementation it is noteworthy that the streaming still has to be performed in velocity space, even if the collision happens in a moment space representation. Consequently the algorithm consists of a forward matrix transform, the collision, a backward matrix transform followed by the streaming step, often times realized as a movement of the entries in the f_i in memory according to their base velocity vector. With regards to this manuscript the MRT representation is particularly useful because it allows for independent access of the hydrodynamically relevant degrees of freedom and allows for adding noise directly to all non-conserved moments while avoiding adding a noise term to the conserved degrees of freedom. An in-depth discussion on the moment representation and what degrees of freedom one still retains in the transforms while reproducing hydrodynamics is given in paper 3. In paper 4 we discuss how a fluctuating lattice Boltzmann method can be implemented by means of the MRT method.

2. CROSS CORRELATORS AND GALILEAN INVARIANCE IN FLUCTUATING IDEAL GAS LATTICE BOLTZMANN SIMULATIONS[1]

2.1. Abstract

We analyze the Lattice Boltzmann method for the simulation of fluctuating hydrodynamics by Adhikari *et al.* [Europhys. Lett. **71**, 473 (2005)] and find that it shows excellent agreement with theory even for small wavelengths as long as a stationary system is considered. This is in contrast to other finite difference and older lattice Boltzmann implementations that show convergence only in the limit of large wavelengths. In particular cross correlators vanish to less than 0.5%. For larger mean velocities, however, Galilean invariance violations manifest themselves.

2.2. Introduction

Fluctuations are important for many hydrodynamic phenomena, from colloid diffusion to phase-separation close to the critical point. Particle based methods such as Stochastic Rotation Dynamics [31], Lattice Gas [32] or Molecular Dynamics simulations [33] naturally give rise to stochastic noise. In contrast the lattice Boltzmann (LB), or finite difference discretization of the Navier-Stokes equations require fluctuations that have to be included manually. The guiding principle for doing this is the theory of the fluctuating Navier Stokes equations [34]. Despite the success of applying the Navier Stokes equations to very small-scale flows formally the hydrodynamic limit

[1]The idea for this publication originated from a discussion regarding Adhikari *et al*'s derivation of the Fluctuation Dissipation theorem for Lattice Boltzmann [13]. We recognized the $\mathbf{u} << 1$ approximation in the normalization condition and investigated it. Goetz Kaehler recognized this approximation and suggested that it might violate Galilean invariance. Alexander Wagner provided the initial working program containing the original Adhikari implementation. On this basis Goetz Kaehler built a new, more general version from which all results in the publication were obtained. All the graphical output from said software was facilitated by means of a graphical user interface written by Alexander Wagner and Johannes Schlosser. The publication itself was written by Goetz Kaehler with very significant editing support by Alexander Wagner. Alexander Wagner also helped in verifying all the calculations that went into this publication.

requires large wavelengths. For fluctuating hydrodynamics the constraint of large wavelengths becomes important and standard discretization will give results that are not in agreement with statistical physics for shorter wavelengths. For a detailed analysis of simulating fluctuating hydrodynamics using finite difference methods and some remedies to improve this situation see the recent manuscript of A. Donev [35]. Similar deficiencies are found for implementations of fluctuating Navier Stokes equations using the Lattice Boltzmann approach introduced by Ladd [10]. It is, however possible to use a more fundamental approach to include fluctuations in the LB method. Adhikari *et al.*[13] introduced noise on all nonconserved modes, not only the hydrodynamic ones, leading to a scheme which shows good agreement with theory even for large wavelengths. Duenweg *et al.* rederived this noise implementation from detailed balance considerations of lattice gases [36]. Both approaches are numerically identical. In this paper we study the degree of improvement achieved and show that many of the deficiencies that plague finite difference discretizations of fluctuating Navier Stokes equations are absent in this Lattice Boltzmann implementation as long as we consider a system with vanishing mean velocity. For large mean velocities Galilean invariance is violated and errors of a similar magnitude to the earlier implementations are observed.

2.3. Fluctuating Lattice Boltzmann with Ghost Noise

Following the derivation of Adhikari *et al.* [13] we start with the Lattice Boltzmann equation (LBE)

$$f_i(\mathbf{x}+\mathbf{v}_i, t+1) = f_i(\mathbf{x},t) + \sum_j \Lambda_{ij}\left[f_j(\mathbf{x},t) - f_j^0(\mathbf{x},t)\right] + \xi_i(\mathbf{x},t). \qquad (68)$$

Here the the f_i are the particle densities at position x, time t associated with with velocity $\mathbf{v}_i$. Λ_{ij} is the collision matrix and ξ_i are the noise terms. We use the standard local equilibrium distribution given by

$$f_i^0 = \rho w_i \left[1 + \frac{3}{c^2}\mathbf{u}.\mathbf{v}_i + \frac{9}{2c^4}\left(\mathbf{u}.\mathbf{v}_i\right)^2 - \frac{3}{2c^2}\mathbf{u}.\mathbf{u}\right], \tag{69}$$

which is the discretized version of a Maxwell distribution [37, 28]. In equilibrium the f_i will fluctuate around this distribution. The noise terms ξ_i must be chosen such that, in the case of isothermal Lattice Boltzmann (LB), the density $\rho = \sum_i f_i$ and momentum $\rho\mathbf{u} = \sum_i f_i\mathbf{v}_i$ are conserved, i.e. $\sum_i \xi_i = 0$ and $\sum_i \xi_i v_i = 0$. Furthermore a proper fluctuation dissipation theorem (FDT) corresponding to the collision operator Λ_{ij} is obeyed. This implies that the ξ_i are correlated. We can find a representation in which the noise terms are uncorrelated by transforming the LBE into moment space. The moments are given by

$$M^a(\mathbf{x}, t) = \sum_i m_i^a f_i(\mathbf{x}, t). \tag{70}$$

So far this is a standard Multi-Relaxation-Time (MRT) representation [27, 38, 39]. The back transform is given by $f_i(\mathbf{x}, t) = \sum_a n_i^a M^a(\mathbf{x}, t)$. However, in order to construct a proper FDT these transforms cannot be orthogonal as in other MRT methods [27, 38], so here we have $n_i^a \neq m_i^a$. Instead the transforms are chosen such that

$$\sum_i w_i m_i^a m_i^b = \sum_i m_i^a n_i^b = \delta^{ab} \tag{71}$$

with $n_i^a = w_i m_i^a$ while maintaining a diagonal moment space representation of the collision operator $\Lambda_{ij} = -\sum_a \sum_b n_i^a \frac{1}{\tau^a}\delta^{ab} m_j^b$. Now the moment transformation matrices are orthogonal with respect to the Hermite norm. Such transforms with weighted norms were proposed before [40, 41, 42] in different contexts. The necessity of the Hermite norm is briefly outlined after Eq. (74) below and allows for a convenient

definition of the moment space noise terms ξ^a as independent random variables. We can now rewrite the collision term of the Lattice Boltzmann equation in terms of the moments M^a as

$$f_i(\mathbf{x}+\mathbf{v}_i, t+1) = \sum_a n_i^a \left\{ M^a(\mathbf{x},t) - \frac{1}{\tau^a}\left[M^a(\mathbf{x},t) - M^{a,0}(\mathbf{x},t)\right] + \xi^a \right\}. \qquad (72)$$

Adhikari *et al.*[13] then obtain the FDT by performing a Fourier transform of the fluctuations from the mean of the moments $\delta M^a = M^a - \langle M^a \rangle$. They then use the k-independence of these for an ideal gas to obtain

$$\langle \xi^a \xi^c \rangle = \frac{\tau^a + \tau^c - 1}{\tau^a \tau^c} \langle \delta M^a \delta M^c \rangle . \qquad (73)$$

One particular result of the derivation is that the moment fluctuations ξ^a decouple because

$$\begin{aligned} \left\langle \delta M^a \delta M^b \right\rangle &= \sum_i \sum_j m_i^a m_j^b \langle \delta f_i \delta f_j \rangle \\ &= \sum_i \sum_j m_i^a m_j^b \bar{f}_i \delta_{ij} \\ &= \sum_i m_i^a m_i^b \bar{\rho} w_i \\ &= \bar{\rho} \delta^{ab}. \end{aligned} \qquad (74)$$

Here we used $\langle \delta f_i \delta f_j \rangle = \bar{f}_i \delta_{ij}$ with $\delta f_i = f_i - \bar{f}_i$ where $\bar{f}_i$ is the spatially uniform global equilibrium distribution function [43]. Adhikari also assumed that $\mathbf{u} \ll 1$ so that $\bar{f}_i = \bar{\rho} w_i$. This allows us to use the orthogonality relation of Eq. (71) in the last step of the calculation above. For a different transformation we would obtain non-diagonal elements in the fluctuation matrix which will then require correlated noise terms which are more cumbersome to implement. For practical applications it

is important to note that the $\mathbf{u} \ll 1$ condition for the noise introduces a non-Galilean invariant contribution. We comment on this in our validation section. Inserting Eq. (74) into Eq. (146) leads to a noise expression of

$$\xi^a = \frac{1}{\tau^a}\sqrt{\bar{\rho}\,(2\tau^a - 1)}N, \tag{75}$$

where N is a random variable with zero mean and a variance of one.

Note that the moments M^a are chosen to include the hydrodynamic moments. In the isothermal case discussed here they are comprised of the conserved quantities ρ and $\mathbf{j}$, and the stress modes $\mathbf{\Pi}$. The remaining degrees of freedom are often called ghost modes as they do not appear in the isothermal Navier Stokes equations. However, the key result of the Adhikari *et al.* paper [13] was that they need to be taken into account when including noise. Thus we add noise on all non conserved quantities, i.e. stress and ghost modes, in Eq. (72) according to Eq. (147).

In practice we implement this algorithm by calculating the moments by means of Eq. (129), performing the collision on the moments, adding the noise term and then transforming back into f-space as indicated in Eq. (72). The streaming step is then done in f-space. This algorithm is almost as efficient as the standard LB implementation. The additional computational cost for calculating the ghost modes and the random numbers results in a computational overhead of less than 20%.

2.4. Correlators in a D2Q9 Implementation

To evaluate this method we present results for the D2Q9 (two dimensions, 9 base velocity vectors) LB model. The results are similar for other models, in particular we also tested D1Q3 and D3Q15. As D2Q9 base velocity set we use $\{v_i\} = \{(0,0),(1,0),(0,1),\,(-1,0),(0,-1),\,(1,1),(-1,1),\,(-1,-1),(1,-1)\}$ and the

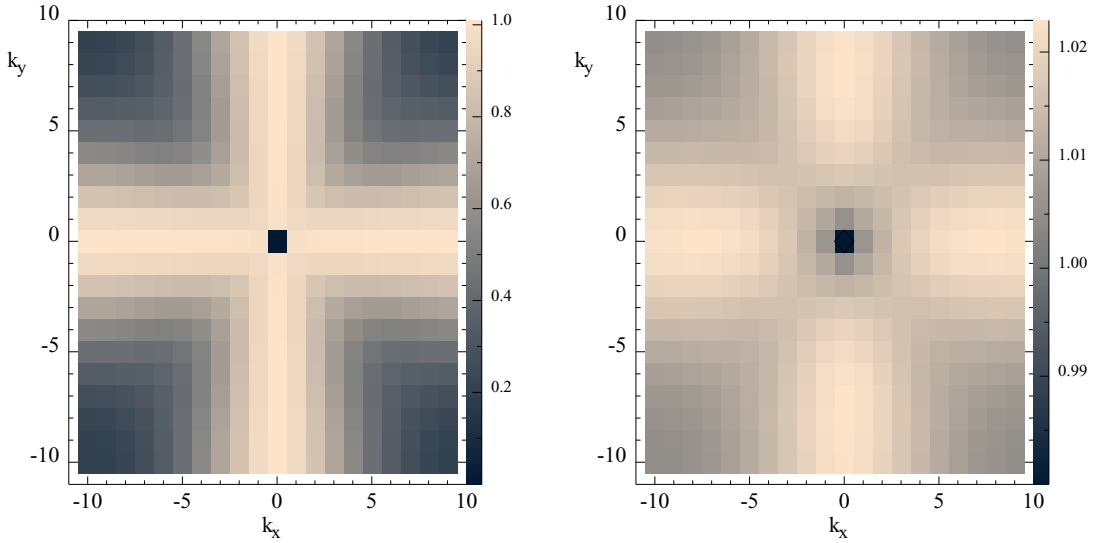

(a) Without ghost noise (b) With ghost noise

Figure 1. $S_{\mathbf{k}}(\rho)$ averaged over 2×10^8 iterations in a $\tau^a = 1$ for all a, $V = 20^2$, fluctuating D2Q9 ideal gas without and with active ghost noise. Note that different scales are used to visualize the slight deviations seen in the ghost noise case.

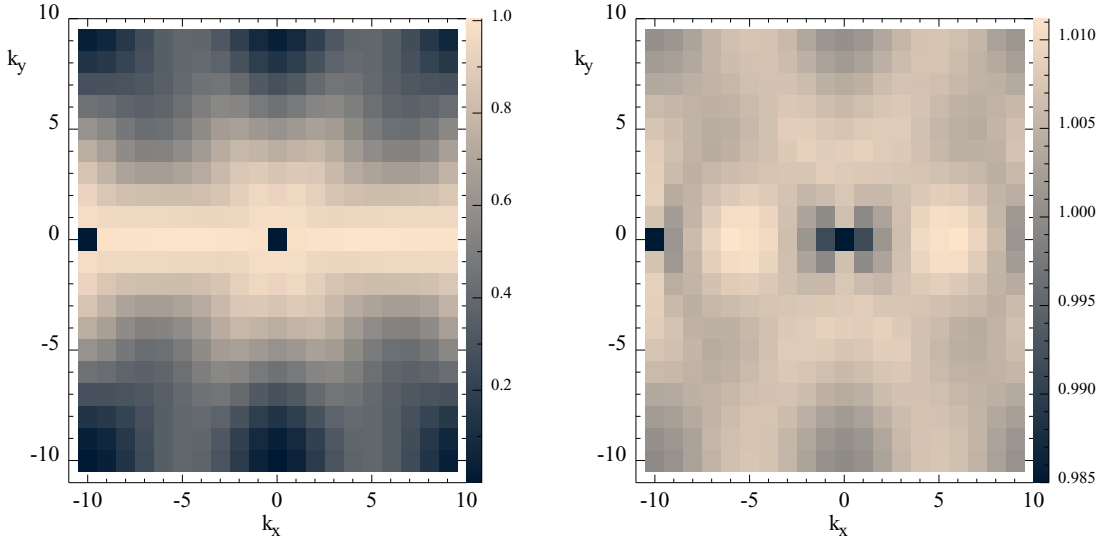

(a) Without ghost noise (b) With ghost noise

Figure 2. $S_{\mathbf{k}}(u_x)$ averaged over 2×10^7 iterations in a $\tau^a = 1$ for all a, $V = 20^2$, fluctuating D2Q9 ideal gas without and with active ghost noise. Note that different scales are used to visualize the slight deviations seen in the ghost noise case.

$\{w_i\} = \{4/9,\ 1/9,\ 1/9,\ 1/9,\ 1/36,\ 1/36,\ 1/36,\ 1/36\}$. The matrix elements m_i^a in transform (129) are then given by

$$\{m_i^a\} = \begin{pmatrix} 1 & 1 & 1 & 1 & 1 & 1 & 1 & 1 & 1 \\ 0 & \sqrt{3} & 0 & -\sqrt{3} & 0 & \sqrt{3} & -\sqrt{3} & -\sqrt{3} & \sqrt{3} \\ 0 & 0 & \sqrt{3} & 0 & -\sqrt{3} & \sqrt{3} & \sqrt{3} & -\sqrt{3} & -\sqrt{3} \\ 0 & \frac{3}{2} & \frac{-3}{2} & \frac{3}{2} & \frac{-3}{2} & 0 & 0 & 0 & 0 \\ 0 & 0 & 0 & 0 & 0 & 3 & -3 & 3 & -3 \\ -1 & \frac{1}{2} & \frac{1}{2} & \frac{1}{2} & \frac{1}{2} & 2 & 2 & 2 & 2 \\ 0 & -\sqrt{\frac{3}{2}} & 0 & \sqrt{\frac{3}{2}} & 0 & \sqrt{6} & -\sqrt{6} & -\sqrt{6} & \sqrt{6} \\ 0 & 0 & -\sqrt{\frac{3}{2}} & 0 & \sqrt{\frac{3}{2}} & \sqrt{6} & \sqrt{6} & -\sqrt{6} & -\sqrt{6} \\ \frac{1}{2} & -1 & -1 & -1 & -1 & 2 & 2 & 2 & 2 \end{pmatrix} . \qquad (76)$$

The corresponding elements n_i^a of the back transform are defined by the requirement $n_i^a = m_i^a w_i$. The zeroth moment then is the density ρ, the first and second are (up to a factor) the components of the momentum, the third and fourth the components

of the shear stress and the fifth resembles the bulk stress [44]. The remaining three moments are the ghost modes. Thus the equilibrium moments $M^{a,0} = \sum_i m_i^a f_i^0$ are

$$\begin{aligned} M^{0,0} &= \rho \\ M^{1,0} &= \sqrt{3}\rho u_x \\ M^{2,0} &= \sqrt{3}\rho u_y \\ M^{3,0} &= \tfrac{3}{2}\rho(u_x^2 - u_y^2) \\ M^{4,0} &= 3\rho u_x u_y \\ M^{5,0} &= \tfrac{3}{2}\rho(u_x^2 + u_y^2) \\ M^{6,0} &= M^{7,0} = M^{8,0} = 0. \end{aligned} \tag{77}$$

We present here results for k-independence of the moment fluctuations predicted by Eq. (74). In particular we consider the normalized static structure factor

$$S_{\mathbf{k}}(M^a) = N^a \left\langle \delta M^a(\mathbf{k}) \delta M^a(-\mathbf{k}) \right\rangle \tag{78}$$

where $\delta M^a(\mathbf{k}) = \sum_{\mathbf{x}} \delta M^a(\mathbf{x}) e^{-i\mathbf{k}\cdot\mathbf{x}}$ is the discrete spatial Fourier transform of δM^a and $\sum_{\mathbf{x}}$ is understood to be the summation over all discrete lattice sites. The normalization constant N^a such that $S_{\mathbf{k}}(M^a) = 1$ is equivalent to $\bar{\rho}$. I. e. for the density $N^\rho = \frac{1}{\bar{\rho}^3 V}$ and velocity components $N^{u_\alpha} = \frac{1}{\bar{\rho} V k_b T}$ where $k_b T = \frac{1}{3}$ for the isothermal D2Q9 model employed. A value of 1 throughout k-space for the structure factor of any of the moments given in Eq. (167) thus indicates agreement with Eq. (74). The volume V is just the number of lattice points $V = \sum_{\mathbf{x}} 1$ and the division by it is just a normalization artifact of the Fourier transform.

According to the argument put forth in [13] we expect the mean square fluctuations of all moments M^a to be unity throughout k-space. For the density ρ this

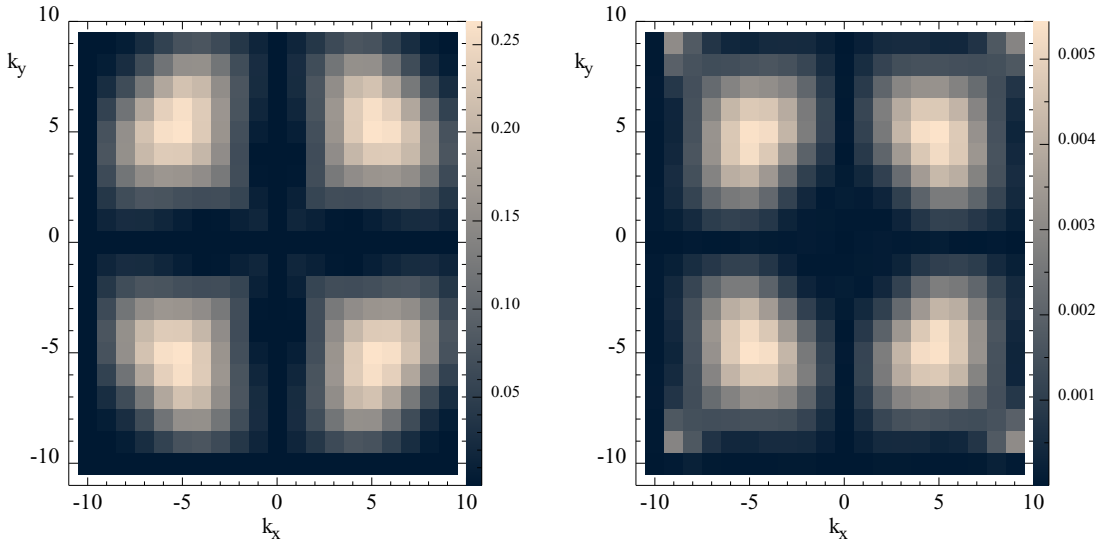

(a) Without ghost noise (b) With ghost noise

Figure 3. $R_{\mathbf{k}}(u_x u_y)$ averaged over 8×10^6 iterations in a $\tau^a = 1$ for all a, $V = 20^2$ fluctuating D2Q9 ideal gas simulation with and without active ghost noise. Again, take note of the different scales.

is confirmed to three orders of magnitude in Fig. 1(b) for $S_{\mathbf{k}}(\rho)$ and in Fig. 2(b) for $S_{\mathbf{k}}(u_x)$. We find similar agreement for all nine moments of the D2Q9 model. For comparison we set the noise on the non-hydrodynamic modes (M^6, M^7, M^8) to zero, recovering the original Ladd method [10] and, as seen in Figures 1(a) and 2(a), the lack of noise on the ghost terms leads to drastic deficiencies for large k_x, k_y values. Note that there are no deficiencies in Fig. 1 for $k_x = 0$ and $k_y = 0$. The reason is that the projection of the D2Q9 model onto one coordinate axis yields a D1Q3 model. The isothermal ideal gas D1Q3 model, however, only has one stress mode and no ghost modes and thus there is no difference between the Ladd and Adhikari implementations in these projections. This is again observed in Fig. 2(a) where $S_{\mathbf{k}}(u_x)$ exhibits white noise along the k_x axis even in the absence of ghost noise. Motivated by private communication with A. Donev who is developing a general finite volume

scheme to solve the fluctuating Navier Stokes Equations [35] based on a third order Runge-Kutta integrator we also measured the cross correlator

$$R_{\mathbf{k}}(u_x, u_y) = N^{u_x} \left\langle u_x(\mathbf{k}) u_y^*(\mathbf{k}) \right\rangle . \tag{79}$$

According to Eq. (74) this quantity is expected to vanish. This is again confirmed nicely in Fig. 3(b) to three orders of magnitude. In contrast measurements of $R_{\mathbf{k}}(u_x, u_y)$ in an implementation without ghost noise exhibits significant correlations of up to $0.25\bar{\rho}$ for intermediate k_x and k_y ranges as seen in Fig. 3(a).

The required condition in Eq. (74), $\mathbf{u} \ll 1$, suggests that this noise implementation may suffer from a lack of Galilean invariance. To estimate the magnitude of this violation we consider an imposed mean velocity in the x-direction. We measured correlators for a fluctuating system with large superimposed velocity of $u_x = 0.1$. The results in Fig. 4 indicate that indeed the moment fluctuations do not completely decouple and Eq. (74) is no longer fulfilled. Compared to the Ladd implementation these errors are still smaller, but they can approach the same order of magnitude for maximal accessible velocities. A more comprehensive investigation of these effects is subject of a forthcoming publication.

2.5. Discussion and Outlook

We have shown here that the Adhikari approach to use an improved LB method presents a promising scheme to simulate fluctuating hydrodynamics. The ability to interprete the ghost degrees of freedom as resulting from discrete particle distributions gives us the ability to systematically introduce fluctuations. This approach recovers fluctuations not only in the hydrodynamic limit but also for much shorter wavelengths.

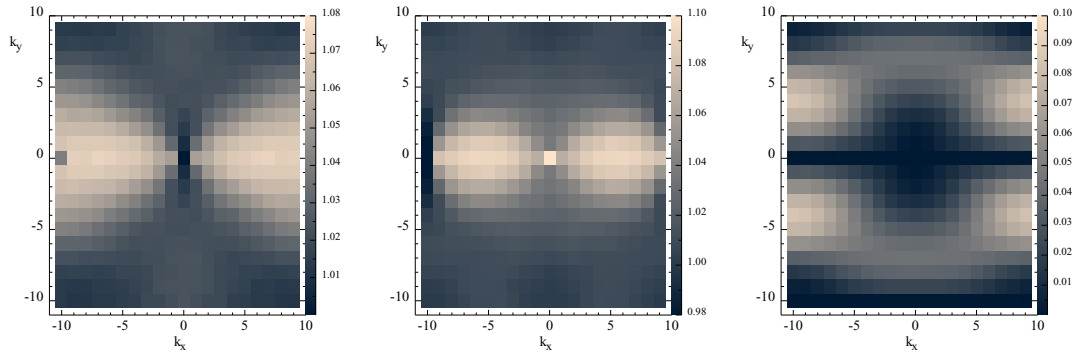

(a) $S_{\mathbf{k}}(\rho)$ (b) $S_{\mathbf{k}}(u_x)$ (c) $S_{\mathbf{k}}(u_x, u_y)$

Figure 4. Correlators $S_{\mathbf{k}}(\rho)$, $S_{\mathbf{k}}(u_x)$, and $R_{\mathbf{k}}(u_x, u_y)$ averaged over 5×10^6 iterations or a $\tau^a = 1$ for all a, $V = 20^2$ fluctuating D2Q9 ideal gas simulation with a constant velocity of $u_x = 0.1$.

However, this is only true in the absence of flow. Since lattice Boltzmann methods are not generally used in this regime one may wonder if Galilean invariance violations may not erase some of the improvement achieved by including noise in the ghost modes. This is a subject to which we will return in a forthcoming paper.

3. PAPER 2: DERIVATION OF HYDRODYNAMICS FOR MULTI-RELAXATION TIME LATTICE BOLTZMANN USING THE MOMENT APPROACH[2]

3.1. Abstract

A general analysis of the hydrodynamic limit of multi-relaxation time lattice Boltzmann models is presented. We examine multi-relaxation time BGK collision operators that are constructed similarly to those for the MRT case, however, without explicitly moving into a moment space representation. The corresponding 'moments' are derived as left eigenvectors of said collision operator in velocity space. Consequently we can, in a representation independent of the chosen base velocity set, generate the conservation equations. We find a significant degree of freedom in the choice of the collision matrix and the associated basis which leaves the collision operator invariant. We explain why MRT implementations in the literature reproduce identical hydrodynamics despite being based on different orthogonalization relations. More importantly, however, we outline a minimal set of requirements on the moment base necessary to maintain the validity of the hydrodynamic equations. This is particularly useful in the context of position and time-dependent moments such as those

[2]While investigating the validity of more general transforms to facilitate a fluctuating lattice Boltzmann method that would not violate Galilean invariance, both Alexander Wagner and Goetz Kaehler recognized that with the multi relaxation time transforms would need to vary depending on the local velocity. The general validity of the hydrodynamic equations with a collision carried out in a velocity dependent multi-relaxation time moment representation was not clear nor documented in the literature. However, it was known that different multi-relaxation time representations exist [45, 27, 41], all of which had been shown to fulfill second order hydrodynamics. Alexander Wagner suggested rederiving the hydrodynamic equations in velocity space directly which Goetz Kaehler did. In doing so Goetz Kaehler realized that the additional conserved quantity eigenvectors only lead to additional higher order appearances of the conservation equations which consequently vanish to in the second order limit. While other authors had hinted at this in the literature before [23] it had never been clearly outlined with an exact specification of the requirements as done in this publication. This discovery was instrumental for the implementation of the Galilean invariant implementation of the fluctuating lattice Boltzmann method with locally velocity dependent multi-relaxation time transforms we discuss in paper 3. This publication was written by Goetz Kaehler with editing support and advice by Alexander Wagner.

used in the context of peculiar velocities and some implementations of fluctuations in a lattice-Boltzmann simulation.

3.2. Introduction

The lattice Boltzmann (LB) method is continuing to increase in popularity as a simulation method for fluid mechanics for a wide range of applications from turbulence [46] to complex fluids [47]. A key of its success is the simplicity of the algorithm. Instead of discretizing the hydrodynamic equations directly the method is based on an underlying microscopic model. Historically the method developed from lattice gases [32] where particles move on a lattice and collide on lattice points. Because such a lattice gas model locally conserves mass and momentum the macroscopic behavior of the system has to be described by the continuity and Navier-Stokes equations [1]. The connections between the microscopic streaming and collision rules and the macroscopic differential equations is established by taking the hydrodynamic limit which requires averaging the locally conserved quantities. This reproduces the Boltzmann equation [18]. Performing a Taylor expansion on the discrete Boltzmann equation then leads to a PDE representation of the discrete evolution equation [41].

At this point there are several routes to proceed. Grad [20] suggests taking moments of the full Boltzmann equation which is a route that has been taken by other groups [21]. Alternatively one can formally expand the distribution function before taking the moments, which is known as the Chapman-Enskog expansion [48]. The maximum entropy method is another viable alternative [49]. In the case of convective scaling either approach will lead to identical results to second order: the continuity and Navier-Stokes equations as well as the heat equation for thermal systems. The higher order equations are, however, quite different. Here neither approach has been particularly successful as the Navier-Stokes level equations appear to be appropriate to length-scales close to molecular scale [50]. There are few attempts to derive higher

order hydrodynamic equations in the LB context. One recent publication succeeded in deriving third order hydrodynamics with an off-lattice approach [51]. Another exception are multi-phase fluids where higher order spatial derivatives giving rise to surface tension have to be taken into account [52].

The development of the method took a major leap when it was discovered that it is feasible to use a Boltzmann–level microscopic model [53, 54], which removes microscopic noise. This approach is referred to as the lattice Boltzmann method. Higuera and Jiminez already introduced the predecessor of what would become the multi-relaxation time (MRT) technique. Qian *et al.* [28] found that the approach is simplified considerably when the collision operator is written as a single-time BGK expression which relaxes local particle distributions towards the equilibrium distribution. To this date this represents the most popular flavor of lattice Boltzmann algorithms employed.

Shortly after the introduction of the single-time relaxation collision operator d'Humieres reemphasized that one can extend the BGK collision with a multi-relaxation time (MRT) approach [27]. In the MRT description the collision is described with a matrix, which allows for a decoupled relaxation of the different stress terms. It thus decouples the different transport coefficients and they no longer need to take their ideal gas values as in the single time BGK case.

Deriving hydrodynamic equations for multi-relaxation time lattice Boltzmann methods is usually achieved by Chapman-Enskog like expansions. These expansions often depend on the specific model [48]. A good review on lattice Boltzmann was published recently by Dünweg and Ladd [23]. Similar in spirit to the work presented here they attempt to derive the isothermal Navier-Stokes equations in a model independent fashion. In particular they list a set of general conditions that are required to retain hydrodynamics [Eqs. (80–84) in [23]]. However, they state that the de-

tails of the implementation of the hydrodynamic stress cannot be done in a model independent manner.

In this context we should also mention a very comprehensive approach presented by Junk *et al.* [55] detailing a very general Chapman-Enskog method for the case of diffusive scaling. In this paper we show that general requirement on the collision matrix is that it must have left eigenvectors for shear and bulk stress degrees of freedom. Furthermore we find that we are free to add any conserved quantity eigenvectors to any of the non conserved modes. Therefore we have a complete and model independent set of requirements that guarantees the validity of second order hydrodynamics. Levermore's [49] maximum entropy approach proposed a general multi-relaxation time like closure hierarchy for kinetic theories in 1996. Levermore's derivation and its application to lattice Boltzmann by Ansumali *et al.* [29] differ from the work presented here in that they do not limit themselves to the isothermal ideal gas and consequently the bulk viscosity is not a free parameter.

The relevance of this general approach stems from our interest in LB methods with locally varying collision matrices. Such an approach is necessary to address Galilean invariance in fluctuating lattice Boltzmann [44].

3.3. Lattice Boltzmann

The lattice Boltzmann equation (LBE) is a representation of the Boltzmann transport equation [18] with three levels discretization taken into account: time t , position $\mathbf{x}$ and velocity $\mathbf{v}$. First LB-methods utilized a two body collision operator derived from lattice gas methods (Higuera *et al.* [56]). Later Qian and d'Humieres realized that the collision operator could be significantly simplified using a BGK approach [19] as $\Omega_i = (1/\tau)(f_i^0 - f_i)$ where f_i^0 is the local equilibrium distribution [27, 28]. In the BGK approximation [19] the collision integral is replaced by a relaxation term that moves the current distribution $f(\mathbf{x}, \mathbf{v}, t)$ function towards the equilibrium

distribution $f^0(\mathbf{x}, \mathbf{v}, t)$ For a general collision operator Ω_i the basic LBE can then be written as

$$f_i(\mathbf{x} + \mathbf{v}_i, t + 1) - f_i(\mathbf{x}, t) = \Omega_i(f_1, \cdots, f_N), \tag{80}$$

where the f_i are the density functions associated with a discrete set of N base velocity vectors $\mathbf{v}_i$, x is the lattice position and t is the discrete time with interval $\Delta t = 1$. The velocities are chosen such that the v_i are lattice vectors. Since collisions conserve certain quantities such as mass and momentum we require

$$\sum_i \psi_i^{a,c} \Omega_i = 0, \tag{81}$$

where the $\psi_i^{a,c}$ are the vectors describing the velocity moments of the conserved quantities. The index c only emphasizes that these vectors are associated with conserved quantities. We will encounter non-conserved vectors ψ^a later in this paper. The first quantity that has to be conserved in the collision is the local density which has a corresponding vector of $\psi_i^{0,c} = 1_i$ where 1_i is simply 1 for every i. Momentum must also be conserved in each spatial direction. In three dimensions the corresponding ψ vectors are $\psi_i^{1,c} = v_{i,x}$, $\psi_i^{2,c} = v_{i,y}$, and $\psi_i^{3,c} = v_{i,z}$. We denote the locally conserved quantities as density ρ and momentum $\mathbf{j}$. They are defined through the vectors $\psi^{a,c}$ as

$$\sum_i \psi_i^{0,c} f_i = \rho, \quad \sum_i \psi_i^{\alpha,c} f_i = j_\alpha. \tag{82}$$

Throughout this paper Greek indices α, β, γ will generally denote the range of spatial dimensions $\{x, y, z\}$ and be treated under the Einstein summation convention. Latin indices i, j, k are used in the context of vector components of the lattice Boltzmann base velocity set and are summed over explicitly.

Most LB models are used to simulate isothermal hydrodynamics and these models are the focus of this paper. Thermal models require the conservation of the addi-

tional moment v_i^2, which we do not treat here. In principle, however, it should be easy to extend the presented approach to thermal systems and generate the corresponding heat equation.

To recover the continuity and Navier-Stokes equations this local equilibrium distribution needs to match the first four velocity moments of the continuum Maxwell-Boltzmann distribution. This distribution is $f^0(\mathbf{v}) = \frac{\rho}{(2\pi\theta)^{3/2}} \exp\left(\frac{(\mathbf{v}-\mathbf{u})^2}{2\theta}\right)$ where local velocity is defined as $\mathbf{u} = \mathbf{j}/\rho$ and θ is the temperature. For thermal models we would need to match velocity moments. The first four moments sufficient to derive isothermal hydrodynamics are

$$\sum_i f_i^0 = \rho, \tag{83}$$

$$\sum_i v_{i\alpha} f_i^0 = \rho u_\alpha = j_\alpha, \tag{84}$$

$$\sum_i v_{i\alpha} v_{i\beta} f_i^0 = \rho\theta\delta_{\alpha\beta} + \rho u_\alpha u_\beta, \tag{85}$$

$$\sum_i v_{i\alpha} v_{i\beta} v_{i\gamma} f_i^0 = \rho\theta\left(u_\alpha\delta_{\beta\gamma} + u_\beta\delta_{\gamma\alpha} + u_\gamma\delta_{\alpha\beta}\right) + \rho u_\alpha u_\beta u_\gamma + Q_{\alpha\beta\gamma}. \tag{86}$$

The tensor quantity $Q_{\alpha\beta\gamma}$ is an arbitrary correction term and vanishes in the continuum case. However, the typical choice is $Q_{\alpha\beta\gamma} = -\rho u_\alpha u_\beta u_\gamma$ which allows us to use a much smaller velocity set. The trade off are small Galilean invariance problems [30]. Note that the conserved moments of the local equilibrium distribution f_i^0 and the distribution f_i are identical because the collision does not change them, *i.e.* $\sum_i \psi_i^{a,c} f_i^0 = \sum_i \psi_i^{a,c} f_i$.

Depending on the base velocity set the conditions Eqs. (83-86) may not uniquely define the equilibrium distribution. For practical implementations of the method we

then require a consistent choice of the f_i^0. From several different general arguments it is usually found that the explicit form

$$f_i^0(\rho, \mathbf{u}) = \rho w_i \left[(\mathbf{1} + \frac{1}{\theta}\mathbf{u}.\mathbf{v}_i + \frac{1}{2\theta^2}(\mathbf{u}.\mathbf{v}_i)^2 - \frac{1}{2\theta}\mathbf{u}.\mathbf{u} \right] \tag{87}$$

is a good choice for the isothermal equilibrium distribution for an appropriate choice of the w_i weight constants [37] although other forms have been used [57]. Note that we require only Eqs. (83-86) in the following analysis.

When deriving the hydrodynamic equations from the continuous Boltzmann equation using the single-relaxation time approximation leads to a fixed ratio of the transport coefficients such as shear viscosity, bulk viscosity, and thermal conductivity [18]. In the discrete case of lattice Boltzmann the same hydrodynamic equations can be derived with transport coefficients containing a re-normalized relaxation time $\omega = (\tau - 1/2)$. For ideal gases the predicted ratios agree quite well with the experimentally measured values [18]. The form of the hydrodynamic equations apply not only to ideal but also non-ideal gases and even fluids. Lattice Boltzmann applications usually consider examples from this more general class of systems. In these more general cases, however, the ratios of transport coefficient are no longer fixed, and it would be advantageous to write a more flexible collision term that allows for independently variable transport coefficients. This was accomplished by D'Humieres [27] by considering a multi-relaxation time BGK collision operator of the form

$$\Omega_i(f_1, \cdots, f_N) = \sum_j \Lambda_{ij}[f_j^0(\rho, \mathbf{u}, \theta) - f_j(\mathbf{x}, t)], \tag{88}$$

where Λ is a collision matrix. If we choose $\Lambda_{ij} = \delta_{ij}/\tau$ we recover the single-relaxation time collision operator. Another numerical rationale for implementing multi-relaxation time Lattice Boltzmann methods is the improvement in stability,

particularly for high Reynolds numbers [58]. There are some requirements on the collision matrix to ensure mass and momentum conservation in the collision. In the single-relaxation time approach the conservation laws were respected because the conserved moments of the local distribution f_i and the local equilibrium distribution f_i^0 are identical. For the multi-relaxation time collision term Eq. (81) requires

$$\sum_i \psi_i^{a,c} \sum_j \Lambda_{ij} \left(f_j^0 - f_j \right) = 0. \tag{89}$$

These equations will be satisfied if we demand that the scalar product of a conserved quantity vector with the collision matrix is a linear combination of conserved quantity vectors, *i.e.* $\sum_i \psi_i^{a,c} \Lambda_{ij} = c^a \psi_j^{a,c}$ for an arbitrary c^a. Note here that the only physically relevant quantity is the collision operator Ω, not the collision matrix Λ. While different choices for c^a will lead to different collision matrices, they will not change the collision operator Ω. Thus Eq. (88) is not bijective. A convenient choice that coincides with the single-relaxation time case sets the conserved moments 1_i and $v_{i\alpha}$ to the left-eigenvectors of our collision matrix with some eigenvalue:

$$\sum_i 1_i \Lambda_{ik} = \frac{1}{\tau_\rho} 1_k, \tag{90}$$

$$\sum_j v_{j\alpha} \Lambda_{ji} = \frac{1}{\tau_{j_\alpha}} v_{i\alpha}, \tag{91}$$

where we used the relaxation times τ to denote the inverse eigenvalues of the collision matrix. This choice also allows us to ensure that Λ is invertible which, while not strictly necessary, simplifies the formalism. Clearly, the values of $1/\tau_\rho$ and $1/\tau_{j_\alpha}$ are entirely arbitrary, meaning that τ_ρ and τ_{j_α} may not appear in the hydrodynamic equations.

3.4. Hydrodynamic Limit by the Moment Method

In this section we present a new approach to obtain the hydrodynamic equations for the multi-relaxation time lattice BGK equation. We generalize the moment approach familiar from single-relaxation time methods [30] to the more general MRT formalism. For the multi-relaxation time collision operator we expand the left hand side of Eq. (80) to second order:

$$\left(\partial_t + v_{i\alpha}\partial_\alpha\right) f_i + \frac{1}{2}\left(\partial_t + v_{i\alpha}\partial_\alpha\right)\left(\partial_t + v_{i\beta}\partial_\beta\right) f_i + O(\partial^3) = \sum_j \Lambda_{ij}\left(f_j^0 - f_j\right). \qquad (92)$$

This allows us to write the f_i in terms of the f_i^0 and higher order derivatives as long as Λ^{-1} exists:

$$f_j = f_j^0 - \sum_i \left(\Lambda^{-1}\right)_{ji}\left[\left(\partial_t + v_{i\alpha}\partial_\alpha\right) f_i\right] + O(\partial^2). \qquad (93)$$

This is important because we can express the equilibrium distributions f_i^0 in terms of ρ and $\mathbf{u}$ in Eq. (87) but not the local distributions f_i. Here we have made the assumption that both, spatial and temporal derivatives, are small quantities of the same order of magnitude. As a byproduct we see that the conservation equations by virtue of Eq. (89) and the $\psi_i^{a,c}$ being left-eigenvectors of Λ_{ij} require

$$\sum_j \psi_j^{a,c} \sum_i \left(\Lambda^{-1}\right)_{ji}\left[\left(\partial_t + v_{i\alpha}\partial_\alpha\right) f_i\right] = \sum_i \tau^a \psi_i^{a,c}\left[\left(\partial_t + v_{i\alpha}\partial_\alpha\right) f_i\right] = O(\partial^2), \qquad (94)$$

which we will use later. Replacing all occurrences of f_i in Eq. (92) with Eq. (93) up to second order we obtain

$$\left(\partial_t + v_{j\alpha}\partial_\alpha\right) f_j^0 - \left(\partial_t + v_{j\alpha}\partial_\alpha\right) \sum_i \left[\left(\Lambda^{-1}\right)_{ji} - \frac{1}{2}\delta_{ji}\right]\left(\partial_t + v_{i\beta}\partial_\beta\right) f_i^0 + O(\partial^3) = \sum_i \Lambda_{ji}\left(f_i^0 - f_i\right). \qquad (95)$$

Because we know f_i^0 as a function of ρ and $\mathbf{j}$ this is an equation expressed entirely in terms of our hydrodynamic variables, except for the collision term. So far the only requirement on the collision Matrix Λ is that it be invertible and fulfill Eq. (89). The general approach now to obtain a conservation equations is to take the inner product of the conserved quantity vectors $\psi^{a,c}$ with Eq. (95). The collision term then vanishes, we retain no dependencies on the f_i, and, after some algebra, we obtain the conservation equations.

3.4.1. The Continuity Equation

To obtain the continuity equation we take the inner product of $\psi_j^{0,c} = 1_j$ with Eq. (95) from the left hand side, *i.e.* we just sum over Eq. (95) while making use of mass conservation in Eq. (89). We get

$$\sum_j 1_j \left(\partial_t + v_{j_\alpha}\partial_\alpha\right) f_j^0 - \sum_j 1_j \left(\partial_t + v_{j\alpha}\partial_\alpha\right) \sum_i \left[\left(\Lambda^{-1}\right)_{ji} - \frac{1}{2}\delta_{ji}\right] \left(\partial_t + v_{i\beta}\partial_\beta\right) f_i^0 + O(\partial^3) = 0. \tag{96}$$

We can rewrite the second order terms as

$$\partial_t \sum_j 1_j \sum_i \left[\left(\Lambda^{-1}\right)_{ji} - \frac{1}{2}\delta_{ji}\right] \left(\partial_t + v_{i\beta}\partial_\beta\right) f_i^0 = O(\partial^3), \tag{97}$$

$$\partial_\alpha \sum_j 1_j v_{j\alpha} \sum_i \left[\left(\Lambda^{-1}\right)_{ji} - \frac{1}{2}\delta_{ji}\right] \left(\partial_t + v_{i\beta}\partial_\beta\right) f_i^0 = O(\partial^3), \tag{98}$$

where we used that both 1_j and $1_j v_{j\alpha} = v_{j\alpha}$ are conserved quantity vectors so that we can apply Eq. (94). We are left with

$$\sum_j \left(\partial_t + v_{j_\alpha}\partial_\alpha\right) f_j^0 + O(\partial^3) = 0, \tag{99}$$

which, using Eq. (83) and Eq. (84), becomes the continuity equation

$$\partial_t \rho + \partial_\alpha \left(\rho u_\alpha\right) + O(\partial^3) = 0. \tag{100}$$

3.4.2. The Navier-Stokes Equation

As the Navier Stokes Equation describes the conservation of momentum we take the first order velocity moment of Eq. (95) and obtain

$$\sum_j v_{j\alpha} \left(\partial_t + v_{j\beta}\partial_\beta\right) f_j^0 \tag{101}$$

$$-\sum_j v_{j\alpha} \left(\partial_t + v_{j\gamma}\partial_\gamma\right) \sum_i \left[\left(\Lambda^{-1}\right)_{ji} - \frac{1}{2}\delta_{ji}\right] \left(\partial_t + v_{i\beta}\partial_\beta\right) f_i^0 + O(\partial^3) = 0. \tag{102}$$

The collision term vanishes according to Eq. (89). We can rewrite the first of the second order terms as

$$\partial_t \sum_j v_{j_\alpha} \sum_i \left[\left(\Lambda^{-1}\right)_{ji} - \frac{1}{2}\delta_{ji}\right] \left(\partial_t + v_{i\beta}\partial_\beta\right) f_i^0 = O(\partial^3), \tag{103}$$

which vanishes to third order due to Eq. (94) much like Eq. (98). To evaluate the remaining gradient term

$$\partial_\gamma \sum_j v_{j\alpha} v_{j\gamma} \sum_i \left[\left(\Lambda^{-1}\right)_{ji} - \frac{1}{2}\delta_{ki}\right] \left(\partial_t + v_{i\beta}\partial_\beta\right) f_i^0 \tag{104}$$

we need to know the stress moments $\sum_j v_{j\alpha} v_{j\gamma} \left[\left(\Lambda^{-1}\right)_{ji} - \frac{1}{2}\delta_{ji}\right]$ of the collision matrix. From the single-relaxation time derivation [30] we know that these terms lead to the stress terms in the Navier-Stokes equation we wish to obtain. Because we want to

distinguish between bulk and shear stress now we separate these into a trace and a traceless velocity moment

$$\sum_j v_{j\alpha} v_{j\gamma} \Lambda_{ji} = \sum_j v_{j\delta} v_{j\delta} \frac{\delta_{\alpha\gamma}}{D} \Lambda_{ji} + \sum_j \left(v_{j\alpha} v_{j\gamma} - v_{j\delta} v_{j\delta} \frac{\delta_{\alpha\gamma}}{D} \right) \Lambda_{ji}. \tag{105}$$

The key requirement is now that the trace and the $(D-1)\left(\frac{D}{2}+1\right)$ elements of the traceless part are left eigenvectors of the collision matrix Λ. For the trace part we demand

$$\sum_j v_{j\delta} v_{j\delta} \frac{\delta_{\alpha\gamma}}{D} \left(\Lambda^{-1}\right)_{ji} = \tau_B v_{i\delta} v_{i\delta} \frac{\delta_{\alpha\gamma}}{D}, \tag{106}$$

where τ_B is the bulk relaxation time and for the traceless part we require

$$\sum_j \left(v_{j\alpha} v_{j\gamma} - v_{j\delta} v_{j\delta} \frac{\delta_{\alpha\gamma}}{D} \right) \left(\Lambda^{-1}\right)_{ji} = \tau_S \left(v_{i\alpha} v_{i\gamma} - v_{i\delta} v_{i\delta} \frac{\delta_{\alpha\gamma}}{D} \right), \tag{107}$$

where the shear stress relaxation time τ_S is the eigenvalue. These eigenvalue equations for the second order velocity moments are the key property of the collision matrix that allows us to recover the Navier-Stokes equation. Because of the freedom to choose different eigenvalues for the trace and the traceless part we can obtain independent bulk and shear stresses.

What follows is essentially the same derivation as in the single-relaxation time case [30], except that we now have two stress terms with associated relaxation times that need to be treated independently. We use the eigenvalue equations (106) and (107) in Eq. (104) to replace Λ^{-1} with the appropriate eigenvalues. The different

velocity moments are substituted by the expressions in Eqs. (83 - 86) and we replace $\tau_B - \frac{1}{2} = \omega_B$ and $\tau_S - \frac{1}{2} = \omega_S$. We get

$$\begin{aligned}
&\partial_\gamma \partial_t \sum_j \sum_i v_{j\alpha} v_{j\gamma} \left[\left(\Lambda^{-1}\right)_{ji} - \frac{1}{2}\delta_{ji} \right] f_i^0 + \partial_\gamma \partial_\beta \sum_j \sum_i v_{j\alpha} v_{j\gamma} \left[\left(\Lambda^{-1}\right)_{ji} - \frac{1}{2}\delta_{ji} \right] v_{i\beta} f_i^0 \\
&= \partial_\gamma \omega_B \left[\partial_t \left(\rho u_\delta u_\delta \frac{\delta_{\alpha\gamma}}{D} + \rho\theta\delta_{\alpha\gamma} \right) + \theta \frac{D+2}{D} \delta_{\alpha\gamma} \partial_\beta \left(\rho u_\beta\right) + \frac{\delta_{\alpha\gamma}}{D} \partial_\beta \left(\rho u_\delta u_\delta u_\beta + Q_{\delta\delta\beta} \right) \right] \\
&+ \partial_\gamma \omega_S \Bigg[\partial_t \left(\rho u_\alpha u_\gamma - \rho u_\delta u_\delta \frac{\delta_{\alpha\gamma}}{D} \right) + \partial_\beta \left(\rho\theta \left(u_\alpha \delta_{\beta\gamma} + u_\beta \delta_{\gamma\alpha} + u_\gamma \delta_{\alpha\beta} \right) + \rho u_\alpha u_\beta u_\gamma + Q_{\alpha\beta\gamma} \right) \\
&\quad - \partial_\beta \left(\theta \frac{D+2}{D} \delta_{\alpha\gamma} \rho u_\beta + \frac{\delta_{\alpha\gamma}}{D} \left(\rho u_\delta u_\delta u_\beta + Q_{\delta\delta\beta} \right) \right) \Bigg].
\end{aligned} \tag{108}$$

To treat the second order terms further we need two identities we obtain by looking at the first order terms of Eq. (102). Inserting the moments (83), (84) and ignoring all second order terms we get

$$\partial_t \left(\rho u_\alpha\right) = -\partial_\beta \left(\rho\theta\delta_{\alpha\beta} + \rho u_\alpha u_\beta \right) + O(\partial^2). \tag{109}$$

Using the continuity equation (100), we obtain the second identity

$$\rho \partial_t u_\alpha = -\rho u_\beta \partial_\beta u_\alpha - \partial_\beta \rho\theta\delta_{\alpha\beta} + O(\partial^2). \tag{110}$$

These two identities and the continuity equation Eq. (100) now replace the time derivatives in Eq. (108)

$$
\begin{aligned}
&\partial_\gamma\omega_B\Big\{ -\theta\delta_{\alpha\gamma}\partial_\beta\left(\rho u_\beta\right) - \frac{\delta_{\alpha\gamma}}{D}\left[u_\delta\partial_\beta\left(\rho\theta\delta_{\beta\delta}+\rho u_\beta u_\delta\right)+u_\delta\left(\rho u_\beta\partial_\beta u_\delta+\partial_\beta\rho\theta\delta_{\beta\delta}\right)\right] \\
&\qquad + \frac{D+2}{D}\theta\delta_{\alpha\gamma}\partial_\beta\left(\rho u_\beta\right)+\frac{\delta_{\alpha\gamma}}{D}\partial_\beta\left(\rho u_\delta u_\delta u_\beta+Q_{\delta\delta\beta}\right)\Big\} \\
+\quad &\partial_\gamma\omega_S\Big\{ -u_\gamma\partial_\beta\left(\rho\theta\delta_{\alpha\beta}+\rho u_\alpha u_\beta\right)-u_\alpha\left(\rho u_\beta\partial_\beta u_\gamma+\partial_\beta\rho\theta\delta_{\gamma\beta}\right)+\partial_\beta\left(\rho u_\alpha u_\beta u_\gamma+Q_{\alpha\beta\gamma}\right) \\
&\qquad + \frac{\delta_{\alpha\gamma}}{D}\left[u_\delta\partial_\beta\left(\rho\theta\delta_{\beta\delta}+\rho u_\beta u_\beta\right)+u_\delta\left(\rho u_\beta\partial_\beta u_\delta+\partial_\beta\rho\theta\delta_{\beta\delta}\right)\right] \\
&\qquad + \partial_\beta\rho\theta\left(u_\alpha\delta_{\beta\gamma}+u_\beta\delta_{\gamma\alpha}+u_\gamma\delta_{\alpha\beta}\right)-\frac{\delta_{\alpha\gamma}}{D}\partial_\beta\left(\rho u_\delta u_\delta u_\beta+Q_{\delta\delta\beta}\right)\Big\}+O(\partial^3) \\
=\quad &\omega_B\left[\frac{2}{D}\theta\partial_\alpha\rho\partial_\gamma u_\gamma+\frac{1}{D}\partial_\alpha\partial_\gamma Q_{\gamma\delta\delta}\right] \\
+\quad &\omega_S\left[\theta\partial_\gamma\left(\partial_\gamma u_\alpha+\partial_\alpha u_\gamma\right)+\partial_\beta\partial_\gamma Q_{\alpha\beta\gamma}-\frac{2}{D}\theta\partial_\alpha\rho\partial_\gamma u_\gamma-\frac{1}{D}\partial_\alpha\partial_\gamma Q_{\gamma\delta\delta}\right]+O(\partial^3).
\end{aligned}
\tag{111}
$$

If we now combine the first order terms Eq. (109) with the second order terms Eq. (111) of the first order velocity moment of the LBE (102) we find the Navier-Stokes equation

$$
\begin{aligned}
\partial_t\left(\rho u_\alpha\right)+\partial_\beta\left(\rho u_\alpha u_\beta\right) =& -\ \partial_\alpha\rho\theta+\partial_\alpha\omega_B\frac{2}{D}\theta\rho\partial_\gamma u_\gamma \\
&+\partial_\gamma\omega_S\left[\rho\theta\left(\partial_\gamma u_\alpha+\partial_\alpha u_\gamma\right)-\frac{2}{D}\theta\rho\partial_\gamma u_\gamma\delta_{\alpha\gamma}\right] \\
&+\ \partial_\alpha\omega_B\frac{1}{D}\partial_\gamma Q_{\gamma\delta\delta}+\partial_\gamma\omega_S\left(\partial_\beta Q_{\alpha\beta\gamma}-\partial_\gamma\frac{1}{D}Q_{\gamma\delta\delta}\right)+O(\partial^3) \\
=& -\ \partial_\alpha\rho\theta+\partial_\alpha\mu\partial_\gamma u_\gamma+\partial_\gamma\eta[(\partial_\gamma u_\alpha+\partial_\alpha u_\gamma)-\frac{2}{D}\partial_\gamma u_\gamma\delta_{\alpha\gamma}] \\
&+O(\partial^2 Q)+O(\partial^3),
\end{aligned}
\tag{112}
$$

where

$$
\mu=\frac{2}{D}\rho\theta(\tau_B-\frac{1}{2}) \tag{113}
$$

is the bulk and

$$\eta = \rho\theta(\tau_S - \frac{1}{2}) \tag{114}$$

the shear viscosity.

In summary we recover the continuity and Navier-Stokes equations in a similar form as found from multi-relaxation time approaches with independently adjustable bulk and shear viscosities provided that three conditions are fulfilled:

1. The first four velocity moments of the equilibrium distribution are given by Eqs. (83-86).

2. The moments of the conserved quantity vectors 1_k and $v_{k\alpha}$ are not altered in the collision step.

3. The collision matrix has the left eigenvectors $v_{k\alpha}v_{k\beta} - v_{k\gamma}v_{k\gamma}\frac{\delta_{\alpha\beta}}{D}$ and $v_{k\gamma}v_{k\gamma}$. This has already been hinted at by Dellar in a similar context [59]. We should mention here that these left eigenvectors retain the freedom to be altered by linear combination of conserved quantity eigenvectors. This is illustrated in the next section.

Unfortunately none of the published multi-relaxation time lattice Boltzmann methods [27, 45] fulfill this last requirement. This is because we have some additional freedom in combining the ψ_i^a vectors with vectors from the conserved quantities as we will explain below. It is interesting to note that we have constraints up to the third order velocity moments for the equilibrium distribution, but only up to second order moments for the collision matrix.

We should mention that the derivation presented here does not impose any requirements on the extra degrees of freedom that are typically present in a lattice-Boltzmann implementation. A DDQQ simulation with a Q component base velocity set in D dimensions only requires $K = 1 + D + D(D+1)/2$ base vectors to reproduce

isothermal hydrodynamics: 1 for the density, D for the momentum components, and $D(D+1)/2$ for the stress tensor. Our derivation makes no assumptions about the structure of the remaining $Q-K$ 'ghost' or kinetic modes or the choice of their corresponding relaxation times. Often the relaxation times for these ghost degrees of freedom are uniformly set to 1. In this case all possible choices for ghost eigenvectors of the collision matrix lead to identical collision matrices. The choice of ghost modes can influence the performance of the LB method if one wants to make use of the freedom to choose arbitrary relaxation times[38]. The introduction of fluctuations to the LBM requires careful treatment of the ghost modes and their relaxation times [13], particularly in the context of boundary conditions [36]. Furthermore Adhikari and Succi suggested a duality between conserved quantity vectors and ghost modes [39] as guideline for constructing base velocity sets for multi-relaxation time implementation.

3.4.3. Limited Freedom of Choice of the Eigenvectors

When we required Eqs. (106) and (107) we ignored that there is a remaining freedom of choice for the eigenvectors. To understand this, let us first remember that the relaxation times for the conserved moments τ_ρ and τ_{j_α} are entirely arbitrary by construction. Because the conserved moments of the f_i and f_i^0 are identical the collision term simply can not alter the values of the conserved quantities, independent of the value of τ_ρ and τ_{j_α}. This also implies that the effect of adding multiples of a conserved mode eigenvector $\psi_j^{a,c}$ to any of the eigenvectors will still result in suitable eigenvectors. Consider an alternative collision matrix $\hat{\Lambda}$ with a left eigenvector $\left(\psi_j^n + \psi_j^c\right)$:

$$\sum_j \left[\left(\psi_j^n + \psi_j^c\right) - \psi_j^c\right] \left(\hat{\Lambda}^{-1}\right)_{ji} = \tau^n \left(\psi_i^n + \psi_i^c\right) - \tau^c \psi_i^c. \tag{115}$$

Here ψ_j^n is an eigenvector of the original matrix Λ^{-1}. The n indicates that it corresponds to a non-conserved quantity and τ^n is the associated eigenvalue. In contrast

ψ_j^c is an eigenvector that corresponds to a conserved quantity, i.e. ρ or v_α, with the associated eigenvalue τ^c. Now, terms that depend on τ^c have to vanish because its value is entirely arbitrary. Therefore we will only retain the $\tau^n\psi_i^n$ terms in the hydrodynamic equations. The collision matrices Λ and $\hat{\Lambda}$ will lead to identical hydrodynamic equations. To illustrate this we re-investigate the bulk stress component in the second order terms in the Navier-Stokes derivation in Eq. (108) for the alternative collision matrix $\hat{\Lambda}$. We replace $v_{j\delta}v_{j\delta}$ with $(v_{j\delta}v_{j\delta} + K1_j) - K1_j$ and use the aforementioned new collision matrix $\hat{\Lambda}^{-1}$ and obtain

$$\begin{aligned}
&\partial_\gamma\partial_t \sum_i \sum_j \left[(v_{j\delta}v_{j\delta} + K1_j) - K1_j\right] \left[\left(\hat{\Lambda}^{-1}\right)_{ji} - \frac{1}{2}\delta_{ji}\right] f_i^0 \\
&\quad + \partial_\gamma\partial_\beta \sum_i \sum_j \left[(v_{j\delta}v_{j\delta} + K1_j) - K1_j\right] \left[\left(\hat{\Lambda}^{-1}\right)_{ji} - \frac{1}{2}\delta_{ji}\right] v_{i\beta} f_i^0 \\
= \;& \partial_\gamma\omega_B \left[\partial_t \left(\rho u_\delta u_\delta \frac{\delta_{\alpha\gamma}}{D} + \rho\theta\delta_{\alpha\gamma}\right) + \frac{D+2}{D}\theta\delta_{\alpha\gamma}\partial_\beta\left(\rho u_\beta\right)\right] \\
&\quad - \partial_\gamma\omega_B K\left[\partial_t\rho + \partial_\beta\left(\rho u_\beta\right)\right]\frac{\delta_{\alpha\gamma}}{D} + \partial_\gamma\omega_\rho K\left[\partial_t\rho + \partial_\beta\left(\rho u_\beta\right)\right]\frac{\delta_{\alpha\gamma}}{D}. \qquad (116)
\end{aligned}$$

For readability we omit the $\rho u_\alpha u_\beta u_\gamma + Q_{\alpha\beta\gamma}$ correction terms from Eq. (86) here as no additional third order velocity moments are generated by the 1_j term in the new bulk viscosity eigenvector. The 1_j contributions lead to additional terms consisting of derivatives of the continuity equation. Since these contributions vanish to third order Eq. (100) the resulting Navier-Stokes equation remains unaffected. If we decided to add a first order velocity moment to one of the non-conserved eigenvectors we would find a Navier-Stokes equation instead of the continuity equation here which again vanishes to third order. We are thus free to add any vectors corresponding to our conserved quantities to the non-conserved eigenvectors. This is the degree of freedom

that allows us to impose orthogonality on the eigenvectors with respect to different inner products.

To recover the approach of d'Humieres we now need to require all of the left eigenvectors of Λ_{ji} be orthogonal, with respect to the inner product $\sum_j \psi_j^m \psi_j^n = \delta_{nm} N^n$ where N^n is the norm of the vector ψ^n which need not be normalized. The only non-orthogonal left eigenvectors here are 1_j and $v_{j\gamma} v_{j\gamma}$. We remedy this by applying a Gram-Schmidt orthogonalization procedure to find the new orthogonalized bulk stress

$$v_{j\gamma} v_{j\gamma} - \frac{\sum_{j'}^{N} 1_{j'} v_{j'\gamma} v_{j'\gamma}}{N} 1_j \tag{117}$$

and thus recover d'Humieres' basis. In contrast recovering the Benzi approach requires that the eigenvectors obey orthogonality with respect to the Hermite norm: $\sum_j \psi_j^m \psi_j^n w_j = \delta_{mn} M^n$. Again only one pair of eigenvectors is not orthogonal, 1_j and $v_{j\gamma} v_{j\gamma}$. We apply the same orthogonalization procedure, however, with the new norm and thus obtain

$$v_{j\gamma} v_{j\gamma} - \frac{\sum_{j'}^{N} 1_{j'} w_j v_{j'\gamma} v_{j'\gamma}}{N} 1_j \tag{118}$$

as the orthogonal bulk stress vector. While d'Humieres' and Benzi's approaches lead to different collision matrices it is important to note that a practical implementation of the approaches is entirely identical. This is because the eigenvectors only differ by a multiple of 1_j, which is the density eigenvector and therefore a conserved quantity eigenvector.

Let us assume that we have two collision matrices Λ and $\hat{\Lambda}$ and two corresponding sets of left eigenvectors that only differ by a conserved quantity vector ψ^a and $\hat{\psi}^a = \psi^a + \psi^c$. Vectors with the same index a correspond to the same physical quan-

tity and will thus correspond to the same time constant τ^a. The eigenvalue equations are then

$$\psi^a \Lambda = \frac{1}{\tau^a} \psi^a \quad \text{, and} \quad \left(\psi^a + \psi^c\right) \hat{\Lambda} = \frac{1}{\tau^a} \left(\psi^a + \psi^c\right). \tag{119}$$

We know that conserved quantity vectors ψ^c are left eigenvectors of both Λ and $\hat{\Lambda}$ and Eq. (89) requires that

$$\sum_i \psi_i^c \sum_j \Lambda_{ij} \left(f_j^0 - f_j\right) = \sum_i \psi_i^c \sum_j \hat{\Lambda}_{ij} \left(f_j^0 - f_j\right) = 0, \tag{120}$$

independent of the actual choice of basis. Now the collision operators Ω and $\hat{\Omega}$ can be defined as

$$\Omega = \sum_j \Lambda_{ij} \left(f_j^0 - f_j\right) \quad \text{, and } \hat{\Omega} = \sum_j \hat{\Lambda}_{ij} \left(f_j^0 - f_j\right). \tag{121}$$

Operators are defined by their action on a basis. Therefore we let Ω act on an arbitrary vector chosen from its own left eigenvector basis. Using Eqs. (121), (119), and (120) we get

$$\begin{aligned}
\sum_i \psi_i^a \Omega_i &= \sum_i \psi_i^a \sum_j \Lambda_{ij} \left(f_j^0 - f_j\right) && (122)\\
&= \frac{1}{\tau^a} \sum_j \psi_j^a \left(f_j^0 - f_j\right) && (123)\\
&= \frac{1}{\tau^a} \sum_j \left(\psi_j^a + \psi_j^c\right) \left(f_j^0 - f_j\right) && (124)\\
&= \sum_i \left(\psi_i^a + \psi_i^c\right) \sum_j \hat{\Lambda}_{ij} \left(f_j^0 - f_j\right) && (125)\\
&= \sum_i \psi_i^a \sum_j \hat{\Lambda}_{ij} \left(f_j^0 - f_j\right) && (126)\\
&= \sum_i \psi_i^a \hat{\Omega}_i. && (127)
\end{aligned}$$

Thus we have proved that as long as two different bases differ only by conserved quantity left eigenvectors, the collision operators are, in fact, identical.

3.5. Summary

We presented a new general formulation for the derivation of hydrodynamics. Based on the framework of generalized or multi-relaxation time formalism we performed a direct asymptotic expansion to second order of the lattice Boltzmann equation and derived the continuity and Navier-Stokes equations for the isothermal ideal gas. Our approach is general in the sense that we do not require specific knowledge of the base velocity set and equilibrium distribution function as long as the velocity moments to third order are identical to those of the continuous case and the collision does not affect the conserved quantities. We therefore do not require an explicit multi-relaxation time representation but instead describe all physically relevant quantities in terms of left eigenvectors of a collision matrix. These left eigenvectors can again be described in terms of velocity moments and thus we maintain a representation independent of the chosen base velocity set. The eigenvalues of the collision matrix are chosen to be the inverse of the relaxation time related to the physical quantity in question. Through the relaxation times associated with bulk and shear stress terms we then get direct access to the bulk and shear viscosities.

The derivation illuminates a degree of freedom in the choice of the left eigenvectors. This is rooted in the fact that the collision does not alter conserved quantities. Therefore linear combinations of conserved quantity eigenvectors can be added to non-conserved moment left eigenvectors without changing the collision operator and by extension the hydrodynamic equations. We identify this degree of freedom as the reason for the equality of multi-relaxation time implementations based on different inner products such as the standard vector and the Hermite norm. In fact, we show that for the simple case of isothermal hydrodynamics the collision operators of any

two realizations of multi-relaxation time Lattice Boltzmann are identical provided they conserve mass and momentum and the appropriate equilibrium distribution is chosen.

The clear description of requirements on the collision operator and base vectors here could be particularly useful in situations where the orthogonality condition of a given MRT implementation changes dynamically and the validity of hydrodynamics in such a case might not necessarily be obvious. One such example would be a fluctuating lattice-Boltzmann implementation where more than the zeroth order of the equilibrium distribution enter the orthogonality condition. An in-depth analysis of this case is subject of a forthcoming publication [44].

The authors would like to thank Guiseppe Gonnella, Paul Dellar, and Eric Foard for enlightening discussion and helpful comments. This work has been supported by an ND EPSCoR seed grant.

4. PAPER 3: FLUCTUATING IDEAL GAS LATTICE-BOLTZMANN WITH FLUCTUATION DISSIPATION THEOREM FOR NON-VANISHING VELOCITIES[3]

4.1. Abstract

Current implementations of fluctuating ideal gas discriptions with the lattice Boltzmann methods are based on a fluctuation dissipation theorem, which, while greatly simplifying the implementation, strictly only holds for zero mean velocity and small fluctuations. We show how to derive the fluctuation dissipation theorem for all $\mathbf{k}$ which was done only for $\mathbf{k} = 0$ in previous derivations. The consistent derivation requires, in principle, locally velocity dependent multi-relaxation time transforms. Such an implementation is computationally prohibitively expensive but, with a small computational trick, it is feasible to reproduce the correct FDT without overhead in computation time. It is then shown that the previous standard implementations break down for non vanishing mean velocity as indicated by violations of Galilean invariance of measured structure factors whereas the new method performs significantly better.

4.2. Introduction

The lattice Boltzmann method is used typically in situations where the velocity $\mathbf{u}$ varies spatially. This is also the case for applications of fluctuating lattice Boltzmann. Examples here are the simulation of bijels [60], polymer transport in a solvent [61], or sedimentation of colloidal suspensions [10, 62] so that the current noise implementations [13, 36] should be verified for $\langle \mathbf{u} \rangle \neq 0$. Including noise in lattice Boltzmann

[3]This publication was the continuation of the previous work. Goetz Kaehler implemented the velocity dependent transforms including the Mathematica scripts. Alexander Wagner helped with input and advice on the implementation. The paper was written by Goetz Kaehler with editing help and advice by Alexander Wagner. The crucial point, the derivation of the fluctuation-dissipation theorem for all $\mathbf{k}$ was done by both authors with primary contribution by Goetz Kaehler after receiving a very insightful referee report from PRE.

simulations has been an active field of research in the last few years. It was pioneered by Ladd[10] who suggested to introduce noise on the non-conserved hydrodynamic modes, i.e. the stress degrees of freedom. This approach works reasonably well for the hydrodynamic limit but for short length scales the fluctuations are underrepresented due to interaction with the non-hydrodynamic degrees of freedom often called the 'ghost'-modes. Adhikari *et al.* [13] recognized the necessity to include noise on all non-conserved degrees of freedom, including the non-physical 'ghost'-modes and Dünweg *et al.* [36] reformulated this approach to follow a detailed-balance condition description. All of these publications describe a fluctuating isothermal ideal gas. Just recently there was significant progress in extending this concept to non-ideal equations of state [63, 25, 64].

The Adhikari implementation and its derivatives [36, 63] employ a multi-relaxation time (MRT) method similar to the one originally introduced by d'Humieres [27] except that the modes are orthogonal with respect to the Hermite norm. This allows for independent relaxation of the stress and ghost moments. More importantly, for the case of fluctuating lattice Boltzmann it simplifies the construction of a noise term that does not violate conservation laws while allowing for non-correlated noise on all other degrees of freedom. The derivation of the fluctuation-dissipation theorem in both, Adhikari's and Dünweg's approaches requires the MRT transforms to be orthogonal with respect to a certain norm. In the case of a fluctuating ideal gas this norm depends on the equilibrium distribution. However, in all previous publications the equilibrium distribution in this norm is taken only to zeroth order, i.e. only the weight factors in the equilibrium distribution are used. The benefit of this approach is that the noise terms introduced are completely independent of the local state of the system which produces a standard Langevin equation without multiplicative noise. The result is that the MRT orthogonality condition employed is identical to what is

typically known as the Hermite norm [45]. This approximation, as we first discussed in [44] and show later in this paper, formally introduces non-Galilean invariant terms. To recover the fluctuation dissipation theorem (FDT) one needs to go to the full description. We investigate the effects of using this zeroth order approximation with respect to fluctuations in the context of non-zero flow speeds. The observed Galilean invariance violations suggest that this approximation may be inappropriate in some cases. To avoid this approximation we developed a novel kind of lattice Boltzmann method which includes the full second order expression, in the normalization condition which we expected to significantly reduce the Galilean invariance violations observed. Such a method necessarily has a local collision matrix that depends on the velocity at the respective lattice site.

The paper is structured as follows: In section two we present a detailed derivation of the fluctuation dissipation theorem for an ideal gas. This is similar to Adhikari's noise implementation but we deviate at the orthogonality condition and show that the FDT can be constructed for all $\mathbf{k}$. We elaborate on the source of the orthogonality condition and the consequences of the zeroth order approximation and illustrate the impact on the MRT transforms. In section three we test the current literature standard for the example of a D2Q9 simulation. We measure the validity of two core assumptions of the derivation in the context of large flow speeds and find that Galilean invariance is indeed violated. In section four we show how to remedy these Galilean invariance violations. In particular we move away from the zeroth order orthogonality condition and attempt to introduce first and second order velocity terms of the equilibrium distribution. As a consequence we derive a lattice Boltzmann method for which the MRT transforms become locally velocity dependent. However, a simplistic implementation of this method is numerically inefficient. This inefficiency can be overcome by introducing look-up tables. The resulting LB scheme's computa-

tional cost is only slightly larger than that of the Hermite norm implementation and Galilean invariance violations are significantly reduced.

4.3. Lattice Boltzmann Simulation of a Fluctuating Ideal Gas

In order illustrate the origin of Galilean invariance violations in fluctuating lattice Boltzmann implementations we present a short derivation of the fluctuating ideal gas in the Lattice Boltzmann context. The derivation is based on Adhikari *et al.*'s work [13] who first recognized the necessity to include noise on all non-conserved degrees of freedom. The derivation given in Adhikari *et al.*'s original paper is strictly only valid for $\mathbf{k} = 0$. We show here that the FDT for all $\mathbf{k}$ can be recovered. We put emphasis on a clear notation that separates the velocity space distribution functions f_i and the moment space moments we call M^a.

The fluctuating lattice-Boltzmann equation is given by

$$\begin{aligned} &f_i(\mathbf{x} + v_i, t + 1) = \\ &f_i(\mathbf{x}, t) + \sum_j \Lambda_{ij} \left[f_j(\mathbf{x}, t) - f_j^0(\mathbf{x}, t) \right] + \xi_i(\mathbf{x}, t), \end{aligned} \tag{128}$$

where the f_i are densities associated with the velocities v_i. The local equilibrium distribution depends on position and time through the local number of particles per lattice cell $\rho = \sum_i f_i$ and velocity $\mathbf{u} = \sum_i f_i \mathbf{v}_i / \rho$. The structure of the collision matrix Λ_{ij} is discussed later in this section. This is the standard BGK lattice-Boltzmann equation with an added noise term $\xi_i(\mathbf{x}, t)$. These noise terms must be chosen such that conserved quantities ρ, $\mathbf{j}$, where $\mathbf{j} = \sum_i f_i \mathbf{v}_i$, are not changed and a proper fluctuation dissipation theorem (FDT) is obeyed. How we obtain the latter while ensuring the former is outlined below.

In order to gain independent access of conserved and non-conserved moments it is useful to shift from Boltzmann type particle distributions f_i to what is called

generalized lattice-Boltzmann, moment space representation, or multi relaxation time representation (MRT)[27, 38]. One thus gains access to the hydrodynamically relevant moments directly. For this purpose a set of a forward transform from velocity space and its density functions f_i to moment space and its so-called moments M^a

$$M^a(\mathbf{x}, t) = \sum_i m_i^a f_i(\mathbf{x}, t). \tag{129}$$

and the corresponding back transform

$$f_i(\mathbf{x}, t) = \sum_a n_i^a M^a(\mathbf{x}, t). \tag{130}$$

must be chosen. While the original matrix elements m_i^a and n_i^a in [27] were identical this is not necessary. But they need to follow the orthogonality conditions

$$\sum_i m_i^a n_i^b = \delta^{ab} \text{ and } \sum_a m_i^a n_j^a = \delta_{ij}. \tag{131}$$

The particular choice of these transforms aims to generate a simple form for the fluctuation dissipation theorem and is of key importance to the validity of the noise derivation and Galilean invariance or lack thereof. As such they differ from those in the publications introducing the MRT formalism [27, 38]. At least in the case of the ideal gas implementation it is convenient to choose the moments M^a such that the representation of the collision matrix Λ in moment space is diagonal $\Lambda^{ab} = -\frac{1}{\tau^a}\delta^{ab}$. For practical purposes it is then useful to perform the collision in moment space. The fluctuating LBE Eq. (128) is then written as

$$\begin{aligned} &f_i(\mathbf{x} + \mathbf{v}_i, t + 1) - f_i(\mathbf{x}, t) = \\ &\sum_a n_i^a \left\{ \sum_b \Lambda^{ab} \left[M^b(\mathbf{x}, t) - M^{b,0}(\mathbf{x}, t) \right] + \xi^a \right\} \end{aligned} \tag{132}$$

where ξ^a is a random variable with $\langle \xi^a \rangle = 0$ and $\langle \xi^{a2} \rangle$ is determined below. In this paper we select the ξ^a from a Gaussian distribution although different ways of random number generation have been suggested[65]. The primary advantage here is that we gain independent access to the hydrodynamically relevant physical moments and we can choose the noise amplitudes ξ^a such that conservation laws are not violated, i.e. $\xi^{a,\text{conserved}} = 0$.

Now we separate the f_i in Eq. (128) into their global mean values and a local fluctuating term

$$f_i = \langle f_i \rangle + \delta f_i \tag{133}$$

and we obtain

$$\begin{aligned} &\langle f_i \rangle + \delta f_i(\mathbf{x} + v_i, t+1) = \langle f_i \rangle + \delta f_i(\mathbf{x}, t) \\ &+ \sum_j \Lambda_{ij} \left[\langle f_j \rangle + \delta f_j(\mathbf{x}, t) - \langle f_j^0 \rangle - \delta f_j^0(\mathbf{x}, t) \right] \\ &+ \xi_i(\mathbf{x}, t). \end{aligned} \tag{134}$$

Here we use the velocity space representation of the collision matrix, i.e. $\Lambda_{ij} = \sum_a \sum_b n_i^a \Lambda^{ab} m_j^b$. Subtracting the $\langle f_i \rangle$ and assuming

$$\langle f_i \rangle = \langle f_i^0 \rangle, \tag{135}$$

where ρ_0 and $\mathbf{u}_0$ are the equilibrium values of the density and the velocity, yields a LBE for the fluctuation part of the distribution

$$\begin{aligned} &\delta f_i(\mathbf{x} + v_i, t+1) = \\ &\delta f_i(\mathbf{x}, t) + \sum_j \Lambda_{ij} \left[\delta f_j(\mathbf{x}, t) - \delta f_j^0(\mathbf{x}, t) \right] + \xi_i(\mathbf{x}, t). \end{aligned} \tag{136}$$

We can now Fourier transform in space and apply the moment space transform $\sum_i m_i^a$ to obtain the moment space evolution equation in k-space where we are careful to keep the advection term on the left hand side of the equal sign

$$\sum_i m_i^a e^{i\mathbf{k}v_i} \sum_b n_i^b \delta M^b(\mathbf{k}, t+1) = \delta M^a(\mathbf{k}, t) + \sum_c \Lambda^{ac} \left[\delta M^c(\mathbf{k}, t) - \delta M^{0,c}(\mathbf{k}, t)\right] + \xi^a(\mathbf{k}, t). \tag{137}$$

Finally, Adhikari requires $\delta M^{0,d} = M^{0,d}(\mathbf{k}, t) - \langle M^{0,d}(\mathbf{k}, t)\rangle = 0$ for all non-conserved moments because $M^{d,0} = 0$ and therefore also $\langle M^{d,0}\rangle = 0$. This statement is correct provided one considers only a linearized fluctuating Boltzmann approach [16, 15, 25] which is the theory underlying Adhikari's derivation[13]. For a fluctuating BGK-approach there are deviations which become particularly relevant at small densities. These deviations will be discussed in detail elsewhere [66]. For the current derivation we make the customary assumption $\delta M^0 = 0$ which is appropriate for large densities. We then obtain

$$\sum_b \Gamma^{ab}(\mathbf{k}) \delta M^a(\mathbf{k}, t+1) = \left(1 - \frac{1}{\tau^a}\right) \delta M^a(\mathbf{k}, t) + \xi^a(\mathbf{k}, t), \tag{138}$$

where we introduced $\Gamma^{ab}(\mathbf{k}) = \sum_i m_i^a n_i^b e^{i\mathbf{k}v_i}$ from the advection operator in Fourier transformed moment space. This expression is the inverse to the one used by Adhikari *et al.* in [13]. The importance of this advection operator lies in the fact that the conserved moments only obtain fluctuations through the operator Γ (i.e. the streaming).

Taking the outer product of δM^a with itself, i.e. computing the structure factor, performing an ensemble average and substituting $r^a = 1 - 1/\tau^a$ we obtain

$$\left\langle \sum_b \Gamma^{ab}(\mathbf{k})\delta M^b(\mathbf{k}, t+1) \sum_d \Gamma^{cd}(-\mathbf{k})\delta M^d(-\mathbf{k}, t+1) \right\rangle = \tag{139}$$
$$\langle r^a \delta M^a(\mathbf{k}, t) r^c \delta M^c(-\mathbf{k}, t)\rangle + \langle \xi^a(\mathbf{k}, t)\xi^c(-\mathbf{k}, t)\rangle \,,$$

where we have used that the noise ξ^a is to be independent of the moment deviations, i.e. $\langle \xi^a \delta M^b \rangle = 0$. We now have to consider $\langle \delta M^a \delta M^c \rangle$ carefully. For an ideal gas we know from Lifshitz [43, §19 in chapter I] that the f_i are Poisson distributed about f_i^0 and with δf_i as defined in Eq. (133) and Eq. (135) one thus obtains

$$\langle \delta f_i \delta f_j \rangle_{|_{\rho_0, u_0}} = \langle f_i \rangle \delta_{ij}. \tag{140}$$

We can then find for the moment correlator

$$\begin{aligned} \langle \delta M^a \delta M^b \rangle &= \sum_i \sum_j m_i^a m_j^b \langle \delta f_i \delta f_j \rangle \\ &= \sum_i \sum_j m_i^a m_j^b f_i^0 \delta_{ij}. \end{aligned} \tag{141}$$

Comparing Eq. (141) with Eq. (131) we notice that if we choose $n_i^a = m_i^a f_i^0/\rho$ such that the orthogonality condition of Eq. (131) becomes

$$\sum_i m_i^a m_i^b \frac{f_i^0}{\rho} = \delta^{ab}, \tag{142}$$

the moment fluctuations in Eq. (141) are effectively decoupled and we obtain

$$\langle \delta M^a \delta M^b \rangle = \rho \delta^{ab}, \tag{143}$$

which for an ideal gas is true for all $\mathbf{k}$. Of course, one has also to show that this is also consistent with identifying the M^a with the hydrodynamic moments. For a detailed discussion of this see [67].

Now, with Eq. (143) and assuming stationarity of equal time correlators, i.e. $\langle \delta M^a(\mathbf{k}, t+1)\delta M^b(-\mathbf{k}, t+1)\rangle = \langle \delta M^a(\mathbf{k}, t)\delta M^b(-\mathbf{k}, t)\rangle$ our expression for the FDT Eq. (139) simplifies to

$$\sum_b \sum_d \sum_i \sum_j m_i^a n_i^b m_j^c m_j^d \frac{f_j^0}{\rho} \rho \delta^{bd} e^{i\mathbf{k}(v_i - v_j)} = \tag{144}$$
$$r^a r^c \rho \delta^{ac} + \langle \xi^a(-\mathbf{k}, t)\xi^c(\mathbf{k}, t)\rangle \,,$$

where we expanded the advection operators $\Gamma^{ab} = \sum_i m_i^a n_i^b e^{i\mathbf{k}v_i}$ and one of the $n_i^a = m_i^a f_i^0/\rho$. Contracting the summation over d, then j and finally b we find

$$\sum_i m_i^a m_i^c f_i^0 e^{i\mathbf{k}(v_i - v_i)} = r^a r^c \rho \delta^{ac} + \langle \xi^a(-\mathbf{k}, t)\xi^c(\mathbf{k}, t)\rangle \,. \tag{145}$$

Here we observe, that we can indeed decouple the the noise terms and find that they are independent of $\mathbf{k}$ such that

$$\langle \xi^a \xi^c \rangle = \rho \delta^{ac}(1 - r^a r^c). \tag{146}$$

The standard deviation of the random number distribution to be chosen thus becomes

$$\sqrt{\langle \xi^{a2} \rangle} = \frac{1}{\tau^a} \sqrt{\rho\,(2\tau^a - 1)}. \tag{147}$$

The actual implementation performs the collision in moment space according to Eq. (132) where the moments M^b are constructed at each time step by the standard

forward transform. The streaming, however, still has to happen in velocity space and consequently each update involves two matrix transforms.

Of course, the problem here is that fulfilling the orthogonality condition Eq. (142) that the transforms become locally dependent on the velocity $\mathbf{u}(\mathbf{x}, t)$. One of the motivations behind the zeroth order approximation of the original implementations [13, 36] to the equilibrium distribution in the orthogonality condition was to have a noise term that is independent of local quantities. If we assume very low mean velocities

$$\lim_{\mathbf{u}\to 0} f_i^0\left(\rho, \mathbf{u}\right) = \rho w_i, \tag{148}$$

thereby avoiding aforementioned problem and the orthogonality condition simplifies to

$$\sum_i m_i^a m_i^b w_i = \delta^{ab}. \tag{149}$$

This implies $n_i^a = m_i^a w_i$ and is identical to what is frequently called the Hermite norm and was originally introduced by Benzi [45]. The orthogonality condition Eq. (149) therefore qualifies the requirements on the transforms in addition to the necessity that they preserve hydrodynamics. An extensive study on the second condition has been published in [67]. There we found that the Hermite norm of Eq. (149), does indeed also preserve hydrodynamics and that, in fact, we are free to add any conserved quantity moments to hydrodynamic modes without impacting the validity of the hydrodynamic equations. The choice of the zeroth order approximation in Eq. (149) is, however, not well documented or motivated in the original literature and gives rise to the question whether Galilean invariance violations of the fluctuations result as a consequence. We should mention here that we are grateful for the comments of [68] on the derivation of the FDT for all $\mathbf{k}$. Furthermore a lot of the considerations here and in other recent work on fluctuating lattice Boltzmann is very similar in spirit to the

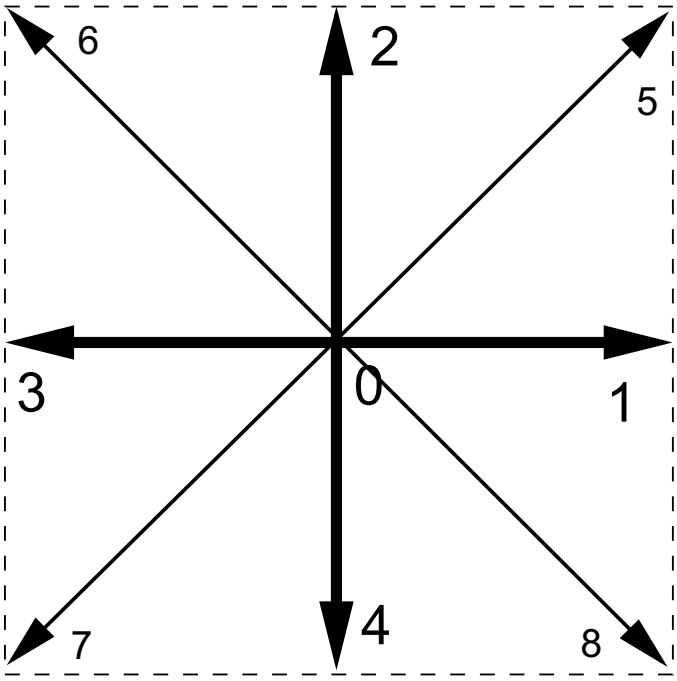

Figure 5. Basis vectors v_i of the D2Q9 scheme used in all simulations in this manuscript.

results of Fox and Uhlenbeck [15] for the case of the continuous linarized Boltzmann equation. There it was already shown that for an FDT in the context of a linearized fluctuating Boltzmann equation it is helpful to decompose the distribution function into velocity-dependent eigenfunctions to eigenvalues of the collision operator. The equivalent of those velocity dependent eigenfunctions is the moment representation used here.

4.4. Galilean Invariance Violations in the Hermite Norm

First we want to evaluate what effect choosing the simplified norm of Eq. (149) has on the Galilean invariance of a fluctuating lattice Boltzmann implementation. Here we show the numerical results for an isothermal D2Q9 fluctuating lattice Boltzmann method with periodic boundary conditions. Moment space transforms are generated with respect to the Hermite norm of Eq. (149). The basis vectors v_i are shown in Fig. Figure 5. All i indices in the following correspond to these basis vectors. The

details of the D2Q9 Hermite norm transforms and the equilibrium moments are documented in appendix (4). We use Qian's second order expansion [28] of the continuous Maxwell-Boltzmann distribution as expression for the equilibrium distribution

$$f_i^0(\rho, \mathbf{u}, \theta) = \rho w_i \left[1 + \frac{1}{\theta}\mathbf{u}.v_i + \frac{1}{2\theta^2}\left(\mathbf{u}.v_i\right)^2 - \frac{1}{2\theta}\mathbf{u}.\mathbf{u}\right]. \tag{150}$$

The results in the following were all obtained in a 2D lattice Boltzmann simulation of size 21×21. The odd side lengths are chosen to avoid the independent conservation of momentum components in odd and even lattice sites in either dimension. They occur for even side lengths because collisions conserve momentum and streaming of the densities that constitute momentum and could interact always moves two lattice sites at once. Consequently momenta in odd and even numbered lattice sites would never interact. All our measurements are done in lattice units. With $\Delta t = 1$ and lattice cell length of $d = 1$ the lattice velocity c becomes $d/\Delta t = 1$. Densities ρ are all given in the number of lattice Boltzmann particles per unit cell. We use a large average density of $\rho_0 = 10^6$ to avoid stability issues due to local negative density events. These can occur when the noise ξ_i on the distribution functions f_i exceeds the value of these distribution functions. This is more likely for small ρ as the noise amplitude in moment space Eq. (147) is proportional to $\sqrt{\rho}$. All averages were taken over a simulation time of 10^6 iterations after a thermalisation phase of 10^5 iterations to equilibrate the system. We then perform simulations for different mean velocities of the system. The mean velocity is changed merely by setting $\mathbf{u}$ in Eq. (150) at initialization time.

The fundamental identity that allows us to decouple the moment fluctuations is given by Eq. (140). We can verify its validity in the simulation directly by measuring $\langle \delta f_i \delta f_j \rangle$ as a function of $u_{x,0}$ and comparing it to f_i^0 and w_i of Eq. (140) and Eq. (151). If the ideal gas hypothesis were to hold we would expect Eq. (140) to be fulfilled

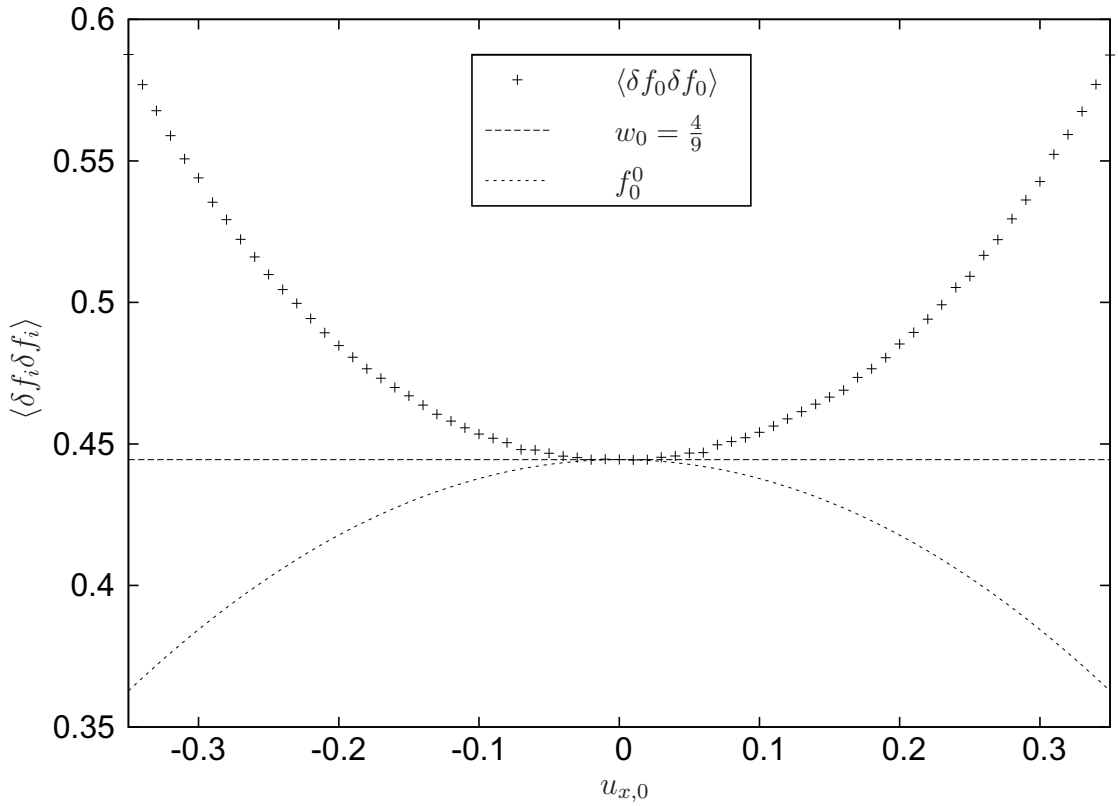

Figure 6. $\langle (\delta f_0)^2 \rangle$ in a 21×21 D2Q9 fluctuating LB simulation employing the Hermite norm. We plot w_i and $f_i^0$for comparison.

independently of **u**. However, using only the Hermite norm Eq. (149) suggests that we might only find Eq. (140) fulfilled to zeroth order, i.e. to the weight factors w_i.

In Figs. 6, 7, 8 we show the simulation results of all unique $\langle \delta f_i \delta f_i \rangle$ correlators as functions of $u_{x,0}$. We find that with increasing velocity $u_{x,0}$ we do indeed deviate strongly from both, the weights w_i, and the equilibrium distributions f_i^0. In this implementation the correlators approach neither the w_i nor the f_i^0 and in some cases not even an intermediate value. For correlators corresponding to base velocities without an x-component ($\langle \delta f_0^2 \rangle$, $\langle \delta f_2^2 \rangle$, $\langle \delta f_4^2 \rangle$) the trend opposes that of the f_i^0. In these plots and all similar figures in this paper the statistical error bars are omitted in the graphs when they are smaller than the symbol size.

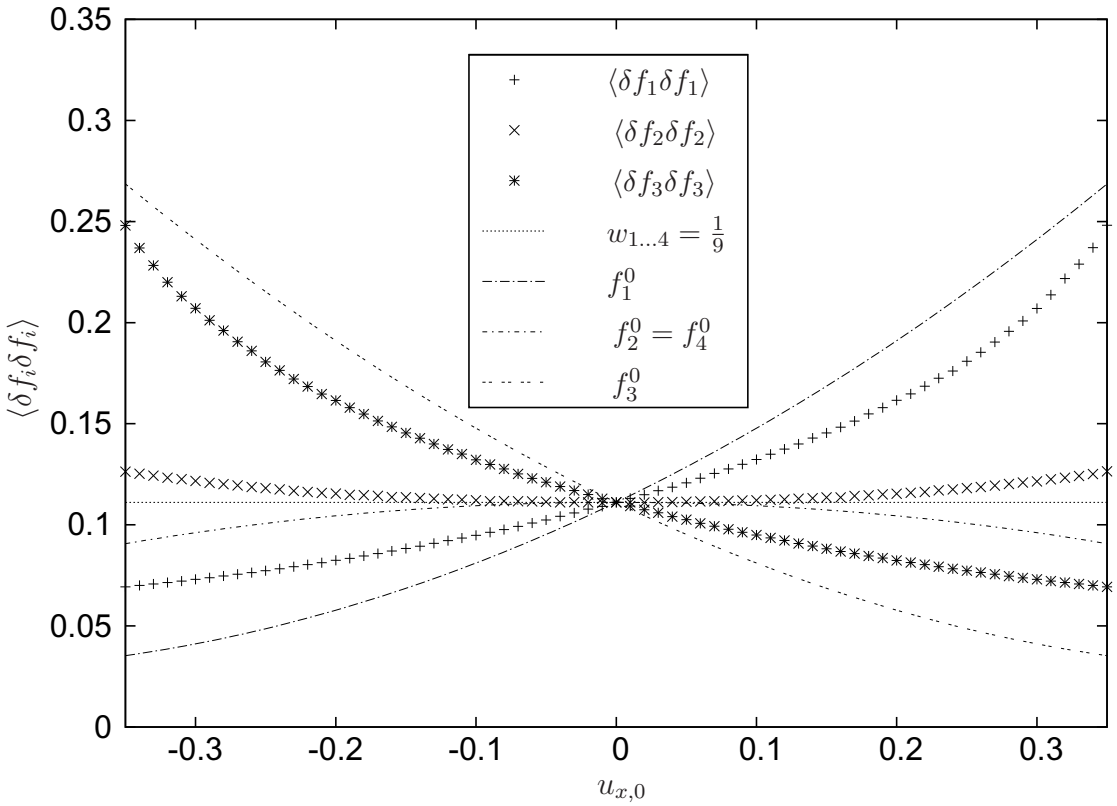

Figure 7. $\langle (\delta f_i)^2 \rangle$ for $i = 1...3$ in a 21×21 D2Q9 fluctuating LB simulation employing the Hermite norm. We plot w_i and f_i^0 for comparison. $\langle (\delta f_4)^2 \rangle$ is not shown as it is identical to $\langle (\delta f_2)^2 \rangle$ for symmetry reasons.

In previous publications [13, 63] the fluctuations were characterized by the fluctuations of the hydrodynamics and ghost moments. The corresponding moment correlators follow directly from the distribution function deviations according to

$$\langle \delta M^a \delta M^b \rangle = \sum_{ij} m_i^a m_j^b \langle \delta f_i \delta f_j \rangle. \tag{151}$$

and are arguably of more practical importance since they represent the fluctuations of the hydrodynamic fields.

These correlators were expected, in the theory of [13, 36, 63, 25, 64] to obey $\langle \delta M^a \delta M^b \rangle = \rho \delta_{ab}$. However, for this to work we would need $\langle \delta f_i \delta f_j \rangle = w_i$ in Eq. (151), which is not the case for non-zero velocities, as we have shown above.

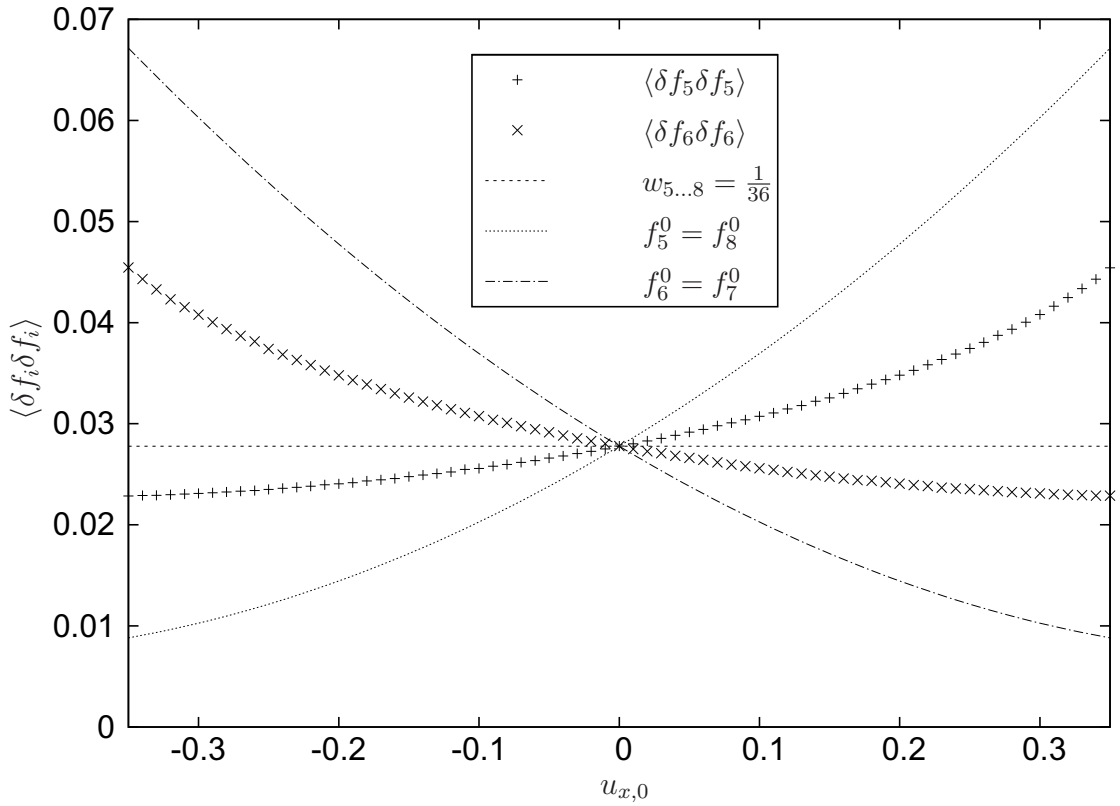

Figure 8. $\langle (\delta f_i)^2 \rangle$ for $i = 5...8$ in a 21×21 D2Q9 fluctuating LB simulation employing the Hermite norm. We plot w_i and f_i^0 for comparison. $\langle (\delta f_8)^2 \rangle$ and $\langle (\delta f_7)^2 \rangle$ are not shown as they appears identical to $\langle (\delta f_5)^2 \rangle$ and $\langle (\delta f_6)^2 \rangle$ respectively in the scale of this plot.

We show the observed deviations for the diagonal correlators in Fig. Figure 10. Here the correlator of the current in x-direction, $\langle \delta j_x \delta j_x \rangle$, exhibits the largest deviations.

To obtain some quantitative measure of the dependency of all 81 (45 unique) correlators in Eq. (151) we fit a second order polynomial $l u_{x,0} + q u_{x,0}^2$ to $\langle \delta M^a \delta M^b \rangle / \rho_0 - \delta^{ab}$. The resulting coefficients l for odd combinations and q for even combinations give a rough estimate of the deviation of the particular moment correlators and are depicted in Fig. Figure 11. We notice in Fig. Figure 11(b) that while the quadratic dependency of the correlations on the velocity is present in several correlators, it is particularly apparent on the square correlators. The linear dependency only ap-

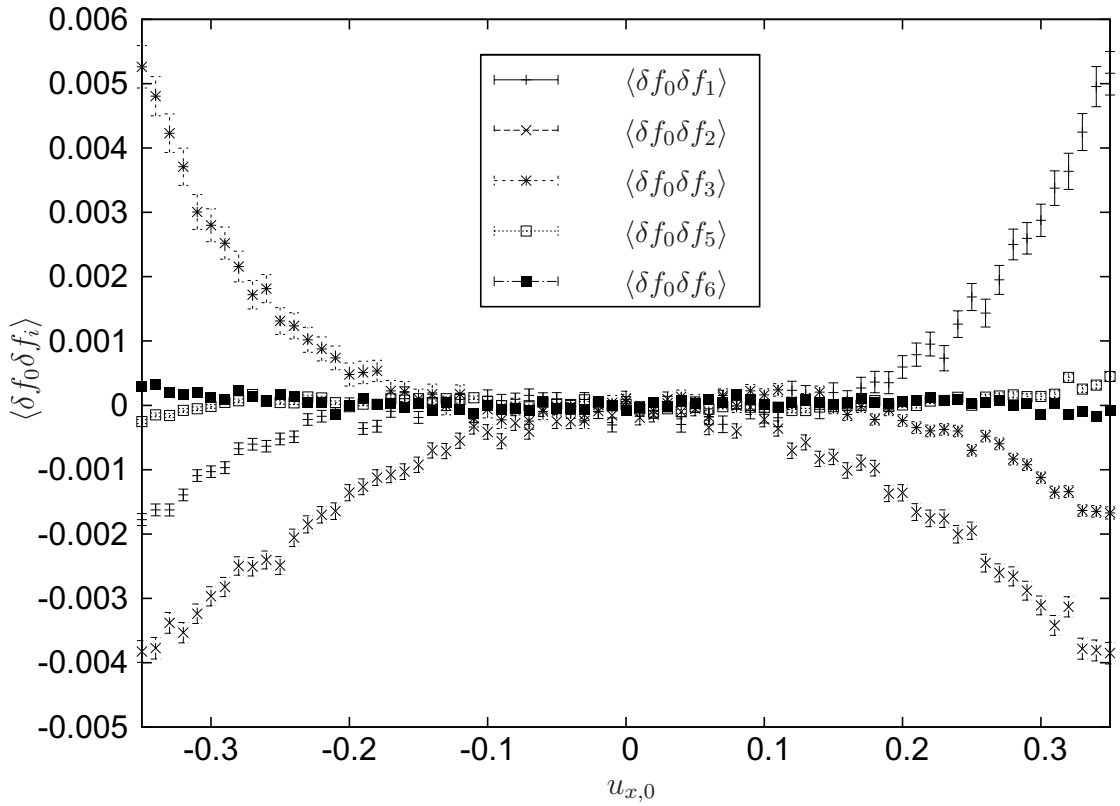

Figure 9. Off-diagonal correlators $\langle \delta f_0 \delta f_i \rangle$ for $i = 1...8$ in a 21×21 D2Q9 fluctuating LB simulation employing the Hermite norm. $\langle \delta f_0 \delta f_4 \rangle$, $\langle \delta f_0 \delta f_7 \rangle$, and $\langle \delta f_0 \delta f_8 \rangle$ are omitted as they behave identical to $\langle \delta f_0 \delta f_2 \rangle$, $\langle \delta f_0 \delta f_6 \rangle$, and $\langle \delta f_0 \delta f_5 \rangle$ respectively.

pears in cross-correlators which are anti-symmetric under $u_{x,0} \to -u_{x,0}$ as seen in Fig. Figure 11(a).

The ensemble averages of the correlation functions shown so far do not resolve the length scale dependency of the deviations we observed. To gain some understanding here we measure the static structure factor

$$S_{\mathbf{k}}(\rho) = \frac{1}{\rho_0} \langle \delta\rho(\mathbf{k}) \delta\rho(-\mathbf{k}) \rangle \,, \tag{152}$$

the j_x momentum correlator

$$S_{\mathbf{k}}(j_x) = \frac{1}{\rho_0} \langle \delta j_x(\mathbf{k}) \delta j_x(-\mathbf{k}) \rangle \,, \tag{153}$$

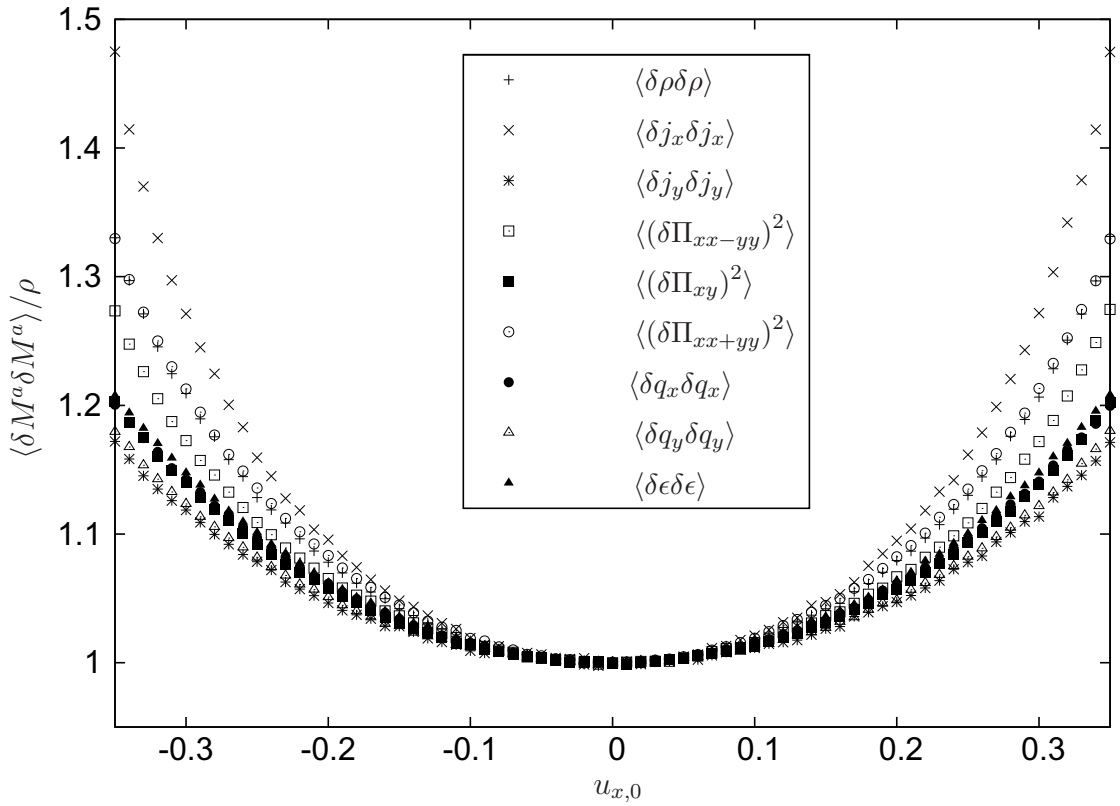

Figure 10. Correlators calculated in the Hermite norm $\langle \delta M^a \delta M^a \rangle$ normalized to ρ according to Eq. (143) in a 21×21 D2Q9 fluctuating LB simulation employing the Hermite norm.

at chosen velocities and the momentum cross correlator

$$R_{\mathbf{k}}(j_x, j_y) = \frac{1}{\rho_0} \langle \delta j_x(\mathbf{k}) \delta j_y(-\mathbf{k}) \rangle \tag{154}$$

at imposed average system velocities $u_{x,0} = 0.0$, $u_{x,0} = 0.1$, and $u_{x,0} = 0.2$. We chose $R_{\mathbf{k}}(j_x, j_y)$ in reference to Donev *et al.*'s investigation of the accuracy of finite volume schemes [35].

Here $\delta\rho(\mathbf{k}) = \sum_{\mathbf{x}} [\rho(\mathbf{x}) - \rho_0] e^{-i\mathbf{k}\cdot\mathbf{x}}$ and $\delta j_x(\mathbf{k}) = \sum_{\mathbf{x}} [j_x(\mathbf{x}) - j_{x,0}] e^{-i\mathbf{k}\cdot\mathbf{x}}$ are the discrete spatial Fourier transforms and $\sum_{\mathbf{x}}$ is understood to be the summation over all discrete lattice sites.

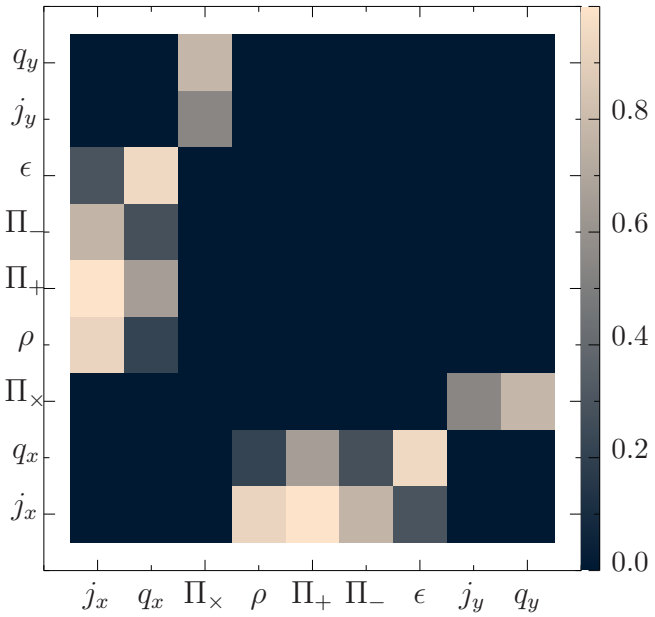

(a) Linear coefficient l, Hermite norm

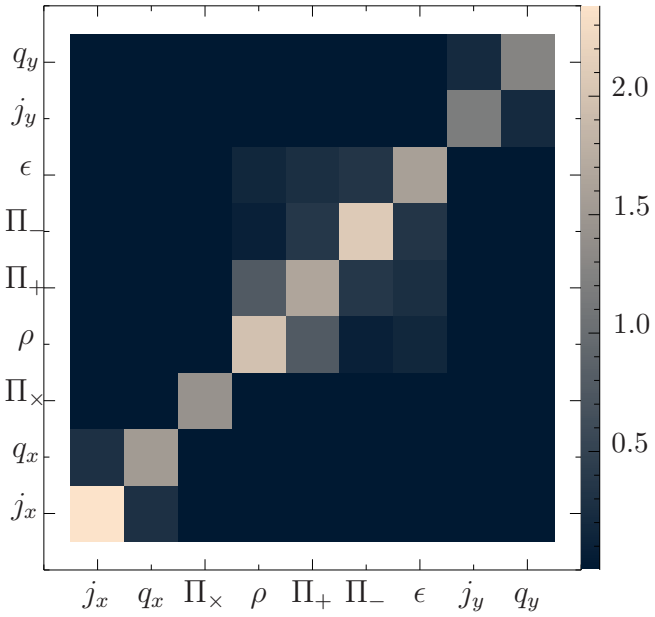

(b) Quadratic coefficient q, Hermite norm

Figure 11. Linear and quadratic coefficient l and q of all 81 (45 unique) correlators as a result of fitting $\langle \delta M^a \delta M^b \rangle (u_{x,0}) - \delta^{ab}$ to $l u_{x,0} + q u_{x,0}^2$. Brighter color indicates larger coefficients. Moments were reordered to visually identify correlations better. To accommodate for symbol size the stress moments were simplified: $\Pi_\times = \Pi_{xy}, \Pi_- = \Pi_{xx-yy}, \Pi_+ = \Pi_{xx+yy}$). The coefficient at position (0, 1) in image (a) would correspond to linear portion of the $\langle \delta j_x \delta q_x \rangle$ correlator. Coefficients were measured on a 21×21 D2Q9 simulation employing the Hermite norm. Fit range used was $-0.25 <= u_x <= 0.25$.

In Figs. 12, 13, and 14 we observe that the correlators lose the relatively good agreement with the isotropy requirement of the ideal gas, i.e. the wave number independence as we increase the velocity. They are sensitive to increased velocities and isotropy at the correlations is destroyed. Errors are not limited to large $\mathbf{k}$ and impinge on the hydrodynamic ($\mathbf{k}$ small) region. Different correlators violate isotropy at different length scales and directions but we can generalize that the violations for certain length scales and spatial directions exceed those observed on the level of the ensemble averaged correlations discussed so far. As an example the density correlator $S_{\mathbf{k}}(\rho)$ deviates by more than 20% on all length scales in the x direction at $u_{x,0} = 0.2$ in Fig. Figure 12(c) while the ensemble average finds a deviation of about 6% in Fig. Figure 10. Comparing Figs. 12, 13, and 14 at $u_{x,0} = 0.2$ with $u_{x,0} = 0.1$ we observe that the structure of the anisotropy is largely independent of the average system speed although there are small deviations. Another observation is that although $\langle j_x j_y \rangle$ is small compared to other cross correlators in Fig. Figure 11 this is mostly due to a fortuitious cancellation of errors for different values of k. The absolute deviations for the $\langle \delta j_x(k) \delta j_y(k) \rangle$ are of similar magnitude compared to $\langle \delta j_x(k) \delta j_x(k) \rangle$.

In summary we can clearly see that as function of the fluid velocity we observe strong deviations from the identities in Eq. (143) and Eq. (140) and the appearance of off-diagonal correlations which are not present in the case of $\mathbf{u} = 0$. We conclude that Galilean invariance is indeed violated and that the fluctuation-dissipation theorem of Eq. (146) is not longer diagonalized by the simple choice of $f_i^0/\rho \approx w_i$ in Eq. (142).

4.5. Local Velocity Dependent Transforms

The question now is whether we can alleviate the difficulties we have encountered by avoiding the approximation of $f_i^0(\mathbf{u} = 0) = \rho w_i$ in the normalization condition. Removing the velocity dependence in the normalization condition could very likely be

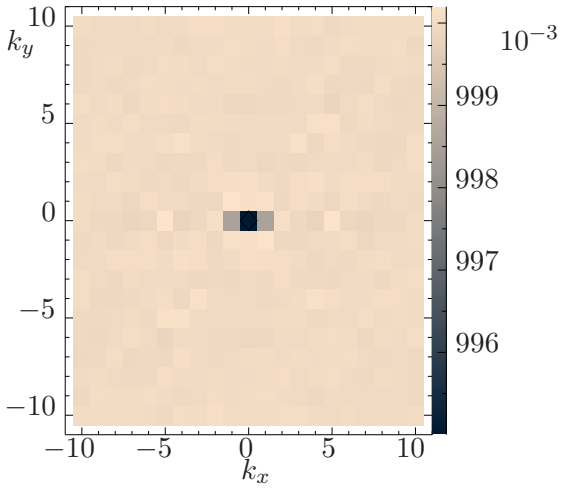

(a) $u_{x,0} = 0.0$

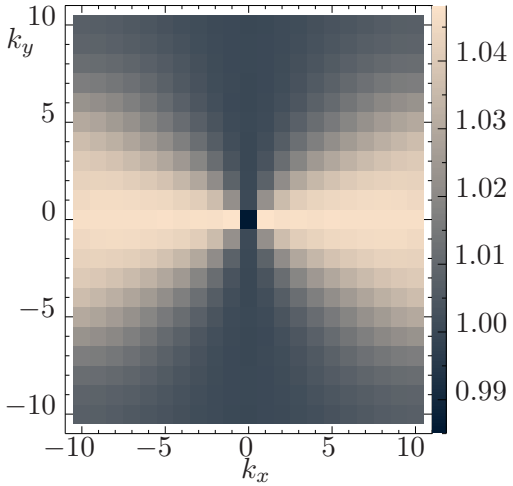

(b) $u_{x,0} = 0.1$

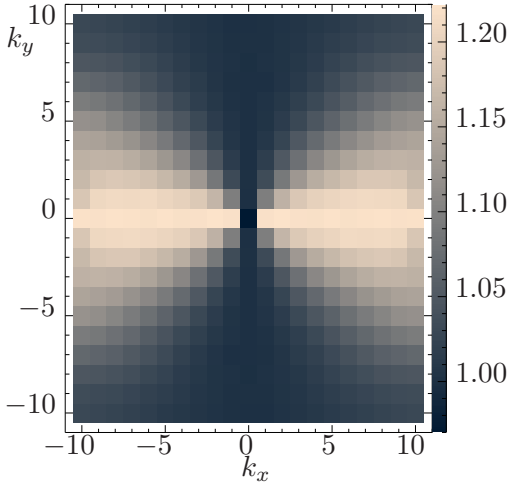

(c) $u_{x,0} = 0.2$

Figure 12. Static structure factor $S_{\mathbf{k}}(\rho)$ at different velocities measured for the Hermite norm.

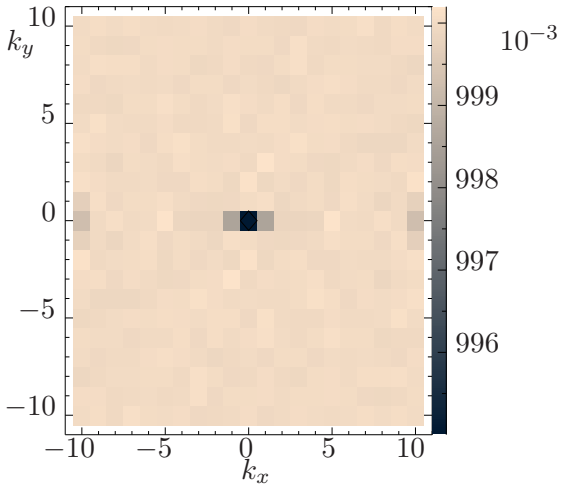

(a) $u_{x,0} = 0.0$

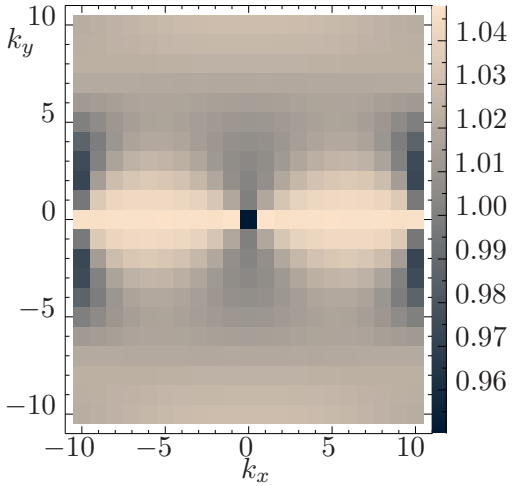

(b) $u_{x,0} = 0.1$

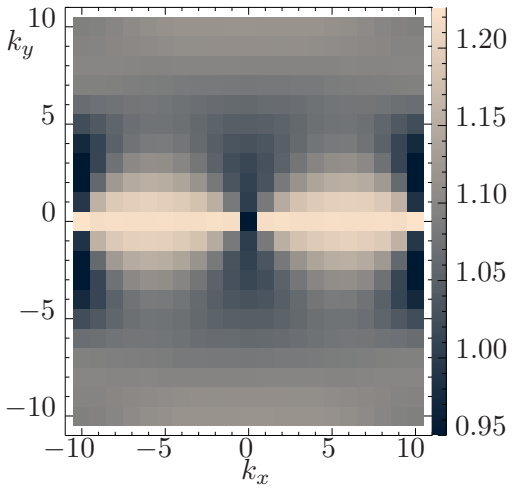

(c) $u_{x,0} = 0.2$

Figure 13. Static structure factor $S_{\mathbf{k}}(j_x)$ at different velocities measured for the Hermite norm.

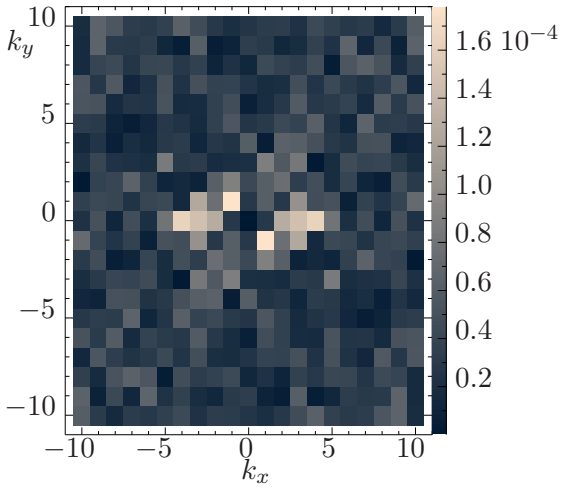

(a) $u_{x,0} = 0.0$

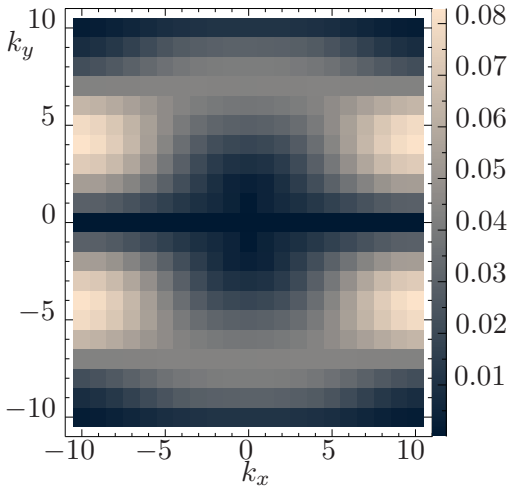

(b) $u_{x,0} = 0.1$

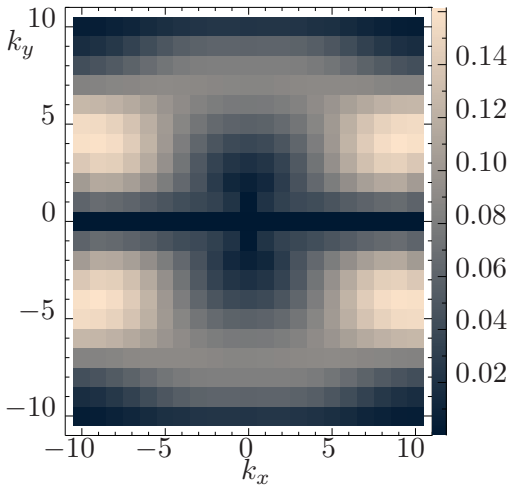

(c) $u_{x,0} = 0.2$

Figure 14. Cross correlator $R_{\mathbf{k}}(j_x, j_y)$ at different velocities measured for the Hermite norm.

the source of the Galilean invariance violations observed. Instead of using Eq. (149) we now include the velocity dependence of the equilibrium distribution in Eq. (142). The orthogonalization condition then becomes

$$\sum_i \tilde{m}_i^a(\mathbf{u})\tilde{m}_i^b(\mathbf{u})w_i\left[1+\frac{1}{\theta}\mathbf{u}.v_i+\frac{1}{2\theta^2}\left(\mathbf{u}.v_i\right)^2-\frac{1}{2\theta}\mathbf{u}.\mathbf{u}\right]=\delta^{ab} \tag{155}$$

where the velocity $\mathbf{u}(\mathbf{r},t)$ is understood to be local to the lattice site $\mathbf{r}$. We obtain a new set of transformation matrices $\tilde{m}_i^a$ by starting with the physical moments, ρ, j_x, j_y, Π_{xx-yy}, Π_{xy}, Π_{xx+yy} and perform a Gram-Schmidt orthogonalization with respect to the new scalar product

$$\sum_i a_i f_i^0 b_i. \tag{156}$$

The iterative procedure then follows

$$\hat{m}_i^a = m_i^a - \sum_{b=0}^{a-1}\tilde{m}_i^b\sum_j \tilde{m}_j^b f_j^0 m_j^a \tag{157}$$

with an intermediate normalization step

$$\tilde{m}_i^a = \frac{\hat{m}_i^a}{\sum_j \hat{m}_j^a f_j^0 \hat{m}_j^a}. \tag{158}$$

With these new matrix elements $\tilde{m}_i^a$ we can define the physically relevant moments

$$\tilde{M}^a = \sum_i \tilde{m}_i^a f_i. \tag{159}$$

This effectively transforms the collision into a reference frame of the peculiar velocities. The equilibrium values for the moments no longer contain a velocity de-

pendence in the reference frame. Explicitly the equilibrium distribution is given by the beautifully simple expression

$$\tilde{M}^{a,0} = \begin{cases} \rho & \text{if } a = 0 \\ 0 & \text{otherwise} \end{cases} \tag{160}$$

It is easy to see this explicitly since it is a direct consequence of condition Eq. (155). We have $\tilde{M}^{a,0} = \sum_i \tilde{m}_i^a f_i^0 \tilde{m}_i^0 = \rho\delta^{a0}$ because the density mode is the one vector $m_i^0 = \tilde{m}_i^0 = 1_i$. One might be concerned that choosing these local moments could have an effect on the hydrodynamic equations we simulate. Here it is important to notice that we only alter the stress moments by adding multiples of the conserved quantities to them. We have previously shown that such an operation has no effect on the hydrodynamic limit, even if the prefactors depend on the local $\mathbf{u}(\mathbf{r}, t)$ and $\rho(\mathbf{r}, t)$ [67]. We will refer to Eq. (155) simply as the "f-norm" in the following.

In order to maintain positive-definiteness of the scalar product Eq. (156) we must be mindful here of the fact that the normalization constant needs to be positive at all times. The second order expansion of the equilibrium distribution Eq. (150) we use here, however, is not. For large enough $|\mathbf{u}|$ the $f_{i,0}(\rho, \mathbf{u}, \theta) < 0$ and the orthogonalization has no solution. In Fig. Figure 15 we show the 0-transition of the second order expansion of the equilibrium distribution in the case of the D2Q9 model as a function of $\mathbf{u}$ for $\theta = \frac{1}{3}$. This plot shows the accessible velocity range. As long as our velocities do not fall outside the central area of Fig. Figure 15 the transformation matrix is guaranteed to be positive definite and the Gram-Schmidt will provide a solution.

The matrix elements $\tilde{m}_i^a(\mathbf{u}(\mathbf{r}))$ we obtain are now functions of the local velocity $\mathbf{u}(\mathbf{r})$ at lattice site $\mathbf{r} = (x, y)^T$. In principle they have to be evaluated at every lattice site during every update cycle. We have implemented a fluctuating LB simulation

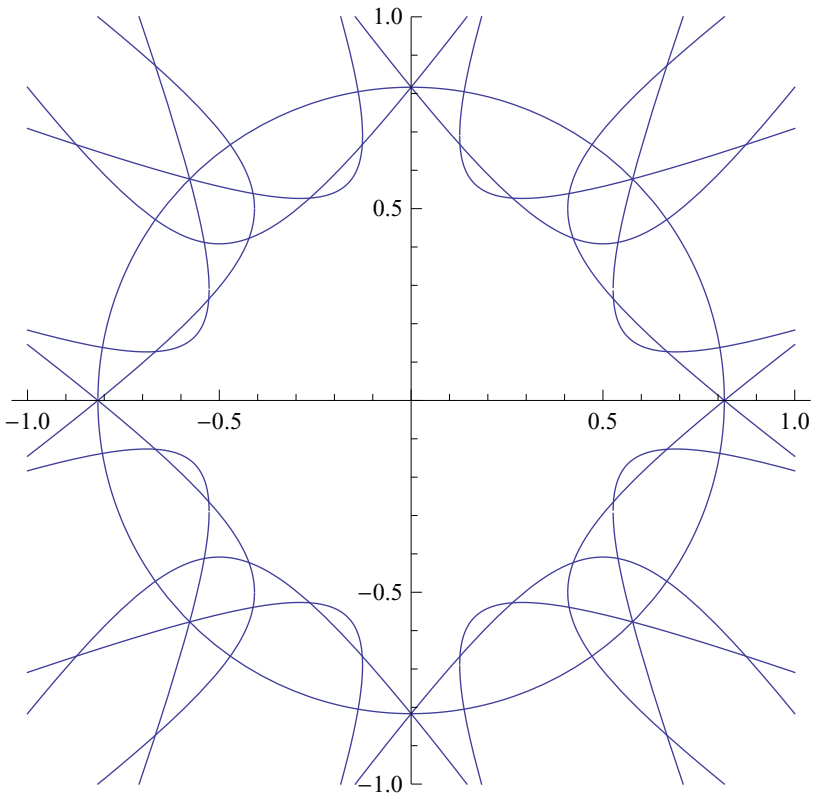

Figure 15. $f_i^0(u_{x,0}, u_y) = 0$ for all i in the case of the D2Q9 model. In the area inside the curves $f_i > 0$ for all i. Outside at least one $f_i < 0$ and consequently the orthogonalization does not find a solution.

with these matrices and the results are encouraging in that Galilean invariance violations are significantly smaller. Some results of these are shown in Figs. Figure 16, Figure 17, and Figure 18. However, even in the relatively simple D2Q9 model the matrix elements of higher order moments are polynomials of $O(\mathbf{u}^{16})$ and therefore the local evaluation of these matrix elements becomes prohibitively costly. Our test implementation used between 95% and 99% of the computation time of an update cycle in the evaluation of the local transforms.

One might think that going to the full second order expansion of f_i^0 might not be necessary and going only to first order in $\mathbf{u}$ would make the structure of the matrix elements significantly simpler. However, working with only the first order expansion introduces anisotropy effects between the different spatial axis. Removing

these effectively makes the expressions for the $\tilde{m}_i^a$ even more complicated than the regular second order expressions where our Gram-Schmidt orthogonalization renders the moments isotropic.

It is, however, not strictly necessary to calculate the transforms to machine precision. Judging from our observations of the Hermite norm implementation it is sufficient to calculate tables of the matrix elements on a velocity grid with velocities $\mathbf{u}_g(g_\alpha)$ where g_α is the grid position and use these matrix elements from a look-up table in the transforms. The benefit is practicality, the pay off is that we may not quite obtain the same amount of improvement we might expect to find otherwise. One caveat is that we lose the convenient form of the equilibrium moments in Eq. (160). In fact the projection of the moments in the representation of current local velocity to that of the nearest look-up table velocity becomes algebraically similarly complex as the calculation of the matrix elements themselves. If, however, we recognize that the matrix elements only depend on $\mathbf{u}_g$, a fixed number for a given velocity grid cell and rewrite the velocities in the equilibrium distributions as $\mathbf{u}_g + \delta\mathbf{u}$ where $\delta\mathbf{u} = \mathbf{u} - \mathbf{u}_g$ the expressions for the equilibrium moments are only second order polynomials in terms of $\delta\mathbf{u}$ with coefficients depending on the fixed $\mathbf{u_g}$. For any given look-up table velocity these coefficients can be calculated and stored just like the matrix elements of the transforms and we maintain the moments to arbitrary precision. An example of these equilibrium moments and the matrix transform elements for D2Q9 can be found in [69].

The velocity grid spacing for the look-up table can be relatively coarse. It is helpful if the entire look-up table of velocities can fit into the second level cache of the CPU the simulation is run on. In our D2Q9 test case we typically use a 51×51 grid with $-0.5 \leq u_{g,x} \leq 0.5$, $-0.5 \leq u_{g,y} \leq 0.5$, and $\Delta u_g = 0.02$. Comparing this velocity range with Fig. Figure 15 we notice that the corners of this square in

velocity space falls outside the valid $f_i^0(\mathbf{u}) > 0$ range. The matrix elements here are simply evaluated to "not a number" and the simulation fails once any one of these velocities are reached. In principle one could also catch outliers in the velocity and just choose the matrix elements for a smaller velocity. The moment projection would still function. However, this would alter the algorithm and the results would not be reliable representations of the method discussed here. For applications, especially at high velocities and low densities it will be necessary to include such an exception handling routine.

One could argue that we might as well have just calculated the matrix elements to a lower order directly, forgo the matrix element look-up tables and use the original simple equilibrium moments. However, in that case we would violate conservation laws and the calculation of the $2q^2$ matrix element polynomials is still significantly more expensive than the evaluation of $q - d - 1$ non-conserved moments in a DdQq lattice Boltzmann configuration.

To evaluate the implementation of the f-norm we perform the same measurements we did for the Hermite norm. We use a D2Q9 ideal gas simulation with periodic boundaries, and a side length of 21. In Fig. Figure 16 we observe the same $\langle \delta f_0 \delta f_0 \rangle$ correlator we did in Fig. Figure 6. We find that with the f-norm the trend actually does follow the f_0^0 prediction and within $-0.2 \leq u_{x,0} \leq 0.2$ we are in good agreement with f_0^0 but at larger speeds we find smaller but noticeable deviations. In Figs. 17, 18 we find much better agreement for all other distribution function correlation functions for the f-norm compared to the Hermite norm in Figs. 7, and 8. Again we notice very good agreement for $|u_x| \leq 0.2$.

The remaining deviations from the equilibrium distributions we find with the f-norm are not an artifact of either the look-up table method or the third order expansion of the equilibrium moments. We performed the same measurement with the

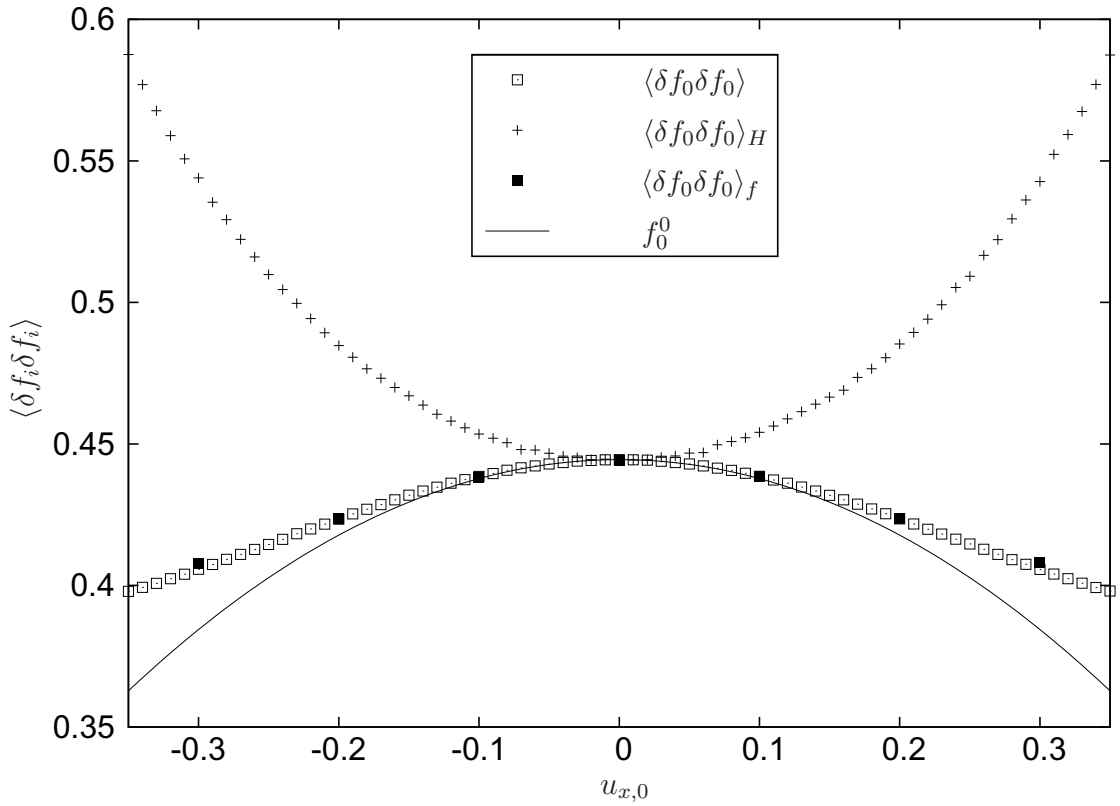

Figure 16. $\langle (\delta f_0)^2 \rangle$ in a 21×21 D2Q9 fluctuating LB simulation employing the f-norm with look-up tables. Equilibrium moments are calculated to third order. $\langle \delta f_0 \delta f_0 \rangle_f$ are data points taken from a fully local implementation that forgoes the look-up table solution. We plot the equilibrium distribution f_0^0 and the Hermite norm correlator $\langle \delta f_0 \delta f_0 \rangle_H$ for comparison.

fully locally orthogonalized set of transforms, albeit with fewer data points due to the much higher computational effort involved. $\langle \delta f_i \delta f_i \rangle_f$ in Figs. Figure 16, Figure 17, and Figure 18 indicate that the deviations from the equilibrium distributions can indeed not be explained with either the look-up table method or the cut off on the equilibrium moments as the results obtained form the look-up table method with third order equilibrium moments appears to be consistent from the fully locally orthogonalized f-norm.

Measuring the moment space correlators in the f-norm poses an interesting question. Do we measure with respect to the Hermite norm or the f-norm and in the case of the latter with respect to which velocity? To answer this question we conduct

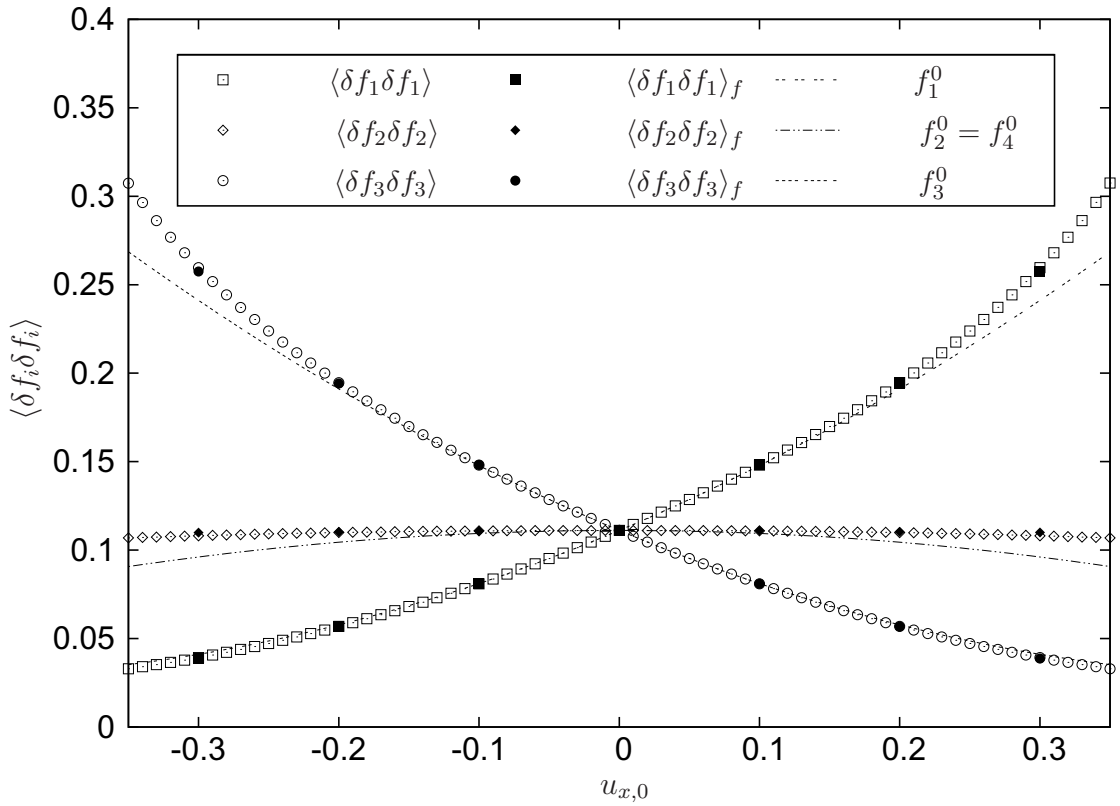

Figure 17. $\langle (\delta f_i)^2 \rangle$ for $i = 1...3$ in a 21×21 D2Q9 fluctuating LB simulation employing the f-norm. We plot f_i^0 for comparison. $\langle \delta f_i \delta f_i \rangle_f$ are data points taken from a fully local implementation that forgoes the look-up table solution. $\langle (\delta f_4)^2 \rangle$ is not shown as it appears identical to $\langle (\delta f_2)^2 \rangle$ within the scale of this plot.

a thought experiment. δM^a should be Galilean invariant for any a, in particular the momentum components. In the Hermite norm we have

$$\delta j_x = \sum_i m_i^a f_i - \sum_i m_i^a f_i^0 = \sqrt{3}\left(\rho u_x - \rho_0 u_{x,0}\right) \tag{161}$$

and for the f-norm

$$\delta \tilde{j}_x = \sum_i \tilde{m}_i^a f_i - \sum_i \tilde{m}_i^a f_i^0 = \sqrt{3}\rho\left(u_x - u_{x,0}\right). \tag{162}$$

Again $\mathbf{u}_0$ is the mean velocity in the system and $\mathbf{u}$ the local velocity at a given lattice site. If we set $\mathbf{u}_0 = 0$ we have $\delta j_x = \delta \tilde{j}_x = \sqrt{3}\rho u_x$. Introducing a constant velocity

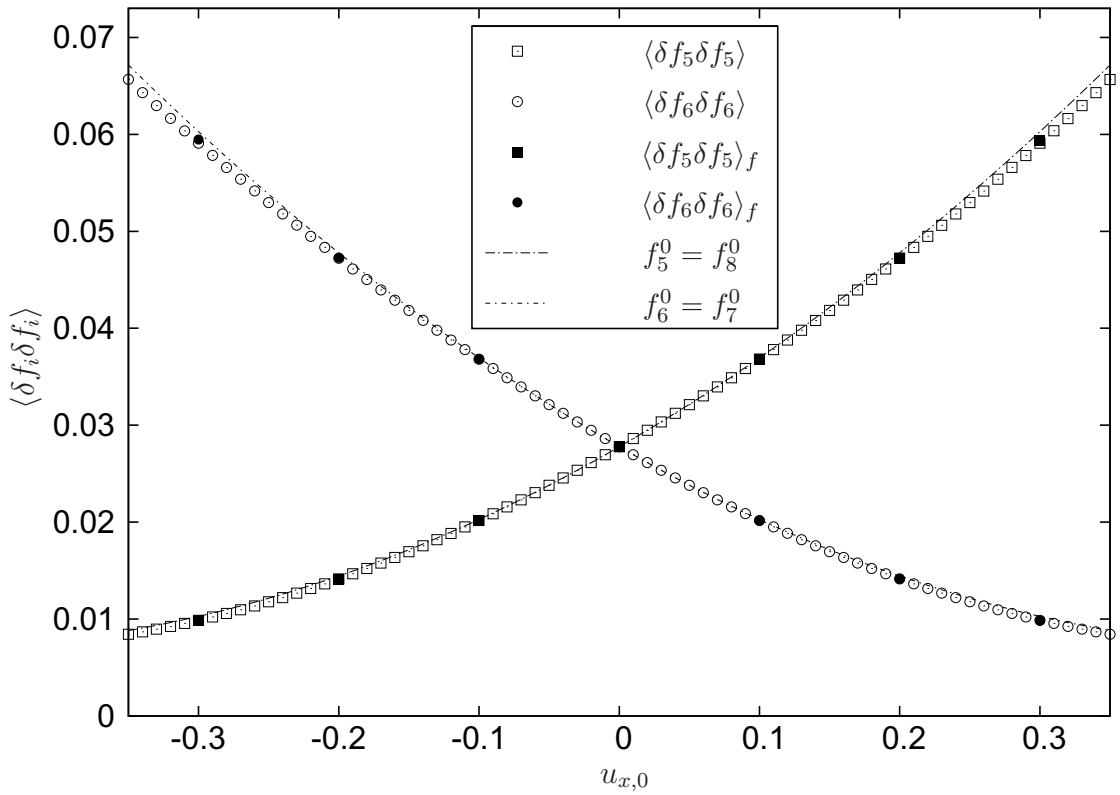

Figure 18. $\langle (\delta f_i)^2 \rangle$ for $i = 5...8$ in a 21×21 D2Q9 fluctuating LB simulation employing the f-norm. We plot f_i^0 for comparison. $\langle \delta f_i \delta f_i \rangle_f$ are data points taken from a fully local implementation that forgoes the look-up table solution. $\langle (\delta f_8)^2 \rangle$ and $\langle (\delta f_7)^2 \rangle$ are not shown as they appears identical to $\langle (\delta f_5)^2 \rangle$ and $\langle (\delta f_6)^2 \rangle$ respectively in the scale of this plot.

offset $-\mathbf{u}_0$ should leave δj_x Galilean invariant, i.e. we expect $\mathbf{u} \to \mathbf{u} - \mathbf{u}_0$. If we now interpret $\mathbf{u}_0$ as such an offset the Hermite norm is clearly not Galilean invariant under velocity offsets as it introduces an extra $u_{x,0}\,(\rho_0 - \rho)$ in Eq. (161) whereas the f-norm in Eq. (162) behaves as required. Consequently we use the f-norm as it provides the correct measurements that leave the $\delta \tilde{M}^a$ invariant under Galilean transformations. Furthermore we measure with respect to the average system velocity $\mathbf{u}_0$ and average density ρ_0. Measuring with respect to the local velocity $\mathbf{u}$ and density ρ is nonsensical as $\delta\rho = 0$ and $\delta\mathbf{j} = 0$ in this case. We thus use the f-norm such that $\tilde{m}_i^a \tilde{m}_i^b \langle f_i \rangle = \delta^{ab}$ where we make the approximation of Eq. (135) $\langle f_i \rangle = f_i^0(\rho_0, \mathbf{u_0})$.

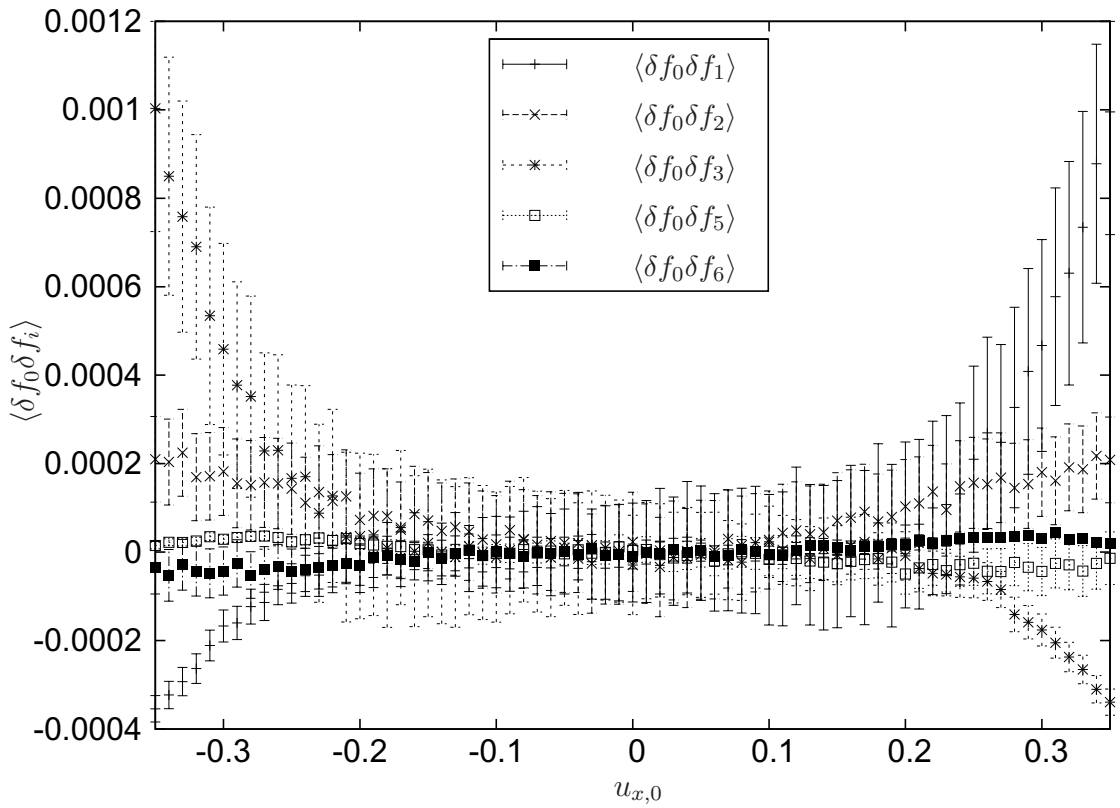

Figure 19. $\langle \delta f_0 \delta f_i \rangle$ for $i = 1...8$ in a 21×21 D2Q9 fluctuating LB simulation employing the f-norm.

Much like the distribution function correlators the moment correlators $\langle (\delta M^a)^2 \rangle$ shown in Fig. Figure 20 exhibit significant improvement compared to those of the Hermite norm in Fig. Figure 10. This improvement is smaller than the general trend of the distribution function correlators would imply for some modes. In particular the $\langle (\delta\tilde{\rho})^2 \rangle$, $\langle (\delta\tilde{\Pi}_{xx-yy})^2 \rangle$, and $\langle (\delta\tilde{j}_y)^2 \rangle$ correlators deviate significantly for larger u_x. Their overall decrease is about 1/3 compared to the Hermite norm. To make a valid comparison between moment correlators computed in the f-norm and the Hermite norm one needs to ensure that for both measurements the moments are obtained in the same way. We therefore measure the moments obtained in a Hermite norm simulation with the f-norm evaluated at $\mathbf{u}_0$ in Fig. Figure 21. We observe that for all moments but $\langle \delta\tilde{\rho}\delta\tilde{\rho} \rangle$ and $\langle \delta\tilde{j}_y\delta\tilde{j}_y \rangle$ the deviations are larger than those measured in the Hermite norm.

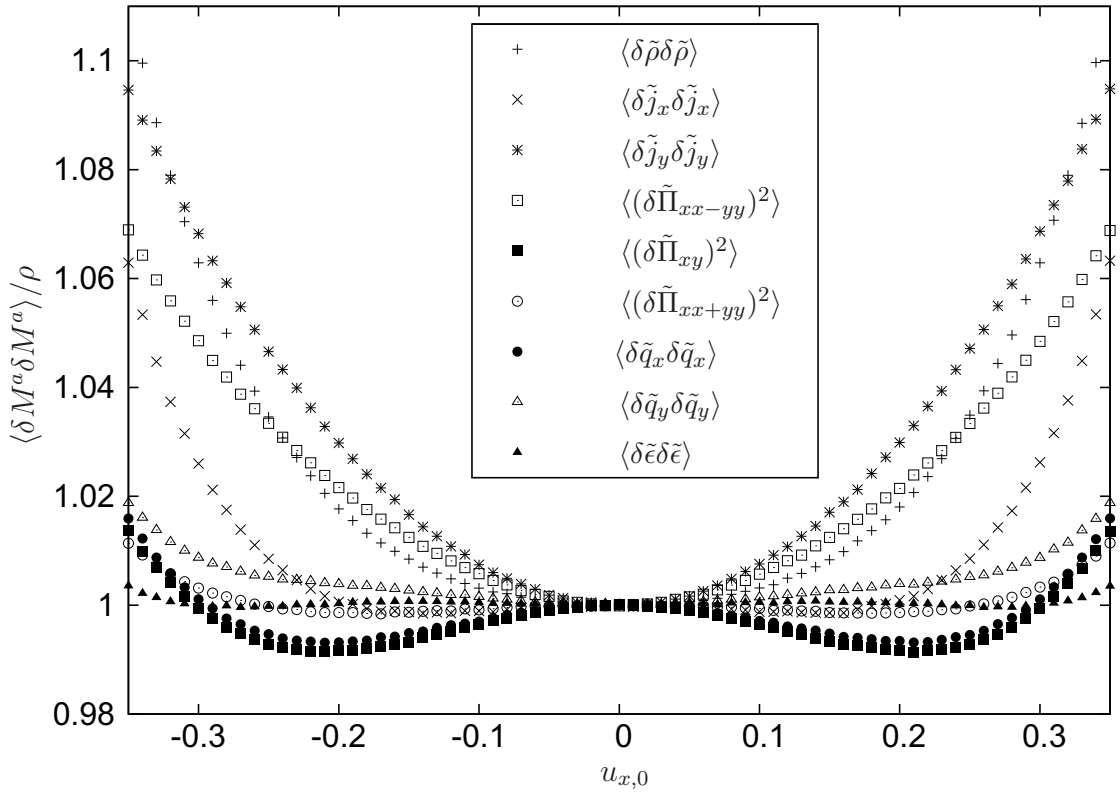

Figure 20. Correlators $\langle \delta\tilde{M}^a \delta\tilde{M}^a \rangle$ normalized to ρ according to Eq. (143) in a 21×21 D2Q9 fluctuating LB simulation employing the f-norm.

As a brief excursion to validate isotropy we also measured the static structure factor as a function of the angle α for both, the Hermite and the f-norm. In Fig. Figure 22 we observe that both Hermite and f-norm are not entirely isotropic. However, the improvement of the f-norm persists. The step like behavior in the data for the f-norm actually exhibits an interesting detail: These steps are observed only at large densities and they occur only near the boundary of a look-up table cell. The short radial lines in Fig. Figure 22 b) mark the position of the steps in a) and they coincide nicely with the points where the velocities chosen for a) match with the indicated look-up table boundaries in b). This effect is only visible for sufficiently large densities and can be explained if we recognize that by virtue of Eq. (147) $\langle \delta u_\alpha \delta u_\alpha \rangle \approx \frac{\langle \delta j_\alpha \delta j_\alpha \rangle}{\rho} \propto \frac{1}{\rho}$ can become significantly smaller than the look-up table velocity grid. At this stage

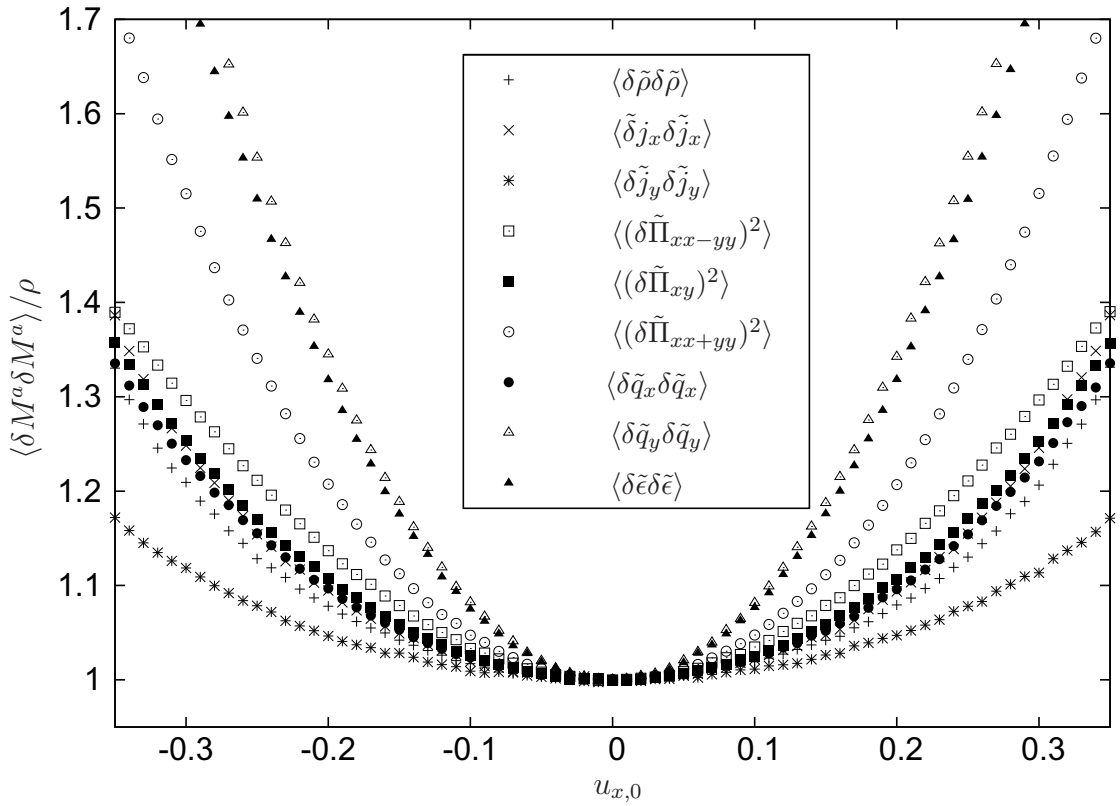

Figure 21. Correlators $\langle \delta\tilde{M}^a \delta\tilde{M}^a \rangle$ normalized to ρ according to Eq. (143) measured in a 21×21 D2Q9 fluctuating LB simulation employing the Hermite norm.

our velocities will stay well within the confines of one look-up table cell. If desired this can easily be remedied by using a higher resolution in the velocity look-up table.

Linear and quadratic fit coefficients for all moment correlators $\langle \delta\tilde{M}^a \delta\tilde{M}^b \rangle$ in Fig. Figure 23 show significant improvement as well. We notice that in particular the coefficients l that apply to those off-diagonal correlators that have a linear dependence on u_x at least a factor of 13 smaller than those measured in the Hermite norm case shown in Fig. Figure 11 (a). We also observe a decrease of the quadratic term q but in line with the observations of Fig. Figure 20 the coefficients corresponding to some correlators decrease less compared to the ones observed in the Hermite norm in Fig. Figure 11 (b): $\langle (\delta\tilde{\rho})^2 \rangle$ from 1.9 to 0.47, $\langle (\delta\tilde{\Pi}_{xx-yy})^2 \rangle$ from 1.6 to 0.54, and $\langle (\delta\tilde{j}_y)^2 \rangle$ from 1.14 to 0.75.

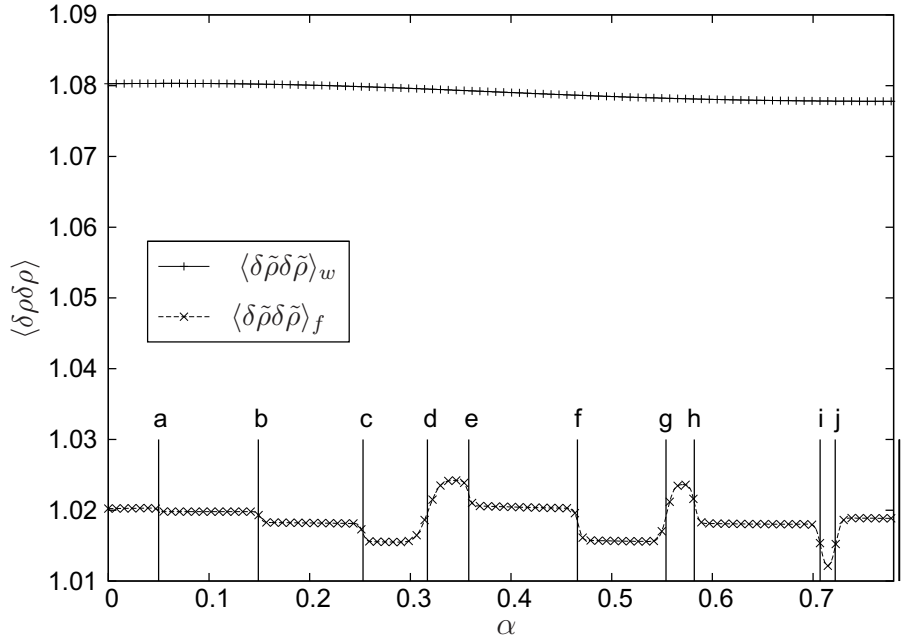

(a) $\langle\delta\rho\delta\rho\rangle$

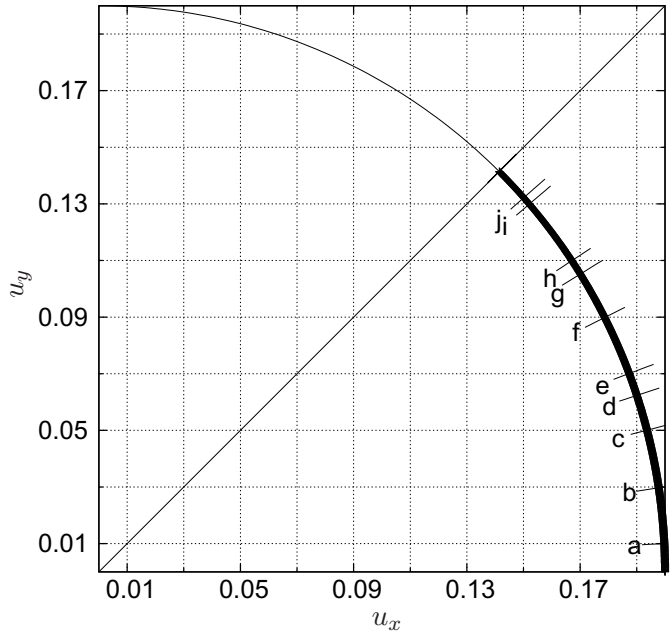

(b) look-up table boundaries intersect with $\sqrt{\mathbf{u}^2 - u_x^2}$

Figure 22. a) Static structure factor $\langle\delta\rho\delta\rho\rangle$ as function of angle α at a velocity of $u = 0.2$ for both, Hermite and f-norm. b) Intersections of the look-up table boundaries with the $\mathbf{u}$ values used in a). All measurements performed on a 21×21 D2Q9 simulation with $\rho = 10^7$ with a look-up table spacing of $\delta u_g = 0.02$. The roman letters indicate the corresponding intersections of the velocity vector with the look-up table boundaries.

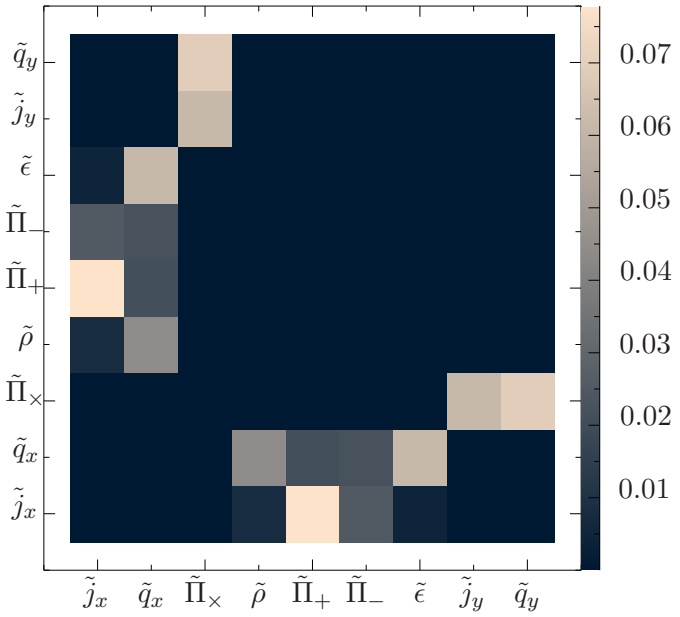

(a) Linear coefficient l, f-norm

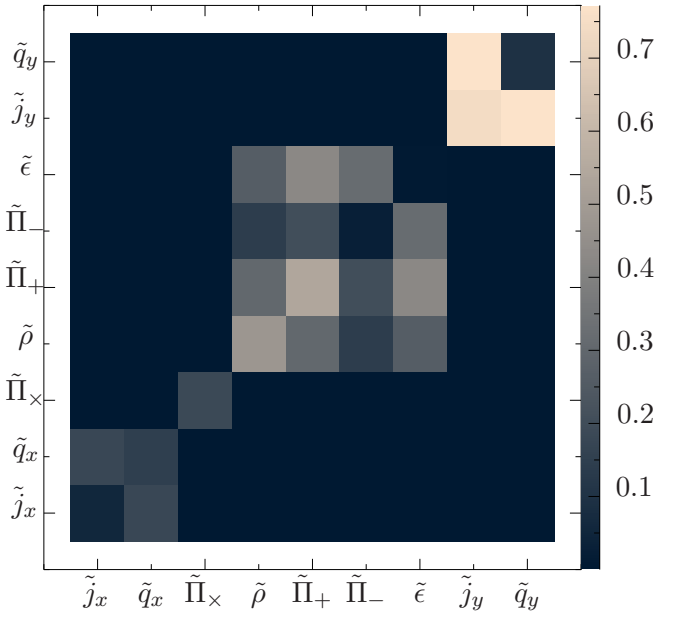

(b) Quadratic coefficient q, f-norm

Figure 23. Linear and quadratic coefficient l and q of all 81 (45 unique) correlators as a result of fitting $\langle \delta\tilde{M}^a \delta\tilde{M}^b \rangle(u_{x,0}) - \delta^{ab}$ to $l u_{x,0} + q u_{x,0}^2$. Brighter color indicates larger coefficients. Moments were reordered to visually identify correlations better. To accommodate for symbol size the stress moments were simplified: $\tilde{\Pi}_\times = \tilde{\Pi}_{xy}, \tilde{\Pi}_- = \tilde{\Pi}_{xx-yy}, \tilde{\Pi}_+ = \tilde{\Pi}_{xx+yy}$). The coefficient at position (0, 1) in image (a) would correspond to linear portion of the $\langle \delta\tilde{j}_x \delta\tilde{q}_x \rangle$ correlator. Coefficients were measured on a 21×21 D2Q9 simulation employing the f-norm with look-up tables, $\delta u_g = 0.02$. Fit range used was $-0.25 <= u_x <= 0.25$.

These findings are confirmed by the structure factor plots for the f-norm in Figs. Figure 24, Figure 25, and Figure 26 which for non-vanishing fixed velocity $u_{x,0}$ are significantly smaller than the one measured for the Hermite norm at the same velocity in Figs. Figure 12, Figure 13, and Figure 14.

We can conclude that employing the f-norm significantly reduces the Galilean invariance effects observed on the Hermite norm implementation. The look-up tables provide a practically feasible approach to implementing the f-norm at a performance loss of about 20 %. All the measurements here were performed on a single CPU.

4.6. Conclusion and Outlook

The current standard implementation of thermal fluctuations in an isothermal ideal gas was tested for Galilean invariance violations. We found that with non zero average velocity the moment space covariance matrix of Eq. (143) is neither diagonal nor are the diagonal elements unity as predicted and required by the derivation of the FDT in both [13] and [36]. We identified an approximation in the orthogonality condition that defines the moment space transforms Eq. (142) as the likely source of the Galilean invariance violations as it directly removes an otherwise necessary velocity dependence from the moment space transforms. The approximation allows for the use of Hermite norm to define the moment space transforms. However, to recover Galilean invariance at least to some degree requires the matrix transforms to be locally velocity dependent, i.e. unique to every lattice site and the Hermite norm is no longer applicable. This led us to introduce a novel variant of the lattice Boltzmann method which effectively transforms the moments in a reference frame of peculiar velocities. Our numerical tests on a standard D2Q9 lattice showed that Galilean invariance can be significantly improved using this method. However, on a fundamental level any lattice Boltzmann method will not be entirely Galilean invariant because the fixed lattice provides a special reference frame. This effect turns up in some velocity moments

of the equilibrium distribution [70, 71, 72]. By enlarging the velocity set, the order of the moment where Galilean invariance is violated can be made arbitrarily large. Typically lattice Boltzmann implementations are considered Galilean invariant when no Galilean invariance violating terms remain in the hydrodynamic equations. We compared our results to the previous implementations by Adhikari and Dünweg [13, 36] who use a standard lattice and equilibrium distribution. These are in themselves not entirely Galilean invariant as terms of order $\rho\mathbf{u}^2$ remain, leading to some violation of Galilean invariance. Our new algorithm, however, is formulated in a velocity set independent form and can therefore also be implemented for velocity sets that lead to formally Galilean invariant lattice Boltzmann methods [71, 30]. It is possible that remaining Galilean invariance violations observed for our new method may be further reduced by using a formally Galilean invariant lattice Boltzmann method. We find that using the local fully velocity dependent f-norm to machine precision in a straight forward manner to be computationally impractical. Evaluating the individual matrix elements leads to an overhead in computational cost of $> 2000\%$ in evaluating the individual matrix elements. However, as the Galilean invariance violations scale quadratically for most moments it is feasible to generate look-up tables for the matrix elements on a velocity grid. This requires to projection of the equilibrium moments into the look-up table reference velocity. This look-up table approach provides comparable benefits to the locally orthogonalized transforms but at only a 20% loss of computation time. All the simulations presented here were performed in a example D2Q9 implementation. However, all calculations and considerations discussed can easily be generalized to other models. We provide a Mathematica notebook [69] that contains the necessary calculations done for the D2Q9 model used here. This new method is potentially important for non-equilibrium situations when locally varying flow fields exist which is the standard realm of lattice Boltzmann simulations.

The authors would like to thank Paul Dellar, Markus Gross and Eric Foard for helpful and insightful discussion. This work has been funded, in part, by the ND EPSCoR SEED grand.

4.7. Hermite Norm D2Q9

For D2Q9 the equilibrium distribution employed is given by Eq. (150) with $\theta = 1/3$

$$f_i^0(\rho, \mathbf{u}, \theta) = \rho w_i \left[1 + 3\mathbf{u}.v_i + \frac{9}{2}\left(\mathbf{u}.v_i\right)^2 - \frac{3}{2}\mathbf{u}.\mathbf{u}\right]. \tag{163}$$

The weights are given by

$$w_i = \begin{cases} \frac{4}{9} & \text{if } i = 0 \\ \frac{1}{9} & \text{if } i = 1, 2, 3, 4 \\ \frac{1}{36} & \text{if } i = 5, 6, 7, 8 \end{cases} \tag{164}$$

In the case of the simple Hermite norm Eq. (149) it is feasible to show the transformation matrices. The forward transform reads

$$\sum_i m_i^a f_i = M^a =$$

$$\begin{pmatrix} 1 & 1 & 1 & 1 & 1 & 1 & 1 & 1 & 1 \\ 0 & \sqrt{3} & 0 & -\sqrt{3} & 0 & \sqrt{3} & -\sqrt{3} & -\sqrt{3} & \sqrt{3} \\ 0 & 0 & \sqrt{3} & 0 & -\sqrt{3} & \sqrt{3} & \sqrt{3} & -\sqrt{3} & -\sqrt{3} \\ 0 & \frac{3}{2} & \frac{-3}{2} & \frac{3}{2} & \frac{-3}{2} & 0 & 0 & 0 & 0 \\ 0 & 0 & 0 & 0 & 0 & 3 & -3 & 3 & -3 \\ -1 & \frac{1}{2} & \frac{1}{2} & \frac{1}{2} & \frac{1}{2} & 2 & 2 & 2 & 2 \\ 0 & -\sqrt{\frac{3}{2}} & 0 & \sqrt{\frac{3}{2}} & 0 & \sqrt{6} & -\sqrt{6} & -\sqrt{6} & \sqrt{6} \\ 0 & 0 & -\sqrt{\frac{3}{2}} & 0 & \sqrt{\frac{3}{2}} & \sqrt{6} & \sqrt{6} & -\sqrt{6} & -\sqrt{6} \\ \frac{1}{2} & -1 & -1 & -1 & -1 & 2 & 2 & 2 & 2 \end{pmatrix} \cdot f_i = \begin{pmatrix} \rho \\ j_x \\ j_y \\ \Pi_{xx-yy} \\ \Pi_{xy} \\ \Pi_{xx+yy} \\ q_x \\ q_y \\ \epsilon \end{pmatrix} \cdot \tag{165}$$

Likewise the back transform from moment space to velocity space is given by

$$\sum_a n_i^a M^a = \begin{pmatrix} \frac{4}{9} & 0 & 0 & 0 & 0 & \frac{-4}{9} & 0 & 0 & \frac{2}{9} \\ \frac{1}{9} & \frac{1}{3\sqrt{3}} & 0 & \frac{1}{6} & 0 & \frac{1}{18} & \frac{-1}{3\sqrt{6}} & 0 & \frac{-1}{9} \\ \frac{1}{9} & 0 & \frac{1}{3\sqrt{3}} & \frac{-1}{6} & 0 & \frac{1}{18} & 0 & \frac{-1}{3\sqrt{6}} & \frac{-1}{9} \\ \frac{1}{9} & \frac{-1}{3\sqrt{3}} & 0 & \frac{1}{6} & 0 & \frac{1}{18} & \frac{1}{3\sqrt{6}} & 0 & \frac{-1}{9} \\ \frac{1}{9} & 0 & \frac{-1}{3\sqrt{3}} & \frac{-1}{6} & 0 & \frac{1}{18} & 0 & \frac{1}{3\sqrt{6}} & \frac{-1}{9} \\ \frac{1}{36} & \frac{1}{12\sqrt{3}} & \frac{1}{12\sqrt{3}} & 0 & \frac{1}{12} & \frac{1}{18} & \frac{1}{6\sqrt{6}} & \frac{1}{6\sqrt{6}} & \frac{1}{18} \\ \frac{1}{36} & \frac{-1}{12\sqrt{3}} & \frac{1}{12\sqrt{3}} & 0 & \frac{-1}{12} & \frac{1}{18} & \frac{-1}{6\sqrt{6}} & \frac{1}{6\sqrt{6}} & \frac{1}{18} \\ \frac{1}{36} & \frac{-1}{12\sqrt{3}} & \frac{-1}{12\sqrt{3}} & 0 & \frac{1}{12} & \frac{1}{18} & \frac{-1}{6\sqrt{6}} & \frac{-1}{6\sqrt{6}} & \frac{1}{18} \\ \frac{1}{36} & \frac{1}{12\sqrt{3}} & \frac{-1}{12\sqrt{3}} & 0 & \frac{-1}{12} & \frac{1}{18} & \frac{1}{6\sqrt{6}} & \frac{-1}{6\sqrt{6}} & \frac{1}{18} \end{pmatrix} \cdot M^a = f_i \qquad (166)$$

where $n_i^a = m_i^a w_i$ The corresponding equilibrium moments $M^{a,0}$ are obtained directly by applying the forward transform to the equilibrium distribution. In the Hermite norm we find

$$\begin{aligned} \rho &= M^{0,0} = \rho \\ j_x &= M^{1,0} = \sqrt{3}\rho u_x \\ j_y &= M^{2,0} = \sqrt{3}\rho u_y \\ \Pi_{xx-yy} &= M^{3,0} = \tfrac{3}{2}\rho(u_x^2 - u_y^2) \\ \Pi_{xy} &= M^{4,0} = 3\rho u_x u_y \\ \Pi_{xx+yy} &= M^{5,0} = \tfrac{3}{2}\rho(u_x^2 + u_y^2) \\ q_x &= M^{6,0} = 0 \\ q_y &= M^{7,0} = 0 \\ \epsilon &= M^{8,0} = 0. \end{aligned} \qquad (167)$$

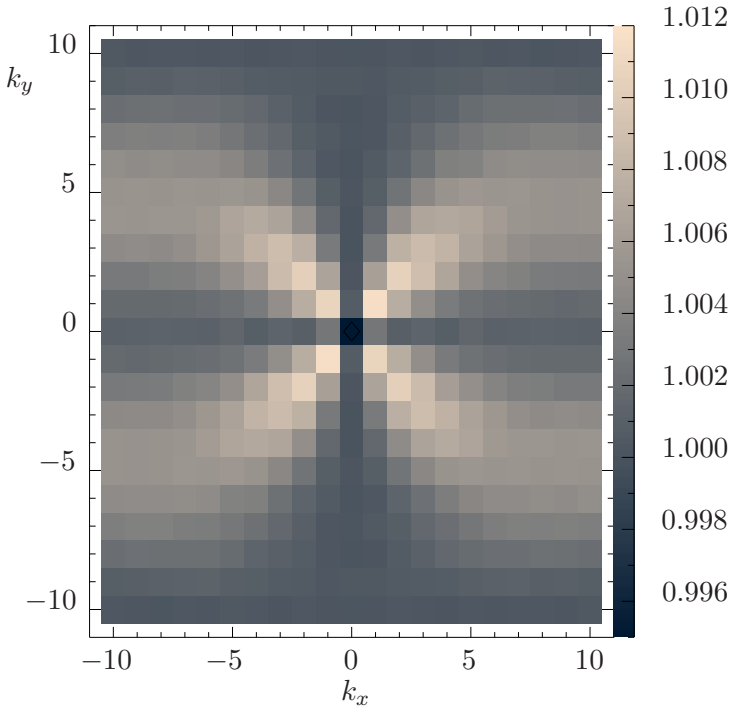

(a) $u_x = 0.1$

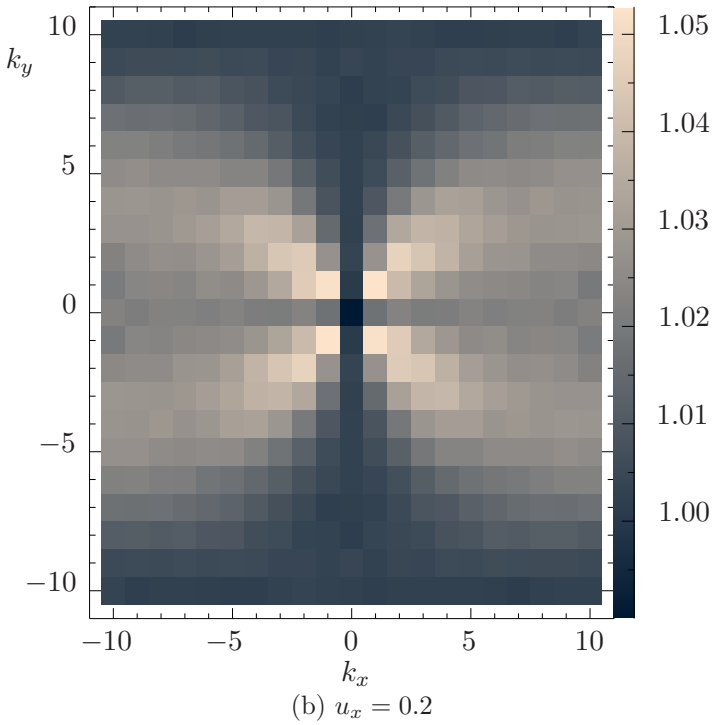

(b) $u_x = 0.2$

Figure 24. Static structure factor $S_{\mathbf{k}}(\tilde{\rho})$ at different velocities measured for the f-norm with the look-up table and $\Delta u_g = 0.02$.

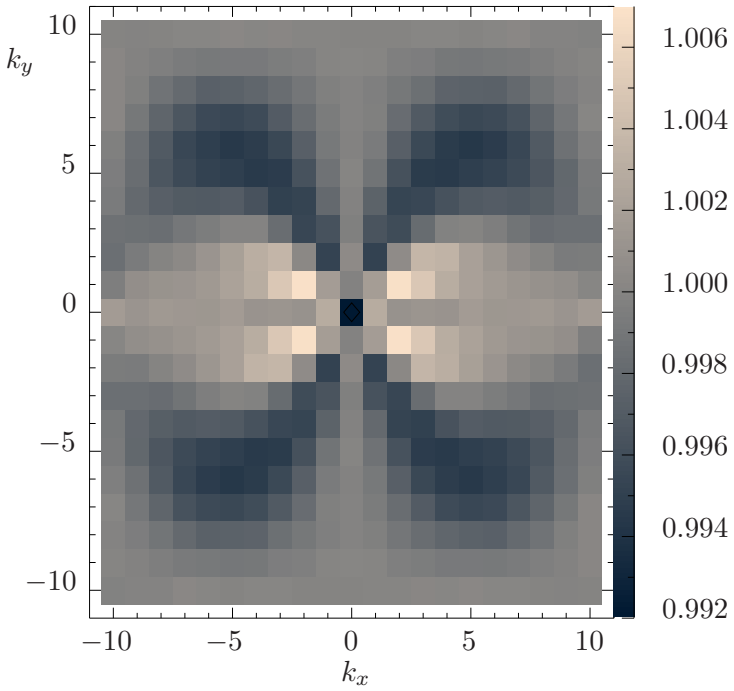

(a) $u_x = 0.1$

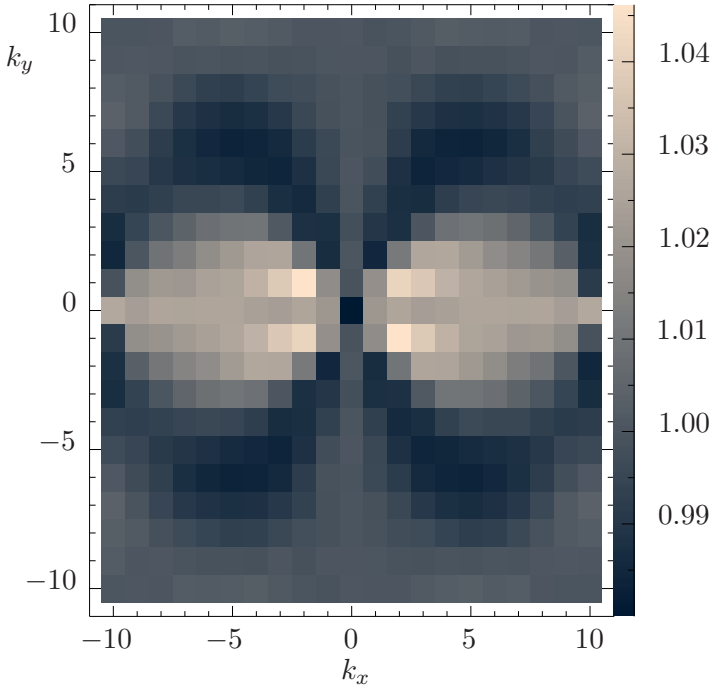

(b) $u_x = 0.2$

Figure 25. Static structure factor $S_{\mathbf{k}}(\tilde{j}_x)$ at different velocities measured for the f-norm with the look-up table and $\Delta u_g = 0.02$.

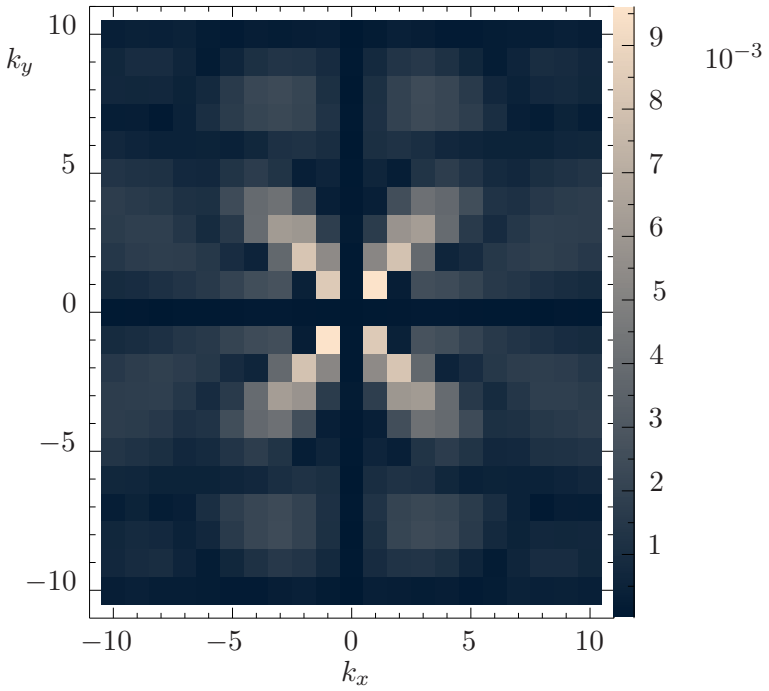

(a) $u_x = 0.1$

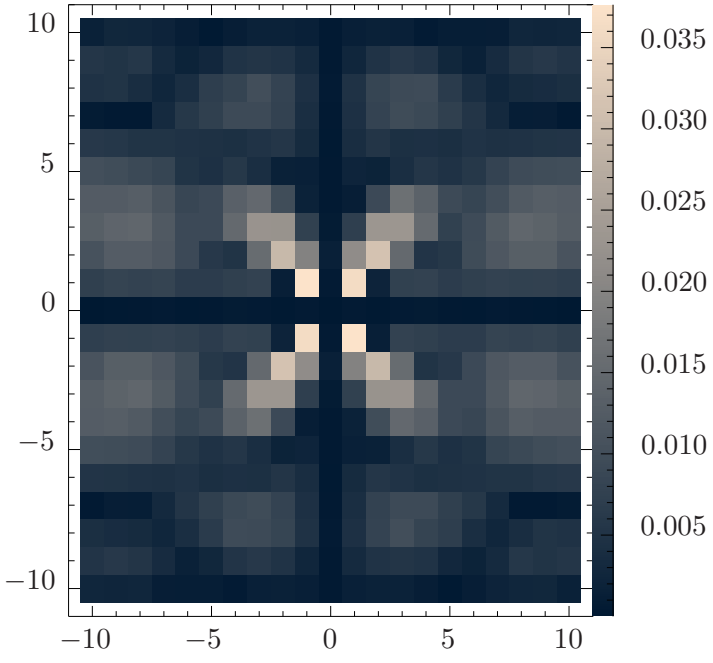

(b) $u_x = 0.2$

Figure 26. Cross correlator $R_{\mathbf{k}}(\tilde{j}_x, \tilde{j}_y)$ at different velocities measured for the f-norm with the look-up table and $\Delta u_g = 0.02$.

5. THE LOCAL FLUCTUATING BGK COLLISION AND ITS EFFECTS AT LOW NUMBER DENSITY

5.1. Local Fluctuations

The Langevin treatment of the linearized Boltzmann equation (see section 1) yields a fluctuation-dissipation theorem for a fluctuating ideal gas in equilibrium. This discussion for the case of a vanishing mean velocity $\mathbf{u} = 0$ is the theoretical foundation for the discussion brought forward in the original Adhikari paper [13] and all other subsequent discussions of fluctuating lattice Boltzmann methods [36, 63, 25]. In chapter 4 we extended this treatment to non-vanishing mean velocities but the derivation presented there is also based on the Langevin treatment of the linearized Boltzmann equation and strictly speaking only valid for the global mean velocity. We found good agreement with this theory in our simulations where we also assumed a global non-vanishing mean velocity. All of the current fluctuating lattice Boltzmann methods base their fluctuation implementations on the global FDT and add a noise term according to Eq. (132) chosen from a Gaussian distribution with variance given by Eq. (147)

$$\xi^a = \frac{1}{\tau^a}\sqrt{\rho\,(2\tau^a - 1)}. \tag{168}$$

In the previous chapter we furthermore argue that the multi-relaxation time transforms used for the moment representation in which the collision is performed are to be velocity dependent such that Eq. (142)

$$\sum_i m_i^a m_i^b \frac{f_i^0(\rho, \mathbf{u})}{\rho} = \delta^{ab} \tag{169}$$

is fulfilled. Following the Langevin theory the density used in Eqs. (168, 169) and the velocity used in the expression for Eq. (169) are to be the equilibrium values. In

the context of the lattice Boltzmann method the limitation to a global equilibrium state is, however, undesirable. In most interesting scenarios the system will not be in equilibrium and then the Langevin theory is, strictly speaking, not applicable.

In fact, if one carefully compares the collision operator of the BGK-approximation Eq. (24)

$$\Omega_{i,\mathrm{BGK}}(f_i) = \sum_i \Lambda_{ij,BGK} \left[f_j^0(\rho(\mathbf{x},t), \mathbf{u}(\mathbf{x},t), \theta) - f_j(\mathbf{x},t) \right] \tag{170}$$

with the one used in the linearized Boltzmann equation Eq. (50)

$$\Omega_{i,\mathrm{linBol}}(f_i) = \sum_i \Lambda_{ij,linBol} \bar{f}_j h_j(\mathbf{x},t) = \sum_i \Lambda_{ij} \left[f_j^0(\bar{\rho}, \bar{\mathbf{u}}, k_b T) - f_j(\mathbf{x},t) \right] \tag{171}$$

it becomes apparent that they differ fundamentally with respect to which distribution function the current local distribution is relaxed to. Here it is implied that the global mean of the distribution function $\bar{f}_i$ in equilibrium is the Maxwell Boltzmann distribution in the second order expansion of Eq. (60) in terms of the equilibrium values of the density $\bar{\rho} = \langle \sum_i f_i \rangle$, the velocity $\bar{u}_\alpha = \frac{1}{\bar{\rho}} \langle \sum_i f_i v_{i\alpha} \rangle$ and the temperature $k_B T$.

While the BGK collision $\Omega_{i,\mathrm{BGK}}$ relaxes towards the local distribution function $f_i^0(\rho(\mathbf{x},t), \mathbf{u}(\mathbf{x},t), \theta)$, the collision operator of the linearized Boltzmann equation, $\Omega_{i,\mathrm{linBol}}$ relaxes towards the global equilibrium distribution $\bar{f}_i = \bar{f}_i(\bar{\rho}, \bar{\mathbf{u}}, k_B T) = \langle f_i \rangle$. This key difference is not discussed in the literature on the fluctuating lattice Boltzmann method [13, 36, 63]. Furthermore it should be noted that the collision matrix $\Lambda_{ij,linBol}$ must have vanishing eigenvalues for the conserved degrees of freedom. This constraint is not necessary in the BGK case for $\Lambda_{ij,BGK}$ as the local equilibrium distribution is generated from the local values of $\rho, \mathbf{u}, \theta$ and thus the collision will not change these conserved quantities. Finally, here we introduce the two different con-

cepts for the temperature, the mean system temperature k_BT, and the temperature local to a lattice site at which a collision takes place, θ. In the context of isothermal lattice Boltzmann methods these are usually not distinguished but in the following section we find that one should tread carefully when discussing temperature, particularly at low densities.

The expectation value of the difference between the local and global equilibrium distributions can be calculated and is relevant for the derivation of the FDT as the term δM^0 needs to vanish to derive the FDT in paper 4 at Eq. (139).

5.1.1. The Meaning of Temperature

In order to calculate this difference we first we need to discuss the difference between the system temperature k_BT and the local lattice Boltzmann temperature θ for which in our isothermal implementations D2Q9 implementations we have $\theta = \frac{1}{3}$ as discussed in section 1. The definition of the mean temperature in the system is

$$\bar{\rho} k_B T = \frac{1}{D} \left\langle \sum_i f_i \left(v_{i\alpha} - \bar{u}_\alpha \right)^2 \right\rangle = \frac{1}{D} \left\langle \sum_i \left(f_i^0 + \delta f_i \right) \left(v_{i\alpha} - \bar{u}_\alpha \right)^2 \right\rangle \tag{172}$$

where we used $f_i = \bar{f}_i + \delta f_i$. In equilibrium $\langle \delta f_i \rangle$ vanishes and thus $\bar{f}_i = \langle f_i^0 \rangle$. We can add and subtract the local velocity in u_α Eq. (172) such that

$$\begin{aligned} \bar{\rho} k_B T &= \frac{1}{D} \left\langle \sum_i f_i^0 \left(v_{i\alpha} - \bar{u}_\alpha \right)^2 \right\rangle \\ &= \frac{1}{D} \left\langle \sum_i f_i^0 \left(v_{i\alpha} - u_\alpha + u_\alpha - \bar{u}_\alpha \right)^2 \right\rangle \\ &= \frac{1}{D} \left\langle \sum_i f_i^0 \left[\left(v_{i\alpha} - u_\alpha \right)^2 + 2 \left(v_{i\alpha} - u_\alpha \right) \left(u_\alpha - \bar{u}_\alpha \right) + \left(u_\alpha - \bar{u}_\alpha \right)^2 \right] \right\rangle . \end{aligned} \tag{173}$$

The middle term vanishes because $\delta u = (u_\alpha - \bar{u}_\alpha)$ is a constant with respect to summation over i that can be pulled out of the sum. We then obtain $(u_\alpha - \bar{u}_\alpha) \sum_i f_i^0 (v_{i\alpha} - u_\alpha)$ which vanishes as $\sum f_i^0 (v_{i\alpha} - u_\alpha) = j_\alpha - \rho u_\alpha = 0$. We are left with

$$\begin{aligned} \bar{\rho} k_B T &= \frac{1}{D} \left\langle \sum_i f_i^0 \left(v_{i\alpha} - u_\alpha\right)^2 + \sum_i f_i^0 (\delta u)^2 \right\rangle \\ &= \frac{1}{D} \left(D\bar{\rho}\theta + \langle \rho \left(\delta u_\alpha\right)^2 \rangle \right). \end{aligned} \tag{174}$$

Now, we estimate $\langle \rho \left(\delta u_\alpha\right)^2 \rangle = \langle \frac{(\delta j_\alpha)^2}{\rho} \rangle \approx \frac{\langle (\delta j_\alpha)^2 \rangle}{\bar{\rho}} = D \frac{\bar{\rho} k_B T}{\bar{\rho}}$ and find the final result

$$\bar{\rho} k_B T = \frac{1}{D} \left(D\bar{\rho}\theta + D k_B T \right). \tag{175}$$

We have thus recovered that the kinetic temperature $k_b T$ is based on an unbiased estimator [73, Chapter 31] of the variance of the velocity Eq. (20) and relate the lattice Boltzmann temperature θ to the equilibrium temperature $k_B T$

$$k_B T = \theta \frac{\bar{\rho}}{\bar{\rho} - 1}. \tag{176}$$

We find good agreement with this prediction in our lattice Boltzmann simulation in Fig. 27. We note that the agreement is better with a local f-norm implementation as opposed to the Hermite norm.

5.2. The Expectation Value of the Distribution Function

The expectation value of the equilibrium distribution

$$f_i^0(\mathbf{x}, t) = \rho w_i \left(1 + \frac{1}{\theta} v_{i\alpha} u_\alpha + \frac{1}{2\theta^2} v_{i\alpha} v_{i\beta} u_\alpha u_\beta - \frac{1}{2\theta} u_\alpha u_\alpha \right) \tag{177}$$

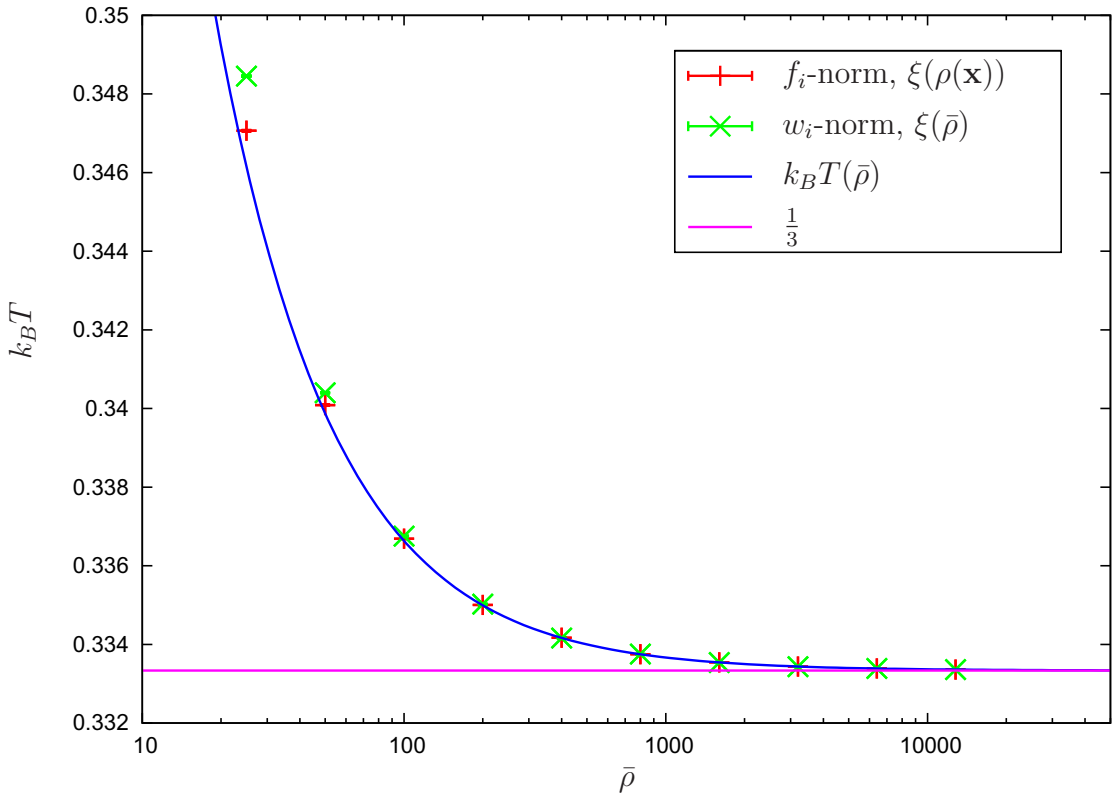

Figure 27. Measured temperature T as a function of mean density ρ_0 in a fluctuating lattice Boltzmann simulation at lattice Boltzmann temperature $\theta = \frac{1}{3}$. We measured with entirely local (f-norm, $\xi(\rho(\mathbf{x}))$ and global(Hermite norm, $\xi(\bar{})$) updates.

as measured in the simulation with fluctuations in the localized transform can be written as

$$\bar{f}_i^0 = \langle f_i^0 \rangle = w_i \left(\langle \rho \rangle + \frac{\langle \rho u_\alpha \rangle}{\theta} v_{i\alpha} + \frac{\langle \rho u_\alpha u_\beta \rangle}{2\theta^2} v_{i\alpha} v_{i\beta} - \frac{\langle \rho u_\alpha u_\alpha \rangle}{2\theta} \right). \tag{178}$$

As $j_\alpha = \rho u_\alpha$ we can write

$$\begin{aligned} \langle \rho u_\alpha u_\beta \rangle = \left\langle \frac{j_\alpha j_\beta}{\rho} \right\rangle &\approx \frac{\langle j_\alpha j_\beta \rangle}{\bar{\rho}} = \frac{\langle (\bar{j}_\alpha - \delta j_\alpha)(\bar{j}_\beta - \delta j_\beta) \rangle}{\bar{\rho}} \\ &= \frac{1}{\bar{\rho}} \left(\bar{j}_\alpha \bar{j}_\beta + \bar{j}_\alpha \langle \delta j_\beta \rangle + \bar{j}_\beta \langle \delta j_\alpha \rangle + \langle \delta j_\alpha \delta j_\beta \rangle \right) \\ &= \frac{\bar{j}_\alpha \bar{j}_\beta + \bar{\rho} k_B T \delta_{\alpha\beta}}{\bar{\rho}} \end{aligned} \tag{179}$$

where we use $\langle \delta j_\alpha \rangle = 0$. We also understand that the temperature has to be adjusted such that $k_B T = \frac{\bar{\rho}}{\bar{\rho}-1}\theta$ to accomodate the unbiased estimator property of the temperature. The corrected expectation value of the distribution functions thus becomes

$$\bar{f}_i = w_i \left[\bar{\rho} + \frac{\bar{j}_\alpha v_{i\alpha}}{\theta} + \frac{\bar{j}_\alpha \bar{j}_\beta v_{i\alpha} v_{i\beta}}{2\bar{\rho}\theta^2} + \frac{k_B T}{2\theta^2} v_i^2 - \frac{\bar{j}_\alpha \bar{j}_\alpha}{\bar{\rho} 2\theta} - \frac{k_B T}{2\theta} D \right] \tag{180}$$

$$= \bar{\rho} w_i \left[1 + \frac{\bar{u}_\alpha v_{i\alpha}}{\theta} + \frac{\bar{u}_\alpha \bar{u}_\beta v_{i\alpha} v_{i\beta}}{2\theta^2} - \frac{\bar{u}_\alpha \bar{u}_\alpha}{2\theta} \right] + \frac{w_i k_B T}{2\theta^2} v_i^2 - \frac{w_i k_B T}{2\theta} D \tag{181}$$

and, with

$$\bar{w}_i = w_i \left(1 - \frac{k_B T}{\bar{\rho} 2\theta} D + \frac{k_B T}{\bar{\rho} 2\theta^2} v_i^2 \right) \tag{182}$$

can be rewritten in the suggestive form

$$\bar{f}_i = \bar{\rho} \bar{w}_i \left[1 + \frac{w_i}{\bar{w}_i} \frac{\bar{u}_\alpha v_{i\alpha}}{\theta} + \frac{w_i}{\bar{w}_i} \frac{\bar{u}_\alpha \bar{u}_\beta v_{i\alpha} v_{i\beta}}{2\theta^2} - \frac{w_i}{\bar{w}_i} \frac{\bar{u}_\alpha \bar{u}_\beta}{2\theta} \right]. \tag{183}$$

We measured $\frac{1}{\bar{\rho}} \langle f_i \rangle$ in a fluctuating D2Q9 simulation and found good agreement with our prediction. In Figs. 28, 29, and 30, the results for the three shells of the D2Q9 base velocity set given in Figure 5 at $\bar{\mathbf{u}} = 0$ show very good agreement with Eq. (181) for the case of $\bar{\mathbf{u}} = 0$. We also note that in this preliminary evaluation that the implementation based on the locally velocity dependent transforms and with a noise amplitude chosen locally appears to be more accurate than the one calculated in the Hermite norm at $\rho^0 = \bar{\rho}$.

We understand now that the FDT obtained from the theory of the linearized Boltzmann equation is strictly not valid for fluctuating BGK lattice Boltzmann and with the estimate of the deviation of the distribution functions we see that δM^0 does not, in fact, vanish as is implied by Adhikari [13] and also in our elaboration of their work in Paper 4 under Eq. (137). Now it should be possible to calculate the

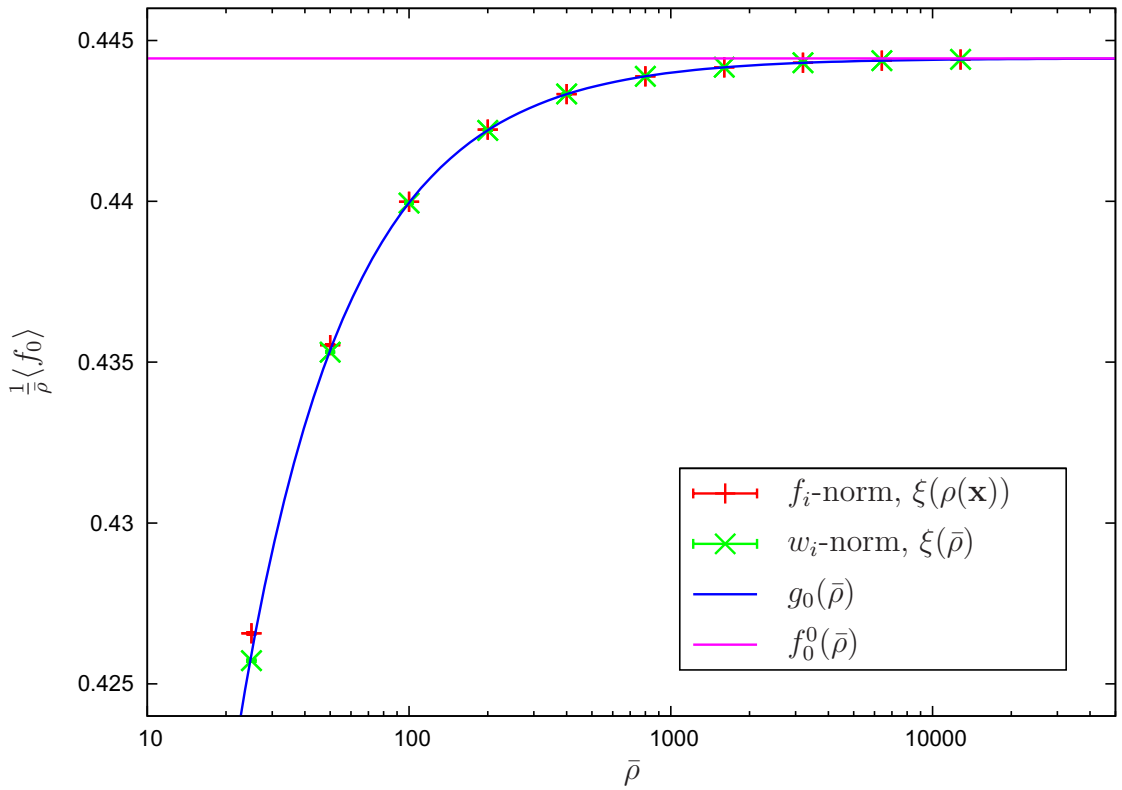

Figure 28. The distribution function $\frac{1}{\rho_0} f_0$ at $\mathbf{u} = 0$ as a function of ρ_0.

necessary corrections for low densities. At the time of this writing, however, we have not finished these calculations.

In Adhikari's derivation [13] and also in our derivation of the FDT in paper 4 the advection term has no effect on the FDT and there is no a priori reason why the noise expression that originates in the local collision should depend on a global mean value that is meaningful only in the equilibrium state which the system may or may not be in. Thus we argue that the density ρ that enters the noise amplitude Eq. (168) should be chosen as the local density $\rho(\mathbf{x})$ and the velocity that enters the multi-relaxation time transforms by means of Eq. (169) should be the local velocity $\mathbf{u}(\mathbf{x})$.

In Figs. 31,32, and 33 we measured the same $\langle (\delta f_i)^2 \rangle$ correlators we observed in Figs. 16, 17, and 18 in Paper 4 for both, f and Hermite norms for low densities $\bar{\rho} = 64$

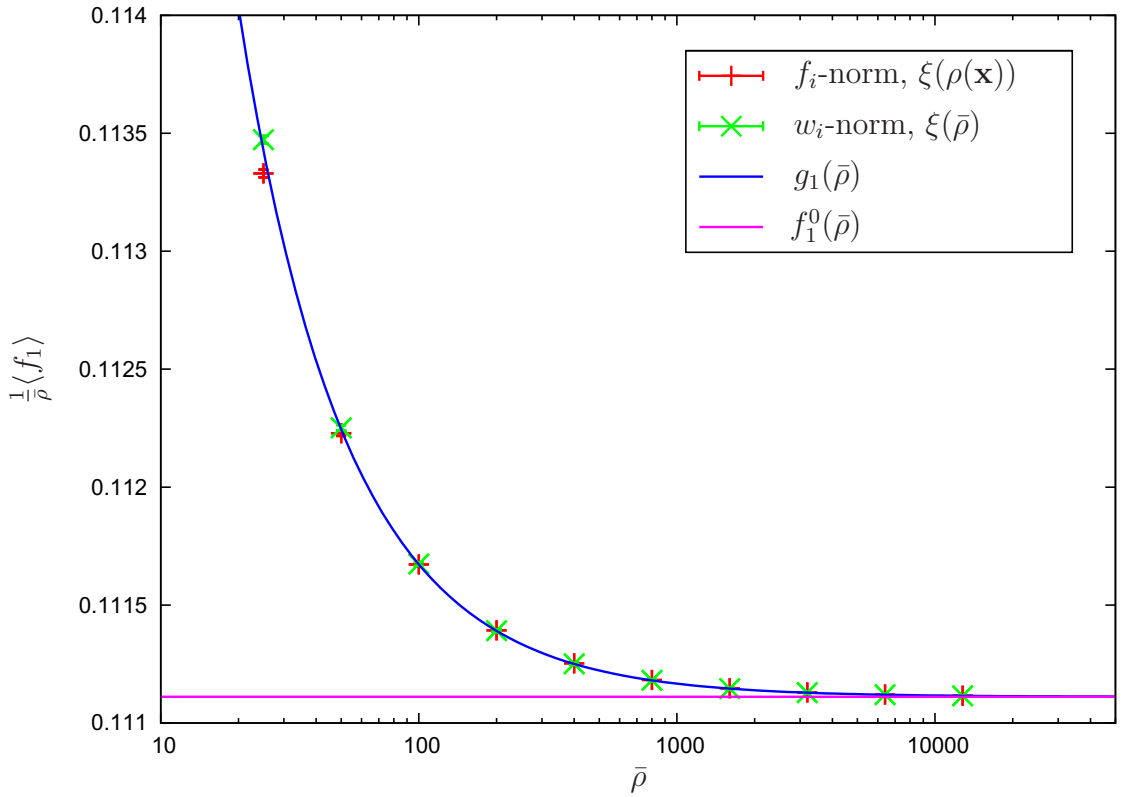

Figure 29. The distribution function $\frac{1}{\rho_0} f_1$ as a function of ρ_0.

as opposed to $\bar{\rho} = 10^6$ in the original paper. We find that our results are similar. However, these measurements were conducted at a significantly lower density than those in the publication on Galilean invariance, $\bar{\rho} = 64$ instead of $\bar{\rho} = 10^6$. We observe that this change introduces significant errors at $\langle (\delta f_0)^2 \rangle$ in Figure 31 but also is very pronounced in the moment space cross correlators Figure 34.

5.3. Stability at Low Densities

There is, however, another benefit to using local velocities in the transforms and local densities which relates to stability. We found that at low densities our fluctuating lattice Boltzmann simulations crash frequently which can be attributed to events of negative values in the distribution functions f_i. In the continuum limit the distribution f_i a Poisson distribution around the maximum value f_i^0. However,

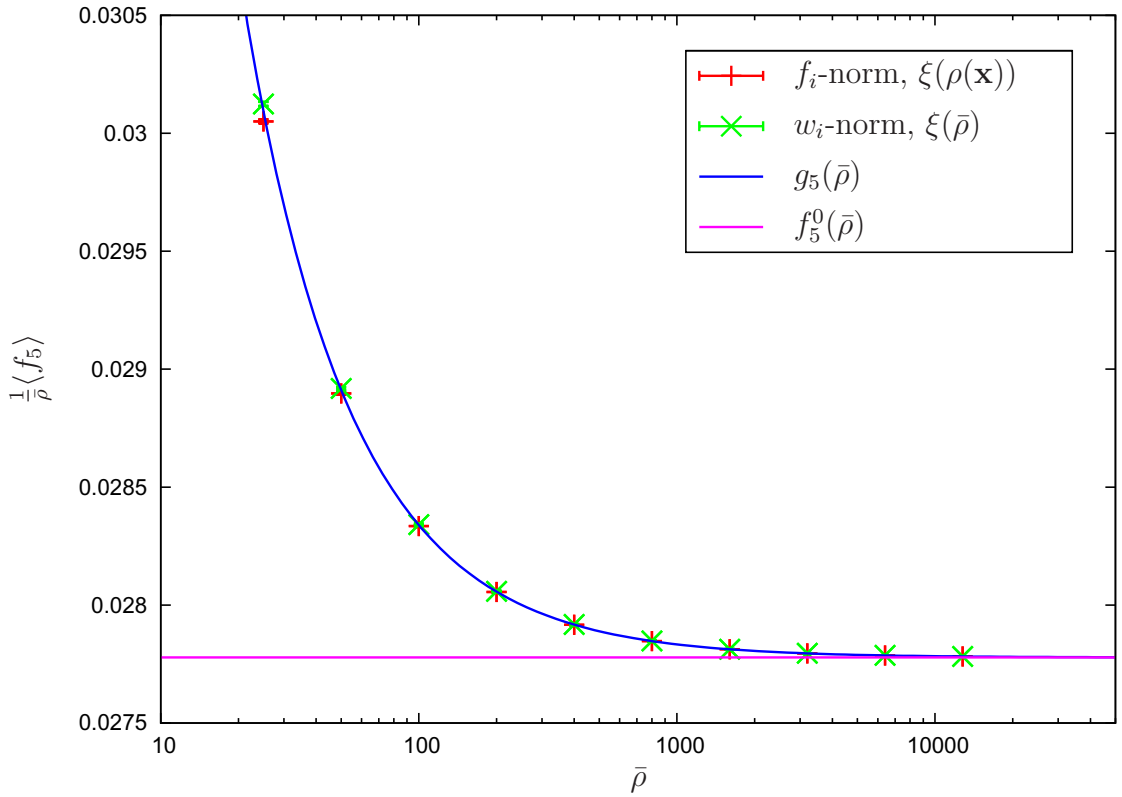

Figure 30. The distribution function $\frac{1}{\rho_0} f_5$ as a function of ρ_0.

in fluctuating lattice Boltzmann methods it is usually modelled as a Gaussian. This is a fundamental shortcoming of the Langevin type discussion of the linearized Boltzmann equation and works nicely in the limit of large number densities but in the description used here there is no reason why number densities local to a lattice cell cannot be small. In the simulations we frequently observe negative density events at low densities that are non-physical and lead to a software crash.

One simple way to measure stability is to initialize a simulation and count lattice site updates until a negative density event occurs. We use this method to obtain a rough measure of the stability of the fluctuating lattice Boltzmann implementations. In Figure 35 we measured the "time to death" for Hermite and f norm each with local density $\rho(\mathbf{x}, t)$ and global mean density $\bar{\rho}$ entering the noise amplitude Eq. (168). We observe that each change, going from global to local density and using the f-norm

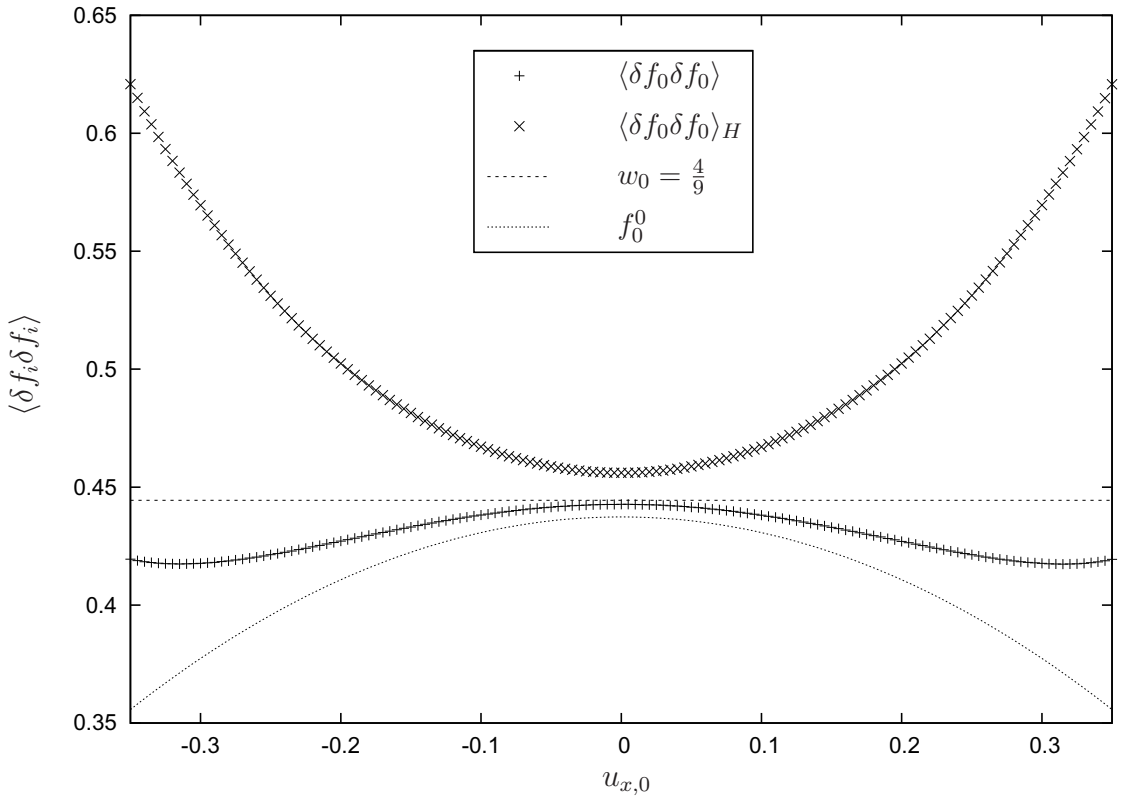

Figure 31. $\langle (\delta f_0)^2 \rangle$ in a 21×21 D2Q9 fluctuating LB simulation employing the local f-norm measured at $\rho_0 = 64$. For comparison $\langle (\delta f_0)^2 \rangle_H$ measured in the Hermite norm is also given.

instead of the Hermite norm improve stability significantly. Both changes combined give the best improvement which exceeds an order of magnitude.

It should be noted that due to the nature of these measurements it is not possible to "thermalize" the system prior to counting the relevant sweeps. Consequently there are finite size effects because the initial system configuration is not in a proper random state. This effect becomes more pronounced, the more unstable the system is and thus this effect is particularly relevant at low densities. We observed this effect in both, the entirely local update (f-norm with local velocities $\mathbf{u}(\mathbf{x}, t)$ and local density $\rho = \rho(\mathbf{x}, t)$) and update with noise depending on global values (Hermite norm and $\bar{\rho}$ in Figure 36 as a function of system size. As expected the effect is more pronounced for larger systems as then more site updates are required to "thermalize" the system.

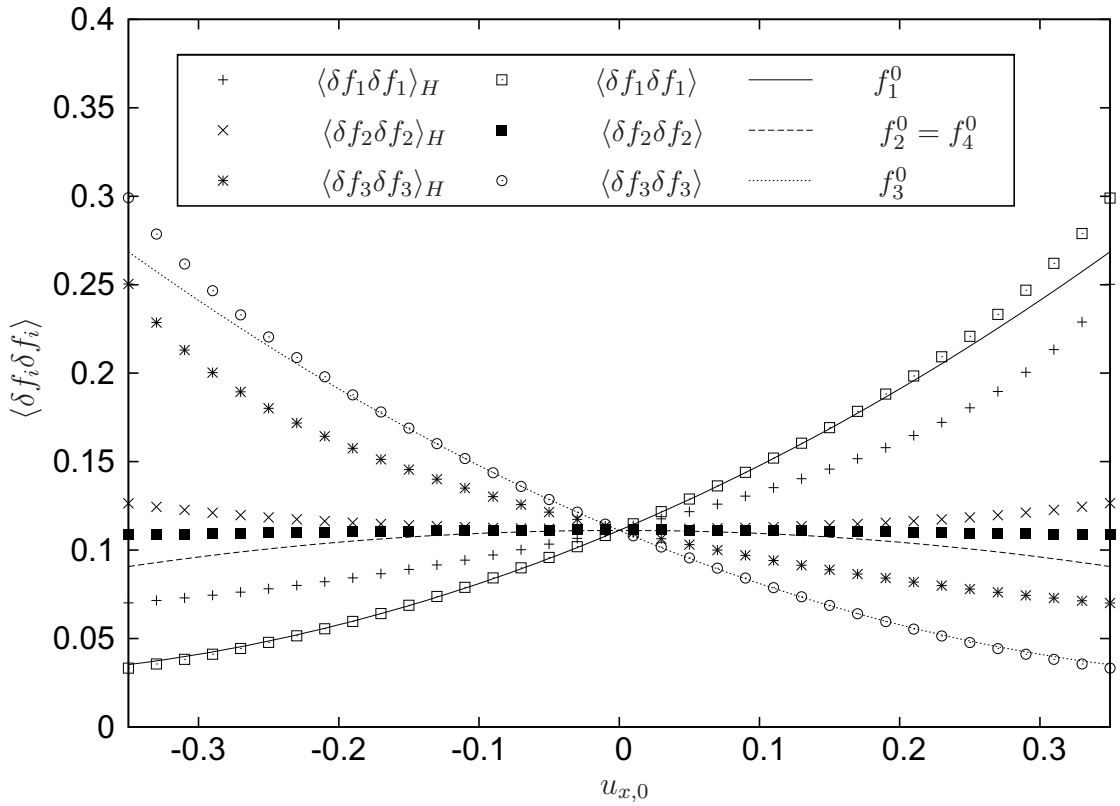

Figure 32. $\langle (\delta f_i)^2 \rangle$ for $i = 1...3$ in a 21×21 D2Q9 fluctuating LB simulation employing the local f-norm measured at $\rho_0 = 64$. For comparison $\langle (\delta f_i)^2 \rangle_H$ measured in the Hermite norm is also given.

There is another variable that is relevant to the stability of the noise implementation. This is the choice of the random number distribution. So far we have used a Gaussian distribution as recommended in the literature [13]. However, the Gaussian distribution does not limit outliers. Motivated by considerations such as those put forward by Ladd [65] who introduced a simple three-value random number generator we tested two more simple distributions: a uniform distribution and a "binary" distribution where only two different values can be found. All three distributions share the vanishing mean and variance of one. The results are given in Figure 37. We observe that choosing random numbers from the "binary" distribution is about one order of magnitude less likely to generate a negative density event than choosing from a Gaussian distribution. The uniform distribution is situated between the two.

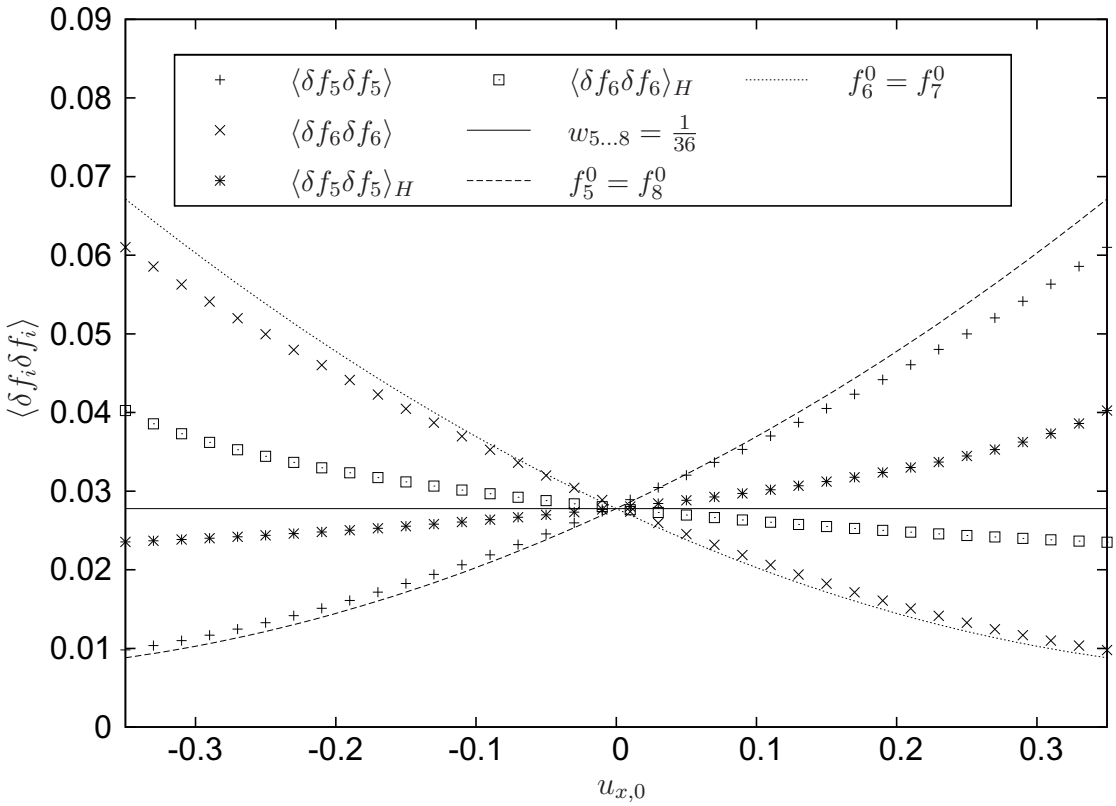

Figure 33. $\langle (\delta f_i)^2 \rangle$ for $i = 5...8$in a 21×21 D2Q9 fluctuating LB simulation employing the local f-norm measured at $\rho_0 = 64$. For comparison $\langle (\delta f_i)^2 \rangle_H$ measured in the Hermite norm is also given.

5.4. The Distribution of the Distribution Functions

One way to investigate the validity of the noise implementations is to investigate the distribution functions of the particles. The initial assumption is taken from Eq. (140). This goes back to the observation that for an ideal gas the distribution function is Poisson distributed [43, chapter I] and that $\langle \delta f_i \delta f_j \rangle = \langle f_i \rangle \delta_{ij}$. If we do recover Poisson distributions as results from including Gaussian distributed noise on our moments we have a good indication of the validity of our method.

Let us assume that we have an ideal lattice gas implementation in the sense of a lattice gas automaton (LGA), i.e. an implementation with discrete particle numbers that are to be distributed amongst a set of base velocities $\mathbf{v}_i$ at each lattice site. The

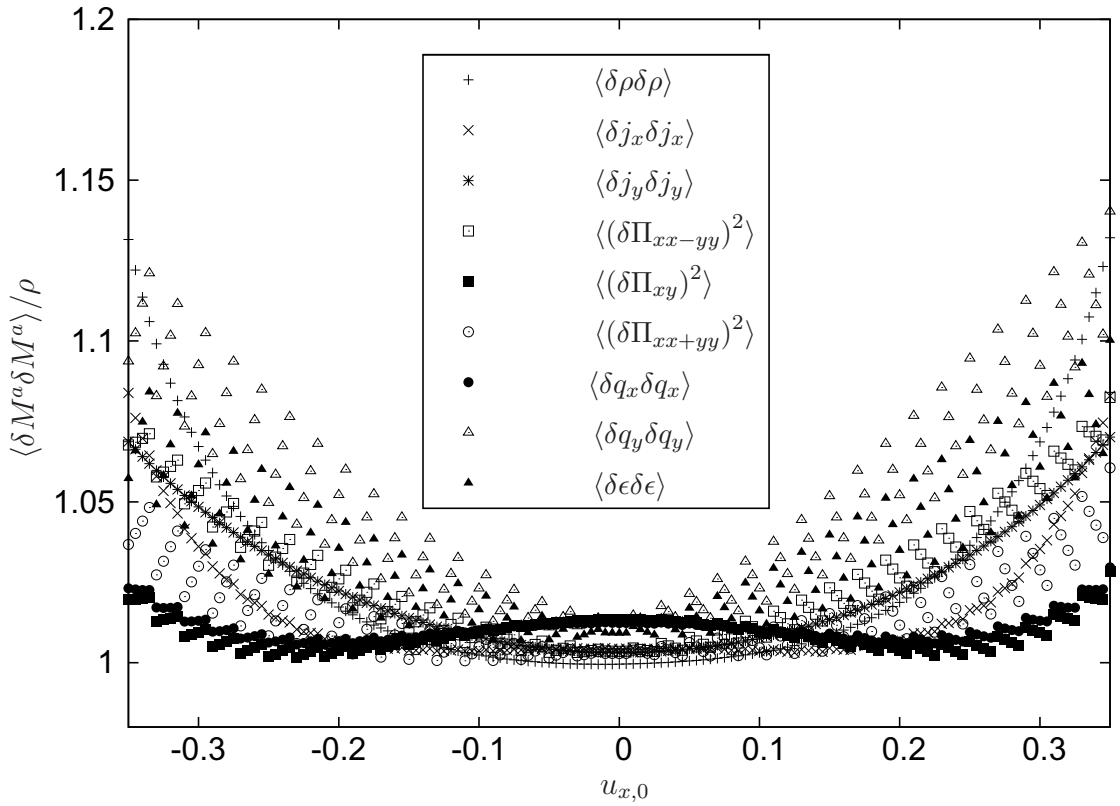

Figure 34. Correlators calculated in the local f-norm $\langle \delta M^a \delta M^a \rangle$ normalized to ρ according to Eq. (143) in a 21×21 D2Q9 fluctuating LB simulation employing the f-norm at $\rho_0 = 64$.

probability to find a certain number of particles g_i associated with a velocity $\mathbf{v}_i$ would then be given by a discrete Poisson distribution

$$P_{Poisson}(g_i; \langle g_i \rangle) = \frac{\langle g_i \rangle^{g_i}}{g_i!} e^{-\langle g_i \rangle} \tag{184}$$

where $\langle g_i \rangle$ is the probability for a particle to move with velocity v_i. This is the assumption that enters the derivation of fluctuating lattice Boltzmann in condition Eq. (140) which we hope to recover. However, contrary to the 'lattice gas' the lattice Boltzmann method does not work with discrete particle numbers but instead all particle distributions f_i and the particle number per unit cell ρ are given by continuous real numbers. We thus want to find the continuous distribution function for the f_i that corresponds best to the discrete Poisson distribution. One approach is to consider

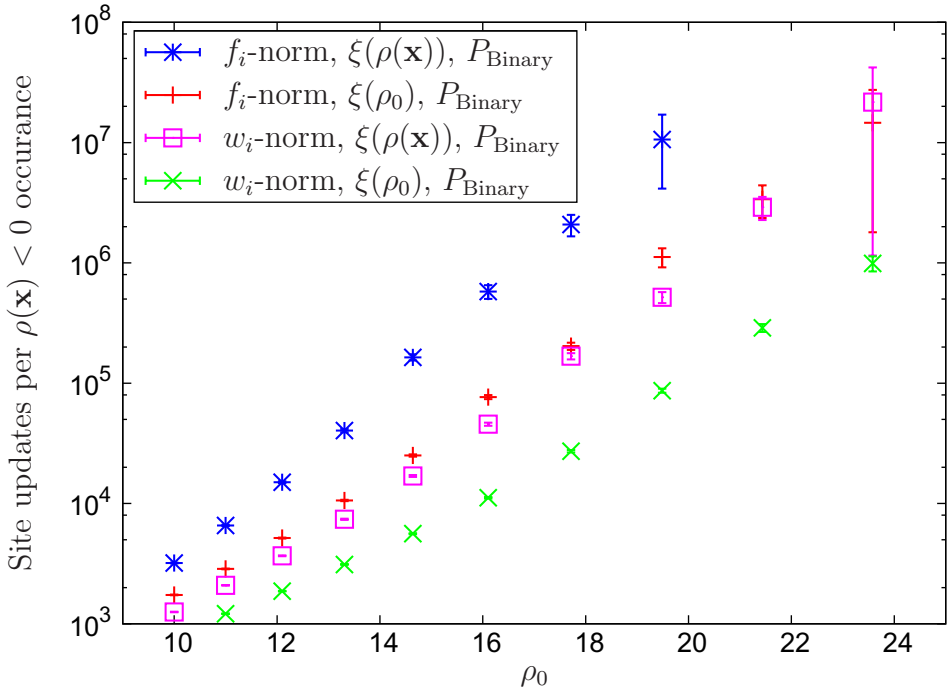

Figure 35. Mean number of lattice site updates until first $\rho(\mathbf{x}, t) < 0$ event occurs. We measure in the Hermite norm and the f norm each with local density $\rho(\mathbf{x}, t)$ and global mean density $\bar{\rho}$ entering the noise amplitudes. Simulations carried out in a 21×21 D2Q9 fluctuating lattice Boltzmann simulation.

the analytical continuation of the discrete Poisson distribution to continuous values given by the continuous Poisson distribution,

$$P_{Poisson}(x; \lambda) = \frac{\lambda^x}{\Gamma(x+1)} e^{-\lambda} \tag{185}$$

where in the case of lattice Boltzmann $x = f_i$ and the mean and variance of the distribution are now given by the expectation value of the lattice Boltzmann equilibrium distribution such that $\lambda = \langle f_i \rangle = f_i^0$. The Γ-function is the continuous extension of the factorial. For positive integer values we have $\Gamma(z+1) = z!$ and it is defined as

$$\Gamma(z) = \int_0^\infty t^{z-1} e^{-t} \, \mathrm{d}\, t. \tag{186}$$

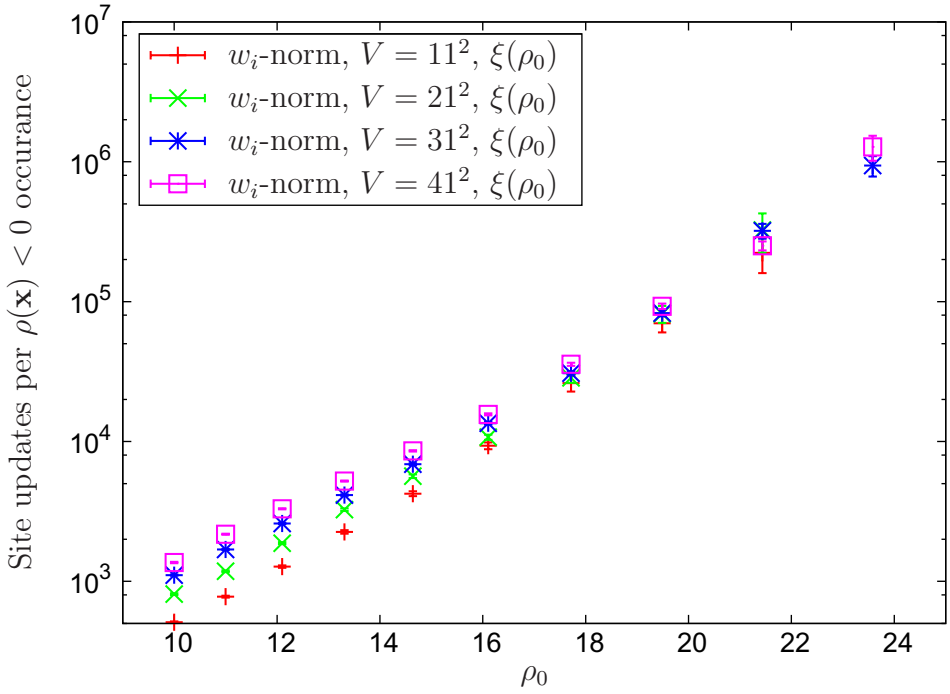

(a) Hermite norm with $\bar{\rho}$

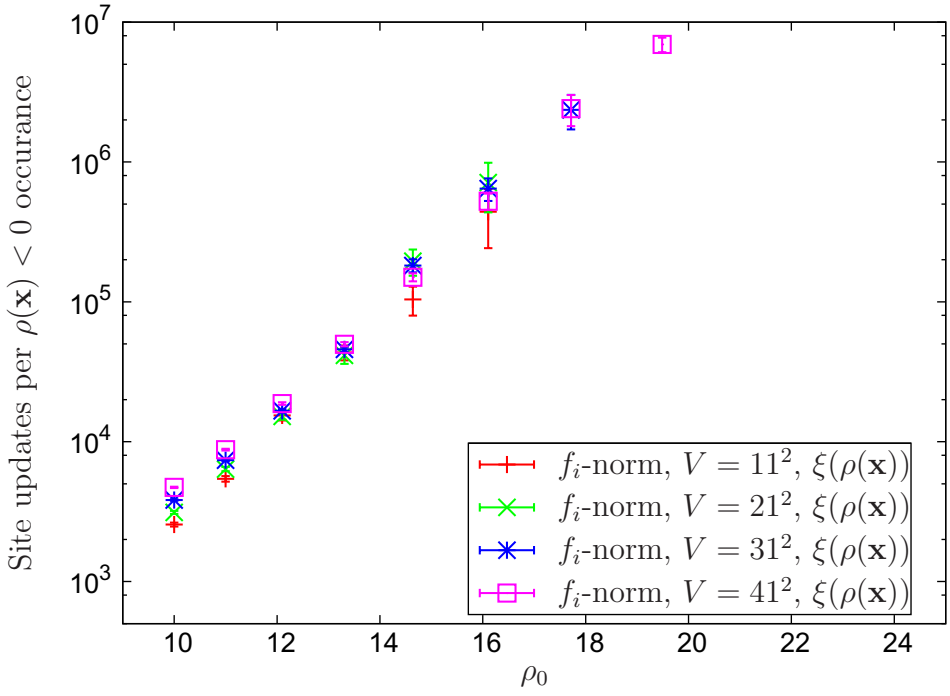

(b) f-norm with $\rho(\mathbf{x}, t)$

Figure 36. Mean number of lattice site updates until first $\rho(\mathbf{x}, t) < 0$ event occurs. Here we measured for different lattice sites and for the update depending only on equilibrium values a) and local values b).

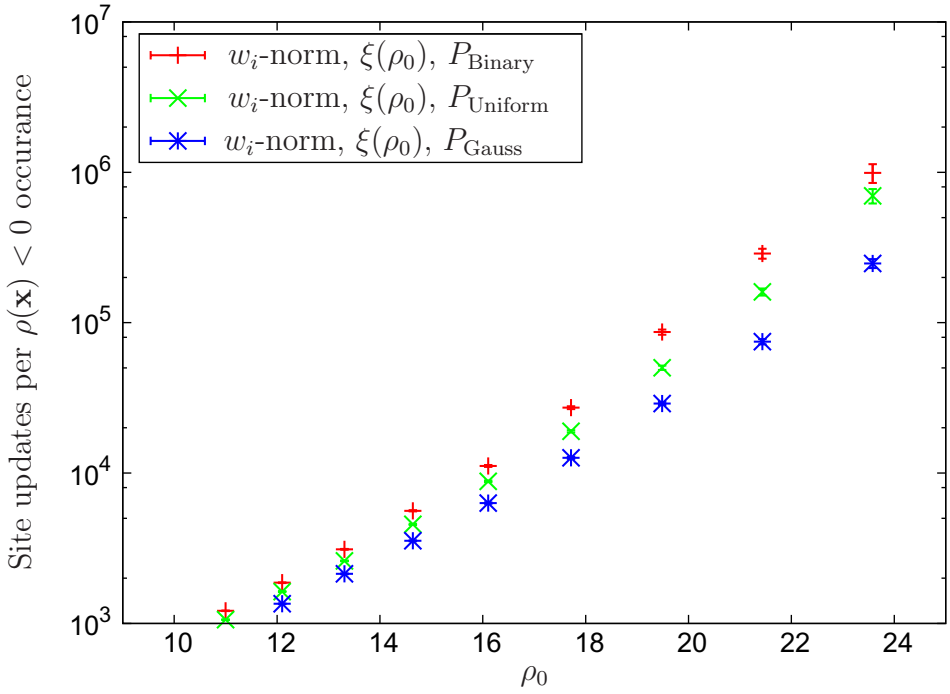

(a) Hermite norm with $\bar{\rho}$

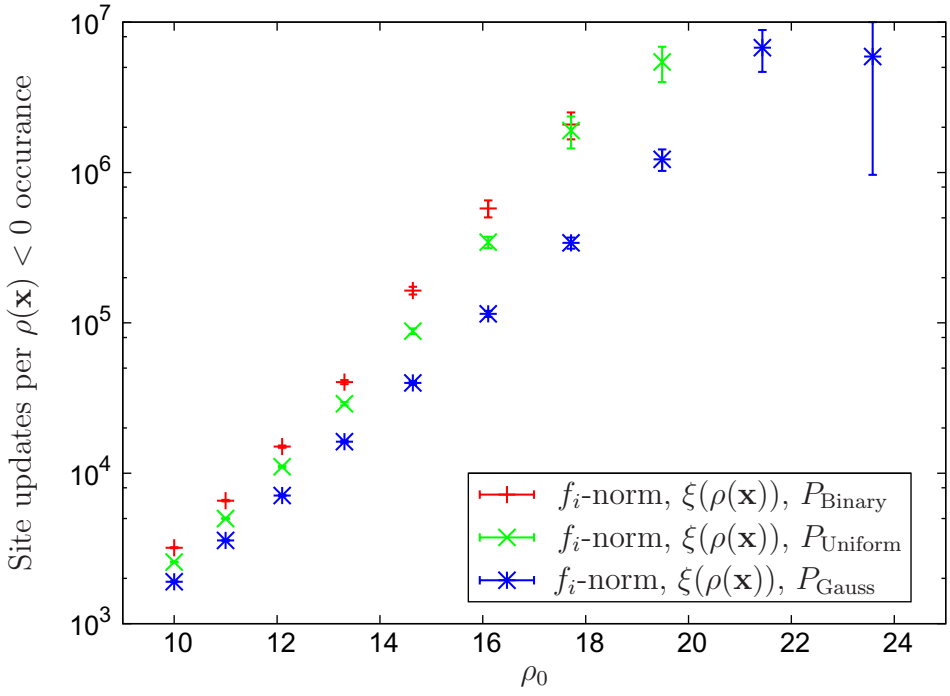

(b) f-norm with $\rho(\mathbf{x}, t)$

Figure 37. Mean number of lattice site updates until first $\rho(\mathbf{x}, t) < 0$ event occurs. Here we used three different random number distributions, again for updates based on global equilibrium values a) and local values b).

The identification of the continuous Poisson distribution with particle numbers is, however, dubious because there remain non-vanishing probabilities for negative values of x in the distribution function. This is more pronounced for very small λ as seen in Figure 38 (a). Even more disturbingly this identification would imply completely non-sensical negative probabilities for non-integer negative values (see Figure 38 (a)). This requires us to cut off this continuous distribution. But whether we cut of at $b = 0$, corresponding to the understanding that negative f_i are unphysical or at $b = -1$ because negative probabilities cannot exist at small λ the distribution function is not well normalized anymore and the first two moments do not reproduce those of the Poisson distribution. For example

$$\mu_b(n) = \int_b^\infty P_{Poisson}(x;\lambda)\frac{x^n}{N}\ \mathrm{d}\ x \tag{187}$$

with $n = 0, 1, 2$ and correspondingly $N = 1, \lambda, \lambda^2 + \lambda$ as seen in Figure 38 for $b = 0$(b) and $b = -1$ (c) are not correct for small λ. Unfortunately this holds independently on whether the integration begins at 0 or the already nonsensical -1. In particular we observe that in both cases we need $\lambda \gtrsim 8$ to have all moments converge. This implies that while we still don't have a good handle on what continuous distribution function is expected for small $\lambda \lesssim 8$, we trust that the continuous extension of the Poisson distribution is a good approximation for $\lambda \gtrsim 8$.

Now that we can describe the probability of the particle distributions at least for $\langle f_i \rangle \gtrsim 8$ the question remains how the hydrodynamic moments M^a should be distributed. Luckily the distribution of combined Poisson distributed variables we need is straight forward. The distribution of the sum of two variables that are distributed according to a Poisson distribution again is a Poisson distribution

$$P_+(n = f_i + f_j; \langle f_i \rangle, \bar{f}_j) = \frac{(\langle f_i \rangle + \bar{f}_j)^n}{\Gamma(n+1)} e^{-(\langle f_i \rangle + \bar{f}_j)}. \tag{188}$$

The distribution of the difference of two Poisson distributed variables yields a Skellam distribution [74]

$$P_-(n = f_i - f_j; \langle f_i \rangle, \bar{f}_j) = 2 \left(\frac{\langle f_i \rangle}{\bar{f}_j} \right)^{\frac{n}{2}} e^{-\left(\langle f_i \rangle + \bar{f}_j\right)} I_{|n|} \left(2\sqrt{\langle f_i \rangle \bar{f}_j} \right) \tag{189}$$

where $I_{|k|}(x)$ is the modified Bessel function of the first kind [75, chapter 9]

$$I_\alpha(x) = \sum_{m=0}^{\infty} \frac{1}{m!\Gamma(m+\alpha+1)} \left(\frac{x}{2} \right)^{2m+\alpha}. \tag{190}$$

We should note that the Poisson distribution converges to a Gaussian distribution at $\lambda \gtrsim 80$ [73, chapter 30]. For the same reason it can be shown that the Skellam distribution Eq. (189) converges to that a normal distribution for either large $\langle f_i \rangle$ or $\bar{f}_j$.

To examine the distribution of densities $P(f_i)$ we performed simulations for our D2Q9 system at an average velocity of $\langle \mathbf{u} \rangle = 0$. Vanishing mean velocities in $D2Q9$ imply $f_1 = f_2 = f_3 = f_4$ and $f_5 = f_6 = f_7 = f_8$ and consequently we only need to observe the distribution functions f_0, f_1, and, f_5.

We choose $\bar{\rho} = 32$ which is close to the smallest reasonably 'stable' density we can simulate for all possible norms and random number generators as discussed in section 5.3 to illustrate the effect of the choice of a noise implementation on the distribution of the distribution functions. For these densities we already obtain a a mean value of $\bar{f}_5 = \bar{\rho}/36 < 1$ for which the continuous and discrete Poisson distributions no longer give the same moments. At this low density we already encounter unrecoverable events of instability in the Hermite norm. Hence in the histograms

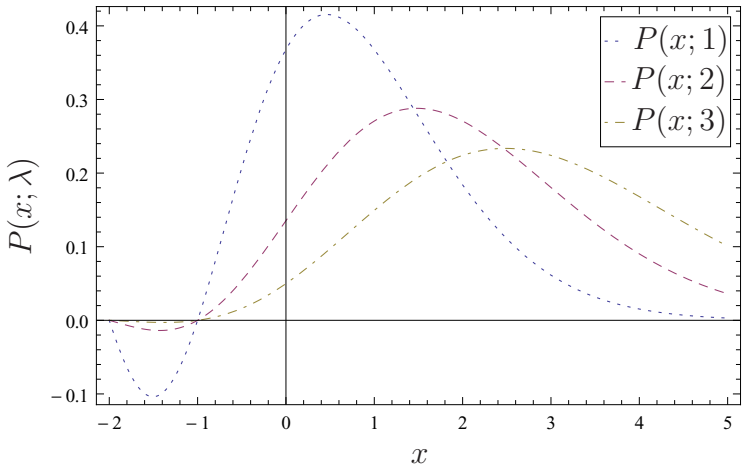

(a) $P(x;\lambda)$ for $\lambda = \{1, 2, 3\}$

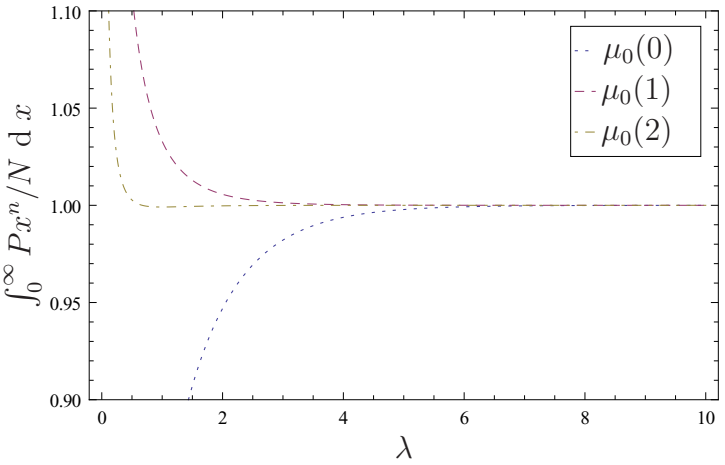

(b) $\int_0^\infty P(x;\lambda)x^n/N \text{ d } x$ for $n = \{0, 1, 2\}$

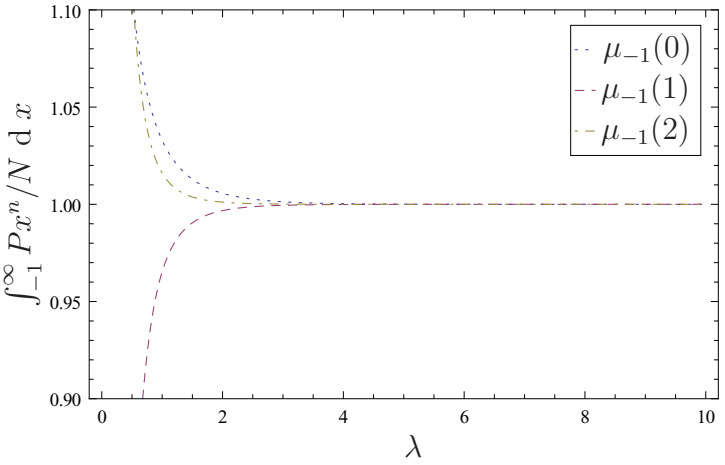

(c) $\int_{-1}^\infty P(x;\lambda)x^n/N \text{ d } x$ for $n = \{0, 1, 2\}$

Figure 38. The continuous Poisson distribution at very small λ (a), and the integral of its zeroth, first and second moment integrated starting at 0 (b) and at -1 (c). In (b) and (c) the first moment is normalized to λ and the second to $\lambda^2 - \lambda$.

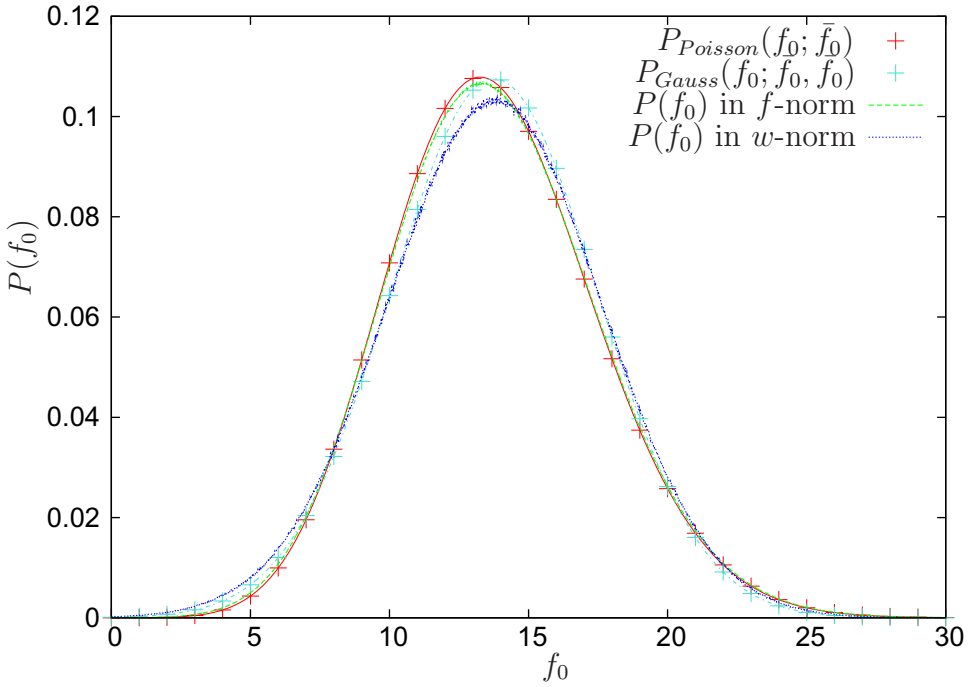

Figure 39. Distribution of f_0 at $\bar{\rho} = 32$, $\bar{\mathbf{u}} = 0$ measured in isothermal fluctuating $D2Q9$ simulation using a Gaussian distribution random number generator.

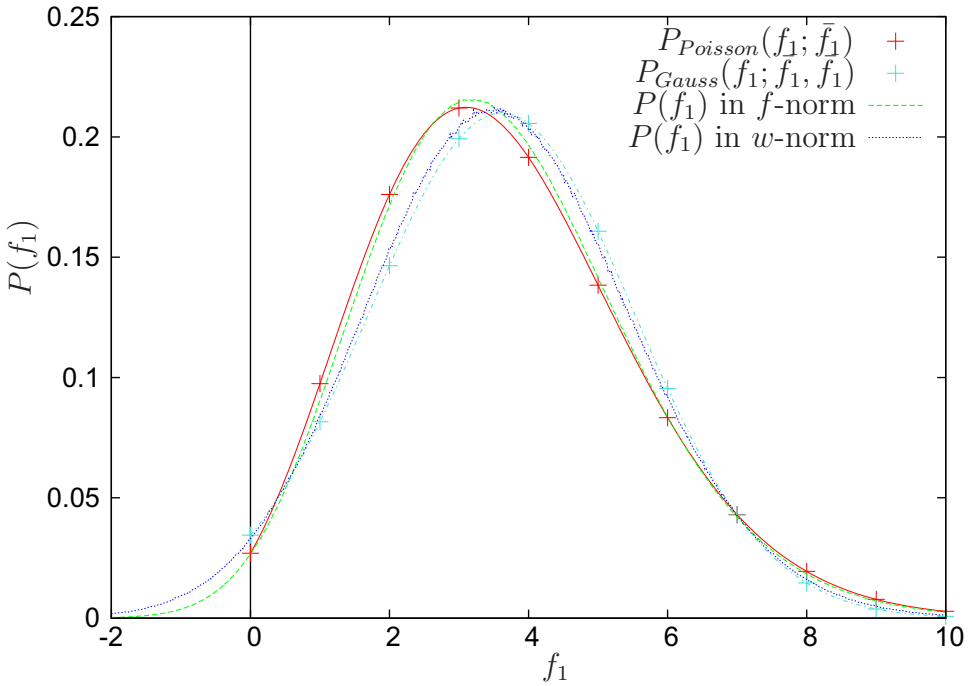

Figure 40. Distribution of f_1 at $\bar{\rho} = 32$, $\bar{\mathbf{u}} = 0$ measured in isothermal fluctuating $D2Q9$ simulation using a Gaussian distribution random number generator.

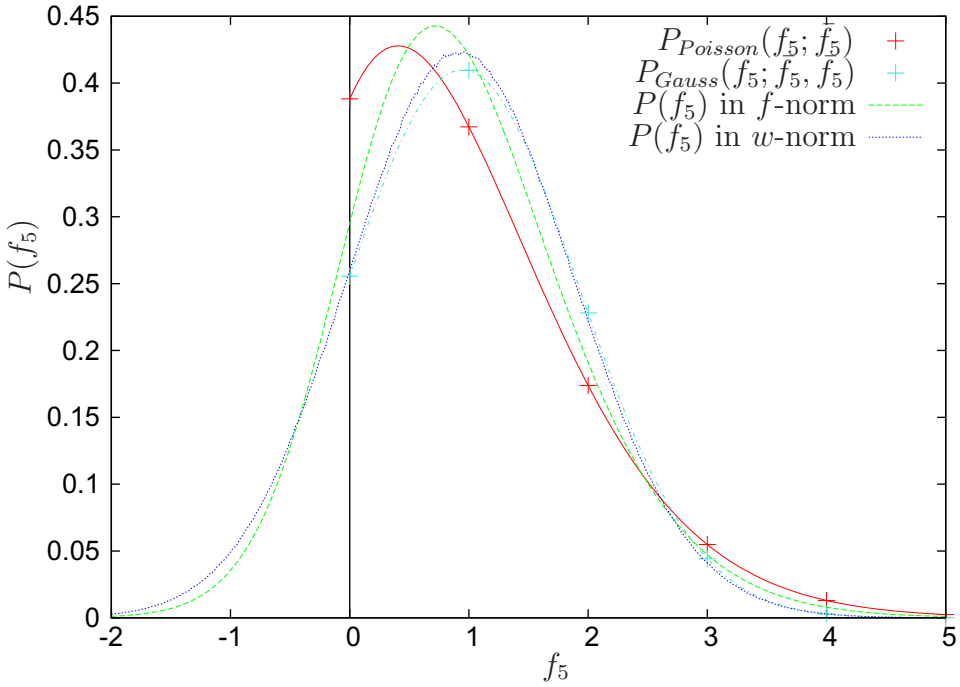

Figure 41. Distribution of f_5 at $\bar{\rho} = 32$, $\bar{\mathbf{u}} = 0$ measured in isothermal fluctuating $D2Q9$ simulation using a Gaussian distribution random number generator.

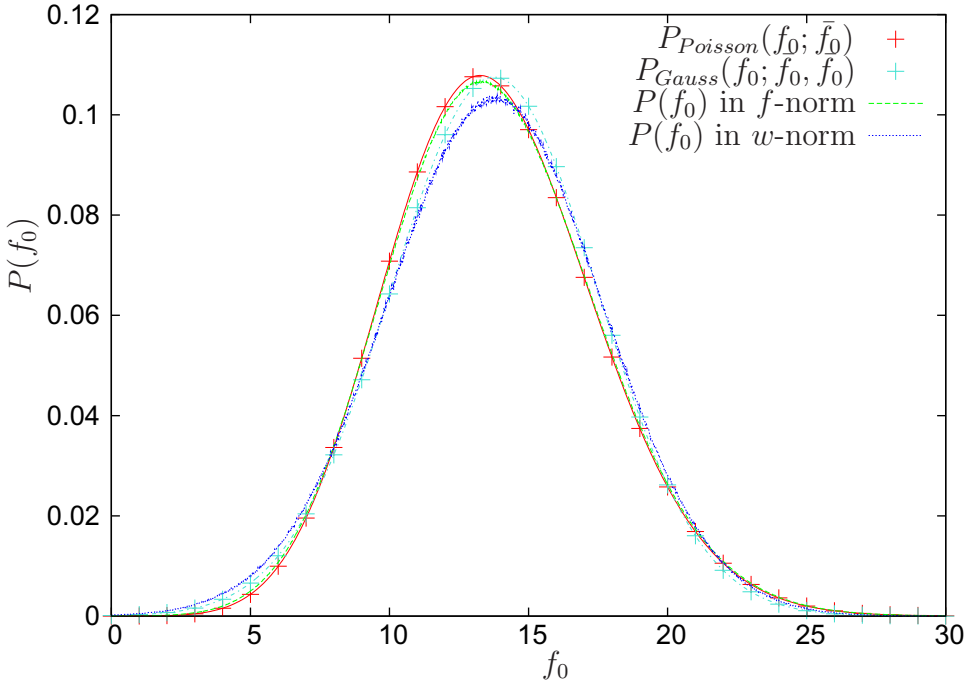

Figure 42. Distribution of f_0 at $\bar{\rho} = 32$, $\bar{\mathbf{u}} = 0$ measured in isothermal fluctuating $D2Q9$ simulation using a Gaussian distribution random number generator.

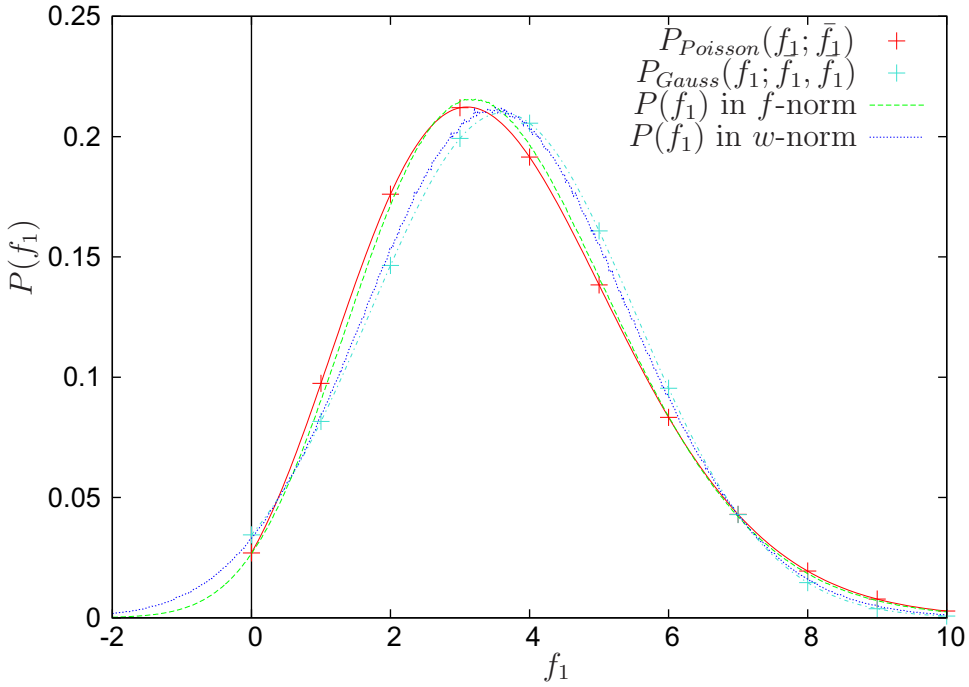

Figure 43. Distribution of f_1 at $\bar{\rho} = 32$, $\bar{\mathbf{u}} = 0$ measured in isothermal fluctuating $D2Q9$ simulation using a Gaussian distribution random number generator.

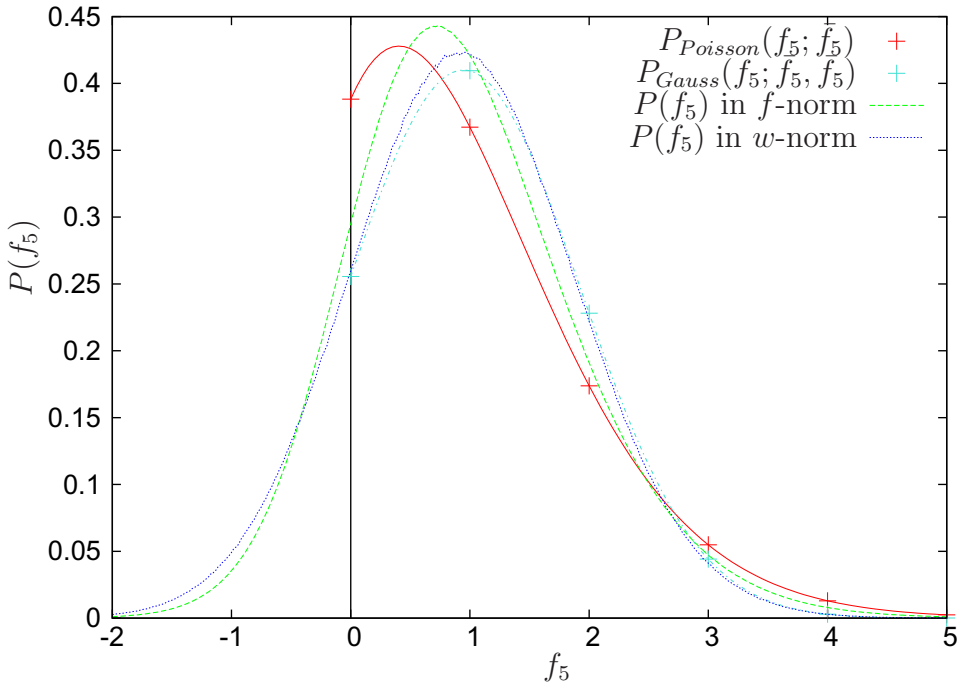

Figure 44. Distribution of f_5 at $\bar{\rho} = 32$, $\bar{\mathbf{u}} = 0$ measured in isothermal fluctuating $D2Q9$ simulation using a Gaussian distribution random number generator.

displayed in the following we have 10^5 lattice Boltzmann lattice updates representing the Hermite norm but 10^7 updates for the f-norm. The bin width in these histograms is $\Delta h(f_i) = 20/(10^4\sqrt{w_i\rho_0})$ for plots of the distribution functions f_i and $\Delta h(M^a 20) = 20/(10^4\sqrt{M^{a,0}})$. In Figure 42 the distributrions of f_0 are shown. The f-norm reproduces the predicted Poisson distribution much more closely than the Hermite norm. An interesting detail is that the Hermite exhibits an increased probability of low f_0 events. This is in agreement with the findings in section 5.3 where we generally observe improved stability for the f-norm due to fewer negative density events.

We observe a similarly improved effect for the f_1 at $\bar{\rho} = 32$ in Figure 43. The results obtained from the f-norm implementation agree significantly better with those of the Hermite norm. Interestingly the Hermite norm results seem to follow a Gaussian distribution even at these low densities. Again, in the f_1 the left side tail of the Hermite norm is larger than that of the f-norm.

Finally in Figure 44 we observe the results for f_5. Taking into account that the expectation value here $\bar{f}_5 \approx \frac{\bar{\rho}}{36} < 1$ we find a significant tail for "negative densities". This is in agreement with Figure 38(b) and does illustrate some of the stability problems we have observed. In contrast to the continuous Poisson and Gaussian distributions, the discrete Poisson distribution does not share this problem and a truly discrete model (i.e. lattice gas implementations) would not share this peculiarity. Again we see that the f-norm is significantly closer to the predicted Poisson distribution than the Hermite norm implementation although this effect is less pronounced than in the cases of f_0 and f_1. We should reiterate here that we don't have a theoretical prediction for the distribution function for $\lambda \approx 1$. The interpretation with regards to stability here is the same as before in that negative density events are more likely for the Hermite norm than the f-norm. In particular as the unphysical event of

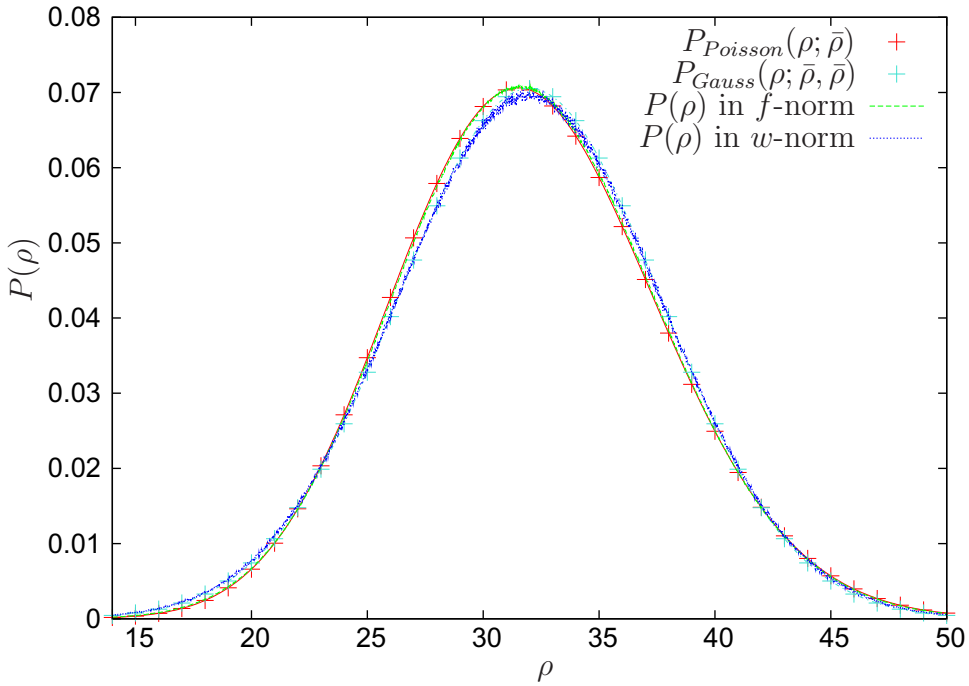

Figure 45. Distribution of the density ρ at $\bar{\rho} = 32$, $\bar{\mathbf{u}} = 0$ measured in isothermal fluctuating $D2Q9$ simulation using a Gaussian distribution random number generator.

finding non-vanishing probabilities of negative particle densities are more pronounced in the Hermite norm than in the f-norm. When interpreting these images, especially for very small λ we have to be mindful of the fact that the displayed graph for the continuous Poisson distribution is not a good representation of an analytic expression. However, for the continuous lattice Boltzmann distributions the discrete Poisson distribution only carries very limited information as well.

In Figure 45 the distribution of the density is shown. We observe significantly better agreement between the predicted Poisson distribution and the f-norm results and again see that the Hermite norm implementation exhibits the behavior of a normal distribution around $\bar{\rho}$.

At $\langle \mathbf{u} \rangle = 0$ all other moments' expectation values are centered about 0 and follow a Skellam distribution. Already at the low mean particle count of $\bar{\rho} = 32$ the Skellam distributions approach normal distributions and it is difficult to make

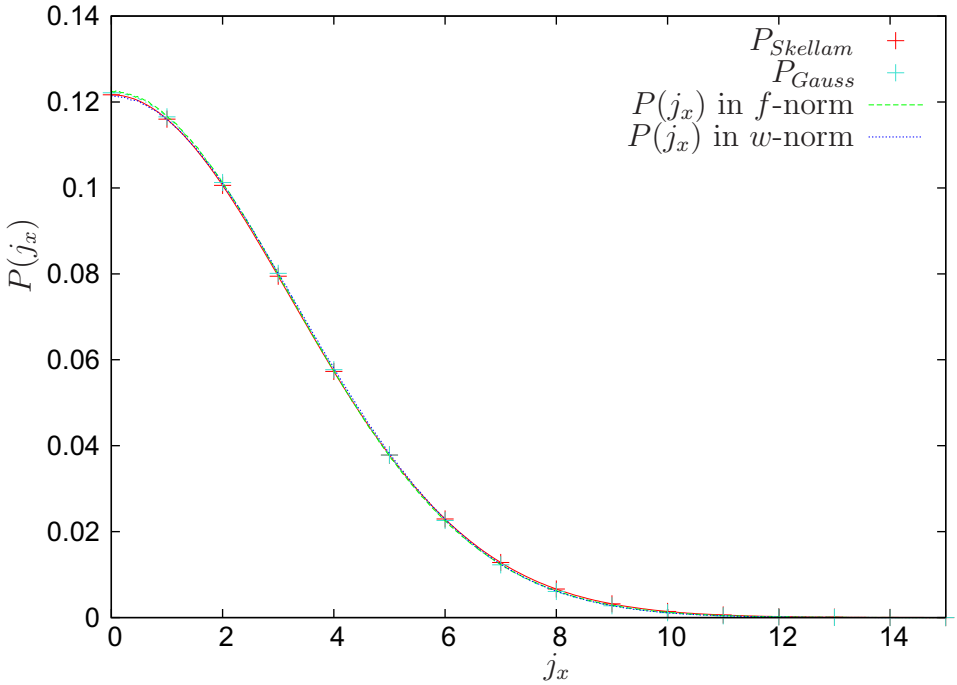

Figure 46. Distribution of the x-component of the momentum j_x at $\bar{\rho} = 32$, $\bar{\mathbf{u}} = 0$ measured in isothermal fluctuating $D2Q9$ simulation using a Gaussian distribution random number generator.

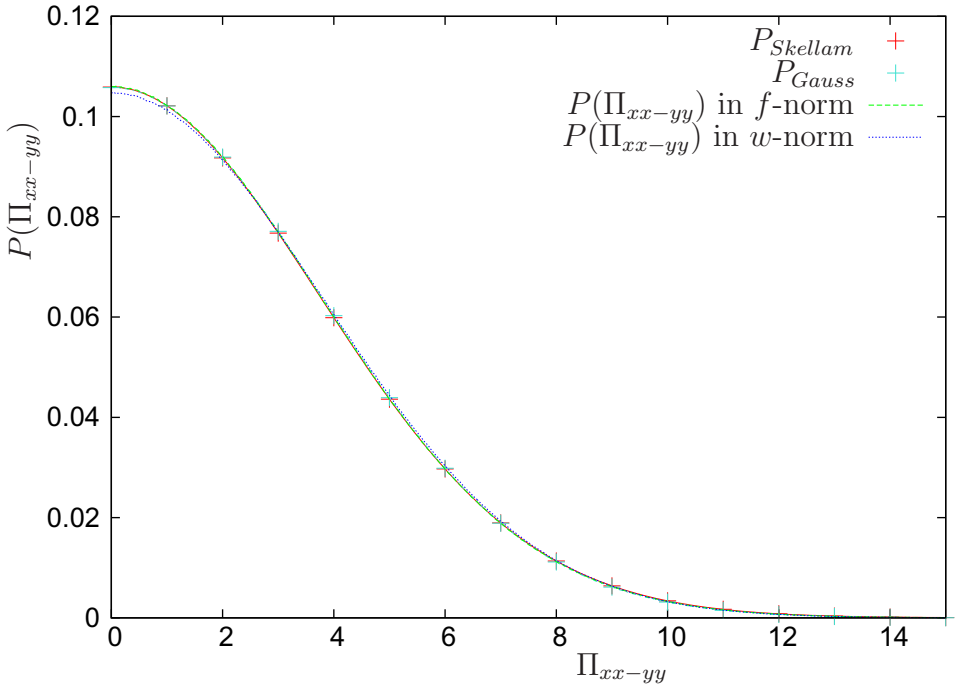

Figure 47. Distribution of the Π_{xx-yy}-component of the stress tensor $\bar{\rho} = 32$, $\bar{\mathbf{u}} = 0$ measured in isothermal fluctuating $D2Q9$ simulation using a Gaussian distribution random number generator.

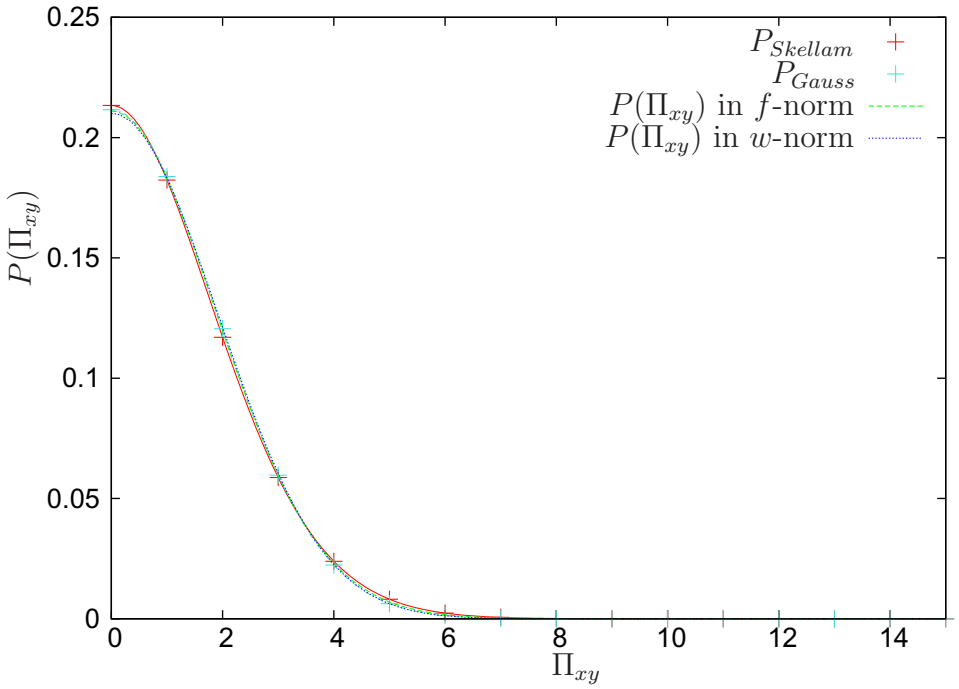

Figure 48. Distribution of the Π_{xy}-component of the stress tensor at $\bar{\rho} = 32$, $\bar{\mathbf{u}} = 0$ measured in isothermal fluctuating $D2Q9$ simulation using a Gaussian distribution random number generator.

different statements regarding the quality of the agreement between predictions and measurements of Hermite norm and f-norm are both good for $\langle \mathbf{u} \rangle = 0$. The notable exception to the vanishing moment expectation values is the bulk stress moment. It is given by

$$\Pi_{xx+yy} = \frac{1}{2}\left(f_1 + f_2 + f_3 + f_4\right) + 2\left(f_5 + f_6 + f_7 + f_8\right) - f_0. \tag{191}$$

and does not vanish. Its expectation value $\langle \Pi_{xx+yy} \rangle$ would vanish without the corrections of Eq. (183) but does not as seen in Figure 49. The value $\langle \Pi_{xx+yy}(\rho_0) = 32) \rangle = 1.1613$ calculated analytically is well reproduced for both norms in Figure 49 and indicated by the vertical line in Figure 49.

To illustrate the effect of the velocity dependent transforms the same distributions were measured for velocity, $u_x = 0.2$. A density of $\rho = 64$ was chosen. Lower

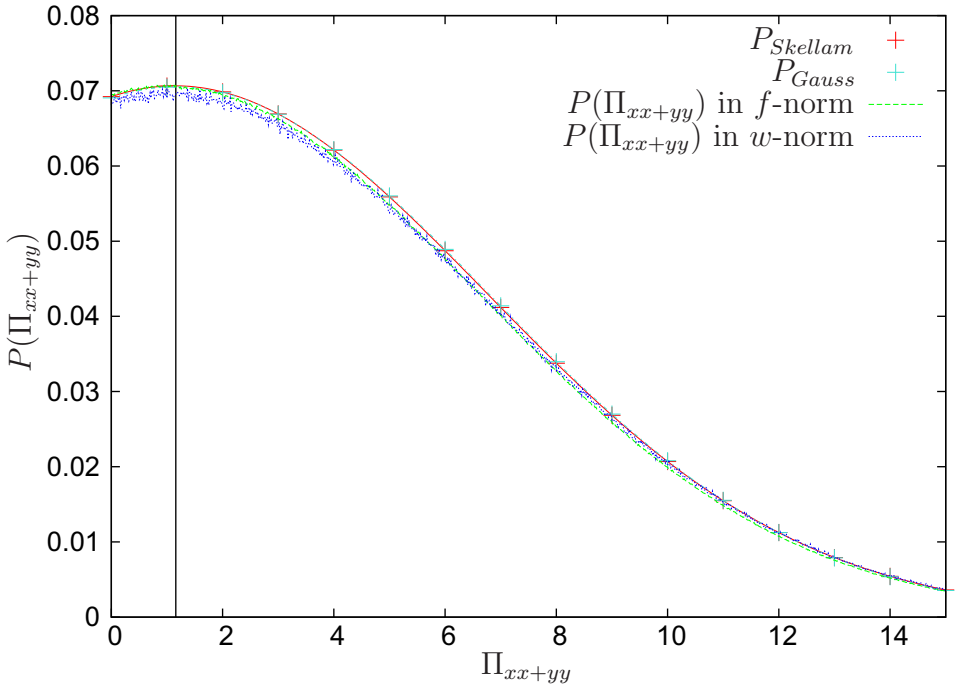

Figure 49. Distribution of the Π_{xx+yy}-component of the stress tensor at at $\bar{\rho} = 32$, $\bar{\mathbf{u}} = 0$ measured in isothermal fluctuating $D2Q9$ simulation using a Gaussian distribution random number generator. The vertical line represents the expectation value calculated according to Eq. (191).

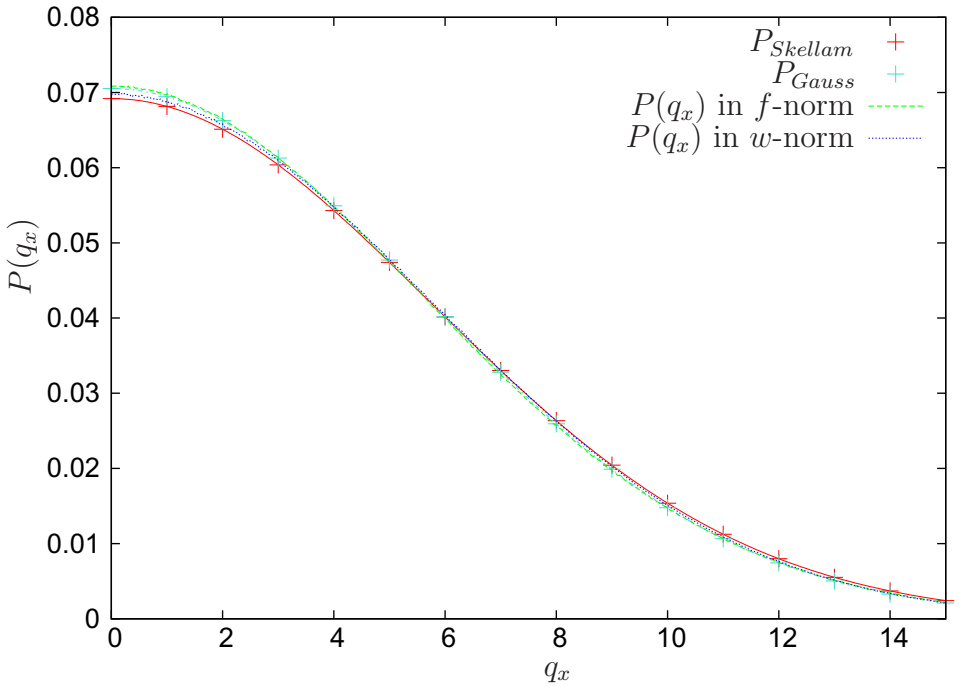

Figure 50. Distribution of the q_x ghost mode at $\bar{\rho} = 32$, $\bar{\mathbf{u}} = 0$ measured in isothermal fluctuating $D2Q9$ simulation using a Gaussian distribution random number generator.

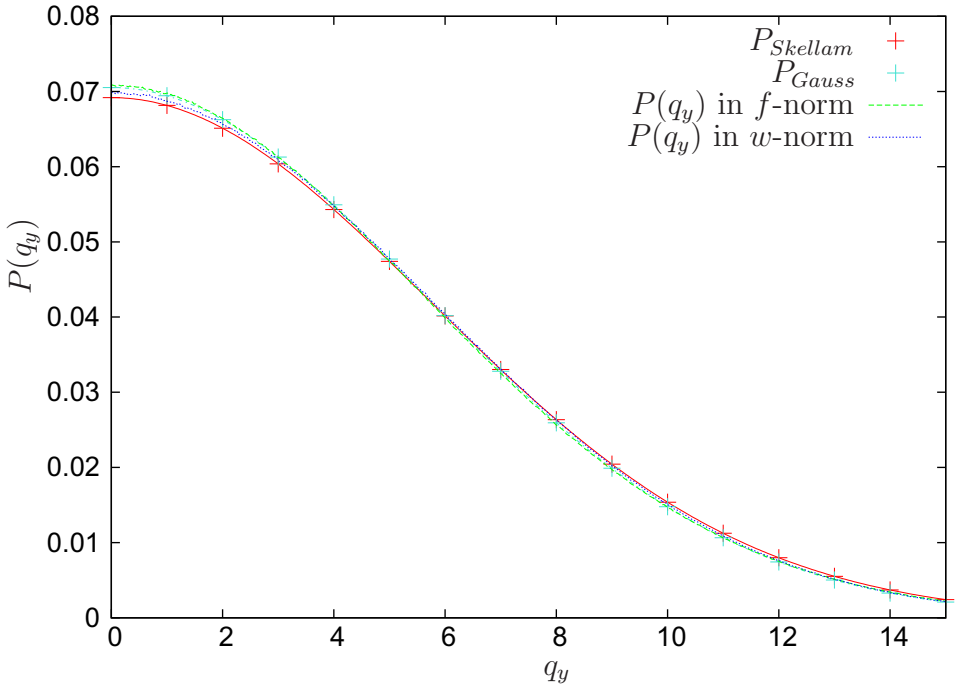

Figure 51. Distribution of the q_y ghost mode at $\bar{\rho} = 32$, $\bar{\mathbf{u}} = 0$ measured in isothermal fluctuating $D2Q9$ simulation using a Gaussian distribution random number generator.

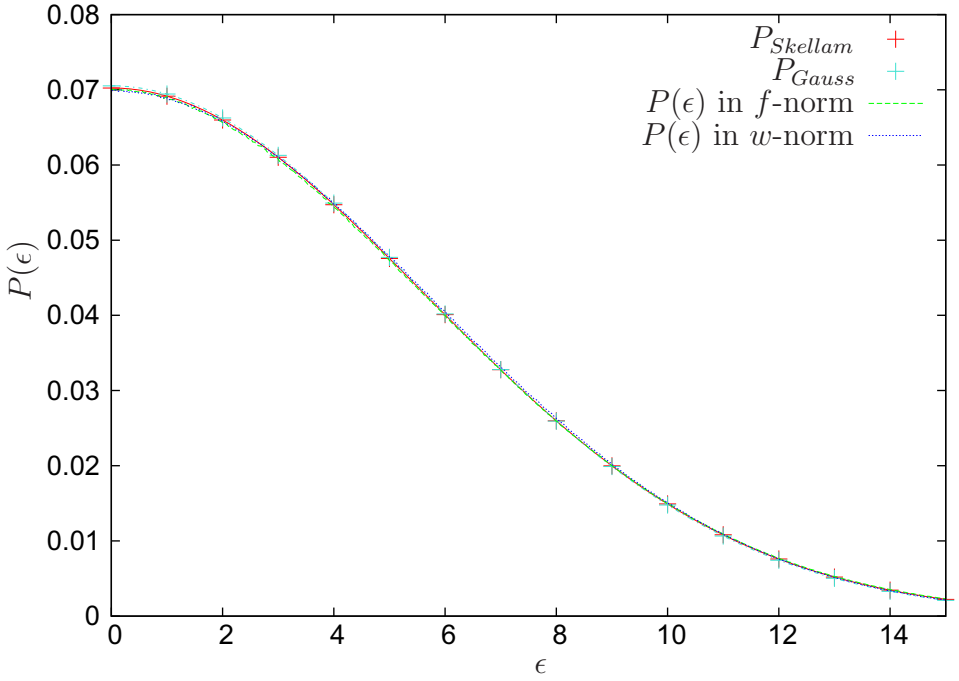

Figure 52. Distribution of the ϵ ghost mode at $\bar{\rho} = 32$, $\bar{\mathbf{u}} = 0$ measured in isothermal fluctuating $D2Q9$ simulation using a Gaussian distribution random number generator.

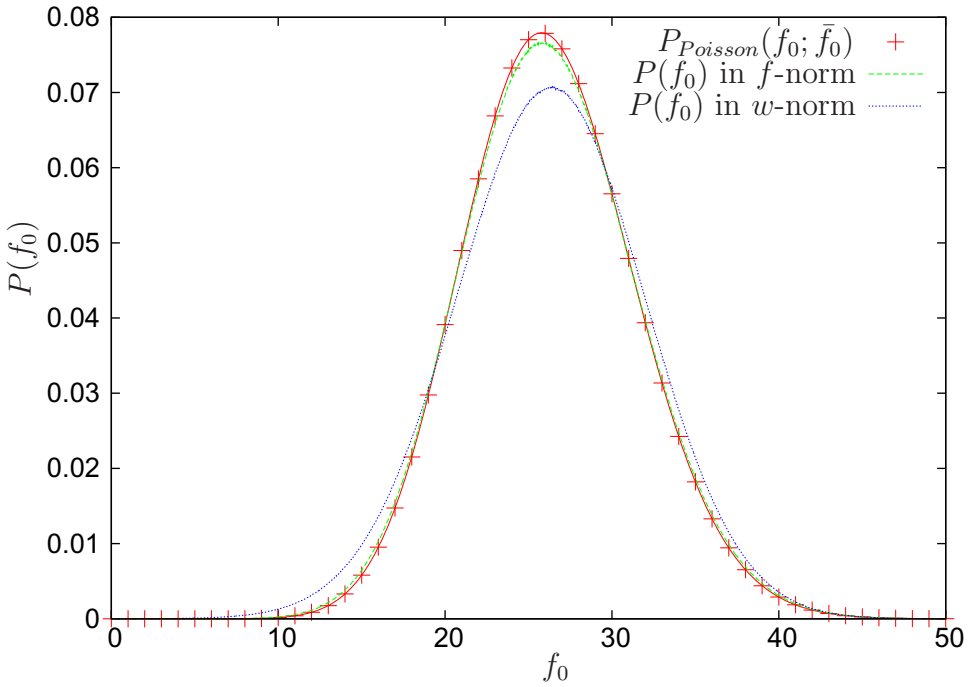

Figure 53. Distribution of f_0 at $\bar{\rho} = 64$, $\bar{\mathbf{u}} = 0.2$ measured in isothermal fluctuating $D2Q9$ simulation using a Gaussian distribution random number generator.

densities are prone to simulation crashes at non vanishing mean velocities. Now the only distribution functions that are, for symmetry reasons, equal are $f_2 = f_4$, $f_5 = f_8$, and $f_6 = f_7$. Consequently $f_0, f_1, f_2, f_3, f_5, f_6$ are displayed.

We observe that for all distribution functions we now find significant disagreement between Hermite and f-norm. In particular in Figure 53 Figure 54 the f-norm results adhere to the continuous Poisson distributions closely provided $\langle f_i \rangle \gtrsim 8$ as discussed earlier in this section. For lower mean values Figure 55 a good statement cannot be made. The distribution functions in the Hermite differ significantly from those of the continuous Poisson distribution as well as from the f-norm results. As in the case of $\rho_0 = 32$, $\langle \mathbf{u} \rangle = 0$ cases they exhibit significantly larger tails in the $f_i < 0$ ranges which likely correlates with significantly worse stability in the low density limit.

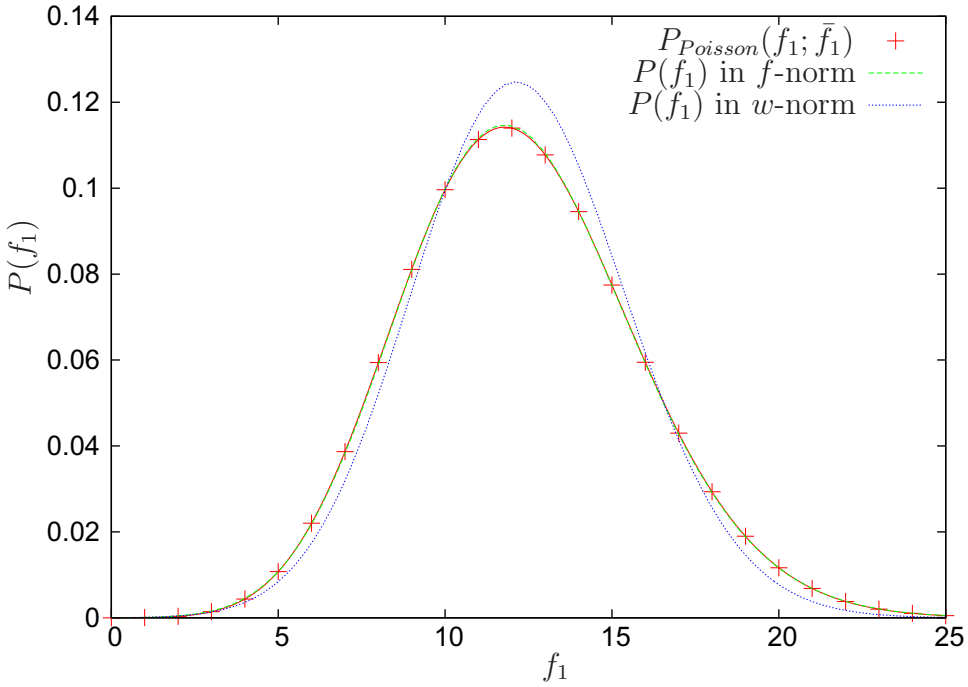

Figure 54. Distribution of f_1 at $\bar{\rho} = 64$, $\bar{\mathbf{u}} = 0.2$ measured in isothermal fluctuating $D2Q9$ simulation using a Gaussian distribution random number generator.

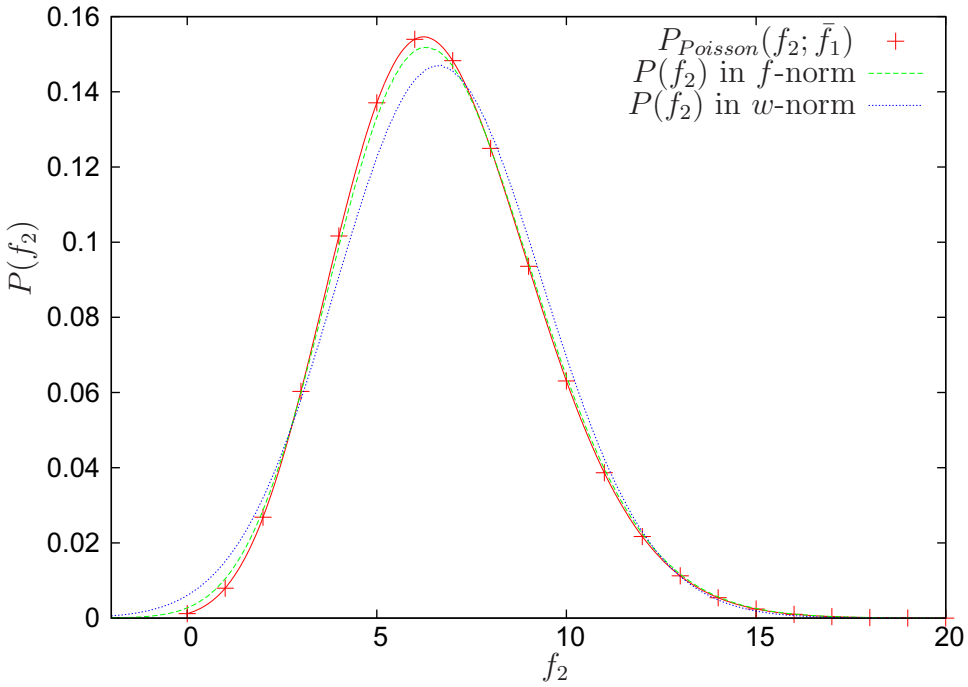

Figure 55. Distribution of f_2 at $\bar{\rho} = 64$, $\bar{\mathbf{u}} = 0.2$ measured in isothermal fluctuating $D2Q9$ simulation using a Gaussian distribution random number generator.

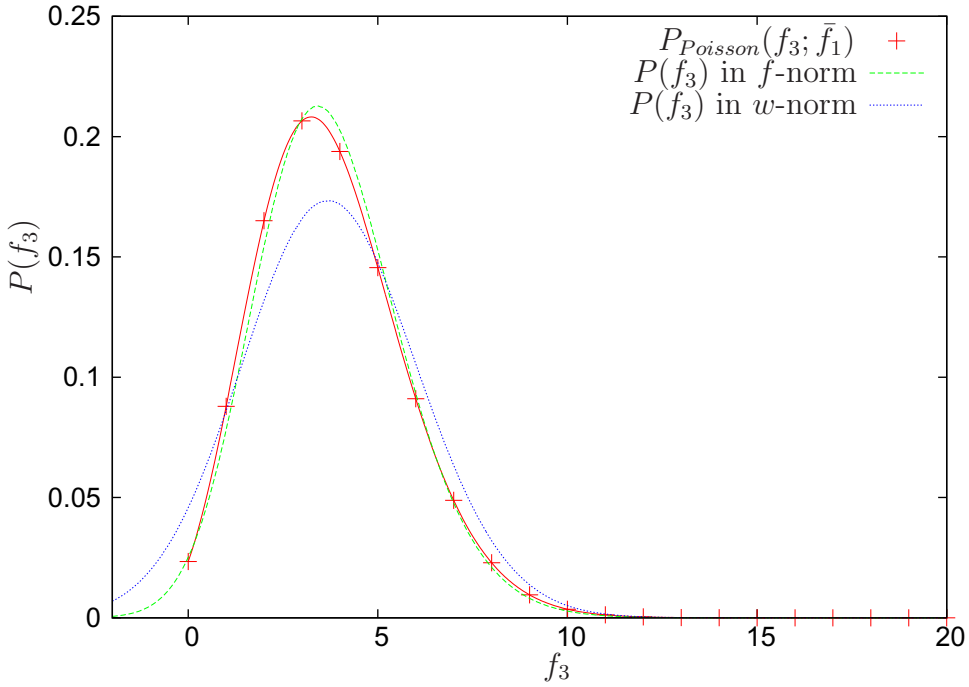

Figure 56. Distribution of f_3 at $\bar{\rho} = 64$, $\bar{\mathbf{u}} = 0.2$ measured in isothermal fluctuating $D2Q9$ simulation using a Gaussian distribution random number generator.

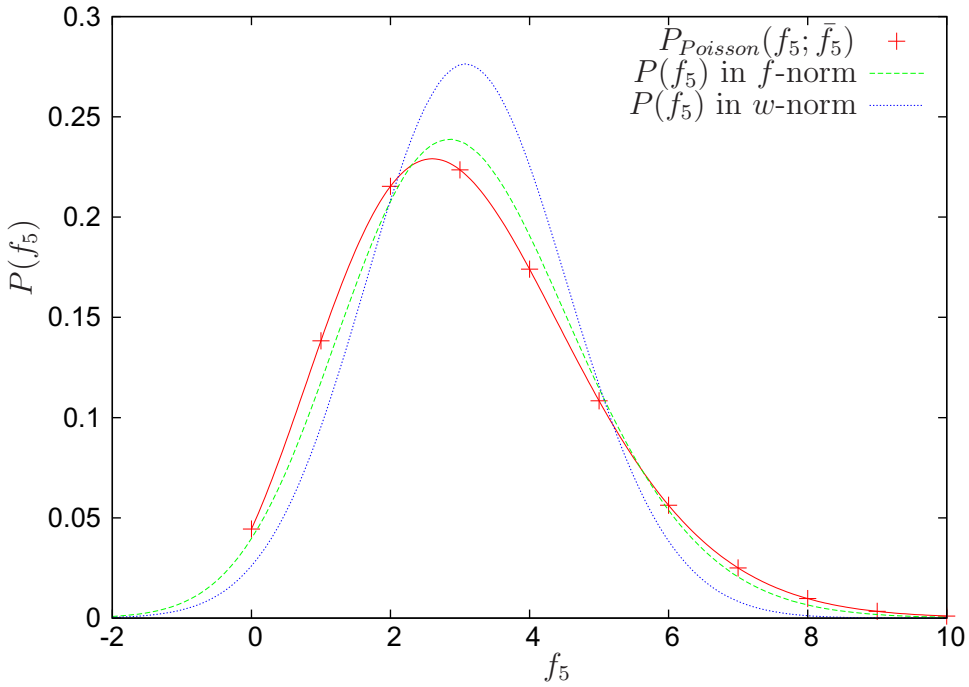

Figure 57. Distribution of f_5 at $\bar{\rho} = 64$, $\bar{\mathbf{u}} = 0.2$ measured in isothermal fluctuating $D2Q9$ simulation using a Gaussian distribution random number generator.

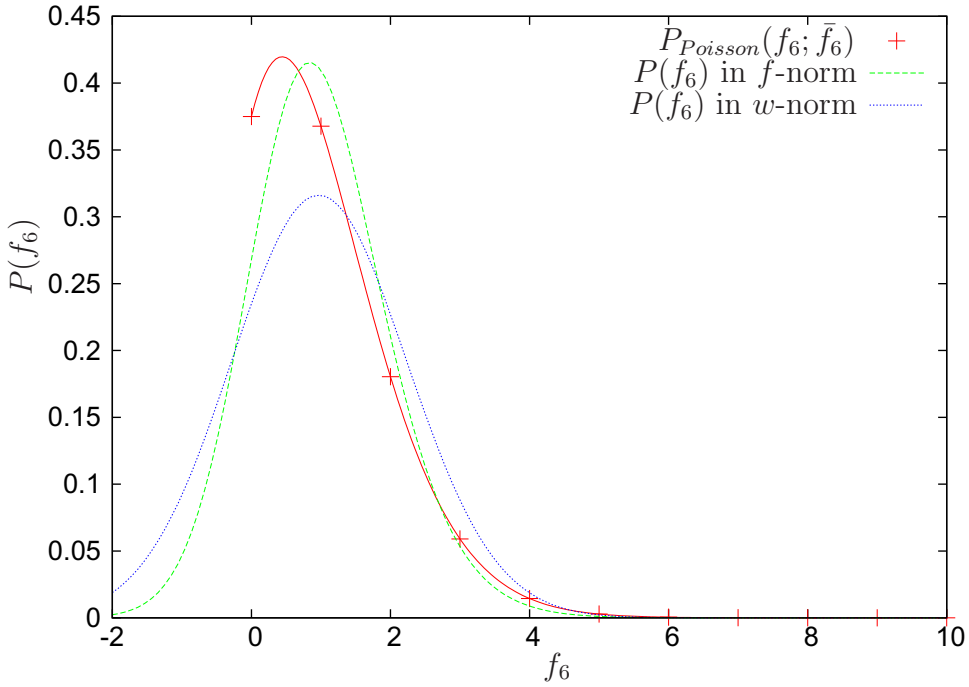

Figure 58. Distribution of f_6 at $\bar{\rho} = 64$, $\bar{\mathbf{u}} = 0.2$ measured in isothermal fluctuating $D2Q9$ simulation using a Gaussian distribution random number generator.

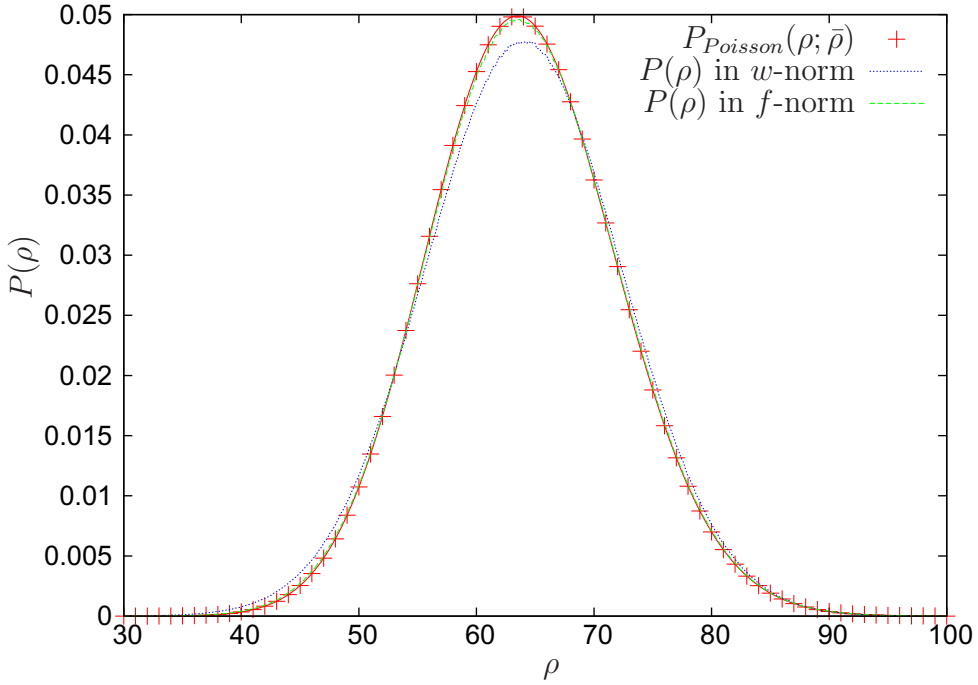

Figure 59. Distribution of ρ at $\bar{\rho} = 64$, $\bar{u}_x = 0.2$ measured in isothermal fluctuating $D2Q9$ simulation using a Gaussian distribution random number generator.

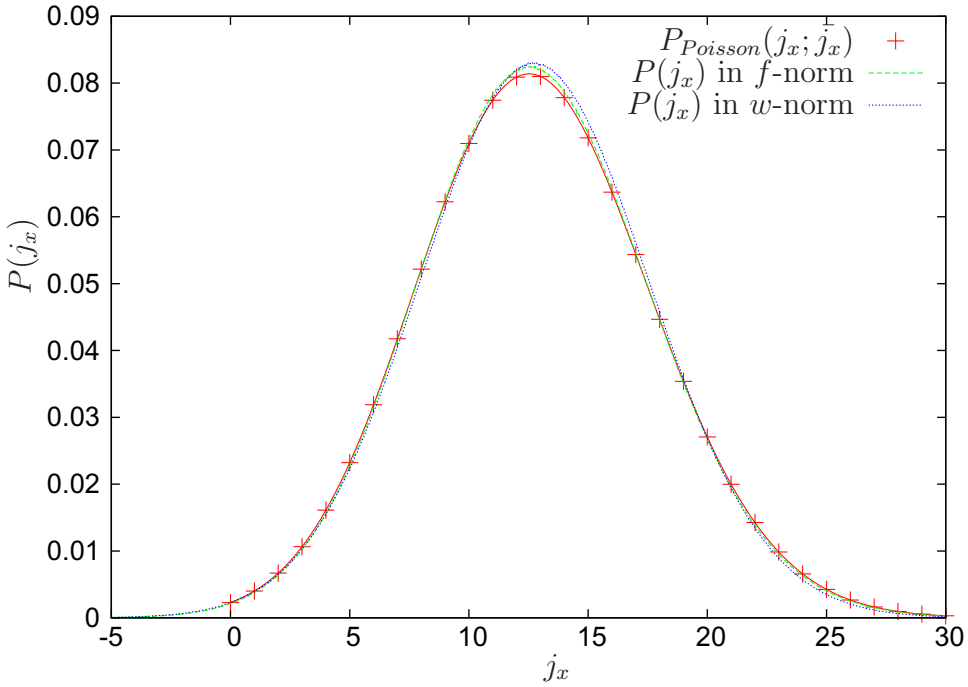

Figure 60. Distribution of j_x at $\bar{\rho} = 64$, $\bar{u}_x = 0.2$ measured in isothermal fluctuating $D2Q9$ simulation using a Gaussian distribution random number generator.

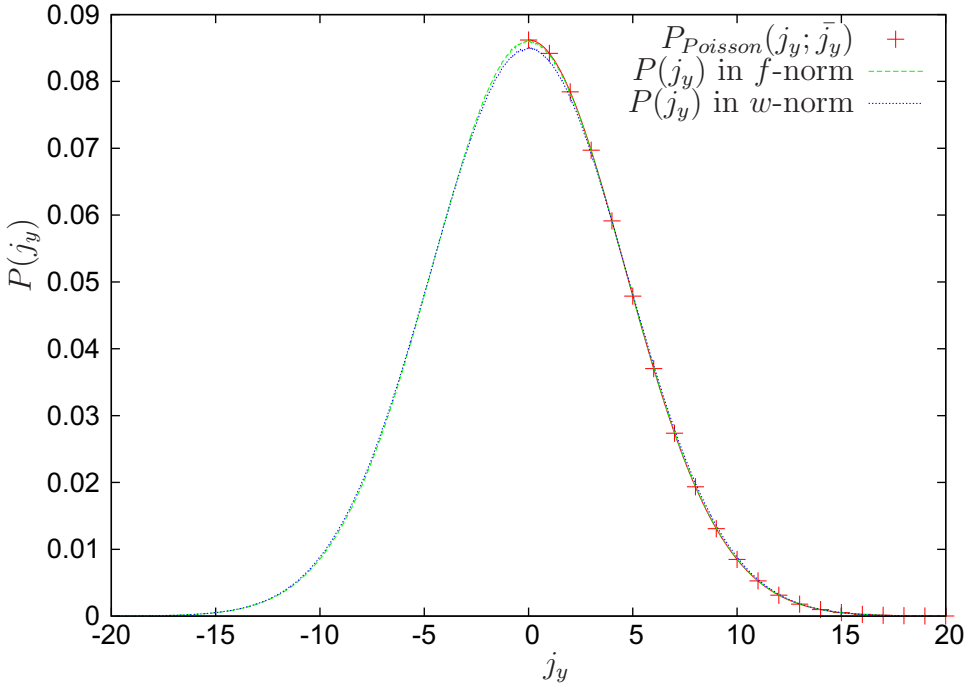

Figure 61. Distribution of j_y at $\bar{\rho} = 64$, $\bar{u}_x = 0.2$ measured in isothermal fluctuating $D2Q9$ simulation using a Gaussian distribution random number generator.

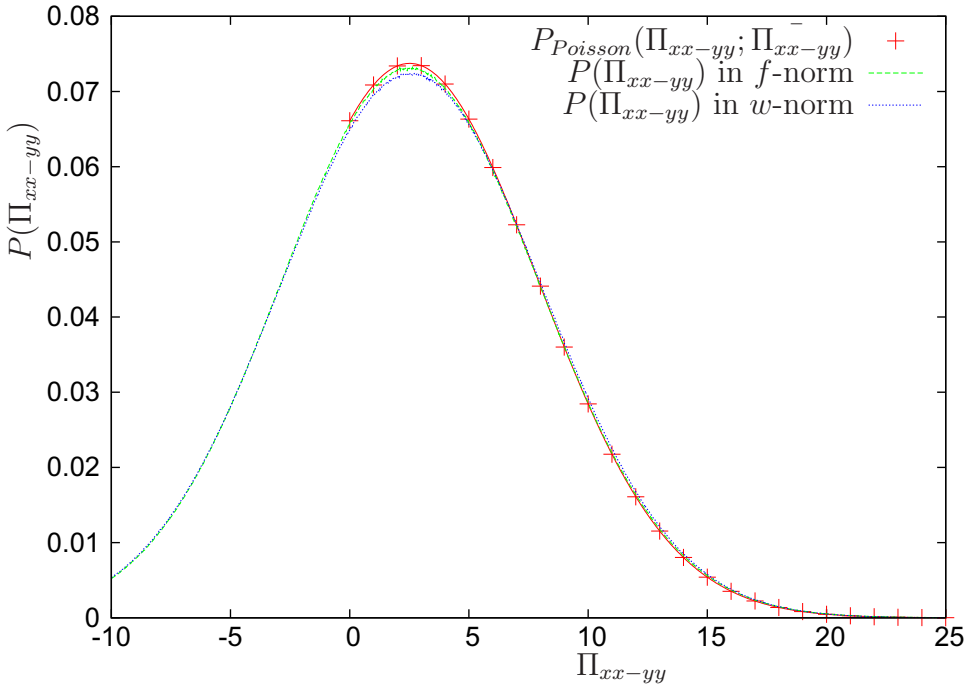

Figure 62. Distribution of Π_{xx-yy} at $\bar{\rho} = 64$, $\bar{u}_x = 0.2$ measured in isothermal fluctuating $D2Q9$ simulation using a Gaussian distribution random number generator.

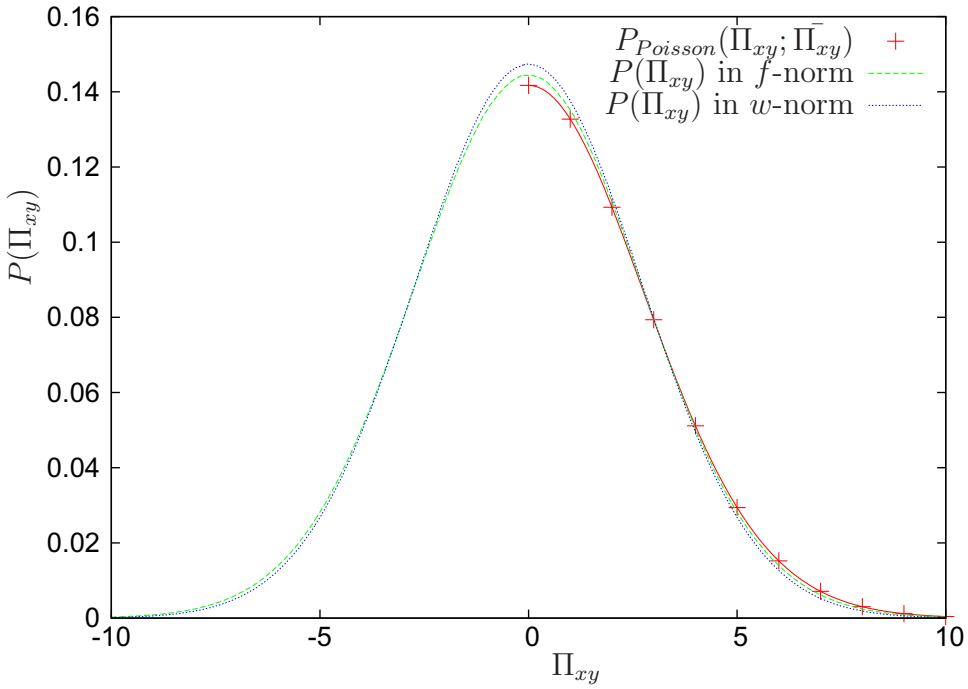

Figure 63. Distribution of Π_{xy} at $\bar{\rho} = 64$, $\bar{u}_x = 0.2$ measured in isothermal fluctuating $D2Q9$ simulation using a Gaussian distribution random number generator.

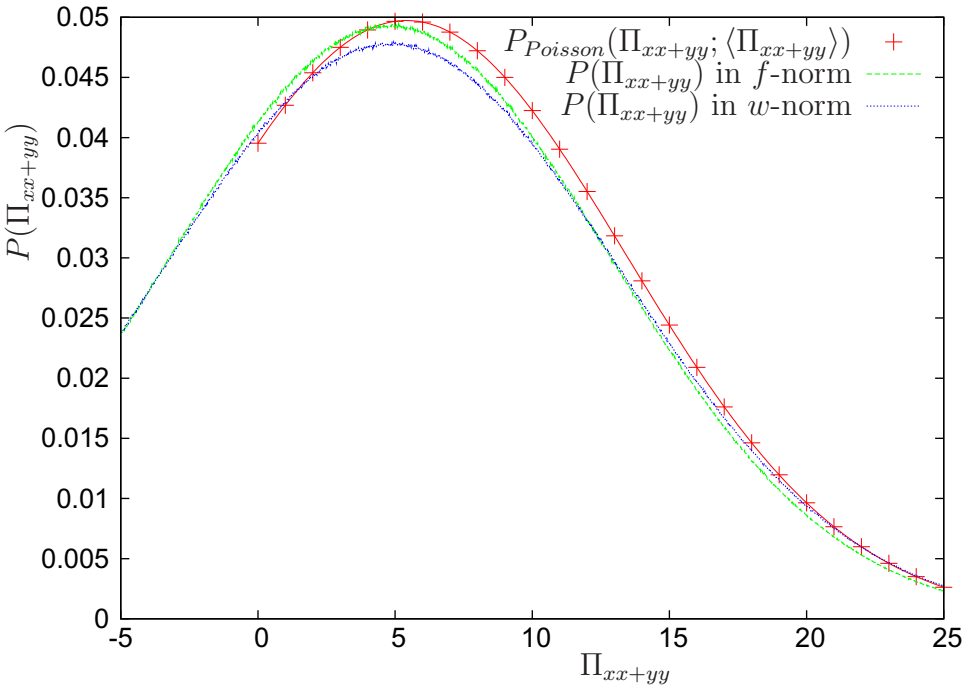

Figure 64. Distribution of Π_{xx+yy} at $\bar{\rho} = 64$, $\bar{u}_x = 0.2$ measured in isothermal fluctuating $D2Q9$ simulation using a Gaussian distribution random number generator.

The same results observed in moment space give a less clear picture. The density distribution function in Figure 59 still shows significantly stronger deviations from the Poisson distribution at $\langle \mathbf{u} \rangle = 0.2$ compared to the one of Figure 45. The remaining hydrodynamic modes, however, do not exhibit larger deviations as seen in Figure 60 and Figure 61 for the momentum components and Figure 62, Figure 63, and Figure 64 for the stress tensor.

5.5. Poiseuille Flow in Two Dimensions

To observe a non-equilibrium system the simple case of a Poiseuille flow was implemented. A Poiseuille flow is a steady driven flow through a channel. For this purpose we used the fluctuating D2Q9 implementation with minor modifications. The

driving component of the Poiseuille flow is implemented as a constant force in the y-direction. We use the forcing term implementation according to [76]

$$F_i = \rho w_i \left[3F_\alpha v_{i\alpha} + \frac{9}{2} \left(F_\alpha u_\beta + F_\beta u_\alpha \right) v_{i\alpha} v_{i\beta} - 3F_\alpha u_\alpha \right] \tag{192}$$

for this purpose. For a constant forcing term without local interaction the fluctuating lattice Boltzmann equation of Eq. (132) can then be written as

$$\begin{aligned} &f_i(\mathbf{x} + \mathbf{v}_i, t+1) - f_i(\mathbf{x}, t) - F_i = \\ &\sum_a n_i^a \left\{ \sum_b \Lambda^{ab} \left[M^b(\mathbf{x}, t) - M^{b,0}(\mathbf{x}, t) \right] + \xi^a \right\}. \end{aligned} \tag{193}$$

The force we use here is a conservative force. In the continuous case this would not impact the collision and in particular the fluctuations and we assume here that this property carries over to the lattice Boltzmann case. Hence the forcing term is applied outside of the local MRT transforms.

To obtain a channel we replace the periodic boundary conditions on the left and right sides of the simulation box with on grid no-slip boundary conditions according to [1, chapter 6]. During the streaming step, taking into account Figure 5, in the column of the left most lattice sites the densities with a velocity component in the x-direction are replaced according to

$$\begin{aligned} f_3(0, y) &\to f_1'(0, y) \\ f_8(0, y) &\to f_6'(0, y) \\ f_5(0, y) &\to f_7'(0, y). \end{aligned} \tag{194}$$

Similarly at the right most lattice boundary,

$$f_1(w,y) \to f_3'(w,y) \tag{195}$$
$$f_8(w,y) \to f_6'(w,y)$$
$$f_5(w,y) \to f_7'(w,y).$$

Here the f' represent the post-streaming density and f the density prior to streaming, i.e. moving the densities according to their velocity vectors. We thus obtain a channel the width of which is the extension in the x-direction of the lattice Boltzmann simulation box. Measured in lattice units this width will be referred to as w in the following.

5.5.1. Navier-Stokes Equation for Fluctuating Stress Tensor

In order to verify the forcing implementation and find an analytic solution of the velocity profile in the Poiseuille-channel we require expressions for the hydrodynamic equations with contributions from the forcing term. This calculation is performed analogously to the discussion in section 3. Unlike that derivation, however, the emphasis here is the effect of fluctuations on the local temperature dependence and its effect on the viscosity terms. We begin with a general expression for the expansion of the ideal lattice-Boltzmann equation with an added forcing term:

$$\sum_{k=1}^{\infty} \frac{(\Delta t)^k}{k!} \left(\partial_t + v_{i\alpha}\partial_\alpha\right)^k f_i = \Delta t \sum_j \Lambda_{ji} \left(f_j^0 - f_j\right) + F_i + \xi_i. \tag{196}$$

Here f_i and f_i^0 describe the current local distribution and the global equilibrium distribution respectively, and F_i will be used to include a constant external force expression according to Eq. (192). To obtain hydrodynamics of mean values we need to calculate the hydrodynamic equations by means of the ensemble average of the

equilibrium distribution $\langle f_i^0 \rangle$. Finally ξ_i is a noise expression in velocity space that can be derived in the moment space representation as discussed in section 4. Now to evaluate the effect of fluctuations on the hydrodynamic equations we take the ensemble average of all quantities. We obtain

$$\sum_{k=1}^{\infty} \frac{(\Delta t)^k}{k!} \left(\partial_t + v_{i\alpha}\partial_\alpha\right)^k \langle f_i \rangle = \Delta t \sum_j \Lambda_{ji} \left(\langle f_j^0 \rangle - \langle f_j \rangle \right) + \langle F_i \rangle. \tag{197}$$

where we used $\langle \xi_i \rangle = 0$ as the noise cannot change expectation value of distribution. The moments for the expectation value of the $\langle f_i^0 \rangle$ are calculated from Eq. (178) and Eq. (181). They are

$$\sum_i \langle f_i^0 \rangle = \bar{\rho} \tag{198}$$

$$\sum_i \langle f_i^0 \rangle v_{i\alpha} = \bar{j}_\alpha \tag{199}$$

$$\sum_i \langle f_i^0 \rangle v_{i\alpha} v_{i\beta} = \theta \bar{\rho} \delta_{\alpha\beta} + k_B T \delta_{\alpha\beta} + \bar{\rho} \bar{u}_\alpha \bar{u}_\beta = k_B T \bar{\rho} \delta_{\alpha\beta} + \bar{\rho} \bar{u}_\alpha \bar{u}_\beta \tag{200}$$

$$\sum_i \langle f_i^0 \rangle v_{i\alpha} v_{i\beta} v_{i\gamma} = \theta \bar{\rho} \left(\bar{u}_\alpha \delta_{\beta\gamma} + \bar{u}_\beta \delta_{\gamma\alpha} + \bar{u}_\gamma \delta_{\alpha\beta} \right) + \bar{\rho} \bar{u}_\alpha \bar{u}_\beta \bar{u}_\gamma + Q_{\alpha\beta\gamma}. \tag{201}$$

We pay particular attention to the second order expression Eq. (200) here where the corrections to the second order terms of Eq. (181) introduce an additional term of $k_B T \delta_{ga\beta}$ compared to the usual second order moment shown in Eq. (85). With

$$\bar{\rho}\theta + k_B T = \bar{\rho}\theta + \frac{\bar{\rho}}{\bar{\rho} - 1}\theta = \frac{\bar{\rho}^2}{\bar{\rho} - 1}\theta = \bar{\rho} k_B T \tag{202}$$

we find Eq. (200). It is worth noting that on the third order moments in Eq. (201) for all models for which $v_{i\alpha}^3 = v_{i\alpha}$, e.g. D1Q3, D2Q9, D3Q19 the expression of the third order moment does not recover $\bar{\rho} \bar{u}_\alpha \bar{u}_\beta \bar{u}_\gamma$ and this introduces Galilean invariance

violations [30]. To accomodate for this deficiency a correction term for this the formal expression $Q_{\alpha\beta\gamma} = -\bar{\rho}\bar{u}_\alpha\bar{u}_\beta\bar{u}_\gamma$ is introduced.

The forcing term moments according to Eq. (192) give

$$\sum_i \langle F_i \rangle = 0 \tag{203}$$

$$\sum_i \langle F_i \rangle v_{i\alpha} = \bar{\rho} a_\alpha \tag{204}$$

$$\sum_i \langle F_i \rangle v_{i\alpha} v_{i\beta} = \bar{\rho} \left(a_\alpha \bar{u}_\beta + a_\beta \bar{u}_\alpha \right) \tag{205}$$

$$\sum_i \langle F_i \rangle v_{i\alpha} v_{i\beta} v_{i\gamma} = \theta \bar{\rho} \left(a_\alpha \delta_{\beta\gamma} + a_\beta \delta_{\gamma\alpha} + a_\gamma \delta_{\alpha\beta} \right) \tag{206}$$

where we understand that components of the acceleration a_α are constants in this example.

The second order expansion of Eq. (197) is found to be

$$\begin{aligned}
&(\partial_t + v_{i\alpha}\partial_\alpha) \left(\langle f_i^0 \rangle + \sum_j \Lambda_{ji}^{-1} \langle F_j \rangle \right) \\
&+ (\partial_t + v_{i\alpha}\partial_\alpha) \sum_j \left[\left(\frac{1}{2} - \Lambda_{ij}^{-1} \right) (\partial_t + v_{j\beta}\partial_\beta) \left(\langle f_j^0 \rangle + \sum_k \Lambda_{jk}^{-1} \langle F_k \rangle \right) \right] \\
&= \sum_j \Lambda_{ij} \left(\langle f_j^0 \rangle - \langle f_j \rangle \right) + \langle F_j \rangle + O(\partial^3).
\end{aligned} \tag{207}$$

Equivalently to the discussion of section 3 the continuity equation is obtained by summation of Eq. (207) over the density eigenvector $\psi^{\rho} = 1_i$ and substitution of all moments of $\langle f_i^0 \rangle$, and $\langle F_i \rangle$ yields

$$\begin{aligned}\partial_t \bar{\rho} + \partial_\alpha \bar{\rho} \bar{u}_\alpha + \tau^{j_\alpha} \partial_\alpha \bar{\rho} a_\alpha + \partial_t \left(\frac{1}{2} - \tau^{\rho} \right) \left[\partial_t \bar{\rho} + \partial_\beta \left(\bar{\rho} \bar{u}_\beta + \tau^{j_\beta} \bar{\rho} a_\beta \right) \right] \\ + \partial_\alpha \left(\frac{1}{2} - \tau^{j_\alpha} \right) \left[\partial_t \left(\bar{\rho} \bar{u}_\alpha + \tau^{j_\alpha} \bar{\rho} a_\alpha \right) \right. \\ \left. + \partial_\beta \left(k_B T \bar{\rho} \delta_{\alpha\beta} + \bar{\rho} \bar{u}_\alpha \bar{u}_\beta + \tau^{\alpha\beta} \left(\bar{\rho} a_\alpha \bar{u}_\beta + \bar{\rho} a_\beta \bar{u}_\alpha \right) \right) \right] \\ = 0 + O(\partial^3). \end{aligned} \tag{208}$$

Similarly we can perform the summation over the momentum eigenvector $\psi^{j_\gamma} = v_{i\gamma}$. For now the expansion to first order will suffice. We find

$$\begin{aligned}\partial_t \left(\bar{\rho} \bar{u}_\gamma + \tau^{j_\gamma} \bar{\rho} a_\gamma \right) + \partial_\alpha \left[k_B T \bar{\rho} \delta_{\alpha\gamma} + \bar{\rho} \bar{u}_\alpha \bar{u}_\gamma + \tau^{\alpha\gamma} \left(\bar{\rho} a_\alpha \bar{u}_\gamma + \bar{\rho} a_\gamma \bar{u}_\alpha \right) \right] \\ = \bar{\rho} a_\gamma + O(\partial^2) \end{aligned} \tag{209}$$

where we recognize the left hand side in Eq. (209) as the contents of the second order spatial derivative of Eq. (208). It can thus be replaced by $\partial_\alpha (1/2 - \tau^{j_\alpha}) \bar{\rho} a_\alpha$. Likewise the terms contained in the second order temporal derivative in Eq. (208) are identical with the first order expressions of the same equation and can thus be absorbed into the remaining third order terms. The second order derivatives thus are completely absorbed into the third order expression except for $\partial_\alpha (1/2 - \tau^{j_\alpha}) \bar{\rho} a_\alpha$ and we find

$$\partial_t \bar{\rho} + \partial_\alpha \bar{\rho} \tilde{u}_\alpha + O(\partial^3) = 0 \tag{210}$$

where we have substituted

$$\tilde{u}_\alpha = \bar{u}_\alpha + \frac{1}{2} a_\alpha \tag{211}$$

as the macroscopic definition of velocity. This is the continuity equation of the local expectation value of the number of particles $\bar{\rho}$. It functionally different from the result obtained in section 3 only through the macroscopic velocity definition of Eq. (211) due to the forcing term introduced in Eq. (197).

To obtain the equation of conservation of momentum we extend the expansion of 209 to second order

$$\begin{aligned}
&\partial_t\left(\bar{\rho}\bar{u}_\gamma + \tau^{j_\gamma}\bar{\rho}a_\gamma\right) + \partial_\alpha\left[k_BT\bar{\rho}\delta_{\alpha\gamma} + \bar{\rho}\bar{u}_\alpha\bar{u}_\gamma + \tau^{\alpha\gamma}\left(\bar{\rho}a_\alpha\bar{u}_\gamma + \bar{\rho}a_\gamma\bar{u}_\alpha\right)\right] \\
\partial_t\left(\frac{1}{2} - \tau^{j_\gamma}\right)&\left[\partial_t\left(\bar{\rho}\bar{u}_\gamma + \tau^{j_\gamma}\bar{\rho}a_\gamma\right) + \partial_\beta k_BT\bar{\rho}\delta_{\beta\gamma} + \bar{\rho}\bar{u}_\beta\bar{u}_\gamma + \tau^{\beta\gamma}\left(\bar{\rho}a_\beta\bar{u}_\gamma + \bar{\rho}a_\gamma\bar{u}_\beta\right)\right] \\
\partial_\alpha\left(\frac{1}{2} - \tau^{\alpha\gamma}\right)&\Big\{\partial_t\left[k_BT\bar{\rho}\delta_{\alpha\gamma} + \bar{\rho}\bar{u}_\alpha\bar{u}_\gamma + \tau^{\alpha\gamma}\left(\bar{\rho}a_\alpha\bar{u}_\gamma + \bar{\rho}a_\gamma\bar{u}_\alpha\right)\right] \\
&+ \partial_\beta[\theta\bar{\rho}\left(\bar{u}_\alpha\delta_{\beta\gamma} + \bar{u}_\beta\delta_{\gamma\alpha} + \bar{u}_\gamma\delta_{\alpha\beta}\right) + \bar{\rho}\bar{u}_\alpha\bar{u}_\beta\bar{u}_\gamma + Q_{\alpha\beta\gamma} \\
&+ \tau^{\alpha\beta\gamma}\theta\bar{\rho}\left(a_\alpha\delta_{\beta\gamma} + a_\beta\delta_{\gamma\alpha} + a_\gamma\delta_{\alpha\beta}\right)]\Big\} \\
&= \bar{\rho}a_\gamma + O(\partial^3).
\end{aligned} \tag{212}$$

Like in the case of the continuity equation we can absorb the temporal second order derivative into third order as its contents exactly reproduces the first order terms in Eq. (212). We do, however, retain $\partial_t(1/2 - \tau^{j_\gamma})\bar{\rho}a_\gamma$ which combines with the first order temporal derivative terms to $\partial_t\bar{\rho}\tilde{u}_\gamma$.

The treatment of the second order terms is slightly more involved and while in spirit very similar to the one in section 3 gives rise to an interesting question and will thus be done in detail here. The first goal is to remove all temporal derivatives from the spatial second order derivative terms. We have

$$\partial_\alpha\partial_t k_BT\bar{\rho}\delta_{\alpha\gamma} = \partial_\alpha k_BT\partial_\beta\bar{\rho}\left(\bar{u}_\beta + \frac{1}{2}a_\beta\right) \tag{213}$$

where we use Eq. (210) and require $\partial_\alpha k_b T = 0$ which is only correct according to the definition in Eq. (176) when there is a time invariant mean density distribution in the system. We treat

$$\partial_\alpha \partial_t \bar{\rho} \bar{u}_\alpha \bar{u}_\gamma = \partial_\alpha \left(\bar{u}_\alpha \partial_t \bar{\rho} \bar{u}_\gamma + \bar{u}_\gamma \bar{\rho} \partial_t \bar{u}_\alpha \right) = \partial_\alpha \left[\bar{u}_\alpha \partial_t \bar{\rho} \bar{u}_\gamma + \bar{u}_\gamma \left(\partial_t \bar{\rho} \bar{u}_\alpha - \bar{u}_\alpha \partial_t \bar{\rho} \right) \right] \tag{214}$$

by chain rule and replace the two occurances of $\partial_t \bar{\rho} \bar{u}_\alpha$ according to

$$\partial_t \bar{\rho} \bar{u}_\alpha = -\partial_\gamma \left(k_B T \bar{\rho} \delta_{\alpha\gamma} + \bar{\rho} \bar{u}_\alpha \bar{u}_\gamma \right) + \bar{\rho} a_\alpha + O(\partial^2). \tag{215}$$

The $\partial_\gamma \tau^{\alpha\gamma} (\bar{\rho} \bar{u}_\alpha a_\gamma + \bar{\rho} \bar{u}_\gamma a_\alpha)$ and $\partial_t \tau^{j_\alpha} \bar{\rho} a_\alpha$ terms are absorbed into the second order terms as $\bar{\rho} a_\alpha$ itself is a derivative term by Eq. (212). The complete second order expression then becomes

$$\begin{aligned} \partial_\alpha \left(\frac{1}{2} - \tau^{\alpha\gamma} \right) \Bigg\{ & k_B T \delta_{\alpha\gamma} \partial_\beta \bar{\rho} \left(\bar{u}_\beta + \frac{1}{2} a_\beta \right) \\ & - \bar{u}_\alpha \partial_\beta k_B T \bar{\rho} \delta_{\beta\gamma} - \bar{u}_\alpha \partial_\beta \bar{\rho} \bar{u}_\beta \bar{u}_\gamma + \bar{u}_\alpha \bar{\rho} a_\gamma \\ & - \bar{u}_\gamma \partial_\beta k_B T \bar{\rho} \delta_{\alpha\beta} - \bar{u}_\gamma \partial_\beta \bar{\rho} \bar{u}_\beta \bar{u}_\alpha + \bar{u}_\gamma \bar{\rho} a_\alpha + \bar{u}_\gamma \bar{u}_\alpha \partial_\beta \bar{\rho} \left(\bar{u}_\beta + \frac{1}{2} a_\beta \right) \\ & + \partial_\beta \theta \bar{\rho} \left(\bar{u}_\alpha \delta_{\beta\gamma} + \bar{u}_\beta \delta_{\gamma\alpha} + \bar{u}_\gamma \delta_{\alpha\beta} \right) + \partial_\beta \bar{\rho} \bar{u}_\alpha \bar{u}_\beta \bar{u}_\gamma + \partial_\beta Q_{\alpha\beta\gamma} \Bigg\}. \end{aligned} \tag{216}$$

For simplicity we do not separate shear and bulk stress terms here unlike the discussion in section 3. By means of the chain rule this expression can be concatenated to

$$\begin{aligned} \left(\frac{1}{2} - \tau^{\alpha\gamma} \right) \Big[& \partial_\alpha k_B T \bar{\rho} \left(\partial_\gamma \bar{u}_\alpha + \partial_\alpha \bar{u}_\gamma \right) + \partial_\alpha \left(\bar{\rho} \bar{u}_\alpha a_\gamma + \bar{\rho} \bar{u}_\gamma a_\alpha \right) + O(\partial^3) \\ & + \partial_\gamma \left(\theta - k_B T \right) \partial_\beta \bar{\rho} \bar{u}_\beta - \partial_\alpha \left(\partial_\gamma \bar{u}_\alpha k_B T + \partial_\alpha \bar{u}_\gamma k_B T \right) \Big]. \end{aligned} \tag{217}$$

The first line of Eq. (217) is the regular result for second order terms in the Navier-Stokes equation with a forcing term [77] while the second line contains terms that originate from the local temperature definition used in Eq. (200). The exact treatment of these is not quite clear. Combining Eq. (212) with the results of the second order terms Eq. (217) we obtain the Navier-Stokes equation

$$\begin{aligned}\partial_t\left(\bar{\rho}\tilde{u}_\gamma\right)+\partial_\alpha\left(\bar{\rho}\tilde{u}_\alpha\tilde{u}_\gamma\right)&=\bar{\rho}a_\gamma-\partial_\alpha k_BT\bar{\rho}\delta_{\alpha\gamma}-\partial_\alpha\left[\eta\left(\partial_\gamma\bar{u}_\alpha+\partial_\alpha\bar{u}_\gamma\right)\right]+O(\partial^3)\\&+\left(\tau^{\alpha\gamma}-\frac{1}{2}\right)\left[\partial_\gamma\left(\theta-k_BT\right)\partial_\beta\bar{\rho}\bar{u}_\beta-\partial_\alpha\left(\partial_\gamma\bar{u}_\alpha k_BT+\partial_\alpha\bar{u}_\gamma k_BT\right)\right]\end{aligned}\tag{218}$$

where η is the shear viscosity

$$\eta=\left(\tau^{\alpha\beta}-\frac{1}{2}\right)\bar{\rho}k_BT.\tag{219}$$

Again the last line of Eq. (218) contains the unresolved terms due to the local temperature definition. It is not surprising to find these additional terms when one considers that the changes in the second order moments appear in the derivation in similar fashion as non-ideal pressure tensor contributions would. Similar expressions were found in this conext, for example in [77].

5.5.2. Velocity Profile in the Poiseuille Channel

For the discussion of the Poiseuille flow a fluctuating ideal gas with an external constant forcing term is sufficient. To find the analytic expression for the velocity profile in two dimensions we solve Eq. (218). For this discussion we disregard the the new terms introduced in the derivation with local temperature definition. We assume a steady flow, i.e. all derivatives with respect to time vanish. In a steady state derivatives in the y-direction must also vanish if there are no other forces present and we assume that the fluctuating stress vanishes in the time average even though

we strictly only know this for the equilibrium state. The velocity in the y-direction then follows from Eq. (218) as

$$\partial_t \rho \tilde{u}_y + \partial_x \left(\rho \tilde{u}_x \tilde{u}_y\right) + \partial_y \left(\rho \tilde{u}_x \tilde{u}_y\right) = \rho a_y - \partial_x \tau^{xy} \xi_{xy} - \eta \partial_x^2 \tilde{u}_y \tag{220}$$

Omitting vanishing temporal and spatial derivatives in the x-direction and using that $\tilde{u}_x = 0$ we are left with

$$0 = \frac{a_y}{\eta} + \partial_x^2 u_y. \tag{221}$$

We now use a constant acceleration a_y and that at the boundaries the mean velocity vanishes $u_y(x = 0) = u_y(x = w) = 0$, where we have introduced the channel width w, and find the expression for the velocity profile

$$u_y(x) = \frac{a_y}{2\eta}\left(x - \frac{w}{2}\right)^2 - \frac{a_y}{8\eta} w^2 \tag{222}$$

In Figure 65 we have measured the Poiseuille flow profile for $\rho = 64$, the lowest density for which both Hermite and f-norm reliably function, i.e. simulations with the w_i-norm do not crash. To maintain $\langle u_y \rangle(x) < 0.2$ the small acceleration $a_y = 0.0005$ was chosen. At this low density we observe the impact of the temperature correction and find very good agreement between the temperature corrected prediction $u_y(x, \mu_{corr})$ and the simulation results obtained via the f-norm. The Hermite norm results lie between the corrected and uncorrected velocity profiles. This observation becomes more evident in Figure 66 where we measured the velocity at the center of the Poiseuille channel as a function of mean densities. We show here again, that the f-norm can be successfully simulated at $\langle \rho \rangle = 32$ whereas the Hermite norm simulation has already failed due to instabilitiy issues.

In conclusion we find that the density dependent definition of the viscosity due to the local temperature $k_B T$ derived in Eq. (218) is confirmed in our simulation

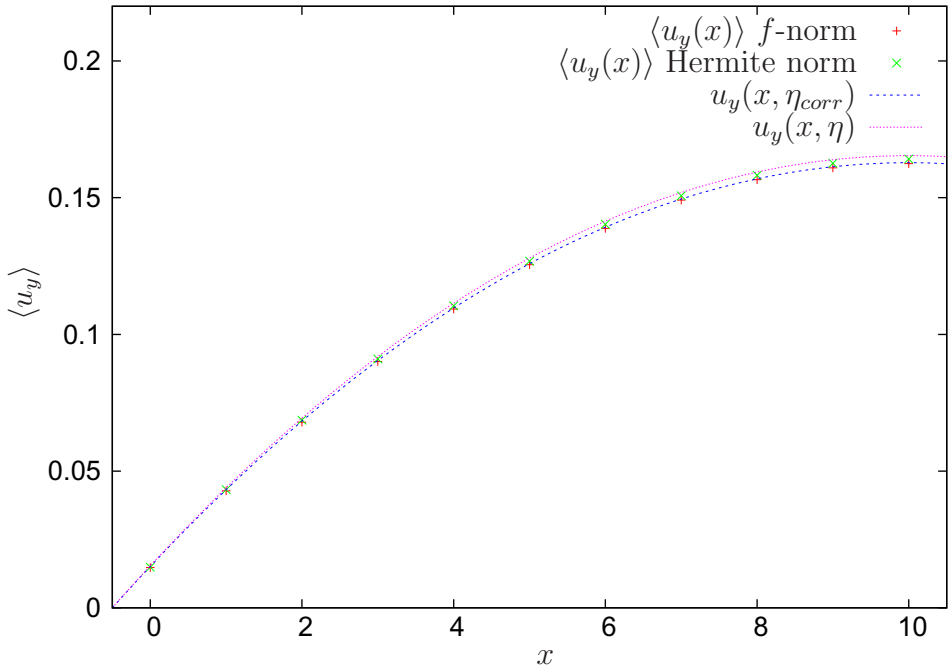

Figure 65. Velocity profile $\langle u_y\rangle(x)$ in a Poiseuille flow measured in an isothermal fluctuating $D2Q9$ simulation at $\rho = 64$ with a constant acceleration of $a_y = 0.0005$ and relaxation time $\tau_B = 1$.

results. This only holds for the f-norm with locally velocity dependent transforms and a noise term that depends on the local density as well. The results for the w-norm implementation underestimate the deviation of the channel center velocity by more than 50% as seen in Figure 66.

While the deviation in the local temperature and the distribution functions will most likely not be of particular relevance to most fluctuating lattice Boltzmann simulations, the discussion of critical phenomena could benefit from the much improved precision and also the significantly better stability.

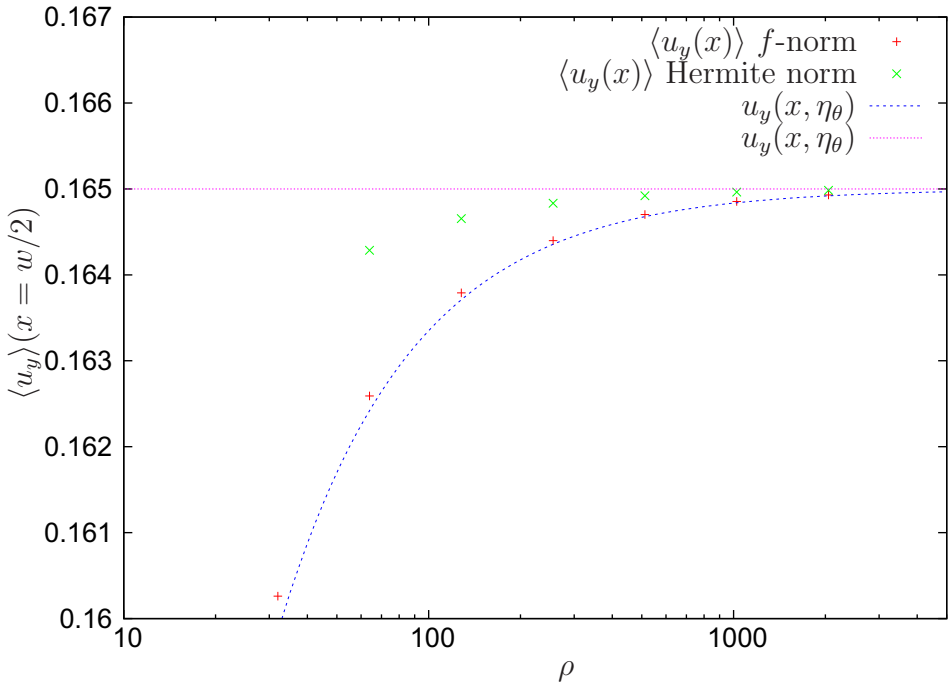

Figure 66. Maximum velocity $\langle u_y \rangle (x = w/2)$ of a Poiseuille flow at the center of a channel of width $w = 21$ as a function of mean particle density ρ measured in an isothermal fluctuating $D2Q9$ simulation with stress relaxation time $\tau_B = 1$ with a constant acceleration of $a_y = 0.0005$.

REFERENCES

[1] S. Succi, *The lattice Boltzmann equation for fluid dynamics and beyond*. Oxford University Press, USA, first ed., 2001.

[2] S. Succi and R. Benzi, "Lattice boltzmann equation for quantum mechanics," *Physica D: Nonlinear Phenomena*, vol. 69, no. 34, pp. 327 – 332, 1993.

[3] S. Succi, "Numerical solution of the schrödinger equation using discrete kinetic theory," *Phys. Rev. E*, vol. 53, pp. 1969–1975, Feb 1996.

[4] L. Zhong, S. Feng, P. Dong, and S. Gao, "Lattice boltzmann schemes for the nonlinear schrödinger equation," *Phys. Rev. E*, vol. 74, p. 036704, Sep 2006.

[5] G. Fogaccia, R. Benzi, and F. Romanelli, "Lattice boltzmann algorithm for three-dimensional simulations of plasma turbulence," *Phys. Rev. E*, vol. 54, pp. 4384–4393, Oct 1996.

[6] P. J. Dellar, "Lattice kinetic schemes for magnetohydrodynamics," *Journal of Computational Physics*, vol. 179, no. 1, pp. 95 – 126, 2002.

[7] M. Mendoza and J. D. Muñoz, "Three-dimensional lattice boltzmann model for electrodynamics," *Phys. Rev. E*, vol. 82, p. 056708, Nov 2010.

[8] L. Boltzmann, "Weitere Studien über das Wärmegleichgewicht unter Gasmolekülen," *Wiener Berichte*, vol. 66, pp. 275–370, 1872.

[9] P. Grosfils, J.-P. Boon, and P. Lallemand, "Spontaneous fluctuation correlations in thermal lattice-gas automata," *Phys. Rev. Lett.*, vol. 68, pp. 1077–1080, Feb 1992.

[10] A. J. C. Ladd, "Short-Time Motion of Colloidal Particles - Numerical-Simulation via a Fluctuating Lattice-Boltzmann Equation," *Phys. Rev. Lett.*, vol. 70, no. 9, pp. 1339–1342, 1993.

[11] D. W. Grunau, T. Lookman, S. Y. Chen, and A. S. Lapedes, "Domain growth, wetting, and scaling in porous media," *Phys. Rev. Lett.*, vol. 71, pp. 4198–4201, Dec 1993.

[12] O. Usta, A. Ladd, and J. Butler, "Lattice-Boltzmann simulations of the dynamics of polymer solutions in periodic and confined geometries," *Journal of Chemical Physics*, vol. 122, p. 094902, March 2005.

[13] R. Adhikari, K. Stratford, M. E. Cates, and A. J. Wagner, "Fluctuating lattice Boltzmann," *Europhys. Lett.*, vol. 71, pp. 473–479, August 2005.

[14] P. bLangevin, "Sur la théorie du mouvement brownien," *C. R. Acad. Sci. (Paris)*, vol. 146, pp. 530–533, 1908.

[15] R. F. Fox and G. E. Uhlenbeck, "Contributions to nonequilibrium thermodynamics. ii. theory of hydrodynamical fluctuations," *Phys. Fluids*, vol. 13, no. 12, p. 2881, 1970.

[16] M. Bixon and R. Zwanzig, "Boltzmann-Langevin Equation and Hydrodynamic Fluctuations," *Phys. Rev.*, vol. 187, no. 1, pp. 267–272, 1969.

[17] J. Logan and M. Kac, "Fluctuations and the boltzmann equation. i," *Phys. Rev. A*, vol. 13, pp. 458–470, January 1976.

[18] K. Huang, *Statistical Mechanics*. Wiley, second ed., 1987.

[19] P. L. Bhatnagar, E. P. Gross, and M. Krook, "A Model for Collision Processes in Gases. I. Small Amplitude Processes in Charged and Neutral One-Component Systems," *Phys. Rev.*, vol. 94, no. 3, pp. 511–525, 1954.

[20] H. Grad, "On the Kinetic Theory of Rarefied Gases," *Communn. Pure Appl. Math.*, vol. 2, no. 4, pp. 331–407, 1949.

[21] M. R. Swift, E. Orlandini, W. R. Osborn, and J. M. Yeomans, "Lattice Boltzmann simulations of liquid-gas and binary fluid systems," *Phys. Rev. E*, vol. 54, no. 5, pp. 5041–5052, 1996.

[22] P. Rosenau, "Extending hydrodynamics via the regularization of the chapman-enskog expansion," *Phys. Rev. A*, vol. 40, pp. 7193–7196, Dec 1989.

[23] B. Dünweg and A. Ladd, "Lattice boltzmann simulations of soft matter systems," in *Advanced Computer Simulation Approaches for Soft Matter Sciences III* (C. Holm and K. Kremer, eds.), vol. 221 of *Advances in Polymer Science*, pp. 89–166, Springer Berlin / Heidelberg, 2009.

[24] R. F. Fox and G. E. Uhlenbeck, "Contributions to NonEquilibrium Thermodynamics. I. Theory of Hydrodynamical Fluctuations," *Phys. Fluids*, vol. 13, no. 8, p. 1893, 1970.

[25] M. Gross, M. E. Cates, F. Varnik, and R. Adhikari, "Langevin theory of fluctuations in the discrete boltzmann equation," *Journal of Statistical Mechanics: Theory and Experiment*, vol. 03, p. 03030, 2011.

[26] L. E. Reichl, *A Modern Course in Statistical Physics*. Wiley, second ed., 1998.

[27] D. d'Humieres, "Generalized lattice-Boltzmann equations," *Rarefied Gas Dynamics: Theory and Simulations, Prog. Astronaut. Aeronaut.*, vol. 159, pp. 450–458, 1992.

[28] Y. H. Qian, D. d'Humieres, and P. Lallemand, "Lattice BGK Models for Navier-Stokes Equation," *Europhys. Lett.*, vol. 17, no. 6, p. 479, 1992.

[29] S. Ansumali, S. Arcidiacono, S. S. Chikatamarla, N. I. Prasianakis, A. N. Gorban, and I. V. Karlin, "Quasi-equilibrium lattice boltzmann method," *The European Physical Journal B - Condensed Matter and Complex Systems*, vol. 56, pp. 135–139, 2007. 10.1140/epjb/e2007-00100-1.

[30] A. J. Wagner and Q. Li, "Investigation of galilean invariance of multi-phase lattice boltzmann methods," *Physica A*, vol. 362, pp. 105–110, March 2006.

[31] T. Ihle and D. M. Kroll, "Stochastic rotation dynamics: A galilean-invariant mesoscopic model for fluid flow," *Phys. Rev. E*, vol. 63, p. 020201, Jan 2001.

[32] U. Frisch, B. Hasslacher, and Y. Pomeau, "Lattice-Gas Automata for the Navier-Stokes Equation," *Phys. Rev. Lett.*, vol. 56, no. 14, pp. 1505–1508, 1986.

[33] M. P. Allen and D. J. Tildesley, *Computer Simulation of Liquids*. Clarendon, Oxford, 1987.

[34] E. M. Lifshitz and L. P. Pitaevskii, *Statistical Physics, Part 2: Volume 9 (Course of Theoretical Physics)*. Pergamon Press, Oxford, first ed., 1980.

[35] A. Donev, E. Vanden-Eijnden, A. L. Garcia, and J. B. Bell, "On the Accuracy of Finite-Volume Schemes for Fluctuating Hydrodynamics," *CAMCOS*, vol. 5, p. 149, June 2010.

[36] B. Dünweg, U. D. Schiller, and A. J. C. Ladd, "Statistical mechanics of the fluctuating lattice boltzmann equation," *Phys. Rev. E*, vol. 76, p. 036704, Sep 2007.

[37] X. He and L.-S. Luo, "A priori derivation of the lattice boltzmann equation," *Phys. Rev. E*, vol. 55, pp. R6333–R6336, Jun 1997.

[38] P. Lallemand and L. S. Luo, "Theory of the lattice Boltzmann method: Dispersion, dissipation, isotropy, Galilean invariance, and stability," *Phys. Rev. E*, vol. 61, pp. 6546–6562, June 2000.

[39] R. Adhikari and S. Succi, "Duality in matrix lattice Boltzmann models," *Phys. Rev. E*, vol. 78, p. 066701, December 2008.

[40] M. Vergassola, R. Benzi, and S. Succi, "On the hydrodynamic behaviour of the lattice boltzmann equation," *Europhys. Lett.*, vol. 13, pp. 411–416, 1990.

[41] P. J. Dellar, "Nonhydrodynamic modes and a priori construction of shallow water lattice Boltzmann equations," *Phys. Rev. E*, vol. 65, p. 036309, February 2002.

[42] P. J. Dellar, "Incompressible limits of lattice Boltzmann equations using multiple relaxation times," *J. Comput. Phys.*, vol. 190, pp. 351–370, June 2003.

[43] E. M. Lifshitz and L. P. Pitaevskii, *Physical Kinetics: Volume 10 (Course of Theoretical Physics)*. Pergamon Press, Oxford, first ed., 1981.

[44] G. Kaehler and A. J. Wagner, "Cross correlators and Galilean invariance in fluctuating ideal gas lattice Boltzmann simulations," *Commun. Comput. Phys.*, vol. 9, pp. 1315–1322, February 2011.

[45] R. Benzi, S. Succi, and M. Vergassola, "The Lattice Boltzmann-Equation–Theory and Applications," *Phys. Rep.-Rev. Sec. Phys. Lett.*, vol. 222, pp. 145–197, December 1992.

[46] J. G. M. Eggels, "Direct and large-eddy simulation of turbulent fluid flow using the lattice-Boltzmann scheme," *Int. J. Heat Fluid Flow*, vol. 17, no. 3, pp. 307–323, 1996.

[47] X. Shan and H. Chen, "Lattice Boltzmann model for simulating flows with multiple phases and components," *Phys. Rev. E*, vol. 47, pp. 1815–1819, Mar 1993.

[48] L. Giraud, D. dHumieres, and P. Lallemand, "A lattice-Boltzmann model for visco-elasticity," *Int. J. Mod. Phys. C*, vol. 8, no. 4, pp. 805–815, 1997.

[49] C. Levermore, "Moment closure hierarchies for kinetic theories," *Journal of Statistical Physics*, vol. 83, pp. 1021–1065, 1996. 10.1007/BF02179552.

[50] J. Koplik and J. R. Banavar, "Continuum Deductions from Molecular Hydrodynamics," *Annu. Rev. Fluid Mech.*, vol. 27, pp. 257–292, 1995.

[51] W. P. Yudistiawan, S. K. Kwak, D. V. Patil, and S. Ansumali, "Higher-order galilean-invariant lattice boltzmann model for microflows: Single-component gas," *Phys. Rev. E*, vol. 82, p. 046701, Oct 2010.

[52] A. J. Wagner, "Thermodynamic consistency of liquid-gas lattice boltzmann simulations," *Phys. Rev. E*, vol. 74, no. 5, p. 056703, 2006.

[53] G. R. McNamara and G. Zanetti, "Use of the boltzmann equation to simulate lattice-gas automata," *Phys. Rev. Lett.*, vol. 61, pp. 2332–2335, Nov 1988.

[54] F. J. Higuera and J. Jimnez, "Boltzmann approach to lattice gas simulations," *EPL (Europhysics Letters)*, vol. 9, no. 7, p. 663, 1989.

[55] M. Junk, A. Klar, and L. S. Luo, "Asymptotic analysis of the lattice Boltzmann equation," *J. Comput. Phys.*, vol. 210, pp. 676–704, July 2005.

[56] F. J. Higuera, S. Succi, and R. Benzi, "Lattice Gas-Dynamics with enhanced Collisions," *Europhys. Lett.*, vol. 9, pp. 345–349, June 1989.

[57] A. J. Wagner and J. M. Yeomans, "Phase separation under shear in two-dimensional binary fluids," *Phys. Rev. E*, vol. 59, pp. 4366–4373, October 1999.

[58] P. Lallemand and L. S. Luo, "Theory of the lattice Boltzmann method: Acoustic and thermal properties in two and three dimensions," *Phys. Rev. E*, vol. 68, p. 036706, September 2003.

[59] P. J. Dellar, "Multiple-Relaxation-Time Collision Operators in the Lattice Boltzmann Method," August 2008.

[60] F. Jansen and J. Harting, "From bijels to pickering emulsions: A lattice boltzmann study," *Phys. Rev. E*, vol. 83, p. 046707, Apr 2011.

[61] M. Fyta, S. Melchionna, E. Kaxiras, and S. Succi, "Multiscale simulation of nanobiological flows," *Computing in Science and Engineering*, vol. 10, pp. 10–19, 2008.

[62] N.-Q. Nguyen and A. J. C. Ladd, "Sedimentation of hard-sphere suspensions at low reynolds number," *Journal of Fluid Mechanics*, vol. 525, pp. 73–104, 2005.

[63] M. Gross, R. Adhikari, M. E. Cates, and F. Varnik, "Thermal fluctuations in the lattice Boltzmann method for nonideal fluids," *Phys. Rev. E*, vol. 82, p. 056714, Nov 2010.

[64] S. T. T. Ollila, C. Denniston, M. Karttunen, and T. Ala-Nissila, "Fluctuating lattice-Boltzmann model for complex fluids," *J. Chem. Phys.*, vol. 134, no. 6, p. 064902, 2011.

[65] A. J. Ladd, "A fast random number generator for stochastic simulations," *Computer Physics Communications*, vol. 180, no. 11, pp. 2140 – 2142, 2009.

[66] G. Kaehler and A. J. Wagner, "Fluctuating lattice Boltzmann in the low density limit," *In Preparation*, 2013.

[67] G. Kaehler and A. J. Wagner, "Derivation of Hydrodynamics for Multi-Relaxation Time Lattice Boltzmann using the Moment Approach," *accepted for publication in Commun. Comput. Phys., preprint at arXiv:1011.1510*, 2012.

[68] We are very appreciative of deeply insightful comments on this manuscript by the third referee. His review was of key importance of finding the FDT such that it is valid for all k.

[69] See Supplemental Material at [URL will be inserted by publisher] for the Mathematica notebook containing our orthogonalization procedure for the D2Q9 implementation used in this manuscript.

[70] S. S. Chikatamarla and I. V. Karlin, "Entropy and Galilean Invariance of Lattice Boltzmann Theories," *Phys. Rev. Lett.*, vol. 97, p. 190601, Nov 2006.

[71] X. B. Nie, X. Shan, and H. Chen, "Galilean invariance of lattice boltzmann models," *EPL (Europhysics Letters)*, vol. 81, no. 3, p. 34005, 2008.

[72] S. S. Chikatamarla and I. V. Karlin, "Lattices for the lattice boltzmann method," *Phys. Rev. E*, vol. 79, p. 046701, Apr 2009.

[73] K. F. Riley, M. P. Hobson, and S. J. Bence, *Mathematical Methods for Physicists and Engineers*. Cambridge University Press, third ed., 2006.

[74] J. G. Skellam, "The frequency distribution of the difference between two poisson variates belonging to different populations," *Journal of the Royal Statistical Society*, vol. 109, no. 3, p. p. 296, 1946.

[75] M. Abramowitz and I. A. Stegun, *Handbook of Mathematical Functions: With Formulas, Graphs, and Mathematical Tables*. Dover printing, t ed., 1964.

[76] M. R. Swift, W. R. Osborn, and J. M. Yeomans, "Lattice Boltzmann Simulation of Nonideal Fluids," *Phys. Rev. Lett.*, vol. 75, pp. 830–833, July 1995.

[77] A. Wagner, "Theory and applications of the lattice boltzmann method," 1997.

[78] S. Ansumali, I. V. Karlin, and H. C. ttinger, "Minimal entropic kinetic models for hydrodynamics," *EPL (Europhysics Letters)*, vol. 63, no. 6, p. 798, 2003.

APPENDIX A. MATHEMATICA EXAMPLE OF THE F-NORM

Here we give an an example of the Mathematica notebook used to calculate the velocity dependent transforms and the moment coefficients used in paper 4. We begin with an example set of MRT transforms of a D2Q9 implementation. These are stored in the array *M*. Then weight function for the orthogonality condition is defined in *fn*, a scalar product with the additional factor of the equilibrium distribution function *fsg* which is f_i^0/ρ_0 as given in Eq. (156). Then a manual Gram-Schmidt orthogonalization is performed based on this orthogonality condition according to Eqs. (157,158). The reason here is that the manual expressions, while cumbersome, evaluate much faster than the Mathematica internal function (or a recursive function with the same functionality) and we have direct control over what the procedure actually does. The inverse transform is calculated by multiplying the resulting vectors with the equilibrium distribution. We thus obtain the matrix elements of m_i^a and $n_i^a = m_i^a f_i$ as seen in section II of paper 4 and fulfill Eq. (142). Results are stored in the arrays *nfotab* for m_i^a and *nfobtab* for n_i^a. Finally, in line 140 equilibrium moments are calculated as a function of the deviation from the velocity with respect to which the transforms were calculated. The velocity difference is $\delta\mathbf{u} = \mathbf{u} - \mathbf{u}_0$. Taking this approach we can then, for a fixed $\mathbf{u}_0$ expand the equilibrium moments M^0 in terms of $\delta\mathbf{u}$ and, because the equilibrium distribution we use Eq. (163), is a second order expression in u_x and u_y the resulting equilbrium moments also have to be second order expressions in the velocity components, we can thus define the full equilibrium moment by storing the corresponding coefficients of these velocity moments. Finally the orthogonalization and calculation of equilibrium moment coefficients are performed in a stacked loop, where each loop represents one parameter for the look-up table code given in `mlrlt.h` and `mlrlt.c`. In this example case $\theta = 1/3$ is fixed but the velocity grid has a resolution of 100 in both u_x and u_y. The output is written to `mfile.dat` for the forward

transforms, `nfile.dat` the backward transforms and `meqfile.dat` for the coefficients of the equilibrium distribution.

```
autosave option
SetOptions[SelectedNotebook[],NotebookAutoSave->True]
Notebook for Galilean invariance correction on FLBoltzmann on the example of D2Q9.


Definitions of an initial original MRT transform based on d'Humieres work [27]
mc1 = {1, 1, 1, 1, 1, 1, 1, 1, 1};
mc2 = {0, 1, 0, -1, 0, 1, -1, -1, 1};
mc3 = {0, 0, 1, 0, -1, 1, 1, -1, -1};
mc4 = {0, 1, -1, 1, -1, 0, 0, 0, 0};
mc5 = {0, 0, 0, 0, 0, 1, -1, 1, -1 };
mc6 = {-4, -1, -1, -1, -1, 2, 2, 2, 2};
mc7 = {0, -2, 0, 2, 0, 1, -1, -1, 1};
mc8 = {0, 0, -2, 0, 2, 1, 1, -1, -1};
mc9 = {4, -2, -2, -2, -2, 1, 1, 1, 1};
M = {mc1, mc2, mc3, mc4, mc5, mc6, mc7, mc8, mc9};


base velocity vector of D2Q9
v={{0, 0}, {1, 0}, {0, 1}, {-1, 0}, {0, -1}, {1, 1}, {-1, 1}, {-1, -1},
    {1, -1} };


weight factor w_i in the equilibrium distribution
w = {4/9, 1/9, 1/9, 1/9, 1/9, 1/36, 1/36, 1/36, 1/36};
global (ug) and local (u) velocities
ug = {ugx, ugy};
u = {ux, uy};
du = {dux, duy};
Clear[dux, duy, ugx, ugy]
```

```
Dim=2;
Equilibrium distribution definition for local and global distribution functions
General definition of wi as found in Ansumali et al [78]
Ws = Function[i, (1-theta)^Dim (theta/(2*(1-theta)))^(v[[i]].v[[i]])];
ws = Table[Ws[i],{i,1,9}];

Equilibrium distribution in look up table values ug, used for transforms
Fsg = Function[i, ws[[i]] *(1+ ug.v[[i]]/theta + 1/2 /theta^2 (ug.v[[i
    ]])^2 - 1/2 /theta ug.ug )];
fsg = Table[Fsg[i],{i,9}];
Equilibrium distribution in ug+du used for equilibrium moments.
Fsd = Function[i, ws[[i]] *(1+ (ug+du).v[[i]]/theta + 1/2 /theta^2 ((ug
    +du).v[[i]])^2 - 1/2 /theta (ug+du).(ug+du) )];
fsd = Table[Fsd[i],{i,9}];

Fs = Function[i, ws[[i]] *(1+ u.v[[i]]/theta + 1/2/theta^2 (u.v[[i]])^2
     - 1/2/theta u.u )];
fs = Table[Fs[i],{i,9}];

Definition of scalar products for f_i and Hermite norm
fn = Function[{a, b},Simplify[a.(fsg*b)]];
wn = Function[{a, b},Simplify[a.(w*b)]];
icheck = Function[a, If[Abs[Im[a]]>0,0 ,a ]];

Definition of our initial moment base
m1 = mc1;
m2 = mc2;
m3 = mc3;
m4 = m2^2 - m3^2;
m5 = m2*m3;
m6 = m2^2 + m3^2;
```

```
m7 = mc7;
m8 = mc8;
m9 = mc9;

M = {m1, m2, m3, m4, m5, m6, m7, m8, m9}//Simplify;
M2 = {mc1, mc2, mc3, mc4, mc5, mc6, mc7, mc8, mc9}//Simplify;


Clear[ugx, ugy, theta];
ugx = 0.1;
ugy = 0.1;
theta = 1/3.;
ddux = 0.020;
dduy = 0.020;
dtheta = 1/12;
i=0;
Close["/home/kaehler/mfile.dat"];
Close["/home/kaehler/nfile.dat"];
Close["/home/kaehler/meqfile.dat"];
Clear[mfile, nfile, meqfile];
mfile = OpenWrite["~/mfile.dat"]
nfile = OpenWrite["~/nfile.dat"]
meqfile = OpenWrite["~/meqfile.dat"]



Loop over parameter space to generate lookup table files.
z=0;
Clear[ugx, ugy, theta];
theta = 1/3.; ugx = ugy = 0.1;
For[theta= 1/3,theta<=1/3, theta+= dtheta,
For[ugy=-0.5,ugy<.51, ugy+= dduy,
For[ugx=-0.5,ugx<.51, ugx+= ddux,
```

```
Print[z,""^,ugx,""^, ugy,""^, theta,""^, ddux,""^, dduy,""^, dtheta];
z++;


nf1 = m1;
MatrixForm[Simplify[nf1]]
nf2 = m2 - fn[nf1, m2] * nf1/fn[nf1, nf1];
MatrixForm[Simplify[nf2]]
nf3 = m3 - fn[nf1, m3] * nf1 /fn[nf1, nf1]- fn[nf2, m3]*nf2 /fn[nf2, nf2];
MatrixForm[Simplify[nf3]]
nf4 = m4 - fn[nf1, m4] * nf1 /fn[nf1, nf1]- fn[nf2, m4]*nf2 /fn[nf2, nf2]-
    fn[nf3, m4]*nf3 /fn[nf3, nf3];
MatrixForm[Simplify[nf4]]
nf5 = m5 - fn[nf1, m5] * nf1 /fn[nf1, nf1]- fn[nf2, m5]*nf2 /fn[nf2, nf2]-
    fn[nf3, m5]*nf3 /fn[nf3, nf3]-fn[nf4, m5]*nf4 /fn[nf4, nf4];
MatrixForm[Simplify[nf5]]
nf6 = m6 - fn[nf1, m6] * nf1 /fn[nf1, nf1]- fn[nf2, m6]*nf2 /fn[nf2, nf2]-
    fn[nf3, m6]*nf3 /fn[nf3, nf3]-fn[nf4, m6]*nf4 /fn[nf4, nf4]-fn[nf5, m6
    ]*nf5 /fn[nf5, nf5];
MatrixForm[Simplify[ExpandAll[nf6]]]
nf7 = m7 - fn[nf1, m7] * nf1 /fn[nf1, nf1]- fn[nf2, m7]*nf2 /fn[nf2, nf2]-
    fn[nf3, m7]*nf3 /fn[nf3, nf3]-fn[nf4, m7]*nf4 /fn[nf4, nf4]-fn[nf5, m7
    ]*nf5 /fn[nf5, nf5]-fn[nf6, m7]*nf6 /fn[nf6, nf6];
MatrixForm[Simplify[ExpandAll[nf7]]]
nf8 =m8 - fn[nf1, m8] * nf1 /fn[nf1, nf1]- fn[nf2, m8]*nf2 /fn[nf2, nf2]-
    fn[nf3, m8]*nf3 /fn[nf3, nf3]-fn[nf4, m8]*nf4 /fn[nf4, nf4]-fn[nf5, m8
    ]*nf5 /fn[nf5, nf5]-fn[nf6, m8]*nf6 /fn[nf6, nf6]-fn[nf7, m8]*nf7 /fn[
    nf7, nf7];
MatrixForm[Simplify[ExpandAll[nf8]]]
nf9 = m9 - fn[nf1, m9] * nf1 /fn[nf1, nf1]- fn[nf2, m9]*nf2 /fn[nf2, nf2]-
    fn[nf3, m9]*nf3 /fn[nf3, nf3]-fn[nf4, m9]*nf4 /fn[nf4, nf4]-fn[nf5, m9
```

```
    ]*nf5 /fn[nf5,nf5]-fn[nf6, m9]*nf6 /fn[nf6,nf6]-fn[nf7, m9]*nf7 /fn[
    nf7,nf7]-fn[nf8, m9]*nf8 /fn[nf8,nf8];
MatrixForm[Simplify[ExpandAll[nf9]]]

nfo1 = nf1/Sqrt[fn[nf1,nf1]]//Simplify;
nfo2 = nf2/Sqrt[fn[nf2,nf2]]//Simplify;
nfo3 = nf3/Sqrt[fn[nf3,nf3]]//Simplify;
nfo4 = nf4/Sqrt[fn[nf4,nf4]]//Simplify;
nfo5 = nf5/Sqrt[fn[nf5,nf5]]//Simplify;
nfo6 = nf6/Sqrt[fn[nf6,nf6]]//Simplify;
nfo7 = nf7/Sqrt[fn[nf7,nf7]]//Simplify;
nfo8 = nf8/Sqrt[fn[nf8,nf8]]//Simplify;
nfo9 = nf9/Sqrt[fn[nf9,nf9]]//Simplify;

nfob1 = Simplify[nfo1*fsg];
nfob2 = Simplify[nfo2*fsg];
nfob3 = Simplify[nfo3*fsg];
nfob4 = Simplify[nfo4*fsg];
nfob5 = Simplify[nfo5*fsg];
nfob6 = Simplify[nfo6*fsg];
nfob7 = Simplify[nfo7*fsg];
nfob8 = Simplify[nfo8*fsg];
nfob9 = Simplify[nfo9*fsg];

nfotab={nfo1, nfo2, nfo3, nfo4, nfo5, nfo6, nfo7, nfo8, nfo9};
nfobtab = {nfob1, nfob2, nfob3, nfob4, nfob5, nfob6, nfob7, nfob8, nfob9
    };

WriteString[mfile, z//CForm,"\t",ugx//CForm,"\t", ugy//CForm,"\t", theta
    //CForm,"\t", ddux//CForm,"\t", dduy//CForm,"\t", dtheta//CForm,"\n"
    ];
```

```
WriteString[nfile, z//CForm,"\t",ugx//CForm,"\t", ugy//CForm,"\t", theta
    //CForm,"\t", ddux//CForm,"\t", dduy//CForm,"\t", dtheta//CForm,"\n"
    ];
WriteString[meqfile, z//CForm,"\t",ugx//CForm,"\t", ugy//CForm,"\t",
    theta//CForm,"\t", ddux//CForm,"\t", dduy//CForm,"\t", dtheta//CForm
    ,"\n"];

M0 = Simplify[nfotab.fsd];
For[l=1,l<10, l++,
For[m=1,m<10, m++,
WriteString[mfile, Re[nfotab[[l]][[m]]]//CForm,"\t"];
WriteString[nfile, Re[nfobtab[[l]][[m]]]//CForm,"\t"];
]
WriteString[mfile,"\n"];
WriteString[nfile, "\n"];

Print[M0[[l]]];
M0[[l]]-=M0f*dux*duy;
M0a = M0[[l]]/.{dux->0, duy->0};
M0b = Coefficient[M0[[l]], dux,1]/.{dux->0, duy->0};
M0c = Coefficient[M0[[l]], dux, 2]/.{dux->0, duy->0};
M0d = Coefficient[M0[[l]], duy,1]/.{dux->0, duy->0};
M0e = Coefficient[M0[[l]], duy,2]/.{dux->0, duy->0};
M0f = Coefficient[M0[[l]], dux*duy,1]/.{dux->0, duy->0};

WriteString[meqfile, Re[M0a]//CForm,"\t", Re[M0b]//CForm,"\t", Re[M0c]//
    CForm, "\t", Re[M0d]//CForm, "\t", Re[M0e]//CForm, "\t", Re[M0f]//
    CForm, "\n"];
]
WriteString[mfile,"\n"];
WriteString[nfile,"\n"];
WriteString[meqfile,"\n"];
```

```
]]]
```

Listing 1. mlrlt.nb

Here we briefly document the C-implementation of our look-up table method. The idea is that we have a multidimensional array of pointers, each dimension being one parameter of our lookup tables. These pointers then point to structs where each struct contains a table containing the forward transform, a backward transform and a set of equilibrium moment coefficients. The benefit is that we decouple the geometry (now contained in the structs) from the lookup process so that it is easy to extend to more parameters or different geometries or dimensions such as a 3 dimensional implementation with energy conservatoin where we would have a look-up table with four degrees of freedom (three for $\mathbf{u}$ and one additional for the energy ϵ).

```
#ifndef MLRLT
#define MLRLT

#include<math.h>

 temp dependent transformations buffer

struct mlrlt_vector{
  int size;
  double * value;
};

cell, the struct that contains all information to do a collision at one particular set of parameters
struct mlrlt_cell{
  Matrix of the forward transform, Q*Q entries, single index
  double *M;
  Matrix of the backward transform, Q*Q entries, single index
  double *N;
  Vector of equilibrium moments coefficients
  struct mlrlt_vector **meqcoeffs;
  double ugx, ugy, theta;
  int idx;
};

Struct that contains minimum, maximum of a parameter as well as the number of entries.
Main purpose is to have a way to pass parameters to the mlrlt_base constructor.
```

```
struct mlrlt_parameter{
  double min;
  double max;
  double interval;
  int entries;
};

struct mlrlt_base{
  Q = base velocities
  N = total number of mlrlt_cells
  D = dimensionality of parameter space (i.e. 2 for isothermal D2Q9,
      3 for energy conserving D2Q9),
      is also used as size of the mlrlt_parameter array
  int Q, N, D;

  pointer to array of pointers to cells
  struct mlrlt_parameter *para_ptr;
  struct mlrlt_cell ** ltab_ptr;
};

Just a faster way to test validity of malloc-ed memory
#define MTEST(x) \
if(!(x)){fprintf(stderr,"Error allocating memory!\n");exit(-1);}


Function declarations
struct mlrlt_vector* mlrlt_vector_construct(int size);
void mlrlt_vector_destruct(struct mlrlt_vector *this);

struct mlrlt_cell* mlrlt_cell_construct(int Q, int coeffcount);
void mlrlt_cell_destruct(struct mlrlt_cell* cell_ptr);

struct mlrlt_base* mlrlt_base_construct(int Q, int coeffcount, struct
    mlrlt_parameter* paraarray_ptr, int paracount);
void mlrlt_base_destruct(struct mlrlt_base* base_ptr);

struct mlrlt_cell * mlrlt_lookup(struct mlrlt_base * this, struct
    mlrlt_vector * coords);

void mlrlt_base_set(struct mlrlt_base * this, int Q, const char* mfile
    , const char* nfile, const char* meqfile);
```

```
#endif
```

Listing 2. mlrlt.h

```
#include<stdlib.h>
#include<stdio.h>

#include"mlrlt.h"
#include<math.h>


Constructor of mlrlt_vector. Requires size of array to be used.
struct mlrlt_vector* mlrlt_vector_construct(int size){
  int i;
  struct mlrlt_vector * coords_ptr;
  coords_ptr = malloc(sizeof(struct mlrlt_vector));
  MTEST(coords_ptr);
  coords_ptr->value = malloc(sizeof(double)*size);
  MTEST(coords_ptr->value);
  coords_ptr->size = size;
  for(i=0;i<size;i++){
    coords_ptr->value[i] = i;
  }
  return(coords_ptr);
}

void mlrlt_vector_destruct(struct mlrlt_vector *this){
  free(this->value);
  free(this);
}

constructor of mlrlt_cell. Only requires Q and the number of equilibrium moment coefficients
struct mlrlt\_cell* mlrlt\_cell\_construct(int Q, int coeffcount){

  struct mlrlt_cell* cell_ptr;
  int i, j;
  cell_ptr = malloc(sizeof(struct mlrlt_cell));
  MTEST(cell_ptr);

  cell_ptr->M = malloc(sizeof(double)*Q*Q);
  MTEST(cell_ptr->M);
  cell_ptr->N = malloc(sizeof(double)*Q*Q);
  MTEST(cell_ptr->N);
```

```
    cell_ptr->meqcoeffs = malloc(sizeof(struct mlrlt_vector*)*Q);
    MTEST(cell_ptr->meqcoeffs);

    for(i=0;i<Q;i++){
      for(j=0;j<Q;j++){
        cell_ptr->M[i*Q+j] = i;
        cell_ptr->N[i*Q+j] = i;
      }
      cell_ptr->meqcoeffs[i] = mlrlt_vector_construct(coeffcount);
    }
    return(cell_ptr);
  }

  mlrlt_cell destructor
  void mlrlt_cell_destruct(struct mlrlt_cell* this){
    free(this->M);
    free(this->N);
    free(this->meqcoeffs);
    free(this);
  }

  mlrlt_base constructor. takes D, Q, and a struct of mlrlt_parameter
  struct mlrlt_base* mlrlt_base_construct(int Q, int coeffcount, struct
      mlrlt_parameter* paraarray_ptr, int paracount){
    struct mlrlt_base* base_ptr;
    int i, j, k;
    int size=1;

    base_ptr = malloc(sizeof(struct mlrlt_base) );
    MTEST(base_ptr);
    base_ptr->Q = Q;
    for(i=0; i<paracount;i++){
      size*=paraarray_ptr[i].entries;
      paraarray_ptr[i].interval = (paraarray_ptr[i].max - paraarray_ptr[
          i].min)/(paraarray_ptr[i].entries-1.);
    }
    base_ptr->N = size;
    base_ptr->D = paracount;
    base_ptr->para_ptr = paraarray_ptr;

    base_ptr->ltab_ptr = malloc(sizeof(struct mlrlt_cell*) * base_ptr->N
        );
```

```
79      MTEST(base_ptr->ltab_ptr);

        for(i = 0;i < base_ptr->N; i++){
          base_ptr->ltab_ptr[i] = mlrlt_cell_construct(Q, coeffcount);
        }
84      return(base_ptr);
      }
```

This function depends explicitely on the chosen parameters and the geometry. Look-up table parameters are given in the array coords. Function returns pointer to the cell that contains the dataset closest to those of the coords array. Current implementation assumes a standard nd rectangular grid.

```
      struct mlrlt_cell * mlrlt_lookup(struct mlrlt_base * this, struct
          mlrlt_vector * coords){
89      struct mlrlt_cell * cell;
        int index, i, slice, psize;

        psize = this->D;
        index = slice = 0;
94      if(psize != coords->size){
          fprintf(stderr, "Error: para_ptr->size(%i) and coords->size(%i)
              don't match.\n", this->D, coords->size);
          exit(-1);
        }

99      for(i=0;i<psize;i++){
          if( (coords->value[i] < this->para_ptr[i].min) || (coords->value[i
              ] > this->para_ptr[i].max) )
          fprintf(stderr,"Error: coordinate %i at %lf is out of bounds [%lf,
              %lf]\n", i, coords->value[i],this->para_ptr[i].min, this->
              para_ptr[i].max);
        }

104     slice = 1;

        for(i = 0; i < psize; i++){
          if(this->para_ptr[i].entries > 1){
            index+=slice* rint( (coords->value[i] - this->para_ptr[i].min) /
                this->para_ptr[i].interval );
109       }
          slice*=this->para_ptr[i].entries;
        }
```

```
  return(this->ltab_ptr[index]);
}

void mlrlt_base_destruct(struct mlrlt_base* this){
  int i;
  for(i = 0;i < this->N; i++){
    mlrlt_cell_destruct(this->ltab_ptr[i]);
  }
  free(this->ltab_ptr);
  free(this);
}

```

Here ends the general part

D2Q9 with ux, uy, theta dependence and 2nd order equilibrium moments

```
void mlrlt_base_set(struct mlrlt_base * this, int Q, const char* mfile
    , const char* nfile, const char* meqfile){
  int i, j, k, l, m;
  FILE* mf, *nf, *meqf;

  double n, ux, uy, theta, dux, duy, dtheta, junk;

  double mtest[9][9];
  int x, y, z;

  mf = fopen(mfile, "r");
  nf = fopen(nfile, "r");
  meqf = fopen(meqfile, "r");

  printf("%i\n", this->N);
  for(k=0;k< this->N; k++){

    for(x = 0; x < 9; x++){
      for(y = 0; y < 9; y++){
        mtest[x][y]=0;
      }
    }

    fscanf(mf,"%le" ,&n);
    fscanf(mf,"%le" ,&ux);
```

```
        fscanf(mf,"%le" ,&uy);
154     fscanf(mf,"%le" ,&theta);
        fscanf(mf,"%le" ,&dux);
        fscanf(mf,"%le" ,&duy);
        fscanf(mf,"%le" ,&dtheta);

159     this->ltab_ptr[k]->ugx = ux;
        this->ltab_ptr[k]->ugy = uy;
        this->ltab_ptr[k]->theta = theta;
        this->ltab_ptr[k]->idx = k;

164     for(i=0;i<7;i++){
          fscanf(nf,"%le", &junk);
          fscanf(meqf,"%le", &junk);
        }

169     printf("%lf \t %lf \t %lf \t %lf \t %lf \t %lf \t %lf \n", n, ux,
            uy, theta, dux, duy, dtheta);

        for(i=0;i<Q;i++){
          for(j=0;j<Q;j++){
            fscanf(mf,"%le", (&this->ltab_ptr[k]->M[i*Q+j])) ;
174           fscanf(nf,"%le", (&this->ltab_ptr[k]->N[i*Q+j])) ;
          }
          for(j=0;j<this->ltab_ptr[k]->meqcoeffs[i]->size;j++){
            fscanf(meqf,"%le",&(this->ltab_ptr[k]->meqcoeffs[i]->value[j])
                );
          }
179     }


        for(x = 0; x < 9; x++){
          for(y = 0; y < 9; y++){
184         for(z = 0; z < 9; z++){
              mtest[x][y] += (this->ltab_ptr[k]->M[x*Q+z])*(this->ltab_ptr
                  [k]->N[y*Q+z]);
    }
          }
        }
189   }

      fclose(mf);
```

```
    fclose(nf);
    fclose(meqf);
194 }
```

Listing 3. mlrlt.c

A barebone usage might then look like the following where we have omitted initilization of the

```
  include "mlrlt.h"

system size
  #define XSIZE 21
5 #define YSIZE 21

  global arrays for the distribution functions. There is no good reason to have these as constant
      arrays anymore other than that they are part of an old working code base.
  double f0[XSIZE][YSIZE], f1[XSIZE][YSIZE], f2[XSIZE][YSIZE], f3[XSIZE
      ][YSIZE], f4[XSIZE][YSIZE], f5[XSIZE][YSIZE], f6[XSIZE][YSIZE], f7
      [XSIZE][YSIZE], f8[XSIZE][YSIZE];


10

  mlrlt declarations
  struct mlrlt_parameter mlrlt_tpara[3];
  struct mlrlt_base * mlrlt_tbase;

15 int main(){
    int i,newdata;
    struct timespec timer;

    mlrlt initialization, this referers to the parameters used in the mathematica file.
20  $u_x$
    mlrlt_tpara[0].min = -0.5;
    mlrlt_tpara[0].max = 0.5;
    mlrlt_tpara[0].entries = 51;

25  $u_y$
    mlrlt_tpara[1].min = -0.5;
    mlrlt_tpara[1].max = 0.5;
    mlrlt_tpara[1].entries = 51;

30  $\theta$
    mlrlt_tpara[2].min = 3/12.;
    mlrlt_tpara[2].max = 5/12.;
```

```
    mlrlt_tpara[2].entries = 3;

    mlrlt_tbase = mlrlt_base_construct(9, 6,mlrlt_tpara, 3);
    mlrlt_base_set(mlrlt_tbase, 9, "mfile.dat", "nfile.dat", "meqfile.
        dat");

    for(i=0;i<100;i++){
      iteration();
    }
  }

  void iteration(){
    double meq[9], feq[9]; vector of equilibrium moments
    double dux, duy, dtheta;
    static struct mlrlt_cell * mlrlt_tcell;
    static struct mlrlt_vector * mlrlt_coords;

    int x, y, xm, xp, ym, yp, i, a, b, Q;
    int collision;

    double M[9];
    double noise[9];

    double f1y[ydim],f3y[ydim],f5y[ydim],f6y[ydim],f7y[ydim],f8y[ydim];
    double f2x[xdim],f4x[xdim],f5x[xdim],f6x[xdim],f7x[xdim],f8x[xdim];

    double ux,uy,uxx,uyy,nl,sn, uxy, usq;
    double uxt, uyt;

    Q = 9;

    mlrlt_coords = mlrlt_vector_construct(3);

    for (x=0;x<xdim;x++){
      for (y=0;y<ydim;y++){
        n[x][y]=f0[x][y]+f1[x][y]+f2[x][y]+f3[x][y]+f4[x][y]
        +f5[x][y]+f6[x][y]+f7[x][y]+f8[x][y];
        ux=f1[x][y]-f3[x][y]+f5[x][y]-f6[x][y]-f7[x][y]+f8[x][y];
        uy=f2[x][y]-f4[x][y]+f5[x][y]+f6[x][y]-f7[x][y]-f8[x][y];

        nl = n[x][y];
```

```
ux/=nl;
uy/=nl;

uxx=ux*ux;
uyy=uy*uy;

uxt = ux;
uyt = uy;
```

Here we limit $u < .5$ to ensure that the velocity remains inside the valid velocity range as in Figure 15.

```
if( ( uxx + uyy ) > .25 ){
  if(uxx>0.16){
    if(ux>0.4) uxt = 0.4;
    if(ux<-0.4) uxt = -0.4;
  }
  else{
    uxt = ux;
  }
  if(uyy>0.16){
    if(uy>0.4) uyt = 0.4;
    if(uy<-0.4) uyt = -0.4;
  }
  else{
    uyt = uy;
  }
}
if(isnan(uxt)) uxt = 0;
if(isnan(uyt)) uyt = 0;

mlrlt_coords->value[0] = uxt;
mlrlt_coords->value[1] = uyt;
mlrlt_coords->value[2] = theta;

mlrlt_tcell = mlrlt_lookup(mlrlt_tbase, mlrlt_coords);

dux = ux - mlrlt_tcell->ugx;
duy = uy - mlrlt_tcell->ugy;
dtheta = theta - mlrlt_tcell->theta;

for(a = 0; a < Q; a++){
  M[a]=0;
```

```
            i=0; M[a]+= mlrlt_tcell->M[a*Q+i]*f0[x][y];
            i=1; M[a]+= mlrlt_tcell->M[a*Q+i]*f1[x][y];
            i=2; M[a]+= mlrlt_tcell->M[a*Q+i]*f2[x][y];
            i=3; M[a]+= mlrlt_tcell->M[a*Q+i]*f3[x][y];
            i=4; M[a]+= mlrlt_tcell->M[a*Q+i]*f4[x][y];
            i=5; M[a]+= mlrlt_tcell->M[a*Q+i]*f5[x][y];
            i=6; M[a]+= mlrlt_tcell->M[a*Q+i]*f6[x][y];
            i=7; M[a]+= mlrlt_tcell->M[a*Q+i]*f7[x][y];
            i=8; M[a]+= mlrlt_tcell->M[a*Q+i]*f8[x][y];

            Here the equilibrium moments are assembled from the precomputed coefficients
                stored in the lookup table and the powers of the deviations from the lookup
                table velocity δu_x, δu_y, (δu_x^2), (δu_y^2), δu_xδu_y as seen in section IV in paper 3.
            meq[a] = 0;
            meq[a] += mlrlt_tcell->meqcoeffs[a]->value[0];
            meq[a] += mlrlt_tcell->meqcoeffs[a]->value[1]*dux;
            meq[a] += mlrlt_tcell->meqcoeffs[a]->value[2]*dux*dux;
            meq[a] += mlrlt_tcell->meqcoeffs[a]->value[3]*duy;
            meq[a] += mlrlt_tcell->meqcoeffs[a]->value[4]*duy*duy;
            meq[a] += mlrlt_tcell->meqcoeffs[a]->value[5]*dux*duy;
            meq[a] *= nl;
          }

          sn=sqrt(nl);

          noise[0] = noise[1] = noise[2] = 0;

          noise[3] = sn*rndgen(&idum);
          noise[4] = sn*rndgen(&idum);
          noise[5] = sn*rndgen(&idum);
          noise[6] = sn*rndgen(&idum);
          noise[7] = sn*rndgen(&idum);
          noise[8] = sn*rndgen(&idum);


          Here we perform the actual collision step according to Eq. (132)
          for(a=0;a<Q;a++){
    M[a] = 1./tau[a] * ( meq[a] + ( tau[a] - 1. ) * M[a] + sqrt( 2 * tau
        [a] - 1. ) * noise[a] );
          }
```

```
        f0[x][y] = f1[x][y] = f2[x][y] = f3[x][y] = f4[x][y] = f5[x][y]
            = f6[x][y] = f7[x][y]= f8[x][y] = 0;
        for(a = 0; a < Q; a++){
          i = 0; f0[x][y] += mlrlt_tcell->N[a*Q+i] * M[a];
          i = 1; f1[x][y] += mlrlt_tcell->N[a*Q+i] * M[a];
          i = 2; f2[x][y] += mlrlt_tcell->N[a*Q+i] * M[a];
          i = 3; f3[x][y] += mlrlt_tcell->N[a*Q+i] * M[a];
          i = 4; f4[x][y] += mlrlt_tcell->N[a*Q+i] * M[a];
          i = 5; f5[x][y] += mlrlt_tcell->N[a*Q+i] * M[a];
          i = 6; f6[x][y] += mlrlt_tcell->N[a*Q+i] * M[a];
          i = 7; f7[x][y] += mlrlt_tcell->N[a*Q+i] * M[a];
          i = 8; f8[x][y] += mlrlt_tcell->N[a*Q+i] * M[a];
        }
      }
    }
```

Arrays of boundaries are read

```
    for (y=0;y<ydim;y++){
      f1y[y]=f1[xdim-1][y];
      f3y[y]=f3[0][y];

      f5y[y]=f5[xdim-1][y];
      f6y[y]=f6[0][y];
      f7y[y]=f7[0][y];
      f8y[y]=f8[xdim-1][y];
    }
    for (x=0;x<xdim;x++){
      f2x[x]=f2[x][ydim-1];
      f4x[x]=f4[x][0];

      f5x[x]=f5[x][ydim-1];
      f6x[x]=f6[x][ydim-1];
      f7x[x]=f7[x][0];
      f8x[x]=f8[x][0];
    }
```

The streaming is done according to the velocity vectors v_i associated with the distribution functions f_i.

```
    memmove(&f1[1][0],&f1[0][0],(xdim-1)*ydim*sizeof(double));
    memmove(&f3[0][0],&f3[1][0],(xdim-1)*ydim*sizeof(double));
    memmove(&f2[0][1],&f2[0][0],(xdim*ydim-1)*sizeof(double));
    memmove(&f4[0][0],&f4[0][1],(xdim*ydim-1)*sizeof(double));
```

```
    memmove(&f5[1][1],&f5[0][0],((xdim-1)*ydim-1)*sizeof(double));
    memmove(&f7[0][0],&f7[1][1],((xdim-1)*ydim-1)*sizeof(double));
    memmove(&f6[0][1],&f6[1][0],((xdim-1)*ydim)*sizeof(double));
    memmove(&f8[1][0],&f8[0][1],((xdim-1)*ydim)*sizeof(double));

    Periodic boundary conditions are generated by writing the saved boundary arrays in the
        appropriate positions.
    for (y=0;y<ydim;y++){
      f1[0][y]                =f1y[y];
      f3[xdim-1][y]           =f3y[y];

      f5[0][(y+1)%ydim]       =f5y[y];
      f6[xdim-1][(y+1)%ydim]=f6y[y];
      f7[xdim-1][y]           =f7y[(y+1)%ydim];
      f8[0][y]                =f8y[(y+1)%ydim];
    }
    for (x=0;x<xdim;x++){
      f2[x][0]                =f2x[x];
      f4[x][ydim-1]           =f4x[x];
      f5[(x+1)%xdim][0]       =f5x[x];
      f6[x][0]                =f6x[(x+1)%xdim];
      f7[x][ydim-1]           =f7x[(x+1)%xdim];
      f8[(x+1)%xdim][ydim-1]=f8x[x];
    }
    iterations++;
    mlrlt_vector_destruct(mlrlt_coords);
  }
```

Listing 4. FLD2Q9.c